Vasculogenic Mimicry: Regulation and Function in Melanoma

Lih Yin Tan

Bachelor of Health Sciences (Honours)

A thesis submitted for the degree of

Doctor of Philosophy

School of Pharmacy and Medical Sciences

Division of Health Sciences



University of
South Australia

January 2018

Table of Contents

List of Figures ..... **iii**
List of Tables ..... **v**
Abbreviations ..... **vi**
Publications arising from this thesis ..... **xii**
Future publications arising from this thesis ..... **xii**
Abstract ..... **xiii**
Declaration ..... **xv**
Acknowledgements ..... **xvi**
Chapter 1. Introduction **1**
1.1. General Introduction 2
1.2. Melanoma and Key Driver Pathways 2
1.2.1. Key Signalling Pathways Driving Melanoma 2
1.2.2. Therapies Targeting Key Signalling Pathways in Melanoma 6
1.3. Melanoma and the Immune System 6
1.3.1. General Introduction 6
1.3.2. Roles of Different Leukocyte Subsets in Melanoma 7
1.3.3. Immunotherapy 11
1.3.4. "Immunotherapy" with other Treatment Approaches 14
1.4. Melanoma and Blood Vessels 14
1.4.1. Introduction 14
1.4.2. Conventional Endothelial Cell Lined Blood Vessels 15
1.4.3. Alternative Melanoma Cell Lined Blood Vessels 26
1.5. The Research Project 32
1.5.1. Regulation of Vasculogenic Mimicry 32
1.5.2. Function of Vasculogenic Mimicry 32
Chapter 2. Materials and Methods **34**
2.1. Ethics Statement 35
2.1.1. Human Ethical Statement 35
2.1.2. Murine Ethical Statement 35
2.2. Materials and Methods 35
2.2.1. Cell Culture 35
2.2.2. Isolation and Preparation of Bulk Mononuclear Cells 40
2.2.3. Transfection and Transduction Protocols 41
2.2.4. Characterisation of Gene Expression 43
2.2.5. Characterisation of Protein Expression 48
2.2.6. Functional Assays 55

2.2.7. In Vivo Murine Experiments 59
2.2.8. In Silico Analysis 61
2.2.9. Statistical Analysis 61
Chapter 3. Regulation of Melanoma VM: Role of Desmoglein 2 63
3.1. Introduction 64
3.1.1. General Introduction 64
3.1.2. Desmoglein 2 (DSG2) 64
3.2. Hypothesis and Aims 70
3.3. Results 71
3.4. Discussion 95
Chapter 4. Function of Melanoma VM: Leukocyte Recruitment *in Vitro* 102
4.1. Introduction 103
4.1.1. General Introduction 103
4.1.2. Leukocyte Recruitment by EC Vessels 103
4.1.3. Leukocyte Recruitment by Melanoma EC Vessels 107
4.2. Hypothesis and Aims 108
4.3. Results 110
4.4. Discussion 157
Chapter 5. Function of Melanoma VM: Leukocyte Recruitment *in Vivo* 170
5.1. Introduction 171
5.1.1. General Introduction 171
5.1.2. Strengths and Limitations of Intravital Microscopy 171
5.1.3. Intravital Microscopy on VM Vessels 173
5.2. Hypothesis and Aims 173
5.3. Results 174
5.4. Discussion 189
Chapter 6. Final Discussion 193
Appendix A. Summary of RNA Sequencing Statistics 200
Appendix B. Gating Strategy for Flow Cytometric Phenotyping of Mononuclear Cells 202
References 204

List of Figures

Figure 1.1. Key signalling pathways driving melanoma progression and the different targeted therapies available. 5
Figure 1.2. Roles of different leukocyte subsets in regulating melanoma disease and the effect of various treatment approaches on leukocyte numbers and function. 13
Figure 1.3. The leukocyte recruitment cascade, and the adhesion molecules/ligands which are relevant for each step. Figure adapted from (Tan et al. 2017). 18
Figure 1.4. Vasculogenic mimicry and the pathways involved in its regulation. 31
Figure 3.1. Schematic diagram of desmosomes. 66
Figure 3.2. The human melanoma cell lines C32, CHL-1 and SK-Mel-28 express DSG2. (Immunofluorescence image for HaCaT keratinocytes kindly provided by Dr Lisa Ebert). 72
Figure 3.3. C32, CHL-1 and SK-Mel-28 form VM structures when seeded on Matrigel. 74
Figure 3.4. DSG2 expression can be downregulated with siRNA transfection. 76
Figure 3.5. DSG2 knockdown leads to disruption of melanoma VM formation. 79
Figure 3.6. DSG2 knockdown does not affect melanoma cell proliferation. 81
Figure 3.7. DSG2 knockdown does not alter melanoma cell actin cytoskeleton structure. 83
Figure 3.8. The xCELLigence assay does not allow for accurate measurement of melanoma cell migration. 86
Figure 3.9. DSG2 knockdown does not affect melanoma cell migration. 87
Figure 3.10. DSG2 knockdown impairs melanoma cell-cell adhesion. 90
Figure 3.11. Pre-existing DSG2 expression levels on melanoma cells may be affected by hypoxia. 92
Figure 3.12. The DSG2 promoter region has putative hypoxia response elements (HRE). 93
Figure 3.13. EGFR and ADAM17 gene expression levels are not affected by hypoxia. 94
Figure 4.1. Leukocytes can roll and adhere on a VM-competent melanoma cell monolayer. 115
Figure 4.2. Some leukocyte subsets can transmigrate across a melanoma monolayer in response to an FBS gradient. 120
Figure 4.3. Leukocytes can transmigrate across a melanoma monolayer in response to a CXCL12 gradient. 124
Figure 4.4. 0.5% O_2 culture conditions stimulate the expression of hypoxia responsive genes in C32, CHL-1 and SK-Mel-28. 129
Figure 4.5. TrHBMEC do not show altered adhesion molecule expression or reduced leukocyte adhesion after culture in 0.5% O_2. 132
Figure 4.6. C32, CHL-1 and SK-Mel-28 express mRNA for adhesion molecules characteristic of endothelial cells under both ambient and hypoxic conditions. 135
Figure 4.7. C32, CHL-1 and SK-Mel-28 express adhesion molecules characteristic of endothelial cells on the cell surface under both ambient and hypoxic conditions. 138
Figure 4.8. The effect of blocking ICAM-1 on leukocyte adhesion to melanoma cells could not be assessed. 141
Figure 4.9. C32, CHL-1 and SK-Mel-28 express mRNA for chemokines under both ambient and hypoxic conditions. 144
Figure 4.10. C32, CHL-1 and SK-Mel-28 secrete chemokines into the supernatant under both ambient and hypoxic conditions. 146
Figure 4.11. The adhesion molecules and chemokines expressed in melanoma cell lines C32, CHL-1 and SK-Mel-28 are also expressed at the RNA level in human melanoma samples. 153
Figure 4.12. The expression of adhesion molecules and chemokines in the TCGA dataset may be attributed to both ECs and melanoma cells. 156

Figure 5.1. C32 human melanoma cells which are VM-competent in vitro are also VM-competent in vivo. (Combined effort between Ms Kay Khine Myo Min and myself to generate xenografts, immunohistochemistry results kindly provided by Ms Kay Khine Myo Min).....175
Figure 5.2. C32 human melanoma cells transduced to stably express GFP retain VM-competency and adhesion molecule expression in vitro. 178
Figure 5.3. Setup of mouse model for examination of leukocyte recruitment via VM vessels. (Group effort co-ordinated by myself but with input from Associate Professor Claudine Bonder, Dr Eli Moore, Ms Michaelia Cockshell and Ms Kay Khine Myo Min).....180
Figure 5.4. C32-GFP cells can bind to DyLight® 594 tomato lectin. 182
Figure 5.5. Intravenously injected CellTracker™ Blue CMAC labelled MNC can be detected in excised C32-GFP tumours......186
Figure 5.6. Excised C32-GFP tumours retain expression of adhesion molecules required for leukocyte recruitment......188
Figure B1. Gating strategy for flow cytometric phenotyping of MNC from parallel plate flow chamber and Transwell assays. 203

List of Tables

Table 2.1. Media and reagents used for cell culture and their contents.....36
Table 2.2. Cell lines used and their culture conditions.....38
Table 2.3. Media and reagents used for the isolation and preparation of bulk mononuclear cells and their contents.....40
Table 2.4. Media and reagents used for the protocols related to quantitative real time polymerase chain reaction and their contents.....43
Table 2.5. List of primers used for qPCR.....45
Table 2.6. Media and reagents used for the preparation of cells for flow cytometric analysis and their contents.....48
Table 2.7. List of antibodies and reagents used for flow cytometric phenotyping of MNC.....50
Table 2.8. List of antibodies and reagents used for flow cytometric analysis of melanoma adhesion molecule expression.....52
Table 2.9. List of reagents used for immunofluorescence analysis and their contents.....53
Table 2.10. List of reagents used for immunohistochemical analysis and their contents.....60
Table 4.1. Endothelial cell adhesion molecules implicated in the leukocyte recruitment cascade and their respective receptors/ligands on leukocytes. Table adapted and modified from (Tan et al. 2017)......105
Table 4.2. List of chemokines currently demonstrated to recruit $CD8^+$ T cells, TAM, TAN and NK cells to melanoma, and their respective receptors on leukocytes. Table adapted and modified from (Tan et al. 2017)......106
Table 4.3. Summary of the known roles of the various chemokines and chemotactic cytokines secreted by the melanoma cells, their corresponding receptors, the leukocyte subsets expressing these receptors and the disease model whereby the recruitment of the respective leukocyte subsets were demonstrated......150
Table 4.4. Summary of key findings on the three VM-competent melanoma cells.....158
Table A1. Summary of reads and alignment rates of RNA sequencing performed on the melanoma cell lines C32, CHL-1 and SK-Mel-28 cultured under ambient (21% O_2) and hypoxic (0.5% O_2) conditions for 3 (D3) and 7 days (D7)......201

Abbreviations

2D	2 dimensional
3D	3 dimensional
7-AAD	7-aminoactinomycin D
ACK	ammonium chloride potassium
ACT	adoptive cell transfer
ADAM	a distintegrin and metalloproteinase
ADM	adrenomedullin
AKT	AKT serine/threonine-protein kinase
ANGPTL4	angiopoietin-like 4
ANKRD37	ankyrin repeat domain 37
APC	allophycocyanin
bFGF	basic fibroblast growth factor
BNIP3	BCL2/adenovirus E1B 19kDa protein-interacting protein 3
bp	basepair
BRAF	B-Raf serine/threonine-protein kinase
BSA	bovine serum albumin
BUV	Brilliant Ultraviolet
BV	Brilliant Violet
CAR T cell	chimeric antigen receptor T cell
CCL	CC chemokine ligand
CCR	CC chemokine receptor
CD	cluster of differentiation
CDK	cyclin dependent kinase

cDNA	complementary deoxyribonucleic acid
CMAC	7-amino-4-chloromethylcoumarin
CO_2	carbon dioxide
CPM	counts per million
CTLA-4	cytotoxic T-lymphocyte associated protein 4
CX3CL1	fractalkine
CXCL	CXC chemokine ligand
CXCR	CXC chemokine receptor
DAPI	4’,6-diamidino-2-phenylindole
DLL	delta-like ligand 4
DMEM	Dulbecco’s Modified Eagle Medium
DMSO	dimethyl sulfoxide
DNA	deoxyribonucleic acid
dNTP	dinucleotide triphosphate
DPBS	Dulbecco’s phosphate-buffered saline
DSG2	desmoglein 2
DSC	desmocollin
EC	endothelial cell
ECGS	Endothelial Cell Growth Supplement
EDTA	ethylene diamine tetra acetic acid
EGFR	epidermal growth factor receptor
EMCN	endomucin
ENO1	enolase 1
EphA	ephrin A
ERK	extracellular signal-regulated kinases

ESL	E-selectin ligand
ET-1	endothelin 1
ET_BR	endothelin B receptor
FACS	fluorescence activated cell sorting
FAK	focal adhesion kinase
FasL	Fas ligand
FBS	fetal bovine serum
FcR	Fc receptor
FITC	fluorescein isothiocyanate
FOXP3	forkhead box P3
FSC	forward scatter
FVS	Fixable Viability Stain
Fwd	Forward
GFP	green fluorescent protein
HA	hyaluronic acid
HBSS	Hank's Balanced Salt Solution
HEK293T	human embryonic kidney cell line
HEPES	4-(2-Hydroxyethyl)piperazine-1-ethanesulfonic acid
HIF	hypoxia inducible factor
HRE	hypoxia response element
HUVEC	human umbilical vein endothelial cell
ICAM	intercellular adhesion molecule
IF	immunofluorescence
IFN	interferon
IgG	immunoglobulin G

IL	interleukin
JAM	Junctional adhesion molecule
KD	knockdown
KLF	Kruppel-like factor
LDHA	lactate dehydrogenase A
LFA-1	lymphocyte function-associated antigen 1
MAC-1	macrophage-1 antigen
MAdCAM	mucosal vascular addressin cell adhesion molecule
MAPK	mitogen activated protein kinase
MDK	midkine
MDSC	myeloid derived suppressor cells
MEK	mitogen activated protein kinase kinase
MFI	mean fluorescence intensity
MHC	major histocompatibility complex
MITF	microphthalmia-associated transcription factor
MMP	matrix metalloproteinase
MNC	mononuclear cell
mRNA	messenger ribonucleic acid
N_2	nitrogen
NCBI	National Centre for Biotechnology Information
NICD	notch intracellular domain
NK cell	Natural Killer cell
NKG2D	Natural Killer Group 2D receptor
NO	nitric oxide
O_2	oxygen

PAS	Periodic Acid Schiff
PBS	phosphate buffered saline
PCR	polymerase chain reaction
PD-1	programmed cell death protein 1
PDL-1	programmed death-ligand 1
PE	Phycoerythrin
PECAM-1	platelet endothelial cell adhesion molecule-1
PE-Cy5	Phycoerythrin-Cyanine 5
PE-Cy7	Phycoerythrin-Cyanine 7
PerCP-Cy5.5	PerCP Cyanine 5.5
PGK1	phosphoglycerate kinase 1
PI3K	phosphatidylinositol-4,5-bisphosphate 3-kinase
PIP_2	phosphatidylinositol-4,5-bisphosphate
PIP_3	phosphatidylinositol-3,4,5-trisphosphate
PNAd	peripheral node addressin
PSGL	P-selectin glycoprotein ligand
PTEN	phosphatase and tensin homolog
qPCR	quantitative real-time polymerase chain reaction
RB	retinoblastoma
Rev	Reverse
RNA	ribonucleic acid
ROS	reactive oxygen species
RPMI	Roswell Park Memorial Institute
RT	room temperature
RTK	receptor tyrosine kinase

SD	standard deviation
SEM	standard error of the mean
siRNA	small interfering RNA
shRNA	short hairpin RNA
SLC2A1	solute carrier family 2 member 1
SSC	side scatter
TAM	tumour associated macrophage
TAN	tumour associated neutrophil
TCGA	The Cancer Genome Atlas
TFPI	tissue factor pathway inhibitor
TGF	transforming growth factor
Th	helper T cell
TNF	tumour necrosis factor
Treg	regulatory T cell
UTR	untranslated region
UV	ultraviolet
VCAM	vascular cell adhesion molecule
VEGF	vascular endothelial growth factor
VEGFR	vascular endothelial growth factor receptor
VLA-4	very late antigen-4
VM	vasculogenic mimicry
WST	water-soluble tetrazolium salt
x g	times gravity

Publications arising from this thesis

1. **Tan, L.Y.**, Mintoff, C., Johan, M.Z., Ebert, B.W., Fedele, C., Zhang, Y.F., Szeto, P., Sheppard, K.E., McArthur, G.A., Foster-Smith, E. and Ruszkiewicz, A., 2016. Desmoglein 2 promotes vasculogenic mimicry in melanoma and is associated with poor clinical outcome. *Oncotarget*, *7*(29), p.46492.
2. **Tan, L.Y.**, Martini, C., Fridlender, Z.G., Bonder, C.S., Brown, M.P. and Ebert, L.M., 2017. Control of immune cell entry through the tumour vasculature: a missing link in optimising melanoma immunotherapy?. *Clinical & translational immunology*, *6*(3), p.e134.

Future publications arising from this thesis

1. **Tan, L.Y.**, Myo Min, K.K., Ebert, B.W., Cockshell, M., Moore E., Bonder, C.S. and Ebert, L.M.. Vasculogenic mimicry structures in melanoma participate in the recruitment of pro-tumourigenic monocytes. *Manuscript under preparation.*

Abstract

Vasculogenic mimicry (VM) is a process where cancer cells align along a deposited basement membrane to form vessel-like structures which are capable of conducting blood. The overarching aim of this thesis is to address key gaps in our knowledge of melanoma VM. More specifically, two hypotheses relating to the regulation and function of melanoma VM respectively will be investigated.

The role of the cadherin desmoglein 2 (DSG2) in regulating melanoma VM is examined in Chapter 3 of this thesis. When $DSG2^+$ melanoma cells were subjected to a Matrigel tube formation assay, these cells readily rearranged and intimately associated to form networks of elongated structures extending from cell clusters, an indication of their VM capabilities. This was significantly impaired following siRNA-mediated DSG2 knockdown. Further investigation of the mechanism underlying this observation revealed that DSG2 knockdown significantly decreased cell-cell adhesion. Preliminary results suggested a potential role of hypoxia in regulating DSG2 expression levels, although further investigations are warranted.

To date, no studies have directly assessed the actual function of VM in melanoma. The possibility that VM-competent melanoma cells mediate selective leukocyte recruitment *in vitro* is examined in Chapter 4. Parallel plate flow chamber assays and Transwell assays performed on VM-competent melanoma cell monolayers confirmed their ability to promote leukocyte rolling, adhesion and transmigration. While melanoma cells were able to promote adhesion of all the different leukocyte subsets assessed, including $CD4^+$ T cells, $CD8^+$ T cells, $CD14^+$ monocytes, $CD16^+$ NK cells and $CD19^+$ B cells, there was a trend towards preferential monocyte adhesion observed for some of the melanoma cell lines. In line with their leukocyte recruitment capabilities, RNA sequencing and flow cytometry analyses confirmed the expression of various adhesion molecules characteristic of endothelial cells (ECs) in mediating leukocyte recruitment on the melanoma cells. VM-competent melanoma cells expressed at least one adhesion molecule required for each step of the leukocyte recruitment cascade, such as CD44 for leukocyte rolling, ICAM-1 for leukocyte adhesion and JAM for leukocyte transmigration. These cells also secreted various chemokines that have been reported to be chemoattractive towards T cells, NK cells, B cells, monocytes, neutrophils and regulatory T cells. Unlike that reported on ECs, the expression of these adhesion molecules and chemokines on the melanoma cells was largely unaffected upon hypoxic stimulation. This suggests that these VM-competent melanoma cells could

potentially retain their leukocyte recruitment capabilities under physiological conditions where the tumour is constantly under hypoxic stress.

Chapter 5 describes the approaches taken to establish a mouse model to examine leukocyte recruitment via VM vessels using intravital microscopy. C32 melanoma cells transduced using a lentiviral vector to express GFP were used to generate tumour xenografts in mice so that the conventional EC-lined blood vessels can be distinguished from the fluorescently green melanoma cell-lined VM vessels. The progress of establishing this model was hindered with the unexpected malfunction of the two photon laser required for imaging, although vessel-like structures could be visualised within the green C32 xenografts, Furthermore, flow cytometric analysis on dissociated tumours confirmed the retention of adhesion molecule expression on the melanoma cells as well as the presence of injected leukocytes within the tumour. These observations suggest the feasibility of this model in assessing leukocyte recruitment via VM vessels,

In summary, this thesis presents novel findings in the regulation and function of VM in melanoma which will form a foundation for future studies aiming to better understand this process, and potentially to target it for therapeutic benefit.

Declaration

This thesis presents work carried out by myself and does not incorporate without acknowledgment any material previously submitted for a degree or diploma in any university; to the best of my knowledge it does not contain any materials previously published or written by another person except where due reference is made in the text; and all substantive contributions by others to the work presented, including jointly authored publications, are clearly acknowledged.

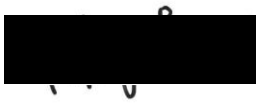

Lih Yin Tan

January 2018

Acknowledgements

Dear God, thank you for making this possible, and fulfilling Your promise that whatever You have started You will see it to completion. Thank you for making this journey as equally (if not more) rewarding in many ways as it is challenging. May all glory and honour be to You. Thank you for surrounding me with wonderful people throughout this journey, for I clearly know that without them, I would not have made it this far. May You bless them abundantly too just as they have blessed me.

Dear Lisa, thank you for all the faith you have had in me throughout and even before I have embarked on this journey, that I am capable of doing a PhD. Thank you for all that you have done- for all the time and effort that you have put into supporting me from little things like positive messages on a rainy day to mammoth tasks like reading this thesis! Thank you too for all the encouragement that you have given me to step out of my comfort zone and to push my limits. There is still a lot for me to learn, but thank you so much for helping me develop into the person I am today.

Dear Claudine, thank you for having me in the laboratory. Thank you for all your time and help in making sure that the work I do is of high calibre, and the support to grab hold of all the opportunities that will help me progress. Thank you for always being there whenever I needed to have a chat, and always generously offering to help far beyond what I could have asked for. You have given me so much comfort and support in times of need and I really appreciate it.

Dear Michael, thank you for taking the time to provide feedback for my experiments and writing even while you are occupied with clinical work. You have added a lot of valuable input from a different perspective and have helped develop my work in many ways.

Dear past and present members of the Vascular Biology and Cell Trafficking laboratory, you are such an awesome bunch to work together and just to be with! Thank you for all the joy and laughter that you have filled my days in the laboratory with. I have had a lot of fun memories in this laboratory. Thank you too for always being understanding when I struggle with things, and always being there to lend a helping hand or a listening ear.

Many thanks to all the members of the Centre for Cancer Biology as well as the staff members of the University of South Australia and CRC for Cell Therapy Manufacturing.

Thank you for all the support that you have generously given, as well as the valuable opportunities to participate in various events that I would not have had otherwise. Many thanks to the Commonwealth Government too for providing financial support through an "Australian Government Research Training Program Scholarship", as well as the CRC for Cell Therapy Manufacturing for providing financial support through the ePhD program.

Dear family, thank you so much for always keeping me in your thoughts and prayers. Thank you for always being there to celebrate my successes and helping me out in every possible way when things got overwhelming. I hope I have made you proud. Many thanks to Ignatius, Ethan and Elyse too for all your hugs, kisses and little gifts. You never fail to brighten up my day. And Vincent, thank you for always seeing the best in me and seeing me through the most challenging period of my PhD.

Dear friends near and far (special shout out to Siew), senseis, senpais and peers from South Australian Kendo Association, brothers and sisters in Christ from Goodwood Methodist Church, thank you for being the wonderful people you are. You have all enriched my life in many ways and broaden my horizon outside of my PhD studies. Thank you for all the much needed support and kindness throughout these four years.

I am very blessed to have every single one of you as part of this journey. You have all made a significant impact in my life, and I would not be here today without you, so thank you, thank you, thank you.

Chapter 1. Introduction

1.1. General Introduction

Melanoma is a cancer of melanocytes, the pigment producing cells of neuroectodermal origin that reside in the skin, eyes and gut. In the skin, melanocytes act as the first line of defence against detrimental ultraviolet (UV) light. When exposed to high levels of UV, these cells undergo melanogenesis to produce melanin that absorbs the infiltrating UV rays and protects the deeper layers of the skin from radiation damage. However, both intrinsic factors such as familial genetic predispositions and extrinsic factors such as excessive sun exposure can lead to defects in melanocyte function and "oversaturation" in melanogenesis. This sparks the occurrence of melanoma. Melanoma initiates as a benign nevus, and progresses through to a radial growth phase melanoma (where the melanoma remains localised within the upper epidermal layer of the skin), followed by a vertical growth phase (where the melanoma invades into the deeper dermal layers of the skin). Eventually, melanoma can metastasise to diverse sites including the lungs, brain and bone marrow.

While a simple surgical excision is sufficient to fully cure melanoma when it is confined to the upper layers of the skin, once the melanoma invades and gains metastatic potential, surgery becomes a less effective treatment. Initial modalities to treat metastatic melanoma have largely focused on the use of chemotherapy (such as dacarbazine and fotemusine) as well as radiation. Unfortunately these treatments have provided little efficacy and are often accompanied with serious side effects.

In order to grow and spread, melanoma requires the activation of multiple proliferation pathways, active editing of the immune microenvironment, and expansion of the nutrient supply. This introduction will focus on our current knowledge of these processes, and how a better understanding of these processes has led to the breakthrough development and evolution of therapies that have dramatically converted the treatment approach and outlook of this disease. In addition, key knowledge gaps will also be highlighted.

1.2. Melanoma and Key Driver Pathways

1.2.1. *Key Signalling Pathways Driving Melanoma*

Melanoma is enriched with both directly UV-induced mutations (C>T, G>T transitions) (Hodis et al. 2012), as well as mutations which are thought to arise from secondary free radical damage following UV-melanin interaction (Noonan et al. 2012). These mutations

affect multiple critical cellular signalling pathways and in turn drive melanoma development and progression.

A key signalling pathway governing melanoma progression is the mitogen activated protein kinase (MAPK) pathway (Figure 1.1). Under physiological conditions, this pathway is initiated in response to growth factor-receptor tyrosine kinase interactions, which in turn stimulate the subsequent RAS-RAF-MEK-ERK signal transduction pathway to regulate a range of cellular processes including proliferation and survival. One of the most prominently mutated proteins in this pathway is the serine/threonine protein kinase BRAF, where a point mutation in *BRAF* results in the substitution of valine to glutamic acid at the 600th amino acid (V600E) residing in the BRAF kinase (Davies et al. 2002). The resulting BRAF^{V600E} mutant kinase is constitutively active, allowing for continual activation of the MAPK pathway. This mutation is found to be present in ~50% of melanoma patients, and is already prevalent in benign nevi (Pollock et al. 2003). Alternatively, ~15-20% of patients harbour mutations in the NRAS protein owing to *NRAS*$^{Q61L/R}$ mutations (Jakob et al. 2012), which similarly allow for constitutive activation of the MAPK pathway. The *BRAF*^{V600E} and *NRAS*$^{Q61L/R}$ mutations are mutually exclusive, and together MAPK pathway mutations are present in ~70% of patients.

The MAPK pathway has also been found to cooperate with other pathways to drive melanoma progression. One of these is the RAS-PI3K-PTEN-AKT pathway, which is also activated in response to growth factor-receptor tyrosine kinase interactions (Figure 1.1). Amplifications in the gene encoding the AC serine/threonine kinase AKT3 allowing for constitutive activation of the PI3K pathway have been reported in ~50% of melanomas (Stahl et al. 2004). Another frequent defect that affects this pathway is the loss-of-function point mutations and deletions in the *PTEN* gene encoding the phosphatase PTEN, which is important in dephosphorylating PI3K and thereby negatively regulating the PI3K pathway (Stark & Hayward 2007). PTEN mutations are present in ~40% of melanomas (Guldberg et al. 1997). The combination of BRAF and PTEN mutations has been reported in ~40% of melanoma (Hodis et al. 2012), and has been found to be key in inducing melanoma metastasis (Dankort et al. 2009).

Alternatively, the MAPK pathway has also been found to cooperate with cell cycle regulatory pathways, in particular the p14^{ARF}-p53 and the p16^{INK4A}-CDK4/CDK6-RB pathways to promote melanoma progression (Figure 1.1). Loss of function mutations in the tumour suppressor proteins p14^{ARF} and p16^{INK4A} arising from mutations in the *CDKN2A* gene that

encodes for both $p14^{ARF}$ and $p16^{INK4A}$ result in downstream degradation of the tumour suppressor p53 and the activation of the cyclin-dependent kinases CDK4/CDK6 which in turn drive cell cycle progression. Mutations in these pathways are found to be present in ~90% of melanomas (Walker et al. 1998).

Taken together, over-activation of the MAPK, PI3K and cell cycle pathways are key in driving melanoma progression.

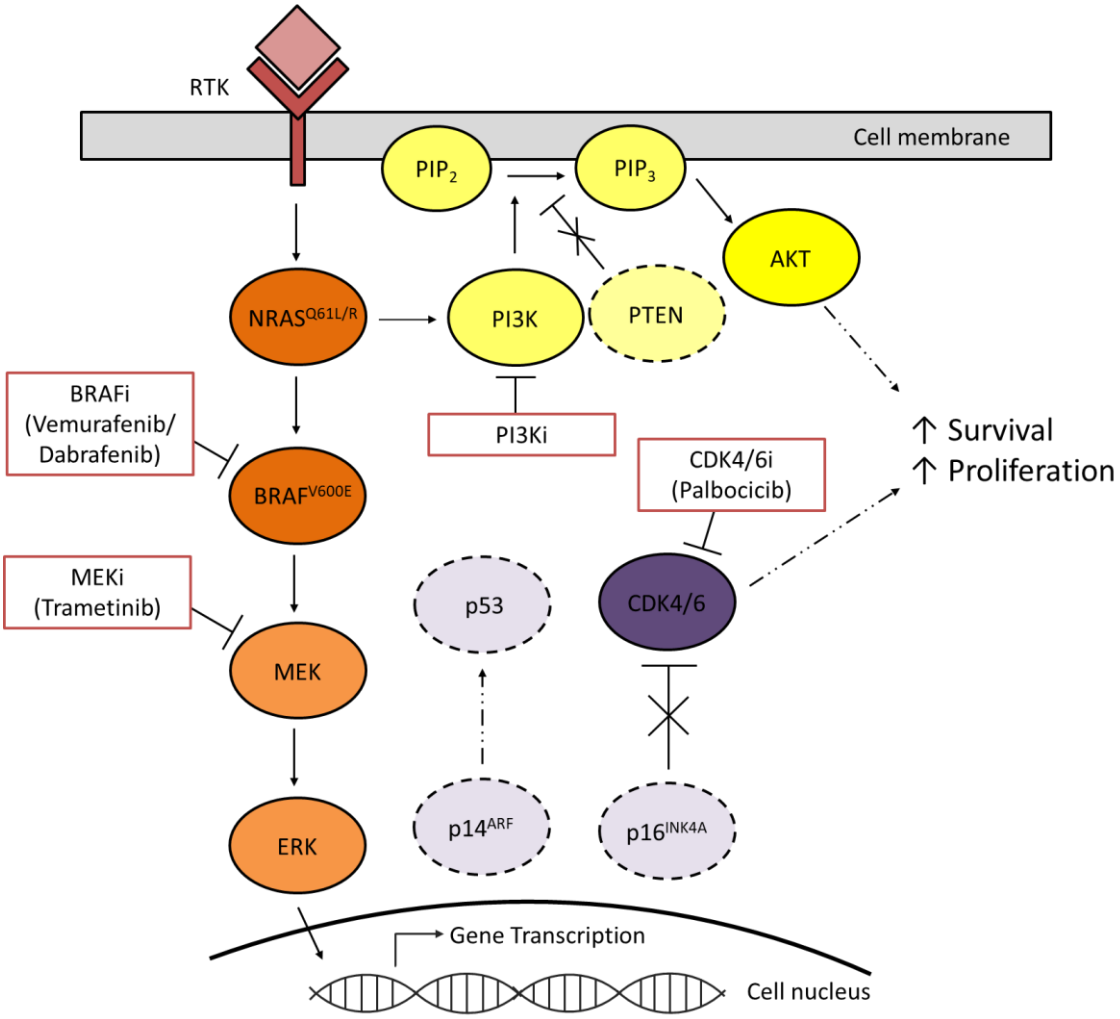

Figure 1.1. Key signalling pathways driving melanoma progression and the different targeted therapies available.

Gain-of-function mutations in the Mitogen Activated Protein Kinase (MAPK; highlighted in orange) signalling pathway, gain- and loss-of-function mutations in the Phosphoinositide 3-kinase (PI3K; highlighted in yellow) signalling pathway, and loss-of-function mutations in cell cycle regulation pathways (highlighted in purple) cooperatively drive the progression of melanoma. Identification of such mutations have led to the development of targeted therapies (highlighted in red boxes). Solid ovals (◯) with darker shades indicate molecules that are over-activated, while dashed ovals (◌) with lighter shades indicate molecules with reduced expression.

1.2.2. *Therapies Targeting Key Signalling Pathways in Melanoma*

The identification of prominent mutations within the pathways described above has allowed for the recent development of targeted therapies for melanoma. These include small molecule kinase inhibitors targeting the signalling flux of the MAPK pathway, in particular the BRAF inhibitors (BRAFi) vemurafenib and dabrafinib, and the MEK inhibitor (MEKi) trametinib (Figure 1.1). While patients receiving these inhibitors generally experience drastic tumour regression, relapse almost inevitably occurs within 6 months as tumours develop resistance. To date, several resistance mechanisms have been reported, including amplification of BRAF copy number (Shi et al. 2012), expression of alternative BRAF splice variants (Poulikakos et al. 2011), or expression of the constitutively active *NRAS*$^{Q61L/R}$ (Nazarian et al. 2010) or MEK mutants (Long et al. 2014). Of note, all of these mechanisms allow for reactivation of the MAPK pathway, thereby highlighting the importance of this pathway in melanoma disease.

Alternative forms of targeted therapy that are currently under development include PI3K inhibitors that target the PI3K pathway, as well as CDK4/CDK6 inhibitors, such as palbocicib, that target the cell cycle pathway (Figure 1.1). Similar to BRAFi and MEKi, preliminary results show that treatment with the single agents eventually result in resistance (Sheppard et al. 2016). However, *in vitro* and mouse studies suggest that using these inhibitors in combination can overcome resistance and achieve sustained tumour cell death and regression (Hoeflich et al. 2012; Sheppard et al. 2016; Villanueva et al. 2010). Clearly, there is much clinical benefit in further refining these combination targeted therapy regimes to allow them to be eventually used in the clinic to achieve maximal efficacy and prolonged tumour regression in patients.

1.3. Melanoma and the Immune System

1.3.1. *General Introduction*

Due to the high prevalence of mutations in melanoma, there is an inevitable increase in the production and display of antigens that are foreign to the immune system on the melanoma cell surface. This makes melanoma a highly immunogenic disease. Hence melanoma is the best understood cancer in terms of its interaction with the immune system. Two of the important immune-related factors that can affect melanoma progression are leukocyte function and leukocyte entry to the tumour microenvironment (reviewed in (Tan et al. 2017)).

The roles of various leukocyte populations in melanoma will be discussed first below, and the recruitment of these subsets to the tumour discussed later in this Chapter. Wherever possible, there will be a focus on evidence gathered from human patient samples and clinical studies, rather than animal studies. As will become evident, the activity and function of leukocytes can be enhanced, dampened or polarised depending on environmental cues. This in turn significantly affects both disease progression and treatment outcome (Figure 1.2).

1.3.2. *Roles of Different Leukocyte Subsets in Melanoma*

$CD8^+$ T cells are well described as the key effector leukocytes in cancer eradication. They mediate their tumour-killing function upon receiving two positive signals - one initiated upon T cell receptor (TCR) recognition of foreign peptides presented on MHC class 1a molecules on antigen presenting cells (APCs), and the other following engagement of co-stimulatory molecules on T cells (e.g. CD28) with their ligands on APCs (e.g. B7) (reviewed in (Chen, L 2004)). Upon recognition of the foreign antigen on the tumour cell surface, the activated $CD8^+$ T cells induce apoptosis in target cells through caspase activation or perforin-mediated mechanisms. The proliferation and function of $CD8^+$ T cells are also highly dependent on the presence of IL-2 (Boyman, Cho & Sprent 2010). Therefore, $CD8^+$ T cell expansion and cytotoxicity can be dampened in the event IL-2 is sequestered, or when a co-inhibitory molecule on the T cell, such as cytotoxic T-lymphocyte-associated antigen 4 (CTLA-4) or programmed death 1 (PD-1) is engaged (reviewed in (Chen, L 2004)). Due to their important role in cancer cell killing, there has been a clear positive correlation between the presence of intratumoural activated $CD8^+$ T cells and good patient prognosis, as well as treatment responsiveness (Ladányi et al. 2004; Piras et al. 2005; van Houdt et al. 2008).

In addition to $CD8^+$ T cells, natural killer (NK) cells also play a role in cancer cell death. NK cell cytotoxicity does not depend on antigen presentation. Instead, NK cell activity is governed by the balance between activating and inhibitory molecule expression on the target cells (reviewed in (Vivier et al. 2011)). An increase in activating NKG2D ligands which indicate cellular stress triggers NK cells to lyse target cells (reviewed in (Vivier et al. 2011)). In addition, downregulation of MHC class Ia molecules, which effectively hides the foreign cells from $CD8^+$ T cell detection, has been reported to increase the susceptibility of the respective cells to NK cell lysis (reviewed in (Vivier et al. 2011)), indicating the presence of highly complementary measures between $CD8^+$ T cells and NK cells to ensure complete eradication of foreign cells. Similar to $CD8^+$ T cells, immunohistochemistry on patient

melanoma tissues has revealed an increase in intratumoural $CD56^+$ NK cells in regressing melanoma tumours, thereby hinting at their role in tumour control (McKay et al. 2011). This is in line with *in vivo* murine experimental data, where NK cells were found to be important in controlling B16 melanoma tumour growth (Ballas et al. 2013). More specifically, the adoptive transfer of NK cells into NK cell-deficient mice prior to the intravenous injection of B16 melanoma cells resulted in the inhibition of pulmonary and liver B16 metastasis (Ballas et al. 2013).

Due to the ability of B cells to participate in antigen presentation (Crawford et al. 2006), the presence of B cells has been found to affect $CD8^+$ T cell infiltration and function *in vivo*. B cell depletion in mice harbouring B16 melanoma tumours impaired the expansion of tumour antigen specific $CD8^+$ T cells, resulting in enhanced tumour growth (DiLillo, Yanaba & Tedder 2010). Furthermore, mice receiving adoptive B cell transfer exhibited increased infiltration of $CD8^+$ T cells with interferon gamma (IFNγ) and tumour necrosis factor alpha (TNFα) production, which in turn impaired B16-F10 melanoma tumour growth (Kobayashi, T et al. 2014). In line with that, increased B cell infiltration in both primary (Garg et al. 2016) and metastatic melanoma (Erdag et al. 2012) has been associated with better patient survival.

Monocytes, which circulate in the blood, or their tissue-residing counterparts macrophages, as well as neutrophils and helper T (Th) cells, all exhibit dual roles in mediating the immune response as they can be polarised to be either pro-inflammatory or anti-inflammatory depending on cytokines and other factors in the surrounding microenvironment. When there is a prevalence of pro-inflammatory cytokines, these cells are induced to form type 1 cells which assist in amplifying the inflammatory response. Conversely, when there is an enrichment of anti-inflammatory cytokines, these cells are polarised to form type 2 cells which assist in dampening the immune response. The differing roles of type 1 and type 2 immune cells will be discussed in more detail below.

Th1 cells are formed following exposure to IL-12 and in turn they exert various pro-inflammatory effects (reviewed in (Murphy, KM & Reiner 2002)). These cells secrete IL-2 which stimulates $CD8^+$ T cell proliferation, IFNγ and TNFα which can initiate caspase-dependent apoptosis in foreign cells, as well as IL-12 which sustains Th1 polarisation within the environment (reviewed in (Murphy, KM & Reiner 2002)). The IFNγ secreted by Th1 cells also polarises macrophages into a pro-inflammatory M1 phenotype (Stein et al. 1992). In addition, Th1 cells can enhance the uptake and presentation of foreign tumour antigens by

APCs, thereby augmenting the $CD8^+$ T cell cytolytic response (reviewed in (Murphy, KM & Reiner 2002)). Th2 cells on the other hand are formed following exposure to IL-4 (reviewed in (Murphy, KM & Reiner 2002)). These cells in turn secrete cytokines such as IL-4, IL-5, IL-10 and IL-13 and act to dampen the immune response by decreasing pro-inflammatory cytokine production, sustaining the polarisation of both Th cells and macrophages into an anti-inflammatory type 2 phenotype and inhibiting cytotoxic T cell functions (reviewed in (Murphy, KM & Reiner 2002)). Hence, Th1 cells are pro-inflammatory mediators whereas Th2 cells are anti-inflammatory mediators. While there is no clear correlation of Th1 or Th2 cells with patient prognosis, the importance of $CD4^+$ T cells is clearly demonstrated in animal studies, as $CD8^+$ T cell activity in B16 mice lacking $CD4^+$ T cells was impaired partly due to the lack of IL-2 (Antony et al. 2005).

Tumour associated macrophages (TAM) can be polarised upon IFNγ stimulation into an M1 phenotype which exhibits anti-tumorigenic properties. These cells are able to mediate tumour cell lysis via the production of reactive nitrogen and oxygen species as well as caspase-activating TNFα (reviewed in (Biswas & Mantovani 2010)). They also secrete IL-12 which can polarise local Th cells to an anti-tumourigenic Th1 phenotype and activate NK cells (reviewed in (Biswas & Mantovani 2010)). In addition, M1 macrophages exhibit an upregulation in MHC molecules, resulting in an enhanced capacity to present antigens to T cells (reviewed in (Biswas & Mantovani 2010)). Alternatively, TAM can be polarised into an M2 phenotype upon IL-4 stimulation, which exhibit pro-tumorigenic activities (reviewed in (Biswas & Mantovani 2010)). These cells are characterised by their secretion of the anti-inflammatory factors IL-1RA, IL-1 decoy receptor and IL-10 which act to either decrease the production or dampen the effects of pro-inflammatory cytokines and chemokines (reviewed in (Biswas & Mantovani 2010)). They also secrete the chemokines CCL17, CCL22 and CCL24 which leads to the recruitment of Th2 cells and regulatory T cells (reviewed in (Biswas & Mantovani 2010)), and arginase which can assist in supporting tumour growth (Sinha et al. 2007). In comparison with M1 macrophages, M2 macrophages were found to have a poorer capability in presenting antigens (reviewed in (Biswas & Mantovani 2010)). Immunohistochemistry on primary melanoma biopsies revealed an increase in TAM infiltration with melanoma progression (Torisu et al. 2000), which also correlated with increased melanoma invasiveness and metastasis (Varney, Michelle L, Johansson & Singh 2005).

Tumour associated neutrophils (TAN) can also be polarised into an anti-tumorigenic N1 phenotype following IFNβ stimulation. Upon activation, N1 neutrophils release a series of cytotoxic factors such as reactive oxygen species (ROS) and TNFα which can lead to tumour cell lysis. In addition, they are also able to activate $CD8^+$ T cells to exert cytolytic effects (Fridlender et al. 2009; Piccard, Muschel & Opdenakker 2012). On the other hand, pro-tumourigenic N2 neutrophils secrete vascular endothelial growth factor (VEGF), matrix metalloproteinase 9 (MMP9), as well as the chemokines CCL2 and CCL5, which as will be discussed in section 1.4.2.3 below are important in recruiting monocytes (Fridlender et al. 2009; Piccard, Muschel & Opdenakker 2012). There is increasing evidence in both human and murine studies that neutrophils inside the tumour are predominantly of an N2 pro-tumorigenic phenotype, especially in advanced tumours (Mishalian et al. 2013; Schaider et al. 2003). In a murine melanoma model, it was observed that TAN were more cytotoxic towards primary but not metastatic tumours (Schaider et al. 2003). This was further explained in murine Lewis lung carcinoma and mesothelioma models, where TAN gradually shifted from an N1 phenotype to an N2 phenotype with disease progression (Mishalian et al. 2013). Immunohistochemistry studies on primary melanoma tissues from patients revealed that the presence of intratumoural neutrophils significantly correlated with poor survival (Jensen, TO et al. 2012).

Regulatory T cells (Tregs) are a population of immunosuppressive cells which make up approximately 5-10% of the $CD4^+$ T cell repertoire and can be identified through their co-expression of CD25 and FoxP3. They contribute to immune tolerance through CTLA-4 engagement, IL-2 adsorption and granzyme-mediated apoptosis to suppress $CD8^+$ T cells, as well as IL-10 and transforming growth factor beta (TGFβ) secretion to confine NK cells to an anergic state (Fridman et al. 2012). In addition to that, Tregs can also stimulate FoxP3 expression in naïve T cells to convert them into Tregs (Chen, W et al. 2003). Immunohistochemistry analysis on patient primary melanoma samples revealed a significant increase in Tregs with recurrence (Miracco et al. 2007), and increased intratumoural Treg frequencies were associated with a reduction in melanoma patient survival (Brody et al. 2009).

Myeloid derived suppressor cells (MDSC) are a heterogeneous population of immature myeloid progenitors that can be further subdivided into monocytic-MDSC (M-MDSC) and granulocytic MDSC (G-MDSC). MDSC exert immunosuppressive roles in the tumour via the inhibition of $CD8^+$ T cell and NK cell function, induction of apoptosis in Th1 cells through

NO production, as well as the induction of Tregs through IL-10 and TGFβ secretion (Huang, B et al. 2006). Furthermore, M-MDSC are involved in shaping the premetastatic niche in lungs to encourage melanoma metastasis in mice (Shi et al. 2017). Increased M-MDSC and G-MDSC frequencies were observed in advanced melanoma patients (Schilling et al. 2013), and increased MDSC frequency was associated with poor patient survival (Jordan et al. 2013).

Taken together, there are many different subsets of leukocytes which can play different roles in regulating melanoma progression. Given the abilities of these immune cells to regulate the function of one another, the composition and ratio of the different subsets in the tumour are key in dictating both natural disease progression and treatment outcome (Figure 1.2).

1.3.3. *Immunotherapy*

Having understood how interactions between the immune system and melanoma can affect disease progression, there has been a focus on the development of cancer immunotherapy, which involves the utilisation of the host immune response to target cancerous cells. While there have been many forms of immunotherapy in development, including vaccinations, this introduction will focus on the ones that have demonstrated greatest clinical success. These often focus on reactivating $CD8^+$ T cell cytotoxic activity.

As mentioned above, $CD8^+$ T cell activation requires both a signal from TCR recognition of foreign antigen as well as a signal following co-stimulatory molecule engagement. On the other hand, the engagement of co-inhibitory molecules such as CTLA-4 and PD-1 results in $CD8^+$ T cell suppression. Studies performed on human melanoma samples revealed an upregulation in PD-1 ligand 1 (PDL-1) expression with disease progression (Hino et al. 2010; Taube et al. 2014), thereby highlighting the prevalence of this mechanism in mediating intratumoural $CD8^+$ T cell suppression. The understanding of these signalling processes has led to the development of antibodies targeting these co-inhibitory molecules to alleviate $CD8^+$ T cell suppression. This includes both inhibitors to the CTLA-4 checkpoint molecule (ipilimumab) and inhibitors to the PD-1 checkpoint molecule (nivolumab and pembrolizumab). CTLA-4 blockade with ipilimumab has been found to increase the diversity of the T cell pool (Robert et al. 2014) and enhance the stability of various T cell clones (Cha et al. 2014), while PD-1 blockade reinvigorates the cytotoxic function of intratumoural $CD8^+$ T cells (reviewed in (Topalian, Drake & Pardoll 2015)). Apart from effects on $CD8^+$ T cells, ipilimumab also affects other leukocyte subsets within the tumour. Advanced melanoma

patients receiving ipilimumab have decreased levels of M-MDSCs and Tregs in their blood (Bjoern et al. 2016; de Coana et al. 2017). A reduction of MDSCs and Tregs was also observed within B16 melanoma tumours following the treatment of mice with anti-CTLA-4 and anti-PD-1 combination therapy (Curran et al. 2010). Currently, the clinical tumour response rates for these inhibitors when used as monotherapy are ~20% and ~40% respectively. Now, emerging data from ongoing clinical trials indicates even higher response rates of approximately 60% from the combinations of ipilimumab and nivolumab (Larkin et al. 2015) or ipilimumab and pembrolizumab (Long et al. 2016). Strikingly, many patients who respond to this form of immunotherapy exhibit deep and durable remissions of disease, which has changed a diagnosis of metastatic melanoma from a virtual death sentence to the prospect of cure.

An experimental kind of immunotherapy called adoptive cell transfer (ACT) (reviewed in (Rosenberg, Steven A. & Restifo 2015)) may also have a role in the treatment of metastatic melanoma, especially where other approaches have failed or for melanoma subtypes such as uveal melanoma, which seem to be less responsive to immune checkpoint blockade. ACT with $CD8^+$ T cells involves the reinfusion of autologous and *ex vivo* expanded tumour-specific $CD8^+$ T cells into the body, often following lymphodepleting chemotherapy or radiotherapy. In non-intent to treat analyses, tumour response rates of up to 72%, with 20% of the patients experiencing durable complete regressions, have been reported (Rosenberg, Steven A et al. 2011). Patients responding to ACT were responsive regardless of previous treatments (Rosenberg, Steven A et al. 2011), highlighting the value of continuing to investigate and improve this treatment approach. Alternatively, the autologous $CD8^+$ T cells can be genetically engineered to express either tumour antigen specific T cell receptors (via TCR gene transfer) or chimeric antigen receptors (CAR T cells) before ACT (reviewed in (Rosenberg, Steven A. & Restifo 2015)). Although CAR T cells have demonstrated striking success in CD19-expressing haematological malignancies with objective response rates of up to 90% (reviewed in (Rosenberg, Steven A. & Restifo 2015)), the effectiveness of this approach in melanoma and other solid tumours remains under investigation. For melanoma in particular, GD2-sepcific CAR T cells are currently in phase 1 clinical trial for metastatic melanoma patients (Gargett et al. 2016).

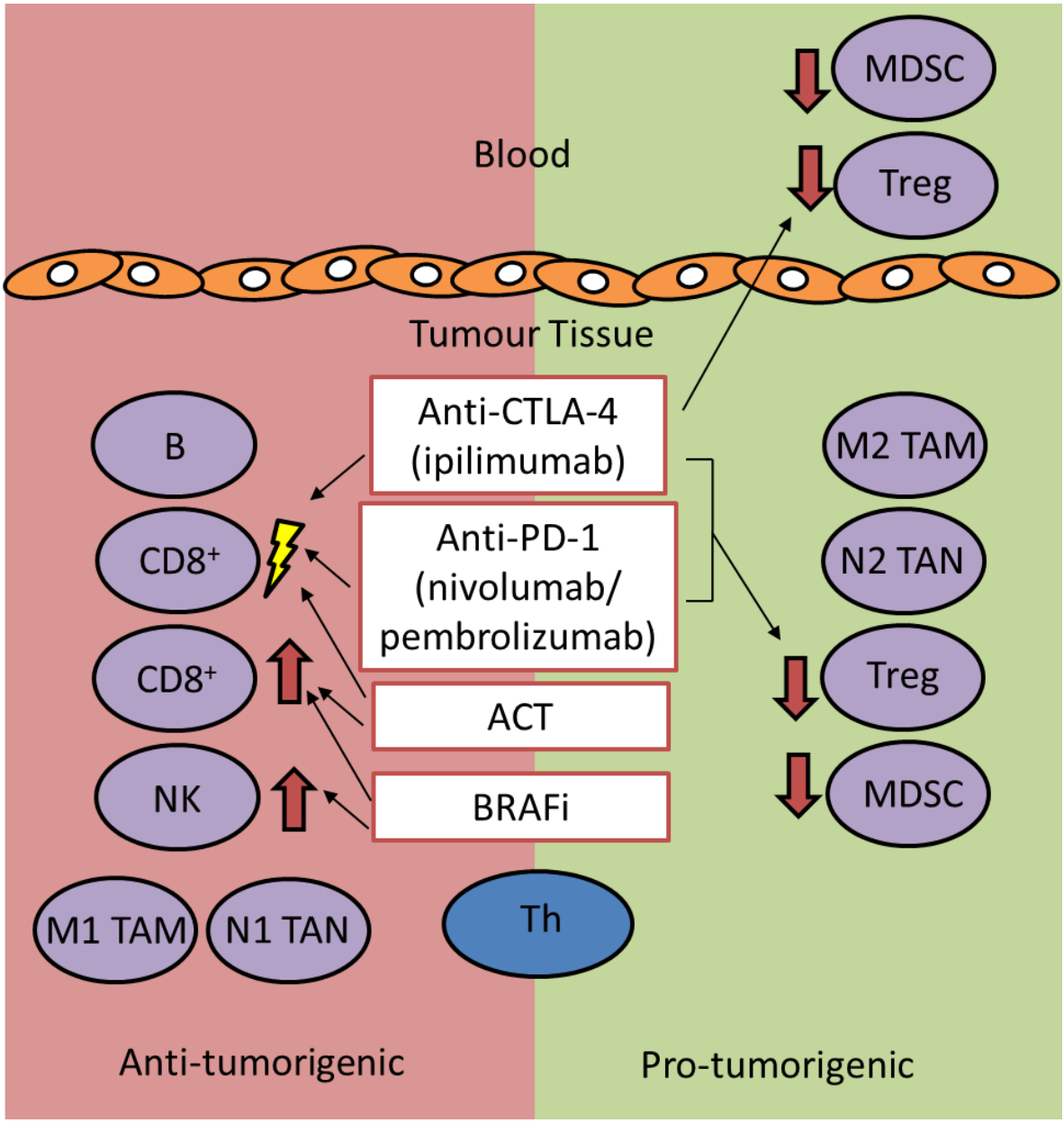

Figure 1.2. Roles of different leukocyte subsets in regulating melanoma disease and the effect of various treatment approaches on leukocyte numbers and function.

The abundance of various leukocyte subsets within both the blood and tumour tissue have been documented to affect melanoma disease. This can in turn be affected by various treatment approaches, where immunotherapy (including checkpoint blockade and adoptive cell transfer (ACT)) as well as targeted therapy can lead to both enhanced (⇧) infiltration and cytotoxic activities (⚡) of certain subsets of anti-tumourigenic leukocytes, as well as decreased (⇩) numbers of pro-tumourigenic leukocytes within the blood and tumour tissue.

1.3.4. *"Immunotherapy" with other Treatment Approaches*

Interestingly, in addition to their direct tumoricidal activity, the BRAF inhibitors vemurafenib and dabrafenib have also been found to promote changes in leukocyte recruitment. Immunohistochemical analysis on metastatic melanoma patient tissue collected before and after vemurafenib treatment revealed an increase in $CD8^+$ T cell infiltration following vemurafenib treatment (Wilmott et al. 2012). In addition, it has also been demonstrated in the B16 mouse melanoma model that BRAFi treatment enhanced NK cell function and frequency, thereby reducing pulmonary metastases (Ferrari de Andrade et al. 2014), and the development of BRAFi resistance was associated with restored levels of MDSC (Steinberg et al. 2017). This highlights the importance of the immune system too in other treatment approaches.

1.4. Melanoma and Blood Vessels

1.4.1. *Introduction*

Melanoma tumours are highly vascularised. Blood vessels serve two major functions within the tumour. Firstly, they act to channel nutrients and oxygen into the tumour. This is to meet the increasing metabolic demands of a tumour as it accumulates mutations that jointly allow for uncontrolled proliferation and apoptosis resistance, and gradually grows in size. In fact, it has been documented that tumours cannot grow past ~$1mm^3$ without an expansion of the pre-existing vasculature (Gimbrone et al. 1972). Secondly, blood vessels serve as a route for leukocyte entry into the tumour. While circulating leukocytes can serve as a useful marker predicting disease progression and responsiveness to treatment, leukocytes need to be physically present within the tumour to exert their function. It is the leukocyte recruitment process, a multistep interaction between the leukocytes and blood vessels, that shapes the leukocyte composition of the tumour (reviewed in (Tan et al. 2017)). The next section first discusses the formation of conventional endothelial cell-lined blood vessels and their roles in leukocyte recruitment, and then expands to discuss an alternative from of vessel formation, vasculogenic mimicry, which is the main focus of this thesis.

1.4.2. ***Conventional Endothelial Cell Lined Blood Vessels***

1.4.2.1. Angiogenesis

Angiogenesis refers to the sprouting and expansion of blood vessels from pre-existing ones. It is a process that is dependent on endothelial cells (ECs), the specialised cells that form the inner lining of all blood vessels in the body. A drop in local oxygen levels activates hypoxia inducible factor (HIF1α) in ECs which in turn stimulates the production of angiogenic factors such as VEGF-A as well as expression of the cognate receptor (VEGFR2) on ECs (Tang, N et al. 2004). The formation of a defined angiogenic gradient then stimulates a phenotypic change in ECs to form tip ECs (Ruhrberg et al. 2002), the cells which lead the angiogenic sprout. Tip ECs first release MMP to degrade the extracellular matrix and then undergo cytoskeletal changes and migrate towards the avascular areas in need of vessel formation (Ruhrberg et al. 2002). During this process, the ECs adjacent to the tip ECs, known as stalk ECs, proliferate to form new blood vessel linings. Delta-like ligand 4 (DLL4) on tip ECs and notch on stalk ECs signalling then comes into play as a negative feedback loop to stop EC proliferation, promote pericyte recruitment, and inhibit MMP production to restore EC phenotype and allow for vessel stabilisation and maturation (Hellström et al. 2007). Blood flow to the newly vascularised area restores the local oxygen levels, reduces VEGF production and stops angiogenesis.

While angiogenesis is tightly regulated under normal physiological conditions, it is highly dysregulated in tumours. Instead of a defined VEGF gradient, VEGF appears to be upregulated throughout the tumour for various reasons (Richard et al. 1999; Tang, N et al. 2004). Apart from VEGF production due to the increased oxygen demand (Tang, N et al. 2004), cancer cells appear to produce enhanced levels of VEGF as a result of mutations within the MAPK pathway that can increase HIF1α activity (Richard et al. 1999). As a result, ECs sprout in all directions and lack a negative feedback loop, leading to the formation of a poorly organised vascular network which is leaky and tortuous, lacks hierarchy and fails to resolve the hypoxic conditions (Konerding et al. 1992).

1.4.2.1.1. Cadherins in Angiogenesis

The cadherins are a large family of transmembrane calcium dependent adhesion molecules. The extracellular domain binds either homotypically or heterotypically to cadherins on

adjacent cells, while the intracellular domain binds to intermediate catenin molecules, which are then anchored to the cytoskeleton (reviewed in (Cavallaro, Liebner & Dejana 2006)).

A major cadherin that is involved in angiogenesis is vascular endothelial cadherin (VE-cadherin). Specifically expressed on ECs, VE-cadherin undergoes direct homotypic interactions to form EC cell-cell junctions, which are required for blood vessel maturation and function (Navarro, Ruco & Dejana 1998). Blocking of VE-cadherin function led to the destabilisation and disassembly of blood vessels within mice allantois, a structure enriched with blood vessels required for gas and waste exchange for the developing embryo (Crosby et al. 2005). In addition, VE-cadherin can also associate with VEGFR to regulate VEGF signalling. This in turn affects EC proliferation and survival, which can profoundly impact angiogenesis (Lampugnani et al. 2003).

Another cadherin that is found to play a role in angiogenesis is neural cadherin (N-cadherin). Initially identified on neuronal cells, N-cadherin has later been found to also be expressed on ECs (Crosby et al. 2005). Unlike VE-cadherin which mediates contact between ECs, N-cadherin is involved in mediating adhesion between ECs and pericytes, which is essential for vessel maturation (Navarro, Ruco & Dejana 1998). Reduction of N-cadherin expression using siRNA resulted in reduced pericyte coverage of EC-lined vessels, which affected their maturation (Paik et al. 2004).

Interestingly, the desmosomal cadherin desmoglein 2 (DSG2) has also been recently reported to regulate angiogenesis. Largely expressed on epithelial tissues, the canonical role of DSG2 is in the formation of desmosomes, which are unique intercellular adhesion structures required for tissues such as skin and heart to withstand mechanical stress (reviewed in (Delva, Tucker & Kowalczyk 2009)). DSG2 forms desmosomes through both homotypic and heterotypic interactions with another group of desmosomal cadherins, the desmocollins. In addition to this canonical function in desmosomes, our group recently reported that DSG2 is expressed on human progenitor cells with angiogenic properties, as well as on specific subsets of ECs (Ebert et al. 2016), the latter observation also being reported by others (Giusti et al. 2013). Blood vessels in mice expressing reduced levels of *Dsg2* have increased leakiness and abnormal morphology (Ebert et al. 2016). Furthermore, siRNA-mediated DSG2 downregulation in human microvascular ECs resulted in impaired actin stress fibre formation, a phenotype that resembles microvascular ECs in systemic sclerosis (Giusti et al. 2013).

Taken together, these studies highlight the importance of cadherins in mediating EC function and blood vessel formation, and reveal DSG2 as a novel player in these processes.

1.4.2.2. The Role of Endothelial Adhesion Molecules in Regulating Leukocyte Recruitment to Melanoma

The endothelium acts as a barrier between leukocytes in the bloodstream and the tumour microenvironment. In order for leukocytes to infiltrate into the tumour, they have to roll along the endothelium (via the engagement of selectins and their ligands), firmly adhere to the ECs (through integrin interactions) and subsequently transmigrate across the endothelium into the underlying tissue to elicit their functions (reviewed in (Vestweber 2015)). Leukocytes can only undergo this series of events if they express an appropriate combination of adhesion molecules which are cognate to those expressed by ECs. Accordingly, adhesion molecule expression is tightly regulated on both leukocytes and ECs, and provides the endothelium with a mechanism to selectively recruit leukocyte subsets appropriate for the immune response required.

The key EC adhesion molecules that regulate leukocyte recruitment include the selectins (P-selectin, E-selectin) for leukocyte rolling, integrin ligands such as intercellular adhesion molecule 1 (ICAM-1), ICAM-2, vascular cell adhesion molecule 1 (VCAM-1) and mucosal vascular addressin cell adhesion molecule 1 (MAdCAM-1) for leukocyte adhesion, as well as junctional adhesion molecules (JAM) and platelet/endothelial cell adhesion molecule-1 (PECAM-1) for leukocyte transmigration (reviewed in (Vestweber 2015)) (Figure 1.3).

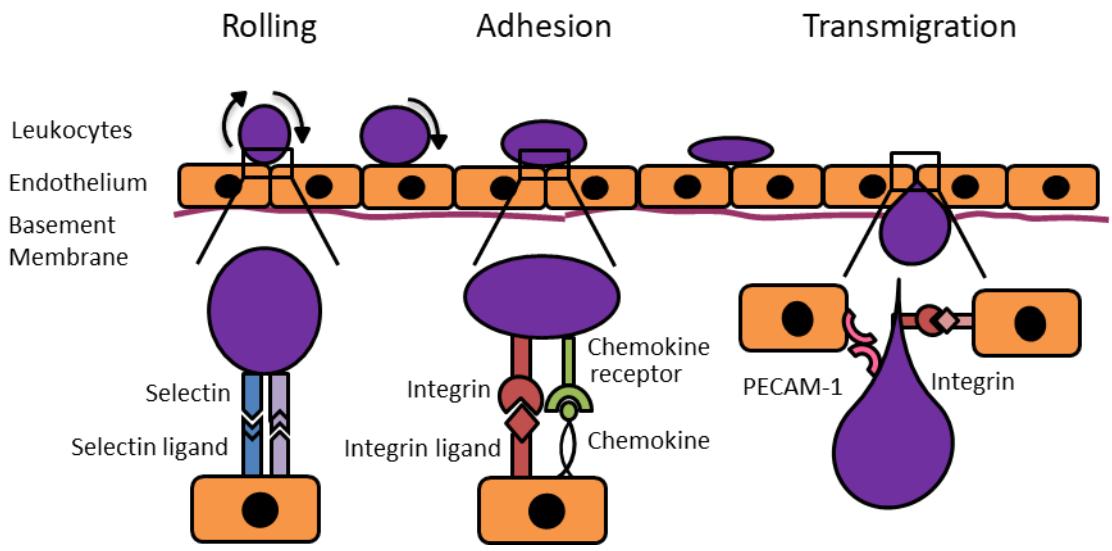

Figure 1.3. The leukocyte recruitment cascade, and the adhesion molecules/ligands which are relevant for each step. Figure adapted from (Tan et al. 2017).

The leukocyte recruitment cascade is a multistep process, with each step mediated by interactions between adhesion molecules/chemokines on the endothelium and their respective counter ligands on the leukocytes.

While the expression levels of these adhesion molecules can be constantly regulated based on environmental stimuli on normal endothelium, tumour ECs are found to be non-responsive ("anergic") to the pro-inflammatory signals that would normally upregulate adhesion molecule expression. Tumour ECs are rendered anergic following chronic stimulation with multiple factors. These include the angiogenic factors VEGF and basic fibroblast growth factor (bFGF), TGFβ, adenosine, as well as nitric oxide (NO). *In vitro*, prolonged VEGF and bFGF exposure modified ECs epigenetically (Hellebrekers et al. 2006), resulting in suppressed adhesion molecule expression, even following pro-inflammatory cytokine TNFα stimulation (Dirkx, AE et al. 2003). Similarly, *in vitro* treatment of IL-1α- or TNFα-activated ECs with TGFβ, adenosine or NO, respectively, was found to differentially downregulate P-selectin, E-selectin, ICAM-1 and VCAM-1 expression (Carlos 2001; Wang, L et al. 2011). Some of these factors are often reported to be upregulated in melanoma with increased disease progression (Mehnert et al. 2010; Van Belle et al. 1996). Furthermore, B16 melanoma vessels are found to express CD73, the enzyme that produces adenosine (Wang, L et al. 2011), as well as endothelin B receptor (ET_BR) and its ligand endothelin-1 (ET-1) which acts through NO (Buckanovich et al. 2008). Together, these observations provide a potential mechanism to explain the low level of adhesion molecule expression observed on ECs in melanoma.

As a result of EC anergy, the endothelium within a melanoma tumour has a distinctly different adhesion molecule expression profile compared to the endothelium of normal, healthy tissue. Immunohistochemical studies of samples from melanoma patients have revealed that intratumoural vessels of primary tumours have reduced P-selectin expression (Nooijen et al. 1998) and VCAM-1 expression (Piali et al. 1995) when compared to non-tumoural blood vessels in adjacent tissues. Furthermore, intratumoural vessels of metastatic melanoma patients also exhibit decreased P-selectin, E-selectin, ICAM-1 and VCAM-1 expression, although these are expressed strongly on non-tumoural blood vessels in adjacent tissue (Nooijen et al. 1998; Piali et al. 1995; Weishaupt et al. 2007). This is also consistently observed in B16 murine melanoma models. Lineage tracing performed on the endothelium of tamoxifen-pulsed VE-cadherin-CreERT2 Rainbow mice engrafted with a B16 melanoma revealed the downregulation of gene expression levels of selectin, ICAM-1, VCAM-1 and MAdCAM-1 in melanoma endothelium compared to normal endothelium with disease progression (Corey, Rinkevich & Weissman 2016).

This altered adhesion molecule profile may translate into changes in leukocyte infiltration. In tumours of metastatic melanoma patients, $CD8^+$ T cells preferentially localised at the tumour periphery where there was high P-selectin, E-selectin and ICAM-1 expression and not at areas within the tumour lacking expression of these adhesion molecules (Weishaupt et al. 2007). Similarly, NK cells are found to be localised within the peritumoral regions in human primary melanomas (Fregni et al. 2013; McKay et al. 2011). The importance of adhesion molecules in T cell and NK cell infiltration of melanoma tumours has also been demonstrated in the B16 murine melanoma model. Mice lacking expression of selectins and/or ICAM-1 had significant reductions in $CD8^+$ T cell, $CD4^+$ T cell and NK cell infiltration of both primary subcutaneous and pulmonary metastasis B16 melanoma, which was associated with enhanced tumour growth and metastasis (Yamada et al. 2006; Yamaoka et al. 2011). Furthermore, an increased expression of adhesion molecules in B16 melanoma tumours was associated with increased T cell infiltration and tumour regression, and relapsed tumours exhibited loss of adhesion molecule expression which correlated with decreased T cell infiltration (Straetemans et al. 2015). In addition, the tumour endothelium specifically expresses Fas ligand (FasL) that can directly kill activated $CD8^+$ T cells, thereby resulting in decreased $CD8^+$ T cell frequencies (Motz et al. 2014).

Interestingly, while monocytes, neutrophils and Tregs are also typically recruited via adhesion molecules such as P-selectin, E-selectin, ICAM-1 and VCAM-1, the downregulation of these EC adhesion molecules in tumours does not appear to correlate with decreased monocyte or neutrophil infiltration. In fact, macrophages were found to constitute the main leukocyte population within melanoma (Hillen, Femke et al. 2008). There were also increased Tregs intratumourally compared to peritumorally (Ahmadzadeh et al. 2008). This suggests that there are additional adhesion molecules involved in recruiting these leukocytes to tumours. However, there is relatively little known about the specific adhesion molecules involved in selectively recruiting monocytes, neutrophils and Tregs into tumours. A potential candidate is the peripheral node addressin (PNAd), an L-selectin ligand normally only expressed in secondary lymphoid tissues but found to be aberrantly expressed on the endothelium in 11 of 18 melanoma primary tumours (Martinet et al. 2011), which can interact with monocytes, neutrophils and Tregs expressing L-selectin. Alternatively, CD44 which can bind homotypically to CD44 expressed on the aforementioned leukocyte subsets, has been found to be elevated on tumour endothelium (Griffioen, Arjan W. et al. 1997). Nonetheless, there is a lack of convincing evidence that these molecules are directly involved in monocyte,

neutrophil and Treg recruitment in melanoma, thereby highlighting the need for further investigation.

1.4.2.3. The Role of Chemokines in Regulating Leukocyte Recruitment to Melanoma

In addition to EC expressed adhesion molecules, chemokines are also critically required for immune cell recruitment. Chemokines, which are anchored in the glycocalix of the endothelium and are displayed to rolling leukocytes, trigger integrin-mediated firm adhesion, while chemokine gradients generated in the underlying tissue guide the transmigrated leukocytes to the site in need of leukocyte function. These chemokines can be produced by melanoma cells, stromal cells such as fibroblasts, as well as the recruited leukocytes.

Of the many chemokines that $CD8^+$ T cells can respond to, those that signal through the CCR5 and CXCR3 axes are suggested to be the most important in recruiting $CD8^+$ T cells into melanoma. These include the CCR5 ligands, CCL3, CCL4 and CCL5; and the CXCR3 ligands, CXCL9, CXCL10 and CXCL11 (González-Martín et al. 2011; Mikucki et al. 2015). Although CCR5 expression is crucial for both the recruitment and effector functions of $CD8^+$ T cells in solid tumours (González-Martín et al. 2011), there is also a non-redundant role for CXCR3 in controlling $CD8^+$ T cell trafficking to human and murine melanoma, not achievable by CCR5 (Mikucki et al. 2015). Similar to $CD8^+$ T cells, NK cells are also found to be recruited to B16 tumours through both the CCR5 (Liu, C et al. 2008) and CXCR3 axes (Wendel et al. 2008; Wennerberg et al. 2015). Therefore, a critical reduction in the signalling ligands for CXCR3 would lead to reduction in both $CD8^+$ T cell and NK cell infiltration.

In mice, a key chemokine for mediating monocyte recruitment to melanoma is CCL2, which signals through the receptor CCR2. CCL2 overexpression in primary murine melanoma led to monocyte infiltration (Nesbit et al. 2001), and CCL2 blockade in a human melanoma xenograft model led to a reduction in macrophage infiltration (Gazzaniga et al. 2007). Although $CD8^+$ T cells also express the receptors for CCL2, post-translational modification of CCL2 such as nitration by reactive nitrogen species in the tumour is found to inhibit $CD8^+$ T cell recruitment via this axis (Molon et al. 2011). Therefore, the enhanced expression of CCL2 in melanoma is likely to result in enhanced monocyte recruitment.

The key chemokines involved in TAN recruitment to murine melanoma signal via the CXCR1 and CXCR2 axes, including CXCL1, CXCL2, CXCL6 and CXCL8. B16-F10

murine melanoma was found to express high levels of CXCL1 and CXCL2, therefore leading to recruitment of TAN to the tumour (Jablonska et al. 2014). Human melanoma xenografts overexpressing murine CXCL6 in mice exhibited increased TAN influx and enhanced tumour growth (Van Coillie et al. 2001). Similarly, CXCL8 overexpression in a human melanoma xenograft model led to increased neutrophil recruitment (Schaider et al. 2003). It has been reported that the expression of CXCL8 is enhanced in melanoma with disease progression (Varney, Michelle L., Johansson & Singh 2006), and therefore this is likely to result in enhanced neutrophil recruitment.

Similar to monocytes, MDSCs have been shown to be recruited to murine melanoma tumours through CCL2-CCR2 signalling (Lesokhin et al. 2012). In addition, the CCR5 signalling axis is also involved in MDSC recruitment, as the blocking of CCL3, CCL4 and CCL5 resulted in reduced MDSC accumulation in murine melanoma lesions (Blattner et al. 2018). While CXCL12 (signalling through the CXCR4 receptor) has also been demonstrated to recruit MDSC in ovarian cancer (Obermajer et al. 2011), its role in melanoma remains to be elucidated.

The key chemokines involved in Treg recruitment to murine melanoma are CCL5 and CCL22. In a B16 melanoma model, enhanced CCL5 increased the levels of intratumoural Treg (Schlecker et al. 2012). Alternatively, vaccination resulting in increased CCL22 expression in mouse skin was found to divert Treg from the lungs and thereby inhibit pulmonary melanoma growth (Klarquist et al. 2016). The CCR10-CCL28, CXCR3-CXCL9/10/11 and CCL20-CCR6 axes have also been found to be involved in Treg recruitment in other cancer models (Chen, KJ et al. 2011; Liu, J et al. 2011; Nishikawa & Sakaguchi 2014), although their role in melanoma remains to be elucidated.

Unfortunately, unlike the aforementioned leukocyte subsets, there is little information on the chemokines important in recruiting B cells into melanoma tumours. B cells however have been shown to express CXCR4, CXCR5, CCR5 and CCR6 (Durig, Schmucker & Duhrsen 2001), thereby suggesting their ability to respond to the corresponding chemokines, although this remains to be confirmed experimentally.

Changes in chemokine expression over time as melanoma progresses have been demonstrated in human melanoma cell lines, human melanoma tissue and mouse studies. The CXCR3 signalling ligands CXCL9, CXCL10 and CXCL11 are often downregulated with disease progression in melanoma. For example, lineage tracing performed on the endothelium of

tamoxifen-pulsed VE-cadherin-CreERT2 Rainbow mice engrafted with a B16 melanoma revealed a downregulation of CXCL9 and CXCL10 gene expression in melanoma endothelium with increased tumour progression (Corey, Rinkevich & Weissman 2016). Furthermore, CXCL9 and CXCL10 expression was found to be reduced with metastasis in a lung metastatic melanoma model, in which CXCL9 and CXCL10 expression were both inhibited by adenosine (Clancy-Thompson et al. 2015).

On the other hand, the expression of the CCR2 ligand, CCL2, is enhanced in melanoma tissues compared to non-melanocytic lesions, and is further upregulated in BRAFi resistant tumours in a small cohort of melanoma patients (Vergani et al. 2016). Similarly, CCL5 expression is detected in melanoma cell lines but not on normal cultured melanocytes (Mattei et al. 1994; Mrowietz et al. 1999). The majority of patient melanoma tumours have also been reported to express significant levels of CXCL8, of which its expression is tightly associated with melanoma progression in patients (Varney, Michelle L., Johansson & Singh 2006), as well as CXCL12 (Harlin, H. et al. 2009).

Taken together, the melanoma tumour microenvironment appears to be depleted of chemokines that recruit $CD8^+$ T cells and NK cells, such as CXCL9, CXCL10 and CXCL11, and yet enriched with chemokines that recruit monocytes, neutrophils, MDSCs and Tregs such as CCL2, CCL5 and CXCL8. This is likely a major factor in the creation of a tumour microenvironment that supports tumour growth and inhibits anti-tumour immunity.

1.4.2.4. Improving Immunotherapy with Endothelium-modifying Approaches

The importance of the endothelium and its associated adhesion molecules and chemokines in disease control is suggested by correlation with disease outcome. Indeed, as we revisit the successful cases where responsiveness to various treatments was observed, these are often associated with increased expression of adhesion molecules and chemokines which allow for better homing of $CD8^+$ T cells to the tumour. This applies to multiple treatment approaches, including BRAFi and immunotherapy. BRAFi therapy has been found to suppress melanoma VEGF production, leading to the enhancement of $CD8^+$ T cell infiltration (Liu, C et al. 2013). Increased expression of CCL4, CCL5, CXCL9, CXCL10 and CXCL11 correlated with increased likelihood to respond to ipilimumab (Ji et al. 2012), while pre-treatment overexpression of CCL5, CXCL9, CXCL10 and CXCL11 in melanoma patients predicted responsiveness to adoptive cell therapy and IL-2 (Bedognetti et al. 2013).

Interestingly, low dose radiation, chemotherapy and anti-angiogenic therapy, all treatments which have had very limited clinical efficacy, have also been found to have endothelium modifying properties *in vivo*. In particular, chemotherapy with dacarbazine increased intratumoural CCL5, CXCL9 and CXCL10 expression, (Hong et al. 2011), while low dose radiation promoted vascular normalisation and enhanced CXCL9 and CXCL10 expression, together allowing for enhanced $CD8^+$ T cell entry *in vivo* (Ganss et al. 2002). In addition, low dose radiation was also found to polarise M2 TAMs to an M1 phenotype, which through the reduction of VEGF production was also found to promote $CD8^+$ T cell infiltration (Klug et al. 2013).

The initial concept of anti-angiogenic therapy, in particular anti-VEGF/VEGFR therapy, was to achieve tumour growth inhibition by blocking blood vessel development in tumours and thereby depriving tumour cells of oxygen and nutrients (reviewed in (Helfrich & Schadendorf 2011)). Despite success in preclinical animal models, anti-angiogenic monotherapy has failed to demonstrate an improvement in overall survival in melanoma clinical trials (reviewed in (Helfrich & Schadendorf 2011)). Nonetheless, there has recently been a conceptual shift to begin using these agents to restore the tumour vasculature to its normal state, a process known as vascular normalisation. Vascular normalisation is observed during a specific window of time following the administration of anti-angiogenics at a high dose (Winkler et al. 2004) or achieved through a reduction in the dosage of administered anti-angiogenics (Huang, Y et al. 2012). Indeed, inhibition of VEGF signalling with the small molecule VEGFR inhibitor sunitinib in B16 murine melanoma models has been found to promote vascular normalisation, restore adhesion molecule expression and enhance CXCL10 and CXCL11 expression, which together increased $CD8^+$ T cell infiltration (Huang, H et al. 2015).

With our increasing understanding of the mechanisms of immune cell entry into tumours and how the immune cell composition can affect treatment response, it is timely to start considering ways to selectively alter leukocyte recruitment to enhance treatment outcomes for melanoma patients. Indeed, a large number of clinical trials in which an immunotherapy backbone is combined with endothelium-modifying components are underway. For example, Phase II trials have revealed that sequencing administration of the BRAFi vemurafenib followed by ipilimumab (Amin et al. 2016) had manageable safety, and patients treated with vemurafenib for 6 weeks remained responsive to ipilimumab treatment and vemurafenib retreatment. The effects of this combination therapy on the endothelium as well as its long term efficacy in comparison to single agent treatment however remains to be elucidated. *In*

vivo, anti-PD-1 and BRAFi combination therapy demonstrated synergistic effects in a $BRAF^{V600E}/Pten^{-/-}$ murine model, with significantly increased $CD8^+$ T cell infiltration and survival compared to BRAFi treatment alone (Cooper et al. 2014). Clinical trials revealed that combination therapy with ipilimumab and the chemotherapy agent fotemusine was efficient in achieving disease control (Di Giacomo et al. 2012), although its efficacy over fotemusine alone is still being assessed (Giacomo et al. 2015). Although phase 1 clinical trials of radiation and ipilimumab in metastatic melanoma patients demonstrated that only 18% of patients had partial response as best response, the therapeutic effects were enhanced by combining radiation, anti-CTLA-4 and anti-PDL-1 in murine melanoma and other tumour models (Twyman-Saint Victor et al. 2015). In a phase 1 clinical trial combining ipilimumab and the VEGF inhibitor bevacizumab (NCT00790010), the ECs of metastatic melanoma patients exhibited enhanced ICAM-1 and VCAM-1 expression post-treatment compared to pre-treatment, resulting in enhanced $CD8^+$ T cell infiltration (Wu, X et al. 2016).

In addition to the aforementioned studies which combine therapies already in clinical use, many new therapeutic agents are currently being developed in animal models which aim to enhance $CD8^+$ T cell recruitment to tumours. While these are yet to be translated into clinical trials, they are discussed here to highlight the exciting future possibilities for clinical immunotherapy.

As discussed above, the tumour endothelium expresses several molecules that inhibit $CD8^+$ T cell infiltration, and therefore can be targets for inhibition to enhance $CD8^+$ T cell entry. *In vivo*, CD73 blockade and anti-CTLA-4 co-therapy enhanced $CD8^+$ T cell infiltration in a B16-F10 melanoma model and inhibited tumour growth compared to anti-CTLA-4 blocking alone (Iannone et al. 2014). Similarly, in multiple *in vivo* solid tumour models, combining adoptive cell transfer with CD73 blockade, FasL blockade or ET_BR inhibition led to enhanced $CD8^+$ T cell homing and infiltration into tumours compared to ACT alone, resulting in tumour regression (Buckanovich et al. 2008; Wang, L et al. 2011).

Another approach to enhance tumour $CD8^+$ T cell infiltration is increasing the expression of CCR5 and CXCR3 ligands within the tumour microenvironment. Tang and colleagues proposed the use of an antibody-guided LIGHT fusion protein to enhance the efficacy of anti-PD-1 therapy (Tang, H et al. 2016). By specifically targeting LIGHT to tumour tissues to stimulate lymphotoxin β receptor (LTβR), the expression of CCL3, CCL4, CCL5, CXCL9

and CXCL10 was increased in tumour cells, resulting in enhanced T cell infiltration and responsiveness to PDL-1 checkpoint blockade treatment.

Improvements in our understanding of the tumour microenvironment could be used for genetic engineering enhancements of CAR T cells that might facilitate their entry into tumours. In particular, T cells could be engineered to express receptors to the aforementioned factors, which are upregulated with disease progression and which also recruit neutrophils and monocytes. Indeed, when T cells were engineered to express CXCR2, their recruitment to B16 murine melanoma overexpressing CXCL1 was increased, resulting in greater tumour regression compared to T cells lacking CXCR2 overexpression (Peng et al. 2010).

Taken together, these studies demonstrate the importance of adhesion molecules and chemokines in regulating the access of leukocytes across the blood vessel barrier, and how this in turn impacts disease progression and treatment outcomes.

1.4.3. ***Alternative Melanoma Cell Lined Blood Vessels***

1.4.3.1. Vasculogenic Mimicry

As discussed in depth in the previous sections, the importance of EC-lined blood vessels in cancer biology and therapy is well established. However, there are alternative forms of vascularisation which are being identified and are gaining attention, one of which is vasculogenic mimicry (VM), and is the main focus of this thesis. VM is a process where the tumour cells mimic EC behaviour and align along a deposited basement membrane forming interconnecting vessel-like structures with lumens. Our current knowledge about the significance and regulation of VM will be discussed in more detail below.

1.4.3.2. Validation and Significance of Vasculogenic Mimicry

In 1999, Manoitis and colleagues reported their discovery of networked structures detected using immunohistochemical analysis on uveal melanoma samples which carried red blood cells but were not lined by ECs (Maniotis et al. 1999). This was in great contradiction with our understanding of blood vessel formation, and soon after sparked debates which openly questioned the reliability of the findings and the actual significance of these structures (McDonald, Munn & Jain 2000). Since then, the evolvement of scientific techniques and further investigations focusing on this phenomenon have allowed for the presentation of evidence validating VM and strengthening its importance in cancer biology.

It has been established in multiple studies with a variety of techniques that VM vessels are involved in blood perfusion and circulation (Dunleavey et al. 2014; Hillen, F. et al. 2008; Ruf et al. 2003). Further to the initial study, immunohistochemistry staining demonstrated that VM vessels are often fused to EC vessels and contain blood cells (Dunleavey et al. 2014). This is also further validated through real time imaging of VM vessels. Ultrasound and Doppler imaging confirmed the flow of microbubbles from EC vessels to VM vessels (Ruf et al. 2003), while intravital microscopy following injection of fluorescently labelled leukocytes confirmed the perfusion through both EC vessels and VM vessels with the injected leukocytes (Hillen, F. et al. 2008). Together, these findings confirmed that VM structures are not merely artefacts of staining and are indeed involved in active blood flow.

The significance of VM in cancer biology has been demonstrated by both *in vivo* studies and analysis of patient data. VM has been established to be a feature of aggressive cancers which have increased metastatic capabilities (Wagenblast et al. 2015). In line with that, blocking VM *in vivo* has been shown to inhibit tumour growth (Francescone et al. 2012; Misra, Bajaj & Kale 2012). A recent meta-analysis confirmed that VM vessels can be present in up to 45% of human melanomas (Yang et al. 2016). More importantly, their presence correlated with increased metastasis and poor overall survival in melanoma, as well as many other cancers such as breast cancer and glioblastoma (Warso et al. 2001; Yang et al. 2016). Taken together, these studies establish both the biological and clinical significance of VM.

1.4.3.3. Regulation of Vasculogenic Mimicry

While there is compelling evidence on the importance of VM in driving disease progression, our understanding of VM is still fairly limited. The current knowledge of VM is largely limited to pathways involved in its regulation, which will be discussed further below (Figure 1.4).

Perhaps unsurprisingly, plasticity of melanoma cells is key to giving rise to this acquired capability of melanoma cells to mimic EC activity, a property that is not characteristic of normal melanocytes. This is demonstrated through the activation of stem cell signalling pathways that are involved in maintaining embryonic stem cell pluripotency during embryogenesis but are silenced after embryo development. One prominent example is the stem cell receptor Notch 4 and embryonic growth factor Nodal (McAllister et al. 2010). The binding of ligands such as the Jagged and Delta like family of ligands to the Notch 4 receptor leads to the cleavage and production of a Notch intracellular domain (NICD) which then

translocates into the nucleus and stimulates the production of Nodal which in turn mediates cell pluripotency and cancer plasticity (Hardy et al. 2010; Topczewska et al. 2006). Both Notch4 and Nodal expression are found to increase with melanoma progression, and are associated with melanoma tumourigenicity and aggressiveness (Hardy et al. 2010; Topczewska et al. 2006). When Nodal is inhibited, melanoma cells appear to revert to a melanocytic phenotype, indicating its importance in maintaining melanoma cell plasticity (Topczewska et al. 2006). More importantly, the inhibition of either Notch 4 or Nodal has been found to suppress VM occurrence (Hardy et al. 2010; Topczewska et al. 2006; Vartanian et al. 2013), highlighting the importance of cell plasticity in regulating melanoma VM.

VM is tightly associated with angiogenesis. Firstly, VM has been found to be regulated by some of the same molecules that regulate angiogenesis. In fact, VE-cadherin, the calcium dependent cell-cell adhesion molecule that has been described previously to be crucial in angiogenesis, was one of the first molecules identified in the regulation of VM (Hendrix, MJ et al. 2001). Subsequent studies revealed that VE-cadherin regulates VM through mediating EphA2 localisation and phosphorylation (Hess et al. 2006). This in turn stimulates the PI3K (Hess et al. 2003) and FAK- Erk1/2 (Seftor et al. 2001) signalling pathways to increase MMP production and activity. MMP remodels the extracellular matrix to enhance production of the basement membrane component Laminin 5γ2, which is important in regulating melanoma cell migration and VM (Seftor et al. 2001). Similar to angiogenesis, hypoxia appears to be a main inducer and stimulator of VM both *in vitro* (Sun, B et al. 2007) and *in vivo* (Hendrix, MJ et al. 2002). Hypoxia can induce the expression of VEGFA, which in turn initiates VEGFR1/PI3K signalling to promote VM (Vartanian et al. 2011). Expression of CD31 (PECAM), another EC associated adhesion molecule, on melanoma cells through the loss of the CD31 transcriptional repressor AP-2α has also been found to promote melanoma VM formation (Dunleavey et al. 2014). In addition, the tissue factor pathway inhibitor (TFPI) molecules which are involved in regulating coagulation pathways during angiogenesis to maintain blood vessel perfusion, are also found to be upregulated in aggressive melanoma (Ruf et al. 2003). These molecules are involved in the regulation of VM and production of blood perfused VM vessels in melanoma xenografts (Ruf et al. 2003).

Secondly, VM appears to be complementary to angiogenesis. Interestingly, while VEGF is also one of the regulators of VM, VM vessels appear to be resistant to anti-VEGF treatment (Dunleavey et al. 2014). Furthermore, VEGF inhibition designed to target angiogenesis

resulted in adaptive resistance in melanoma xenografts, in turn leading to increased VM (Dunleavey et al. 2014; Schnegg et al. 2015). This is likely due to the plasticity of VM competent cells, as well as the abundance of additional molecules other than VEGF that can also regulate VM. Indeed, anti-VEGF treatment enhanced the expansion of $CD31^+$ cells which enabled VM formation and further promoted tumour growth (Dunleavey et al. 2014). Further to that, inherent cellular differences, such as differences in receptor expression between ECs and melanoma cells, have also been found to result in resistance of VM vessels to other anti-angiogenic drugs (van der Schaft et al. 2004). This provides an explanation as to why anti-angiogenic drugs are not always anti-VM, and shows how cancer cells have adapted to evade the effects of anti-angiogenics and still survive by maintaining vascularisation via another method.

Given the multistep process of blood vessel formation (proliferation, cytoskeleton remodelling, migration and cell-cell adhesion), VM has also been reported to be regulated by molecules that control these processes. This includes the molecules BNIP3 and caspase 3 which are normally implicated to play roles in regulating apoptosis. BNIP3 knockdown *in vitro* was found to affect cell-cell interactions and actin cytoskeleton assembly in melanoma cells, which in turn reduced the migratory capacity of the cells and subsequently VM (Maes et al. 2014). Similarly, inhibition of caspase 3 *in vitro* has been found reduce VM due to a reduction in MMP and in turn decreased migration and invasion (Liu, YR et al. 2013).

1.4.3.4. Targeting Vasculogenic Mimicry

To the best of my knowledge, while there have been multiple molecules identified to regulate VM, there is currently only one small molecule, known as CVM-1118, that is present in clinical trials with aims to target VM. *In vitro* work performed on melanoma cells revealed that CVM-1118 acts on multiple signalling pathways, such as Notch4/Nodal signalling and VEGF, which collectively results in decreased cell growth, increased apoptosis and decreased VM (Hendrix, MJC et al. 2016). A phase 1 clinical trial examining the safety of CVM-1118 on advanced cancer patients is currently ongoing, with preliminary results showing manageable side effects and some positive clinical responses in some patients (Tolcher et al. 2017).

Taken together, there is still much to learn about VM. As demonstrated in the sections above, a better understanding of the roles of various signalling pathways, the immune system and blood vessel formation via angiogenesis and leukocyte recruitment in mediating melanoma

disease has enabled the development of better treatment approaches to improve patient outcome, and this will likely be similar as we expand our knowledge on VM.

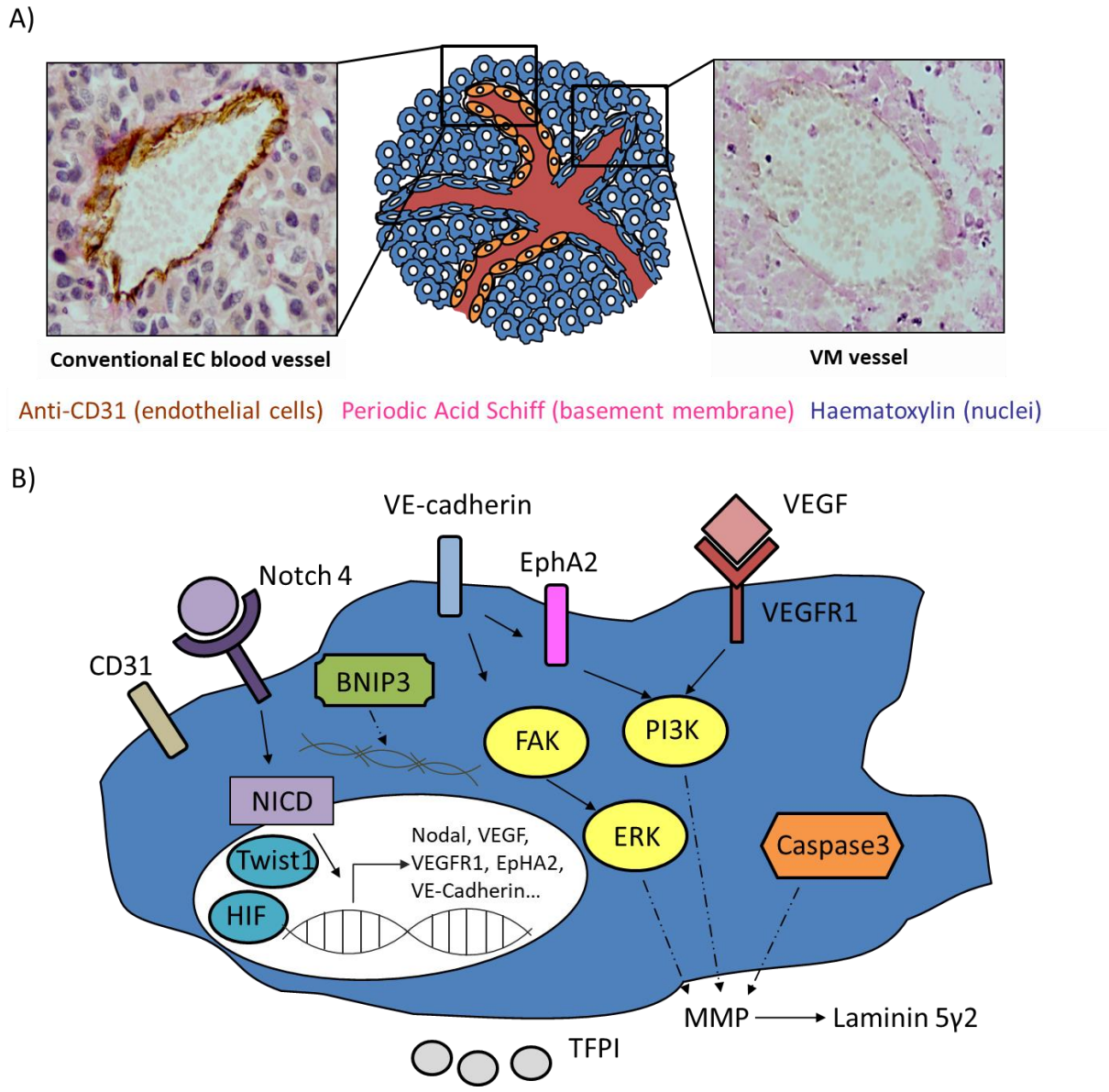

Figure 1.4. Vasculogenic mimicry and the pathways involved in its regulation.

(A) Conventional EC blood vessels and vasculogenic mimicry vessels can be distinguished via immunohistochemical staining with Periodic Acid Schiff (PAS; pink staining) that stains basement membrane components and anti-CD31 antibody that stains ECs (brown staining). EC vessels will appear as pink vessels with an inner brown lining ($CD31^+$ PAS^+), whereas VM vessels will appear as pink vessels without an inner brown lining ($CD31^-$ PAS^+) due to the lack of an inner EC lining. (B) VM is a complex process regulated by multiple signalling pathways including embryonic (Notch4/Nodal) signalling pathways and angiogenic (HIF, CD31, VE-cadherin, EphA2, VEGF, TFPI) signalling pathways. It is also found to be regulated by certain apoptotic (BNIP3, Caspase3) signalling pathways, due to the effects of these molecules on cytoskeletal rearrangement and cell migration, which are critical processes for VM.

1.5. The Research Project

The overarching aim of this thesis is to address key gaps in our knowledge of melanoma VM. Two hypotheses will be investigated, which relate to the **regulation** and **function** of melanoma VM, respectively. These hypotheses and the project aims related to them are introduced briefly below, with further detail to follow in the respective results chapters.

1.5.1. *Regulation of Vasculogenic Mimicry*

The field of VM is rapidly expanding, with more and more molecules being described to play a role in the regulation of this process. This is likely due to the underlying plasticity of the VM competent cells that provides them with the capability of alternating between and utilising multiple molecules to maintain VM. Here, the role of the desmosomal cadherin DSG2, which as discussed above was recently found by ourselves and others to contribute to angiogenesis (Ebert et al. 2016; Giusti et al. 2013), in VM is assessed. It is hypothesised that **DSG2 is a novel regulator of melanoma VM**. The aims to address this hypothesis are to:

1) Examine the role of DSG2 in regulating melanoma VM
2) Examine the mechanism by which DSG2 regulates VM by examining potential roles in melanoma cell proliferation, cytoskeletal rearrangement, migration and cell-cell adhesion

The concept and aims will be further discussed and addressed in Chapter 3 of this thesis.

1.5.2. *Function of Vasculogenic Mimicry*

As mentioned above, our current knowledge of VM is largely limited to its regulation. While studies have shown that blocking VM inhibits tumour growth *in vivo* (Francescone et al. 2012; Misra, Bajaj & Kale 2012), it is unclear how this effect is mediated. To date, no studies have directly assessed the function of VM vessels, and it remains as a big gap in the field. Given the importance of blood vessels in tumour growth, it has been largely deduced that VM vessels act to channel oxygen and nutrients into the tumour, although this has never been directly assessed. While multiple studies have documented the presence and flow of leukocytes within these vessels (Dunleavey et al. 2014; Hillen, F. et al. 2008), the potential function of VM vessels in regulating leukocyte trafficking into tumours has been overlooked. Interestingly, melanoma cells have been reported to express some of the adhesion molecules and chemokines that are expressed by ECs to recruit leukocytes (Denton et al. 1992; Langer et al. 2011; Payne & Cornelius 2002), some of which also appear to be expressed by VM-

competent cells (Dunleavey et al. 2014). The expression of these molecules is primarily thought to allow circulating tumour cells to interact with blood vessels and enter tissues to establish new metastases. However, an intriguing additional possibility is that these molecules allow melanoma cells lining VM channels to actively recruit specific immune cell populations from the circulation.

Based on these observations, it is hypothesised that **VM vessels are involved in leukocyte recruitment to melanoma tumours**. The aims to address this hypothesis are to

1) Examine the ability of leukocytes to roll, adhere and migrate across monolayers of VM-competent melanoma cells
2) Determine the expression of adhesion molecules and chemokines on VM-competent melanoma cell lines under normoxic and hypoxic conditions
3) Establish a mouse model for intravital microscopy examination of VM vessels.

The concept and aims will be further discussed and addressed in Chapters 4 and 5 of this thesis.

Chapter 2. Materials and Methods

2.1. Ethics Statement

2.1.1. *Human Ethical Statement*

The collection of peripheral blood from healthy donors for isolation of bulk mononuclear cells was given ethical clearance from the Royal Adelaide Hospital Human Research Ethics Committee, Adelaide, South Australia, Australia (RAH Protocol Number: 130308). Informed consent was obtained from all subjects in accordance with the "Declaration of Helsinki".

Buffy coats were supplied by the Australian Red Cross Blood Service following ethical clearance and establishment of material supply agreements (Agreement Numbers: 15-04SA-06, 17-05SA-18, 17-04SA-04).

2.1.2. *Murine Ethical Statement*

The execution of animal experiments was given ethical clearance from the Animal Ethics Committee of SA Pathology (Project Number: 12-17) and conforms to the guidelines established by the "Australian Code of Practice for the Care and Use of Animals for Scientific Purposes".

2.2. Materials and Methods

2.2.1. *Cell Culture*

2.2.1.1. Media and Reagents

The recipes for the media and reagents used for cell culture are as listed in Table 2.1.

Table 2.1. Media and reagents used for cell culture and their contents

Cell Culture Media and Reagents	Contents
RF10 media	500 ml Roswell Park Memorial Institute Media (RPMI; Gibco Life Technologies, Carlsbad, California, USA) 10% Fetal Bovine Serum (FBS; Hyclone, GE Healthcare Sciences, Utah, USA) 10 mM HEPES (Gibco Life Technologies) 1x Glutamax (Gibco Life Technologies)
RPMI based serum free media	500 ml RPMI media (Gibco Life Technologies) 10 mM HEPES (Gibco Life Technologies) 1x Glutamax (Gibco Life Technologies)
DMEM based culture media	500 ml Dulbecco's Modified Eagle's Medium (DMEM ; Gibco Life Technologies) 10% Fetal Bovine Serum (FBS; Hyclone, GE Healthcare Sciences, Utah, USA) 10 mM HEPES (Gibco Life Technologies) 1x Glutamax (Gibco Life Technologies)
1x PBS	500 ml of 10x Dulbecco's phosphate-buffered saline, no calcium, no magnesium (DPBS; Gibco Life Technologies) 4500 ml of MiliQ water
Endothelial Cell Growth Supplement (5 mg/ml stock)	100 mg Endothelial Cell Growth Supplement (ECGS; Corning, New York, USA) 20 ml 1x PBS
Heparin (5 mg/ml stock)	50 mg Heparin sodium salt from porcine intestinal mucosa (Sigma-Aldrich, St. Louis, Missouri, USA) 10 ml 1x PBS Final solution filtered using 0.22 µm filter.
HUVE media	500 ml Media 199 (M199; Sigma-Aldrich) 100 ml FBS (Hyclone) 7.5 ml Sodium Bicarbonate (Gibco Life Technologies) 10 ml 1 M HEPES (Gibco Life Technologies) 5 ml 100x Penicillin Streptomycin (Gibco Life Technologies) 5 ml 100 mM Sodium Pyruvate (Sigma-Aldrich) 5 ml Non-essential amino acids (Sigma-Aldrich) Supplemented with fresh heparin and ECGS at 15 µg/ml
HUVE wash	500 ml Media 199 (M199; Sigma-Aldrich) 10 ml FBS (Hyclone) 10 ml 1 M HEPES (Gibco Life Technologies) 5 ml 100x Penicillin Streptomycin (Gibco Life Technologies)
0.5 M EDTA/PBS Stock	186 g Titriplex® III for analysis (EDTA; Merck Millipore, Burlington, Massachusetts, USA) 1 L 1x PBS EDTA dissolved in PBS with pellets of sodium hydroxide. pH adjusted to 7.3 and final solution filtered using 0.22 µm filter.
0.01 M EDTA/PBS	16 ml 0.5 M EDTA/PBS stock 80 ml 10x DPBS (Gibco Life Technologies) 800 ml Water for Irrigation (Baxter, Deerfield, Illinois, USA)

0.25% Trypsin	7.9 ml Water for Irrigation (Baxter) 1 ml 10x Trypsin-EDTA (Millipore, Burlington, Massachusetts, USA) 1.1 ml 0.01 M EDTA/PBS
10x HBSS with Glucose	1 L Water for Irrigation (Baxter) 4 g Potassium chloride (KCl; Merck, Darmstadt, Germany) 0.6 g Potassium dihydrogen phosphate (KH_2PO_4; Merck) 80 g Sodium chloride (NaCl; Ajax Finechem, Taren Point, New South Wales, Australia) 3.5 g Sodium hydrogen carbonate ($NaHCO_3$; Merck) 0.475 g Disodium hydrogen orthophosphate (Na_2HPO_4; Chem Supply, Gillman, South Australia, Australia) 10 g D-glucose (Merck) pH adjusted to 7.3 and final solution filtered using 0.22 µm filter.
Gelatin	750 ml Water for Irrigation (Baxter) 15.39 g Granular gelatin (Sigma-Aldrich) 32.6 ml FBS (Hyclone) 19.6 ml 7.5% sodium bicarbonate ($NaHCO_3$; Merck Millipore) 5.2 ml 10x HBSS with Glucose Gelatin added to warm Baxter Water for Irrigation. Mixture dissolved over low heat (without agitation), autoclaved and then cooled to 4°C to ensure that it would set. Mixture thawed and remaining ingredients added.
Fibronectin (50 µg/ml)	5 mg Fibronectin from human plasma (Roche, Basel, Switzerland) 100 ml 1x PBS

2.2.1.2. Cell Lines

The cell lines used are as listed in Table 2.2.

Table 2.2. Cell lines used and their culture conditions

Cell line	Description	Culture characteristics	Culture conditions
C32	Human melanoma cell line	Adherent	RF10 (Recipe listed in Table 2.1)
CHL-1	Human melanoma cell line	Adherent	RF10
SK-Mel-28	Human melanoma cell line	Adherent	RF10
TrHBMEC	Human endothelial cell line	Adherent	HUVE media (Recipe listed in Table 2.1) Culture flasks/dishes pre-coated with gelatin (Recipe listed in Table 2.1)
HaCaT	Human immortalised keratinocyte cell line	Adherent	DMEM based culture media (Recipe listed in Table 2.1)
HEK293T	Human embryonic kidney cell line	Adherent	DMEM based culture media

2.2.1.3. Protocols

All cell culture was performed under sterile conditions in a Class II Biological Safety Cabinet (Gelaire Pty Ltd, Kew, Victoria, AU).

2.2.1.3.1. Cell Culture in Ambient Oxygen Conditions

Cell cultures were maintained in humidified 5% CO_2 at 37°C in a Hera Cell Incubator. Cells were routinely fed with the appropriate fresh medium and passaged when 80-100% confluent. To passage cells, medium in flasks was aspirated and 0.01 M EDTA/PBS (Recipe listed in Table 2.1) or 0.25% Trypsin (for HaCaT; Recipe listed in Table 2.1) was added into the flasks. The flasks were gently tapped and checked under the microscope to confirm detachment of cells. Detached cells were collected in medium and centrifuged at 475 x g for 5 minutes at room temperature (RT) (Centrifuge 5810; Eppendorf, Hamburg, Germany). After aspiration of the supernatant, the cell pellet was resuspended in fresh cell culture medium and seeded into dishes/flasks at the desired densities. Cells were maintained in continuous culture for no longer than two months, after which fresh vials were thawed.

2.2.1.3.2. Hypoxic Cell Culture

Cells were placed in a modular incubator chamber (Billups-Rothenberg Inc, San Diego, CA, USA) sealed and filled with humidified 0.5% or 3% O_2, 5% CO_2 with N_2 (BOC, Guildford, UK) for 3 or 7 days. The modular incubator chamber was then placed in a Hera Cell Incubator in humidified 5% CO_2 at 37°C. Cells were kept in the modulator incubator chamber without splitting or feeding. The gas in the modular incubator chamber was replaced every 3 days.

2.2.2. *Isolation and Preparation of Bulk Mononuclear Cells*

2.2.2.1. Media and Reagents

The recipes for the media and reagents used for the isolation and preparation of bulk mononuclear cells are as listed in Table 2.1 and Table 2.3.

Table 2.3. Media and reagents used for the isolation and preparation of bulk mononuclear cells and their contents

Media and Reagents	Contents
ACK lysis solution	1 L MiliQ water 8.29 g ammonium chloride (NH_4Cl; Sigma-Aldrich) 1 g potassium bicarbonate ($KHCO_3$; BDH Laboratory Supplies, Poole, England) 0.0372 g EDTA (Merck Millipore) pH adjusted to 7.2-7.4 and final solution filtered using 0.22 µm filter.
0.2% Trypan Blue	100 ml 1x PBS 0.2 g Trypan Blue Dye (Sigma-Aldrich)
Hanks' Balanced Salts Solution (HBSS)	1 L MiliQ water Hanks' Balanced Salts (Sigma-Aldrich) 0.35 g/L sodium bicarbonate ($NaHCO_3$; Merck Millipore) pH adjusted to 7.1 and final solution filtered using 0.22 µm filter.
5% BSA	12 ml RPMI (Gibco Life Technologies) 0.6 g BSA (Sigma-Aldrich) Final solution filtered using 0.22 µm filter.
Chemotactic Buffer	39 ml RPMI (Gibco Life Technologies) 1 ml 1 M HEPES (Gibco Life Technologies) 10 ml 5% BSA (Sigma-Aldrich)

2.2.2.2. Protocols

Peripheral blood or buffy coats were diluted 1:1 in sterile 1x PBS (Recipe listed in Table 2.1), layered onto a gradient medium Lymphoprep™ (Axis-Shield, Oslo, Norway) and subjected to gradient centrifugation at 685 x g for 20 minutes with no brake. The mononuclear cell (MNC) layer was collected and washed twice using HUVE wash (Recipe listed in Table 2.1). Whenever present, red blood cells were lysed by resuspending and incubating the cell pellet in 10 ml ACK lysis buffer (Recipe listed in Table 2.3) for 5 minutes, followed by a neutralisation using HUVE wash (Recipe listed in Table 2.1). The cell suspension was then centrifuged at 475 x g for 5 minutes at RT, and the supernatant was removed.

For parallel plate flow chamber assays, the MNC pellet was resuspended and stained with calcein AM viability dye (1.25 ng/µl in RF10; eBioscience, San Diego, California, USA) for 20 minutes at RT. Following a wash with RF10, cell counts were performed using 0.2% Trypan Blue (Recipe listed in Table 2.3) and the cells were resuspended in Hanks' Balanced Salts Solution (HBSS; Recipe listed in Table 2.3) at $4x10^8$ cells/ml.

For Transwell assays, cell counts were performed using 0.2% Trypan Blue (Recipe listed in Table 2.3) and the cells were resuspended in either RPMI with 0.1% FBS or chemotactic buffer (Recipe listed in Table 2.3) at $8x10^6$ cells/ml.

For intravital microscopy, the MNC pellet was resuspended and stained with CellTracker™ Blue CMAC (7-amino-4-chloromethylcoumarin) (10 µM in RPMI; Thermo Fisher Scientific, Waltham, Massachusetts, USA) for 30 minutes at RT. Following a wash with PBS, cell counts were performed using 0.2% Trypan Blue (Recipe listed in Table 2.3) and the cells were resuspended in 1x PBS (Recipe listed in Table 2.1) at $5x10^7$ cells/ml.

2.2.3. ***Transfection and Transduction Protocols***

2.2.3.1. siRNA Transfection for DSG2 Knockdown

Forward transfections were performed on melanoma cells that were 70%-80% confluent on the day of transfection. "Trilencer-27" siRNA duplexes of three different sequences targeting human DSG2 were purchased from OriGene Technologies (Rockville, MD, USA) and reconstituted to 20 µM according to the manufacturer's instructions. To generate transfection complexes, 10 µl of 606 nM siRNA was diluted in 990 µl Opti-MEM®I reduced serum medium (Life Technologies, Carlsbad, California, USA) and incubated with 5µl

Lipofectamine® RNAiMAX (Invitrogen, Carlsbad, California, USA) for 20-25 minutes at RT. The transfection complexes were then added to a T25 flask of cells in 5 ml RF10 at a final concentration of 1 nM. CHL-1 was used for subsequent assays 48 hours post transfection, while C32 and SK-Mel-28 were used 72 hours post transfection.

2.2.3.2. Overexpressing GFP in C32 cells to Generate C32-GFP Cells

2.2.3.2.1. Lentiviral Production

A mixture containing 1.5 ml Opti-MEM® I reduced serum medium (Life Technologies) and 60 µl Lipofectamine® 2000 (Invitrogen) was mixed with a mixture containing 1.5 ml Opti-MEM® I reduced serum medium (Life Technologies), 15 µg BLIV MSCV-GFP-T2A-Luciferase Lentivector (System Biosciences, Palo Alto, California, USA), 5 µg pLP1 (ViraPower™ Lentiviral Packaging Mix; Invitrogen), 5 µg pLP2 (ViraPower™ Lentiviral Packaging Mix; Invitrogen), and 5 µg VsVG (ViraPower™ Lentiviral Packaging Mix; Invitrogen), and incubated for 20 minutes at RT. The mix was added to a T75 flask of HEK293T to produce lentiviral particles. After 24 hours, the medium was replaced with 15ml of RF10. Viral supernatant was collected 48 hours later, spun at 845 x g for 5 minutes at 4˚C, and filtered with a 0.45 µm filter.

2.2.3.2.2. Lentiviral Transduction of C32

Freshly harvested virus were mixed in RF10 and hexadimethrine bromide (polybrene; Sigma-Aldrich) at 4 different combinations (1:2 virus with 4 µg/ml polybrene, 1:2 virus with 6 µg/ml polybrene, 1:3 virus with 4 µg/ml polybrene, 1:3 virus with 6 µg/ml polybrene) and added to T25 flasks of C32 cells at 70% confluence. The cells were routinely split and fed with fresh medium. Cells transduced with the different viral polybrene concentrations exhibited similar transduction efficacies and viabilities, and hence were pooled together for sorting on the FACSAria II (BD, Franklin Lakes, New Jersey, USA) using the FACS Diva Software version 8.0 (BD).

2.2.4. ***Characterisation of Gene Expression***

2.2.4.1. Quantitative Real Time Polymerase Chain Reaction (qPCR)

2.2.4.1.1. Reagents

Table 2.4. Media and reagents used for the protocols related to quantitative real time polymerase chain reaction and their contents

Reagents	Contents
TE buffer	9.88 ml MiliQ water 100 µl 1 M UltraPure™ Tris (Invitrogen) 20 µl 500 mM EDTA (Merck Millipore)
50x Tris-acetate-EDTA (TAE) Buffer	1 L MiliQ water 242 g UltraPure™ Tris (Invitrogen) 57.1 ml Glacial acetic acid (Chem Supply) 100 ml 0.5 M EDTA/PBS stock pH adjusted to 8.0 and diluted to 1x for use.
1% TAE-Agarose Gel	1 g Agarose (Promega, Madison, Wisconsin, USA) 100 ml 1x TAE Buffer

2.2.4.1.2. Primer Design

Primers were designed using Primer Blast (NIH, Bethesda, Maryland, USA) with the following criteria: i) primer length of 18-25 bp, ii) primer melting temperatures of 58°C-62°C, iii) primer spanning an intron-exon border, iv) PCR product size of 100-250 bp. Self complementarity and potential hairpin formation of primers were assessed using Oligo Calc (Northwestern University, Evanston, Illinois, USA), and specificity of primers were assessed using Primer Blast (NIH). The selected primers were purchased from GeneWorks (Hindmarsh, South Australia, Australia). Primer stocks were reconstituted to 1 µg/µl with sterile miliQ water. Working primer stocks were prepared by diluting primer stocks 1:10 with sterile miliQ water to 100 ng/µl.

2.2.4.1.3. PCR

To confirm primer specificity, PCR was performed using Phusion® High-Fidelity PCR Master Mix with HF Buffer (New England Biolabs; NEB, Beverly, Massachusetts, USA). Each reaction mix contained 2 µl cDNA/control, 4µl 5x HF buffer (NEB), 1 µl 100 ng/µl forward primer, 1 µl 100 ng/µl reverse primer, 0.6 µl DMSO (Sigma-Aldrich), 0.5 µl 10 mM dNTPs, 0.1 µl 0.04 U Phusion® High-Fidelity DNA Polymerase (NEB) and 10.8 µl miliQ water. The samples were placed into a thermocycler (BioRad, Hercules, California, USA) with reactions running at cycling temperatures of 98˚C for 30 seconds, 30-35 cycles of (98˚C for 10 seconds, 60˚C for 15 seconds, 72˚C for 30 seconds) and 72˚C for 15 minutes. The resultant PCR product (10 µl) was then mixed with 2 µl of loading buffer and run on a 2% agarose gel at 120 V for 30-40 minutes. The gel was incubated in 3x Gel Red in 0.1 M NaCl (Biotium, Hayward, California, USA) for 10 minutes at RT and visualised using Uvitec gel documentation system (Uvitec, Cambridge, Cambridgeshire, UK). Only the primer pairs that produce the right size product were used for downstream qPCR.

Table 2.5. List of primers used for qPCR

Primers		Sequence	Company
β-actin	Fwd	5’ ATG TAC GTT GCT ATC CAG GC 3’	GeneWorks Pty Ltd (Thebarton, South Australia, Australia)
	Rev	5’ CTC CTT AAT GTC ACG CAC GA 5’	
CycA	Fwd	5’ AGA CAA GGT CCC AAA GAC AGC AGA 3’	
	Rev	5’ TGT GAA GTC ACC ACC CTG ACA CAT 3’	
GAPDH	Fwd	5’ ACC CAG AAG ACT GTG GAT GG 3’	
	Rev	5’ CAG TGA GCT TCC CGT TCA G 3’	
ADM	Fwd	5’ CAG ATC ACT CTC TTA GCA GGG TC 3’	
	Rev	5’ CAC GAC TCA GAG CCC ACT TA 3’	
ANGPLT4	Fwd	5’ AGA TGA CCT CAG ATG GAG GCT 3’	
	Rev	5’ CCC GTG ATG CTA TGC ACC TT 3’	
ANKRD37	Fwd	5’ AAA TTC TCC CGT GCT AGG GC 3’	
	Rev	5’ TTC AGA CCA TCC ACC TCG GG 3’	
SLC2A1	Fwd	5’ CTT CAC TGT CGT GTC GCT GT 3’	
	Rev	5’ GAT GGC CAC GAT GCT CAG AT 3’	
DSG2	Fwd	5’ CCA TTG CGG AAA GGG CGC CA 3’	
	Rev	5’ GGC AGA AAT GAT GGC ACC ACC TTG T 3’	

2.2.4.1.4. RNA Extraction

Total RNA was isolated using the RNeasy Mini Kit with QIAshredder (Qiagen, Hilden, Germany) according to manufacturer's instructions. Concentration of RNA was assessed using a NanoDrop ND-1000 Spectrophotometer (Thermo Scientific). Extracted RNA was stored at -80˚C.

2.2.4.1.5. cDNA Synthesis

Total RNA (2 µg) was used to synthesise first strand cDNA. RNA was made up to 20 µl with miliQ water. 3' CDS primer (1 µl; 5' AAG CAG TGG TAA CAA CGC AGA GTA CTT TTT TTT TTT TTT TTT TTT TTT TTT TVN 3') was added to each RNA sample and the sample mix was first incubated at 65˚C for 5 minutes, and then incubated on ice for 1 minute. A master reaction mix containing 6.4 µl 5x first-strand buffer (Life Technologies) , 1.6 µl 0.1 M DTT (Life Technologies), 1.6 µl 10 mM dNTPs, and 1 µl SuperScript® III Reverse Transcriptase (Life Technologies) was then added to the RNA samples and mixed well. The samples were placed into a thermocycler (BioRad) with reactions running at cycling temperatures of 50˚C for 30 minutes, 55˚C for 30 minutes and 72˚C for 15 minutes. The 30 µl of resultant cDNA was added to 170 µl TE buffer (Recipe listed in Table 2.1) and stored at -20˚C until further use for qPCR.

2.2.4.1.6. qPCR

qPCR was performed using QuantiTect SYBR Green Master Mix (Qiagen). Each reaction mix contained 2 µl cDNA, 5 µl SYBR Green Master Mix (Qiagen), 0.5 µl 100 ng/µl forward primer, 0.5 µl 100 ng/µl reverse primer and 2 µl miliQ water. Reaction mixes were aliquoted in triplicate in either 72 or 100 well rotors using the QIAgility automated PCR setup instrument (Qiagen).

qPCR was performed using the Rotor-Gene 6000 (Qiagen) at 95˚C for 15 minutes, 45 cycles of cycling temperatures of 95˚C for 10 seconds, 55˚C for 20 seconds and 72˚C for 30 seconds, followed by a melt phase. Data was acquired and analysed using Rotor-Gene Analysis Software version 6 (Corbett Research, Qiagen). Gene expression was normalised to multiple housekeeping genes (β-actin, CycA, GAPDH) using geNorm (https://genorm.cmgg.be/).

2.2.4.2. RNA Sequencing

2.2.4.2.1. RNA Extraction

Following removal from hypoxic chamber, cells were immediately placed on ice. For RNA sequencing, RNA was isolated using the mirVana ™ miRNA isolation kit (Ambion™ by Life Technologies) according to manufacturer's instructions.

2.2.4.2.2. RNA Sequencing

RNA sequencing was outsourced to the ACRF Cancer Genomics Facility (Adelaide, South Australia, Australia). The materials and methods for the RNA sequencing provided from the Facility are as follows:

Poly(A) enriched mRNA was harvested from C32, CHL-1 and SK-Mel-28 cells cultured under ambient (21% O_2) conditions, or after 3 or 7 days in hypoxic conditions (0.5% O_2), in triplicate. These samples were multiplexed and sequenced on the Illumina NextSeq 500 platform (2 runs) using the stranded single end protocol with a read length of 75. Raw reads were adaptor trimmed and filtered for short sequences using cutadapt v1.3 (Martin 2011), setting minimum-length option to 18, error-rate 0.2, overlap 5 and a quality score cut-off of 28. The resulting FASTQ files averaging 18.5 million reads per sample (Table A1) were analysed and quality checked using the FastQC program (http://www.bioinformatics.babraham.ac.uk/projects/fastqc). The filtered reads were mapped against the human reference genome (Hg19) using the TopHat spliced alignment algorithm (Kim, D et al. 2013) (version 2.0.9 with default parameters) returning an average alignment rate of 97% (Table A1). Counts of reads mapping to each gene were calculated using HTSeq v0.6.1p1 (Anders, Pyl & Huber 2015). Differential expression analysis was evaluated from TMM normalized gene counts using R (version 3.2.3) and edgeR (Robinson, MD, McCarthy & Smyth 2010) (version 3.3) following protocols as described in (Chen, Y et al. 2014) and (Lun, Chen & Smyth 2016). Functional analyses were performed using the topGO package in R. Alignments were visualised and interrogated using the Integrative Genomics Viewer v2.3.80 (Thorvaldsdottir, Robinson & Mesirov 2013).

2.2.5. ***Characterisation of Protein Expression***

2.2.5.1. Flow Cytometric Analysis

2.2.5.1.1. Media and Reagents

Table 2.6. Media and reagents used for the preparation of cells for flow cytometric analysis and their contents

Media and Reagents	Contents
RF10 media + sodium azide	RF10 media 0.1% sodium azide (Sigma-Aldrich)
FACS fix	1 L 1x PBS 1% Paraformaldehyde (Sigma-Aldrich) 20 g/L glucose (Sigma-Aldrich) 5 mM sodium azide (Sigma-Aldrich)

2.2.5.1.2. Protocols

Cells were harvested using 0.01 M EDTA/PBS (Recipe listed in Table 2.1), aliquoted in 96 well U-bottom plates and spun down at 685 x g for 2 minutes at RT. Following aspiration of the supernatant, Fc receptor (FcR) blocking was performed by incubating cells with human IgG (0.1 mg/ml in RF10; Thermo Fisher Scientific) for 10 minutes on ice.

2.2.5.1.2.1. DSG2 expression on melanoma cell lines

To examine the expression of DSG2 on melanoma cells, the cells were stained with either a mouse anti human DSG2 primary antibody (5 µg/ml in RF10, Clone 6D8; Thermo Fisher Scientific) or a purified mouse IgG1κ isotype control (5 µg/ml in RF10, Clone MOPC-21; BD Biosciences, San Diego, CA, USA) for 30 minutes at 4°C. After a wash with RF10 and spin at 685 x g for 2 minutes at RT, the cells were stained with a secondary goat anti-mouse IgG H&L DyLight® 650 antibody (5 µg/ml in RF10, polyclonal; Abcam, Cambridge, UK) and 7-AAD (1:20 dilution in RF10; BD Biosciences) for 30 minutes at 4°C in the dark. After another wash with RF10 and spin at 685 x g for 2 minutes at RT, the cells were fixed with FACS fix (Recipe listed in Table 2.6) and stored in the dark at 4°C until being run on the C6 Accuri™ flow cytometer (BD Biosciences) using the CFlow® Plus software (BD).

2.2.5.1.2.2. Phenotyping of MNC

MNC were stained with an antibody master mix made up in RF10 for 30 minutes at 4°C in the dark. After a wash with RF10 and spin at 685 x g for 2 minutes at RT, the cells were fixed with FACS fix (Recipe listed in Table 2.6). Wherever stated, 50 µl of CountBright™ Absolute Counting Beads (Life Technologies) were added to the fixed cell sample to allow for the derivation of absolute cell counts. Samples were stored in the dark at 4°C until being run on the LSR Fortessa (BD) using FACS Diva Software version 8.0 (BD).

Table 2.7. List of antibodies and reagents used for flow cytometric phenotyping of MNC

Antibody/Reagent	Manufacturer	Clone & Isotype	Concentration
Mouse anti-human CD4 PE	BD Pharmingen™, Cat#555347	Clone RPA-T4, monoclonal mouse IgG1κ	1:5
Mouse anti-human CD8 PE-Cy™7	BD Pharmingen™, Cat#557746	Clone RPA-T8, monoclonal mouse IgG1κ	1:20
Mouse anti-human CD14 APC	BD Biosciences, Cat#340436	Clone MϕP9, monoclonal mouse IgG2bκ	1:5
Mouse anti-human CD3 APC-eFluor® 780	eBioscience™, Cat#47-0036-42	Clone SK7, monoclonal mouse IgG1κ	1:20
Mouse anti-human CD56 (NCAM) BUV395	BD OptiBuild™, Cat#742663	Clone MY31, monoclonal mouse IgG1κ	1:20
Mouse anti-human CD16 BV421	BD OptiBuild™, Cat#740098	Clone B73.1, monoclonal mouse IgG1κ	1:20
Mouse anti-human CD16 FITC	BD Pharmingen™, Cat#555406	Clone 3G8, monoclonal mouse IgG1κ	1:5
Mouse anti-human CD19 PE-Cy™5	BD Pharmingen™, Cat#555414	Clone HIB19, monoclonal mouse IgG1κ	1:5
Mouse IgG1κ PE isotype control	BD Pharmingen™, Cat#559320	Clone MOPC-21, mouse IgG1κ	1:5
Mouse IgG1κ FITC isotype control	BD Pharmingen™, Cat#551954	Clone MOPC-21, mouse IgG1κ	1:5
Mouse IgG1κ APC isotype control	BD Pharmingen™, Cat#554681	Clone MOPC-21, mouse IgG1κ	1:5
Mouse IgG2bκ APC isotype control	BD Pharmingen™, Cat#555745	Clone 27-35, mouse IgG2bκ	1:5
Mouse IgG2bκ PE-Cy™7 isotype control	BD Pharmingen™, Cat#560542	Clone 27-35, mouse IgG2bκ	1:20
Mouse IgG1κ BUV395 isotype control	BD Horizon™, Cat#560542	Clone X40, mouse IgG1κ	1:20
Mouse IgG1κ BV421 isotype control	BD Horizon™, Cat#562438	Clone X40, mouse IgG1κ	1:20
Mouse IgG1 κ APC-eFluor® 780 isotype control	eBioscience™, Cat#47-4714-82	Clone P3.6.2.8.1, mouse IgG1κ	1:20
Fixable Viability Stain 700	BD Horizon™, Cat#564997	N/A	0.3 ng/ml
CountBright™ Absolute Counting Beads	Life Technologies, Cat#C36950	N/A	50µl per sample

2.2.5.1.2.3. Adhesion molecule expression on melanoma cell lines

For melanoma cells cultured under hypoxia, cells were immediately placed on ice upon removal from the hypoxic chamber. Media in the flasks were aspirated and the cells were detached with cold 0.01 M EDTA/PBS (Recipe listed in Table 2.1). The detached cells were then collected with cold 1x PBS (Recipe listed in Table 2.1) and spun down at 685 x g for 2 minutes at 4˚C. Following aspiration of the supernatant, Fc receptor (FcR) blocking was performed by incubating cells with human IgG (0.1 mg/ml in RF10 containing 0.1% sodium azide; Thermo Fisher Scientific) for 10 minutes on ice. Cells were stained with an antibody master mix made up in RF10 containing 0.1% sodium azide (Recipe listed in Table 2.6) for 30 minutes at 4°C in the dark. After a wash with RF10 containing 0.1% sodium azide (Recipe listed in Table 2.6) and spin at 685 x g for 2 minutes at 4°C, the cells were fixed with FACS fix (Recipe listed in Table 2.6) and stored in the dark at 4°C until being run on the C6 Accuri™ flow cytometer (BD) using the CFlow® Plus software (BD).

Table 2.8. List of antibodies and reagents used for flow cytometric analysis of melanoma adhesion molecule expression

Antibody	Manufacturer	Clone & Isotype	Concentration
Mouse anti-human CD62P (P-selectin) APC	BD Pharmingen™, Cat#550888	Clone AK-4, monoclonal mouse IgG1κ	1:5
Mouse anti-human CD62E (E-selectin) APC	BD Pharmingen™, Cat#551144	Clone 68-5H11, monoclonal mouse IgG1κ	1:5
Mouse anti-human CD321 (JAM-1) PE	BD Pharmingen™, Cat#552556	Clone M.Ab.F11, monoclonal mouse IgG1κ	1:5
CD323 (JAM-3) VioBright™ FITC	Miltenyi Biotec, Cat#130-106-465	Clone REA429, recombinant human IgG1	1:10
Mouse anti-human CD54 (ICAM-1) PE	BD Pharmingen™, Cat#555511	Clone HA58, monoclonal mouse IgG1κ	1:5
Mouse anti-human CD102 (ICAM-2) APC	BD Pharmingen™, Cat#564677	Clone CBR-IC2/2, monoclonal mouse IgG1κ	1:20
Mouse anti-human CD106 (VCAM-1) FITC	BD Pharmingen™, Cat#551146	Clone 51-10C9, monoclonal mouse IgG1κ	1:5
Mouse anti-human CD44 PE-Cy™7	BD Pharmingen™, Cat#560533	Clone G44-26, monoclonal mouse IgG2bκ	1:20
Mouse anti-human desmoglein-2 (DSG2)	ThermoFisher, Cat#32-6100	Clone 6D8, monoclonal mouse IgG1κ	5 µg/ml
Purified mouse IgG1κ isotype control	BD Pharmingen™, Cat#555746	Clone MOPC-21, monoclonal mouse IgG1κ	5 µg/ml
Goat anti-mouse IgG H&L DyLight® 650	Abcam, Cat#ab96882	Polyclonal goat IgG	5 µg/ml
REA Control (S) VioBright™ FITC	Miltenyi Biotec, Cat#130-106-465	Clone REA293	
Mouse IgG1κ PE isotype control	BD Pharmingen™, Cat#559320	Clone MOPC-21, mouse IgG1κ	1:5
Mouse IgG1κ FITC isotype control	BD Pharmingen™, Cat#551954	Clone MOPC-21, mouse IgG1κ	1:5
Mouse IgG1κ APC isotype control	BD Pharmingen™, Cat#554681	Clone MOPC-21, mouse IgG1κ	1:5
Mouse IgG2bκ PE-Cy™7 isotype control	BD Pharmingen™, Cat#560542	Clone 27-35, mouse IgG2bκ	1:20
7-AAD staining solution	BD Pharmingen™, Cat#559925	N/A	1:20

Further data analysis was performed using FCS Express 4 Flow Cytometry: Research Edition (De Novo Software, California, USA).

2.2.5.1. Immunofluorescence Analysis

2.2.5.1.1. Reagents

Table 2.9. List of reagents used for immunofluorescence analysis and their contents

Reagents	Contents
0.1% Triton-X 100	40 ml MiliQ water 40 ul Triton-X 100 (Merck Millipore)

2.2.5.1.2. Protocols

2.2.5.1.2.1. Examination of Actin Cytoskeleton

Immediately after transfection, cells were seeded into 12 well plates (Falcon, Corning) containing coverslips pre-coated with fibronectin (5 µg/ml in PBS, 30 minute incubation at 37°C; Roche). After 48-72 hours, the culture media was aspirated and the coverslips washed with PBS. The cells were fixed with 4% paraformaldehyde (VWR International, Radnor Pennsylvania, USA) for 10 minutes at RT. Following a wash with PBS, the cells were permeabilised with 0.1% Triton® X-100 (Recipe listed in Table 2.9) for 10 minutes at RT. Later, the cells were washed with PBS and then blocked with 5% human AB serum (Invitrogen) for 30 minutes at RT. After another wash with PBS, the coverslips were flipped with cells facing downwards onto 50µl drops of either mouse anti-human desmoglein 2 (5 µg/ml in RF10, clone 6D8; Life Technologies) or a purified mouse IgG1κ isotype control (5 µg/ml in RF10, Clone MOPC-21; BD Biosciences) on Parafilm M(R) (Bemis NA, Neenah, Wisconsin, USA). Following an overnight incubation at 4°C in the dark, the coverslips were flipped with cells facing upwards back into the 12 well plate and washed once with PBS. Later, the coverslips were flipped with cells facing downwards onto 50µl drops of antibody master mix containing Alexa Fluor 488 goat anti-mouse IgG (H+L) (1:500 in RF10; Molecular Probes, Eugene, Oregon, USA) and Rhodamine Phalloidin (1:1000 in RF10; Life Technologies) on Parafilm M(R) (Bemis NA) and incubated for an hour at RT in the dark. After the incubation, the coverslips were flipped with cells facing upwards back into the 12 well plate and washed once with PBS. They were then mounted onto glass slides using 30 µl drops of ProLong® Gold Antifade Mountant with DAPI (ThermoFisher Scientific) and left to cure for 24 hours at RT in the dark before the edges of the coverslips were sealed with nail polish. Immunofluorescence images were taken on the LSM 710 Two Photon Confocal Laser

Scanning Microscope (Zeiss, Oberkochen, Germany) with the 20x/1.0 DIC W Plan-Apochromat objective (Zeiss) using the Zen 2011 (black edition) software (Zeiss).

2.2.5.1.2.2. Uptake of Tomato Lectin

To examine the ability of C32-GFP cells to take up DyLight® 594 labelled Lycopersicon Esculentum (Tomato) Lectin (Vector Laboratories, Burlingame, California, USA), C32-GFP cells were grown on fibronectin coated coverslips. DyLight® 594 labelled Tomato Lectin (Vector Laboratories) was added to the medium at 100 µg/ml and incubated at 37°C for 30 minutes. The coverslips were rinsed and the cells were fixed with 4% paraformaldehyde (VWR International) for 10 minutes at RT. After another rinse, the coverslips were then mounted onto glass slides using 30 µl drops of ProLong® Gold Antifade Mountant with DAPI (ThermoFisher Scientific) and left to cure for 24 hours at RT in the dark before the edges of the coverslips were sealed with nail polish. Immunofluorescence images were taken on the LSM 710 Two Photon Confocal Laser Scanning Microscope (Zeiss) with the 20x/1.0 DIC W Plan-Apochromat objective (Zeiss) using the Zen 2011 (black edition) software (Zeiss).

2.2.5.2. Examination of Chemokine Production

2.2.5.2.1. Collection of Melanoma Cell Culture Supernatant

Melanoma cell lines C32, CHL-1, SK-Mel-28 were grown to 100% confluency in 25 ml of RF10 in T175 flasks (Greiner Bio-One, Kremsmunster, Austria). The medium was then replaced with 10 ml of RF10 and allowed to grow under ambient or 0.5% O_2 for 3 days. The conditioned media was collected and centrifuged at 475 x g for 5 minutes to pellet any cells which may have been collected. The supernatant was filtered with a Minisart 0.2 µm syringe filter (Sartorius Stedim Biotech, Aubagne, France) and stored at -80°C. Multiple freeze thaws were avoided.

2.2.5.2.2. Chemokine Array

The chemokine profiles of melanoma cell lines C32, CHL-1 and SK-Mel-28 were assessed using the Proteome Profiler Human Chemokine Array Kit (R&D Systems, Minneapolis, Minnesota, USA) according to manufacturer's instructions with 1ml of melanoma cell culture supernatant. The membrane was visualised using the LAS-4000 (FujiFilm, Minato, Tokyo,

Japan). Quantification of the dots on the membrane was performed using ImageQuant™ TL (GE Healthcare Life Sciences, Chicago, Illinois, USA).

2.2.6. ***Functional Assays***

2.2.6.1. Matrigel® Tube Formation Assay

Matrigel® growth factor reduced basement membrane matrix (10µl; Corning) was aliquoted into each well of a "µ-slide Angiogenesis" culture slide (ibidi, Martinsried, Germany) and incubated in humidified 5% CO_2 at 37°C for at least 30 minutes to allow for the solidification of the Matrigel. Melanoma cells transfected with siRNA (as previously described in section 2.2.3.1) or transduced with lentivirus (as previously described in section 2.2.3.2.2) were harvested with 0.01 M EDTA/PBS (Recipe listed in Table 2.1), washed and resuspended in RF10. Cell counts were performed using 0.2% Trypan blue (Recipe listed in Table 2.3), and cell master mixes were prepared to allow for cell seeding at optimised densities (C32: $2x10^4$ cells per well; CHL-1: $1.5x10^4$ cells per well; SK-Mel-28: $5x10^3$ cells per well) in a final volume of 50 µl in RF10 in triplicate. After 3-6 hours of incubation at 37°C, multiple images across the whole well were taken using 4x objective on an IX70 microscope equipped with F-view CCD camera (Olympus, Shinjuku, Tokyo, Japan) and merged using Adobe Photoshop CS6 (Adobe Systems, San Jose, California, USA). The images were blinded and randomised, and the number of tube-like structures formed, stringently characterised as elongated structures formed by multiple cells in intimate association extending from cell clusters were quantified manually using ImageJ (NIH, MD, USA).

2.2.6.2. WST-1 Proliferation Assay

Immediately after siRNA transfection (as previously described in section 2.2.3.1), cells were seeded at 1000-3000 cells in 100 µl RF10 per well in triplicates in a flat bottom 96 well plate (Falcon, Corning). After 48-72 hours, 10µl of Cell Proliferation Reagent WST-1 (Roche) was added to each well and incubated for 30 minutes in humidified 5% CO_2 at 37°C. The plate was then shaken thoroughly on an orbital mixer (Ratek, Victoria, Australia) for 1 minute and the absorbance of the samples was measured using an Epoch™ microplate spectrophotometer (BioTek, Vermont, USA) at 450 nm. The plate was then returned to the incubator, with shaking performed and absorbance readings measured every 30 minutes. To generate an absolute absorbance value, the average absorbance values of the blank triplicate wells (media alone with WST-1) was subtracted from the average absorbance values of the triplicate wells

for each treatment group, and the results were presented as a ratio of the absolute absorbance of the DSG2 siRNA transfected cells over the absolute absorbance of the control siRNA transfected cells.

2.2.6.3. xCELLigence® Migration Assay

RF10 (160 µl) was added to the bottom wells and 30 µl of RPMI based serum free medium (SFM; Recipe listed in Table 2.1) was added to the upper wells of a CIM-Plate 16 (ACEA Biosciences, San Diego, California, USA). The plate was allowed to equilibrate in the xCELLigence® RTCA DP instrument (ACEA Biosciences) for 1 hour and the background impedance was measured. Transfected melanoma cells (prepared as previously described in section 2.2.3.1) were harvested with 0.01 M EDTA/PBS, washed with SFM, resuspended in SFM and counted using 0.2% Trypan Blue (Recipe listed in Table 2.3). Cells were then seeded at $3x10^4$ cells in 100 µl of SFM to the upper wells in duplicates. The plate was then replaced into the xCELLigence® RTCA DP instrument and impedance readings were taken at 5 minute intervals for at least 24 hours. The rate of cell migration was obtained by generating slopes of the curves using the RTCA Software (ACEA Biosciences).

2.2.6.4. Scratch Wound Assay

Immediately after transfection (as previously described in section 2.2.3.1), melanoma cells were seeded in T25 flasks (Greiner Bio-One). One day before the scratch wound assay, the cells were detached using 0.01 M EDTA/PBS and seeded at 30,000 cells per well in at least quintuples into a flat bottom 96 well plate (Falcon, Corning) to allow for the formation of a confluent monolayer overnight. For cells to be treated with mitomycin C (Sigma-Aldrich), prior to the introduction of scratches, the medium was aspirated and replaced with RF10 containing 10 µg/ml of mitomycin C. Following an hour of incubation at 37˚C, the mitomycin C was aspirated and the cells washed twice with RF10 before the addition of fresh RF10. Scratches were made using a WoundMaker™ (Essen Bioscience, Ann Arbor, Michigan, USA) according to the manufacturer's instructions. The medium was aspirated, and the wells were washed with RF10 at least twice to remove any unbound cells. After the addition of fresh RF10 into the wells, the plate was then placed into the IncuCyte ZOOM® (Essen Bioscience), with 10x images taken across the scratch wound every hour for at least 24 hours. The area of the wound across time was assessed using ImageJ with the MRI Wound Healing Tool macro (http://dev.mri.cnrs.fr/projects/imagej-macros/wiki/Wound_Healing_Tool) and a graph depicting the percentage of wound size

relative to the starting wound size across time was generated. The rate of cell migration was obtained by analyzing the area under the curve.

2.2.6.5. Adhesion Assay

One day prior to the adhesion assay, transfected melanoma cells were harvested and seeded at $8x10^5$- $1x10^6$ cells in 1.2 ml onto 35 mm x 10 mm culture dishes (Corning) to allow the formation of a confluent monolayer overnight. On the day of the assay, additional transfected melanoma cells were harvested and labelled with calcein AM viability dye (5 μg/ml in RF10; eBiosciences) for 20 minutes. The calcein AM-labelled cells were washed, resuspended in RF10 and added onto the 35 mm x 10 mm culture dishes containing the confluent monolayer at $8x10^5$- $1x10^6$ cells in 1.2 ml RF10. Following a 15 minute incubation at 37°C and 5% CO_2, the dishes were placed under a parallel plate flow chamber assay setup (setup as described in more detail in section 2.2.6.6, using a silicon gasket with 1.00 cm flow width) and any unbound calcein AM-labelled cells were washed off via a flow of Hanks' Balanced Salts Solution (HBSS; Recipe listed in Table 2.3) at a flow rate of 0.156 ml/min and a shear stress of 2 dynes/cm^2 for 5 minutes. Following removal from the parallel plate flow chamber assay setup, the dishes were rinsed and filled with HBSS. Avoiding the edges, brightfield and fluorescent images were taken at 3-5 fields of view across the gasket window under a 4x/0.10 objective on an IX71 inverted epifluorescence microscope (Olympus) using the analySIS LS Research FIVE software (Olympus). The number of bound fluorescent cells was quantified using ImageJ (NIH).

2.2.6.6. Parallel Plate Flow Chamber Assay

Melanoma cell lines C32, CHL-1, SK-Mel-28, EC line TrHBMEC, keratinocyte cell line HaCaT and fibroblast cell line BJ6 were seeded and cultured in 35 mm x 10 mm cell culture dishes (Corning) until a confluent monolayer was formed. For TrHBMEC treated with hypoxia, cell culture dishes were maintained as previously described in section 2.2.1.3.2 for 3 days prior to assay. For TrHBMEC treated with TNFα, cells were treated with 50 ng/ml TNFα (R&D Systems) in HUVE media for 4 hours prior to the assay.

Parallel plate flow chamber assays were performed using a circular flow chamber kit (GlycoTech Corporation, Rockville, MD). Briefly, a circular flow deck with a silicon rubber gasket with a flow width of 1.00 cm and thickness of 0.0254 cm was attached onto the culture dishes. One connector of the circular flow deck was attached to a vacuum port to generate a

tight seal between the flow deck and the culture dish while another connector was attached to a syringe on a syringe pump to achieve a controlled flow of HBSS/calcein AM-stained MNC across the monolayer at a flow rate of 0.323 ml/min to achieve a shear stress of 0.5 dynes/cm^2.

For each cell culture dish, the cell monolayer was first rinsed with a flow of HBSS for 2 minutes to remove floating cells. Subsequently, 8x10^6 calcein AM-stained MNC (prepared as previously described in section 2.2.2.2) were flowed across the cell monolayer. Later, the monolayer was rinsed again with a HBSS flow for 8 minutes to wash off any unbound MNC. The whole process was monitored under a 10x objective on an IX70 microscope equipped with F-view CCD camera (Olympus), with brightfield videos and images taken using the analySIS LS Research FIVE software (Olympus).

At the end of the assay, fluorescence images of the MNC adhered on the cell monolayer were imaged under a 4x objective using the EVOS® FL Cell Imaging System (Life Technologies). All the cells in the dishes were detached using 0.01 M EDTA/PBS, collected with 1x PBS and then centrifuged at 845 x g for 5 minutes at RT. The cells were subjected to flow cytometry analysis as previously described in section 2.2.5.1.2.2 to examine the phenotype of the bound MNC.

2.2.6.7. Transwell Migration Assay

Melanoma cell lines C32, CHL-1, SK-Mel-28, endothelial cell line TrHBMEC and keratinocyte cell line HaCaT were seeded into gelatin (Recipe listed in Table 2.1) coated 8.0 μm pore Transwell® polycarbonate membrane cell culture inserts (Corning) and allowed to grow for 72 hours to form a confluent monolayer. Cell culture medium was replaced once throughout the 72 hours.

To assess the permeability of the monolayer, 100μl of 2000kDa fluorescein isothiocyanate-dextran (FITC-dextran; 1 mg/ml in PBS; Sigma-Aldrich) was added onto the Transwell, and the Transwell was transferred into a 24 well plate (Falcon, Corning) containing 600 μl of RF10. After a 15-minute incubation, 100 μl of media was collected from the 24 well plate and the fluorescence was measured using a FLUOstar OPTIMA microplate reader (BMG LABTECH, Ortenberg, Germany). FITC-dextran was aspirated from the Transwells and the Transwells were rinsed with media twice.

To assess the morphology of the monolayer, the cells were stained with 100 μl calcein AM viability dye (1 ng/μl in RF10; eBiosciences) for 20 minutes at RT. Following two rinses with

RF10 and the addition of fresh media, the monolayer was imaged using the EVOS® FL Cell Imaging System (Life Technologies). Monolayers that were fully confluent with no holes or tears were selected for subsequent assay.

For Transwell migration assays performed under an FBS gradient, $8x10^5$ MNC (prepared as previously described in section 2.2.2.2) resuspended in 100 µl of RPMI with 0.1% FBS were added into the top chambers of Transwell inserts containing confluent cell monolayers, and the Transwells were transferred into 24-well plates containing 600 µl of either RPMI with 0.1% FBS (as a control for non-specific migration) or RF10 (for specific FBS-directed migration). Cells were allowed to transmigrate for 3 hours in humidified 5% CO_2 at 37°C. Later, the Transwells were removed and the transmigrated MNC in the bottom chamber were collected. The MNCs were subjected to flow cytometry analysis as previously described in section 2.2.5.1.2.2 to examine the phenotype of the transmigrated MNCs.

For Transwell migration assays performed under a CXCL12 gradient, $8x10^5$ MNC (prepared as previously described in section 2.2.2.2) resuspended in 100 µl of chemotactic buffer were added into the top chambers of Transwell inserts containing confluent cell monolayers, and the Transwells were transferred into 24-well plates containing 600 µl of either chemotactic buffer (as a control for non-specific migration; Recipe listed in Table 2.3) or CXCL12 (100 ng/ml in chemotactic buffer; R&D Systems). MNCs were allowed to transmigrate for 3 hours in humidified 5% CO_2 at 37°C. Later, the Transwells were removed and the transmigrated MNC in the bottom chamber were collected. The MNCs were subjected to flow cytometry analysis as previously described in section 2.2.5.1.2.2 to examine the phenotype of the transmigrated MNCs.

2.2.7. ***In Vivo Murine Experiments***

2.2.7.1. Generating C32-GFP Xenografts

Female nu/nu mice aged 6-8 weeks were purchased from Animal Resources Centre (Perth, Australia). C32-GFP cells ($2x10^6$) resuspended in 100 µl PBS were injected subcutaneously into both flanks of anaesthetised mice. Tumours were allowed to grow to a maximum of 1 cm^3. Mice were checked and weighed daily. The width and the length of the tumours were measured using digital vernier callipers at least three times per week and the volume of the tumour was calculated based on the formula of a modified ellipsoid (Tumour volume = ½ (length x $width^2$)) (Jensen, MM et al. 2008).

2.2.7.2. Intravital Microscopy

Tumour-bearing mice were anaesthetised with isofluorane/O_2 and an intraperitoneal injection of ketamine/xylazine (10 mg/ml). DyLight® 594 labelled Lycopersicon Esculentum (Tomato) Lectin (100 µl at 1 mg/ml; Vector Laboratories) was injected retro-orbitally. The midline of the mouse was then surgically opened and the skin separated from the abdominal cavity to expose the subcutaneous tumour on one flank. MNC pre-labelled with CellTracker™ Blue CMAC ($5x10^6$ in 100 µl of PBS, prepared as previously described in section 2.2.2.2) were injected intravenously through the tail vein. The mouse was then positioned under the LSM 710 Two Photon Confocal Laser Scanning Microscope (Zeiss) with the tumour exposed on a coverslip. The tumour was excited with the Argon Laser at 488 nm to visualise the C32-GFP cells, the DPSS 561-10 laser at 561 nm to visualise the DyLight® 594 Tomato Lectin, and the MaiTai laser at 710 nm to visualise the MNC pre-labelled with CellTracker™ Blue CMAC. Images were taken using the 20x/1.0 DIC W Plan-Apochromat objective (Zeiss) using the Zen 2011 (black edition) software (Zeiss).

2.2.7.3. Collection and Processing of Tumours

2.2.7.3.1. Reagents

Table 2.10. List of reagents used for immunohistochemical analysis and their contents

Reagents	Contents
10% Phosphate Buffered Formalin	10 ml 37-40% Formaldehyde (Asia Scientific, Singapore) 90 ml 1x PBS

2.2.7.3.2. Protocols

Tumours from both flanks were carefully excised and used for either flow cytometry or to prepare formalin-fixed paraffin-embedded (FFPE) tissue blocks. For flow cytometry analysis, the tumours were dissociated into single cell suspensions using the Human Tumour Dissociation Kit (Miltenyi Biotec, Bergisch Gladbach, Germany) and gentleMACS™ Octo Dissociator with Heaters (Miltenyi Biotec) according to the manufacturer's instructions. The dissociated cells were then subjected to flow cytometry analysis (as previously described in section 2.2.5.1.2.2 and 2.2.5.1.2.3) to detect the presence of injected MNC pre-labelled with CellTracker™ Blue CMAC and examine adhesion molecule expression.

To prepare FFPE tissue blocks, the tumours were rinsed once with PBS, fixed in 10% buffered formalin solution (Recipe listed in Table 2.10) overnight, and then stored in 70% ethanol before being embedded in paraffin.

2.2.8. ***In Silico Analysis***

2.2.8.1. Analysing the Promoter Region of DSG2 for Putative Hypoxia Responsive Elements (HRE)

The gene sequence encoding for DSG2 is obtained through The Nucleotide database of The National Centre for Biotechnology Information (NCBI; https://www.ncbi.nlm.nih.gov/nuccore; NCBI Reference Sequence: NG_007072.3). The sequence of the first exon was confirmed via Ensembl (http://www.ensembl.org/index.html; (Aken et al. 2016)). The sequence preceding the first exon is considered as the promoter region. A search was performed to identify potential HIF-1 binding hypoxia response elements with the consensus sequence of 5' (A/G)CGTG 3' within this region (Semenza 1998).

2.2.8.2. The Cancer Genome Atlas (TCGA) Analysis

Analysis of The Cancer Genome Atlas (TCGA) to examine gene expression of various adhesion molecules and chemokines within melanoma patient samples was performed by a laboratory member, Mr Brenton Ebert (Centre for Cancer Biology, Adelaide, South Australia, Australia). The materials and methods for this analysis provided by Mr Brenton Ebert are as follows:

The RNA sequencing data from TCGA melanoma dataset (Akbani et al.) was downloaded from the Data Portal at http://cancergenome.nih.gov/. Gene expression values were extracted in R using the edgeR package from Bioconductor.

2.2.9. ***Statistical Analysis***

All statistical analyses were performed using GraphPad Prism (GraphPad Software, San Diego, California, USA). Analyses were performed using two-tailed paired t-tests or one way repeated measures ANOVA wherever suitable. Bonferroni's Multiple Comparison Test was performed to compare individual groups. Results with $p < 0.05$ were considered to be

statistically significant, with * = $p < 0.05$, ** = $p < 0.01$, *** = $p < 0.001$ indicated on the graphs and figure legends.

Chapter 3. Regulation of Melanoma VM: Role of Desmoglein 2

3.1. Introduction

3.1.1. *General Introduction*

Melanoma is a disease that originates from melanocytes. In order to progress, melanoma tumours require an expansion of the pre-existing vasculature to increase nutrient and oxygen supply. While our current knowledge of tumour vascularisation is mainly focused on angiogenesis (the sprouting of EC-lined blood vessels), there is a growing interest in an alternative form of vessel formation known as vasculogenic mimicry (VM). As described in detail in Chapter 1, VM is the phenomenon whereby cancer cells mimic EC behaviour and align along a deposited basement membrane to form vessel-like structures capable of conducting blood. The occurrence of VM in melanoma is associated with decreased patient survival. This Chapter focuses on characterising the role of a cadherin, desmoglein 2 (DSG2), in mediating melanoma VM.

3.1.2. ***Desmoglein 2 (DSG2)***

3.1.2.1. DSG2 as a desmosome forming cadherin

Desmoglein 2 (DSG2) is one of the four isoforms of desmogleins (DSG1-4) that belong to the larger family of desmosomal cadherins, which are calcium dependent transmembrane cell adhesion molecules. DSG2 was initially described to be expressed on epithelial cells and cardiomyocytes (Schafer, Koch & Franke 1994), where it performs its canonical function in the formation of cell-cell adhesion complexes known as demosomes (Figure 3.1). The extracellular domain of DSG2 binds both homotypically with other DSG2 molecules and heterotypically with another desmosomal cadherin desmocollin (DSC2) expressed on adjacent cells to link both cells together, while the intracellular domain of DSG2 interacts with the Armadillo family proteins plakoglobin and plakophilin to anchor the bound adjacent cells to the intermediate filament cytoskeleton network (Figure 3.1) (reviewed in (Brooke, Nitoiu & Kelsell 2012)). Such structures allow epithelial tissues to experience and withstand mechanical stress. The importance of DSG2 in desmosome formation has been especially demonstrated in the heart where DSG2 is the only desmoglein isoform that is expressed (Pilichou et al. 2006). Mutations in DSG2 leading to defects in desmosome formation result in the occurrence of arrhythmogenic right ventricular cardiomyopathy, a heart disease characterised by the excessive dilation of the ventricles, infiltration of fat and occurrence of

fibrosis which eventually displaces the cardiomyocytes (Krusche et al. 2011; Pilichou et al. 2006).

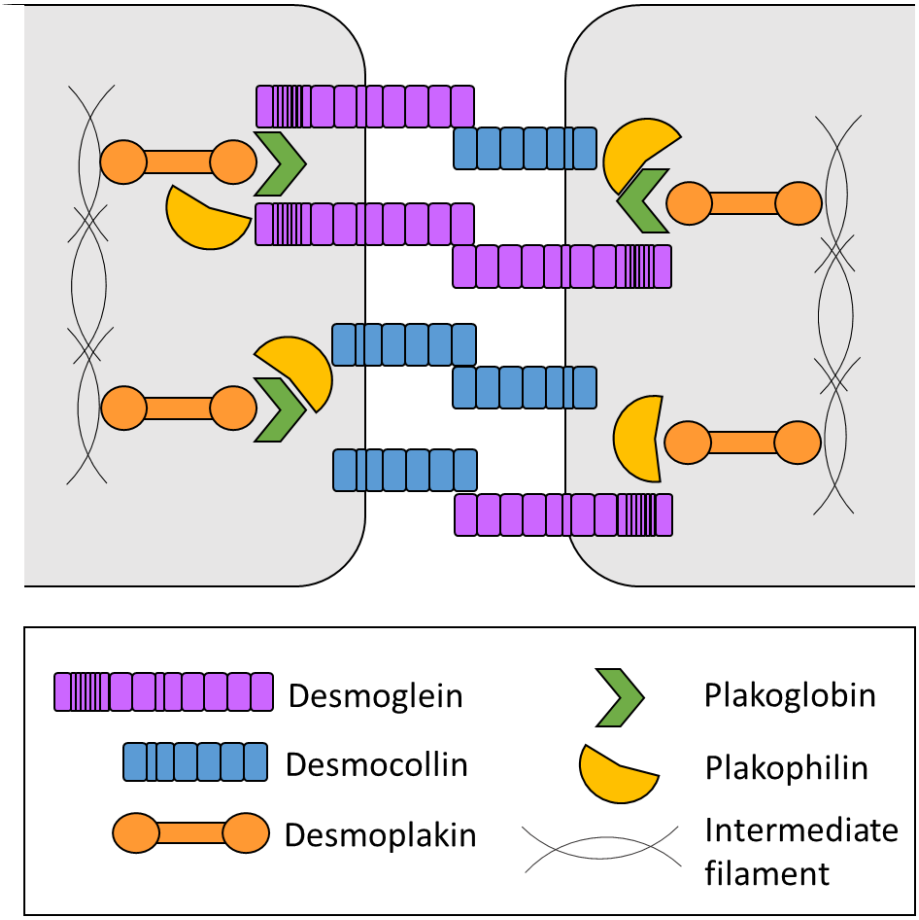

Figure 3.1. Schematic diagram of desmosomes.

Desmosomes are cell-cell adhesion structures that are present in epithelium and myocardium. Desmogleins and desmocollins bind both homotypically and heterotypically through their extracellular domains to link adjacent cells together. Their intracellular domains in turn bind to the Armadillo family proteins plakoglobin and plakophillin linked to desmoplakin to anchor the structure to intermediate filaments.

3.1.2.2. Roles of DSG2 outside of desmosome function

Since its first description as a desmosomal cadherin, DSG2 has been recognised to have other biological roles outside of desmosome formation. One important function of DSG2 is the regulation of cellular proliferation. The first documentation of *Dsg2*$^{-/-}$ mice suggested that loss of *Dsg2* causes embryonic lethality at the time of blastocyst implantation due to defects in embryonic stem cell viability and proliferation (Eshkind et al. 2002). Notably, this study also suggested that Dsg2 participates in non-desmosomal junctional adhesion of embryonic stem cells and that lethality is background strain dependent (Eshkind et al. 2002). While not assessed in the same study, this impaired proliferation may be associated with changes in cellular signalling, as later studies revealed that DSG2 downregulation in both colon cancer cells and keratinocytes suppressed epidermal growth factor receptor (EGFR)-dependent cell proliferation (Kamekura et al. 2014; Overmiller et al. 2016). More specifically, DSG2 knockdown led to a reduction in EGFR internalisation and changes in phosphorylation of downstream signalling molecules which led to reduced EGFR signalling (Kamekura et al. 2014). In support of these findings, transgenic mice wherein keratinocytes overexpressed Dsg2 exhibited enhanced EGFR-dependent proliferation (Brennan et al. 2007).

In addition to regulating cell proliferation, DSG2 has also been found to regulate apoptosis. Keratinocytes overexpressing Dsg2 in transgenic mice were found to be resistant to contact dependent apoptosis (anoikis) (Brennan et al. 2007). This was further enhanced with EGFR signalling stimulation, and inhibited with NF-κB signalling inhibitors.

Another relatively newly reported role of DSG2 that is of great relevance to this study is its role in regulating angiogenesis. Our group has recently shown that reduced expression of Dsg2 in mice (Dsg2$^{lo/lo}$) resulted in aberrant formation of blood vessels with altered morphology and compromised barrier integrity (Ebert et al. 2016). The underlying mechanism was further investigated *in vitro* with the bone marrow EC line TrHBMEC. Small interfering RNA (siRNA)-mediated knockdown of DSG2 on TrHBMEC led to significantly impaired vessel formation on the Matrigel tube formation assay. An adhesion assay performed on these cells revealed impaired cell-cell adhesion, highlighting that DSG2 can participate in homotypic cell-cell adhesion outside of desmosomes (Ebert et al. 2016). Further to that, enhanced invasion and migration following DSG2 knockdown was observed.

DSG2 has also been shown to regulate actin stress fibre formation. The two important cell cytoskeletal structures which F-actin can assemble into are stress fibres and cortical fibres

(Prasain & Stevens 2009). Stress fibres extend throughout the cell and generate tensions within the cell. Cells anchor to focal adhesions formed between neighbouring cells and the extracellular matrix through actin stress fibres to generate pulling forces required for cell migration during angiogenesis. These structures are also important in generating inward pulling forces which, when greater than the outward pulling forces, result in increased cell-cell permeability. The formation of cortical fibres on the other hand limits the availability of F-actin to assemble into stress fibres. Our study revealed an increase of stress fibre formation following DSG2 knockdown, which could explain the enhanced permeability of blood vessels observed in $Dsg2^{lo/lo}$ mice (Ebert et al. 2016). A role for DSG2 in angiogenesis has also been reported by another group (Giusti et al. 2013). siRNA-mediated downregulation of DSG2 in human microvascular ECs impaired the formation of actin stress fibres, resulting in impaired tube formation on Matrigel. Further to that, there was also a loss in DSG2-integrin β8 complex formation required to trigger signalling pathways important in driving angiogenesis. These findings highlight the complexity of angiogenesis, and how DSG2 can influence this process through the regulation of multiple processes critical in blood vessel formation.

Taken together, there is mounting evidence that, in addition to the canonical role of cell-cell adhesion via desmosomes, DSG2 contributes to the regulation of numerous biological processes, including angiogenesis.

3.1.2.3. Regulation of DSG2 expression

The specific pathways by which the expression of DSG2 is regulated remain largely unclear. There are however some hints that we can draw from some of our published findings. In particular, we have done extensive work on characterising DSG2 expression on hematopoietic stem cells, mature leukocytes, endothelial progenitor cells and ECs (Ebert et al. 2016). Our work revealed a downregulation of DSG2 expression as hematopoietic stem cells differentiate down different lineages to form mature leukocytes (Ebert et al. 2016). DSG2 expression is also reduced on ECs compared to their progenitor counterparts (Ebert et al. 2016). As will be discussed below, this reduction of DSG2 expression with increased stem cell differentiation is also observed in other cell types, such as melanocytes. These observations suggest that DSG2 can be transcriptionally regulated, although the exact transcription factor or factors responsible remain to be elucidated. We however have unpublished information that the Kruppel-like factor 2 and 4 (KLF2/4) transcription factors

may be involved in regulating Dsg2 expression (Jain and Bonder, unpublished). Interestingly, KLF2/4 are known to be primary regulators of EC genes (Villarreal et al. 2010), which further links the emerging roles of DSG2 in angiogenesis.

Apart from transcriptional regulation, there are also some studies describing how the levels of surface DSG2 can be altered during certain cellular processes. For example, EGFR signalling has been found to promote internalisation of DSG2 from the cellular surface (Klessner et al. 2009). The internalised DSG2 is then cleaved by metalloproteinases (MMP) and ADAM family proteases, thereby resulting in a reduction in intercellular adhesion (Klessner et al. 2009). Another study showed that overexpression of the transcription factor Snail in human squamous cell carcinoma increased the internalisation of DSG2, which in turn promoted the occurrence of epithelial mesenchymal transition and increased cell migration (Kume et al. 2013). Interestingly, EGFR signalling has been found to promote Snail expression (Hipp et al. 2009), thereby linking the relevance of these two molecules in regulating DSG2 expression. While these studies describe the pathways involved in downregulating DSG2 expression, there is currently not much known about how DSG2 can be overexpressed, which as will be discussed below, occurs in melanoma.

3.1.2.4. DSG2 in melanoma

DSG2 has been found to be expressed in some nevi, primary melanoma as well as melanoma metastases via immunofluorescence and immunohistochemical analysis of melanoma tissue microarrays and full tissue samples from both our group and other laboratories (Rickelt et al. 2008; Schmitt et al. 2007; Tan et al. 2016). However, immunofluorescence analysis of normal skin revealed a lack of DSG2 protein expression in melanocytes (Rickelt et al. 2008; Tan et al. 2016). Further analysis of publically available microarray data performed by our laboratory revealed a gradual downregulation of *DSG2* gene expression as embryonic stem cells differentiate into melanocyte precursors and subsequently mature melanocytes (Tan et al. 2016). This suggests that DSG2 is abnormally upregulated in melanoma. More importantly, analysis of melanoma patient gene expression datasets within The Cancer Genome Atlas (TCGA) confirmed that *DSG2* expression is strongly correlated with poor prognosis in patients (Tan et al. 2016), thereby suggesting the potential of DSG2 in regulating melanoma progression. Further analysis of patient samples confirmed the lack of expression of other components involved in desmosome formation, which excludes the possibility of DSG2 exerting its canonical role in mediating desmosome formation. Indeed, to the best of our

knowledge, melanoma has not been reported to form desmosome structures. Together, this suggests that DSG2 may be involved in regulating non-canonical functions in melanoma cells. One study showed that DSG2 knockdown in melanoma cell lines resulted in overexpression of genes associated with cell migration, TGF-β receptor signalling and cell adhesion (Peitsch et al. 2014). This translated to an increase in cell migration towards a serum gradient (Peitsch et al. 2014). However, this function was associated with decreased DSG2 levels, as opposed to the increased expression observed in melanoma disease and does not explain the acquired benefits of DSG2 upregulation in melanoma disease progression. Clearly, further investigation is required to better understand the role of DSG2 in melanoma.

3.2. Hypothesis and Aims

Given the role of DSG2 in mediating angiogenesis, and based on the observation that VM shares similar pathways with angiogenesis and our observation that DSG2 is overexpressed in melanoma, it is hypothesised that **DSG2 is a novel regulator of melanoma VM**. The aims to address this hypothesis are to:

1) Examine the role of DSG2 in regulating melanoma VM
2) Examine the mechanism by which DSG2 regulates VM, by assessing the role of DSG2 in regulating melanoma cell proliferation, cytoskeletal rearrangement, migration and cell-cell adhesion

It is expected that changes in DSG2 expression will affect melanoma cell function and in turn influence VM formation.

3.3. Results

Previous work in the laboratory had identified several melanoma cell lines which express high levels of DSG2, including C32, CHL-1 and SK-Mel-28. To confirm DSG2 expression levels, the keratinocyte cell line HaCaT which also expresses high levels of DSG2 were included as a comparator cell line. As demonstrated in Figure 3.2A, flow cytometric analysis performed on cells positively stained with an anti-human DSG2 antibody confirmed that melanoma cells expressed DSG2 on the cell surface at levels similar to the HaCaT keratinocyte cell line. This was also confirmed through immunofluorescence staining as demonstrated in Figure 3.2B. In particular, DSG2 appeared to be diffused across the melanoma cells, which is in accordance with previous reports (Schmitt et al. 2007). This distribution is different to that of HaCaT keratinocytes, where DSG2 was observed to be punctate and localised to intercellular junctions where it is involved in desmosome formation. This suggests that DSG2 is playing a role outside of desmosome formation on melanoma cells.

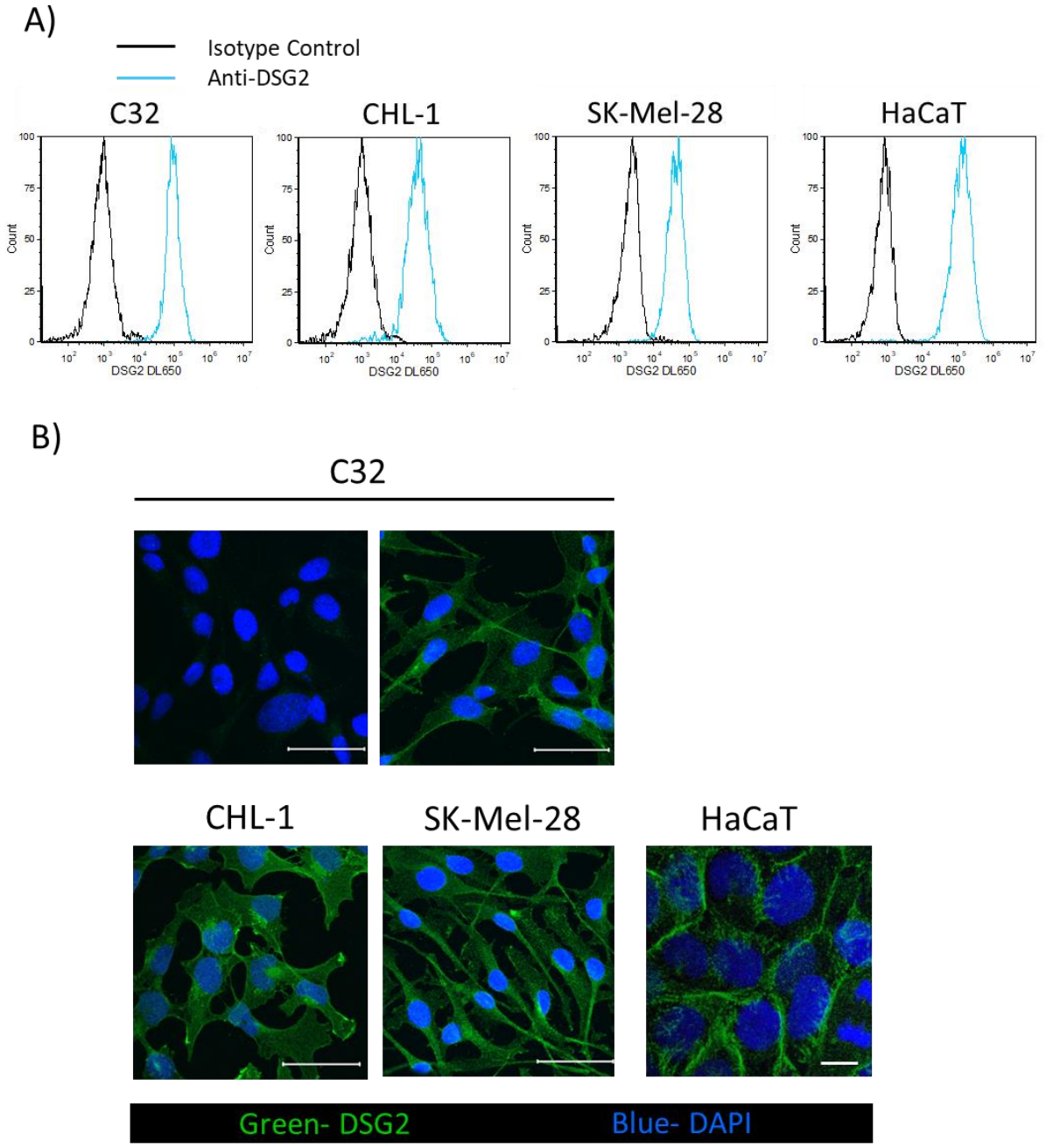

Figure 3.2. The human melanoma cell lines C32, CHL-1 and SK-Mel-28 express DSG2. (Immunofluorescence image for HaCaT keratinocytes kindly provided by Dr Lisa Ebert).

(A) C32, CHL-1 and SK-Mel-28 were stained with either an anti-DSG2 or an isotype matched control, followed by a secondary DyLight® 650 antibody and subjected to flow cytometric analysis. 7-AAD was included in the antibody mastermix to allow dead cells (7-AAD$^+$) to be gated out from analysis. HaCaT keratinocytes were included as a positive control. Representative histograms showing DSG2 expression on the respective cell lines for n≥3 independent experiments. (B) Immunofluorescence staining was performed on fixed and permeabilised C32, CHL-1 or SK-Mel-28 cells grown on coverslips with either an anti-DSG2 or an isotype matched control, followed by a secondary Alexa Fluor 488 antibody. HaCaT keratinocytes were included as a positive control. Representative images shown from n≥3 independent experiments. Scale bars for C32, CHL-1 and SK-Mel-28= 50 µm, scale bar for HaCaT= 10 µm.

Next, the DSG2$^+$ melanoma cell lines were subjected to a Matrigel tube formation assay to assess their VM capabilities. This involves seeding the cells onto Matrigel, a gelatinous substance derived from mouse sarcoma, which is rich in extracellular matrix components important for supporting vessel formation. It is an assay well established to assess EC vessel forming capacity *in vitro* that is reflective of their blood vessel forming capabilities *in vivo* (Ponce 2009), and has also been adapted to assess VM formation by cancer cells (Francescone Iii, Faibish & Shao 2011). VM structures are stringently defined as elongated structures formed by multiple cells in intimate association extending from cell clusters. It has been previously demonstrated that these *in vitro* VM structures are hollow and can be perfused with dye (Hendrix, MJ et al. 2003; Sood et al. 2001), thereby indicating their resemblance with vessels *in vivo*. As demonstrated in Figure 3.3, the DSG2$^+$ melanoma cell lines grew as monolayers on cell culture plastic. Following seeding onto Matrigel, these cells actively rearranged and organised into networks of elongated VM structures extending from cell clusters formed by multiple intimately associated cells within the course of 4-6 hours, thereby highlighting their VM capability.

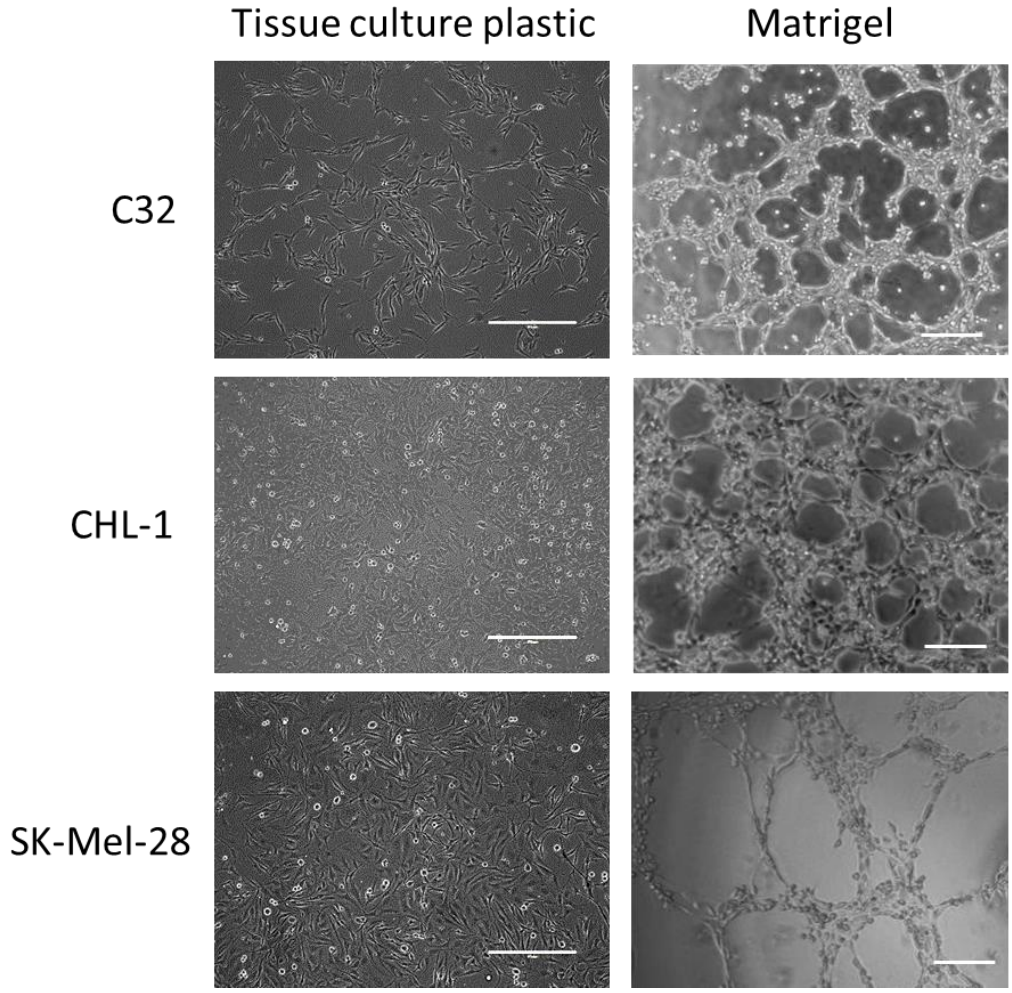

Figure 3.3. C32, CHL-1 and SK-Mel-28 form VM structures when seeded on Matrigel.

C32, CHL-1 and SK-Mel-28 melanoma cells were grown on tissue culture plastic under normal conditions. Images of these cells taken using a 10x objective lens were included here as comparison. To assess their tube formation capabilities, the cells were harvested and seeded onto Matrigel® growth factor reduced basement membrane matrix. After 3-6 hours, multiple images across the whole well were taken using a 4x objective lens. Representative Matrigel images shown from n≥3 independent experiments. Scale bars for cells cultured on tissue culture plastic= 400 µm, scale bars for Matrigel images = 200 µm.

To investigate the role of DSG2 and its potential function in regulating VM in melanoma, a range of cellular properties was compared between melanoma cells expressing usual levels of DSG2 and those with reduced DSG2 expression. The approach to reduce DSG2 expression was through transient transfection with three distinct DSG2-targeting siRNAs. A time course study was first performed to determine the optimal time-point for DSG2 knockdown for each cell line (results not shown). The results revealed that DSG2 knockdown was optimal for CHL-1 at 48 hours post transfection, and optimal for both C32 and SK-Mel-28 at 72 hours post transfection. Therefore, these time points were selected for further assays. As shown in Figure 3.4A, in comparison to the cells transfected with a control siRNA (referred to hereon as control cells), the cells transfected with either one of three siRNAs targeting DSG2 (referred to hereon as DSG2 knockdown (KD) cells) had significantly reduced DSG2 protein expression at the aforementioned timepoints post transfection when assessed via flow cytometry. Importantly, 7-AAD analysis revealed that viability of the cells was not affected following DSG2 knockdown (Figure 3.4B), indicating that any effect observed downstream of DSG2 knockdown is unlikely to be due to impaired cell viability.

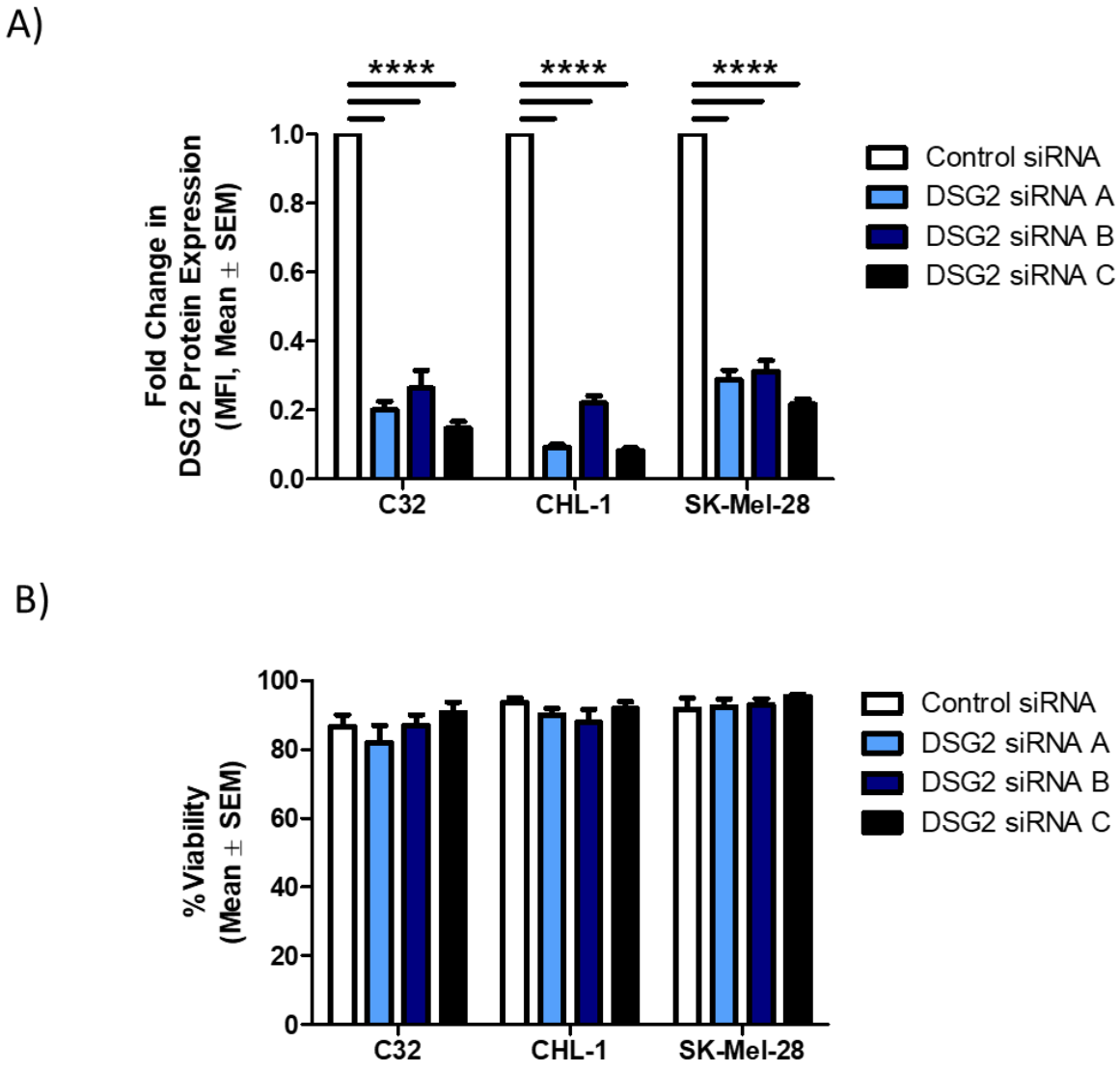

Figure 3.4. DSG2 expression can be downregulated with siRNA transfection.

C32, CHL-1 and SK-Mel-28 cells were transfected with either a control siRNA or one of three siRNAs targeting DSG2. After 48-72 hours, the transfected cells were harvested and stained with either an anti-DSG2 or an isotype matched control, followed by a secondary DyLight® 650 antibody and subjected to flow cytometric analysis. 7-AAD was included in the antibody mastermix to determine cell viability. (A) The DSG2 protein expression was quantified by assessing the mean fluorescence intensity (MFI) within viable cells and presented as a fold change over that of control cells. Bar graph shows mean fold change in DSG2 protein expression (MFI) (normalised over isotype control) ± SEM for n≥3 independent experiments. *** = $p < 0.0001$, two-tailed paired t-test. (B) The viability of transfected cells was assessed with 7-AAD. Bar graph shows percentage (%) of viable (7-AAD-) transfected cells ± SEM for n≥3 independent experiments. Two-tailed paired t-test.

The transfected cells were subjected to Matrigel tube formation assays to assess the effect of DSG2 knockdown on VM capabilities. As shown in Figure 3.5A, the control cells retained their ability to form networks of elongated VM structures formed by multiple intimately associated cells extending from cell clusters like that of the untransfected cells (shown previously in Figure 3.2). This however was impaired on DSG2 KD cells. In particular, the majority of cells transfected with DSG2 siRNA A and DSG2 siRNA B remain scattered as single cells or cell clumps. While cells transfected with DSG2 siRNA C were still able to form some elongated structures, these were generally thin extensions from single cells and were not part of an extensive network like that of the control cells. Quantification of the VM structures formed confirmed that DSG2 KD cells formed significantly less VM structures than the control cells (Figure 3.5B). This indicated that DSG2 plays a role in regulating melanoma VM *in vitro*.

A)

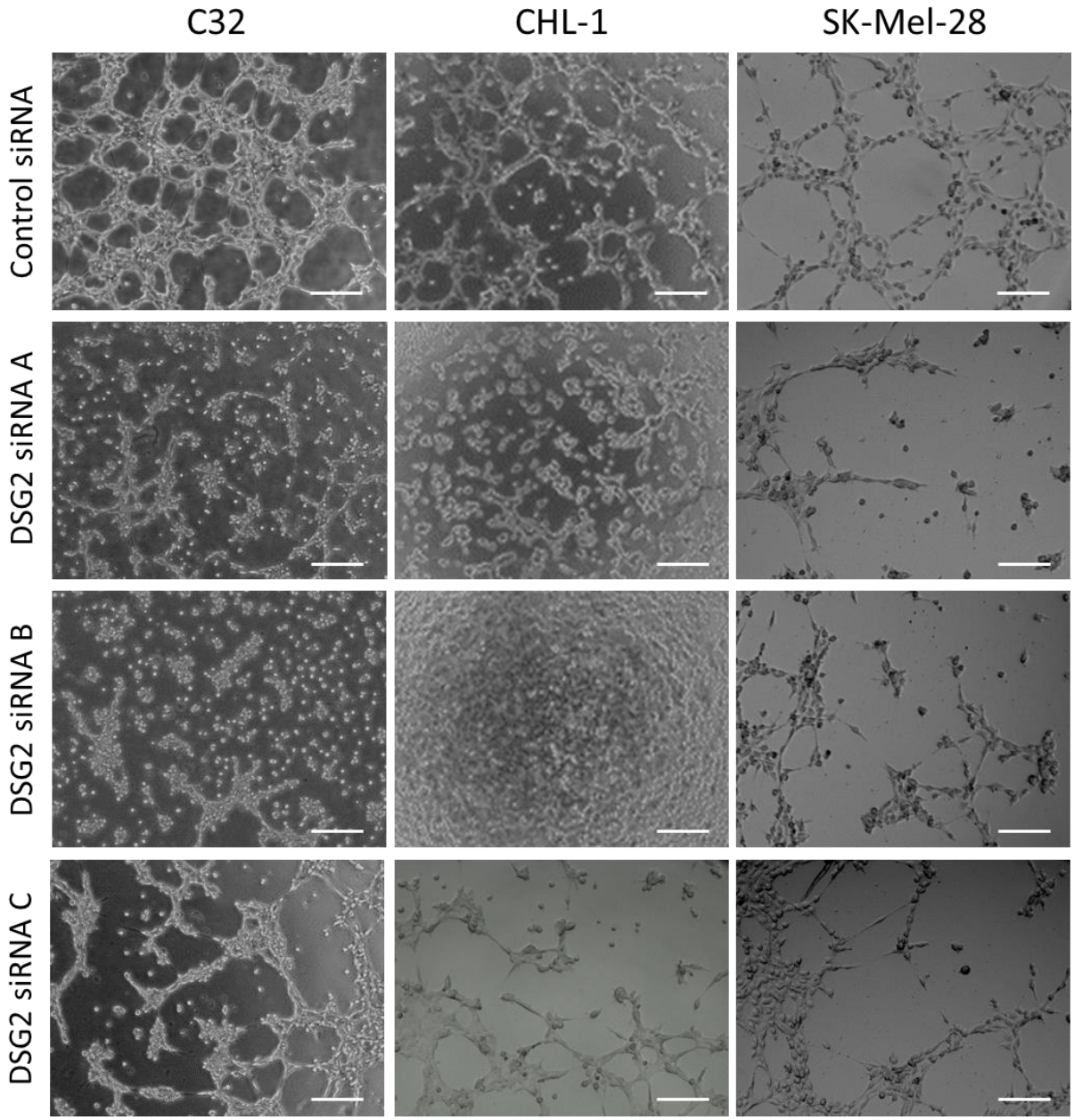
C32
CHL-1
SK-Mel-28
Control siRNA
DSG2 siRNA A
DSG2 siRNA B
DSG2 siRNA C

B)

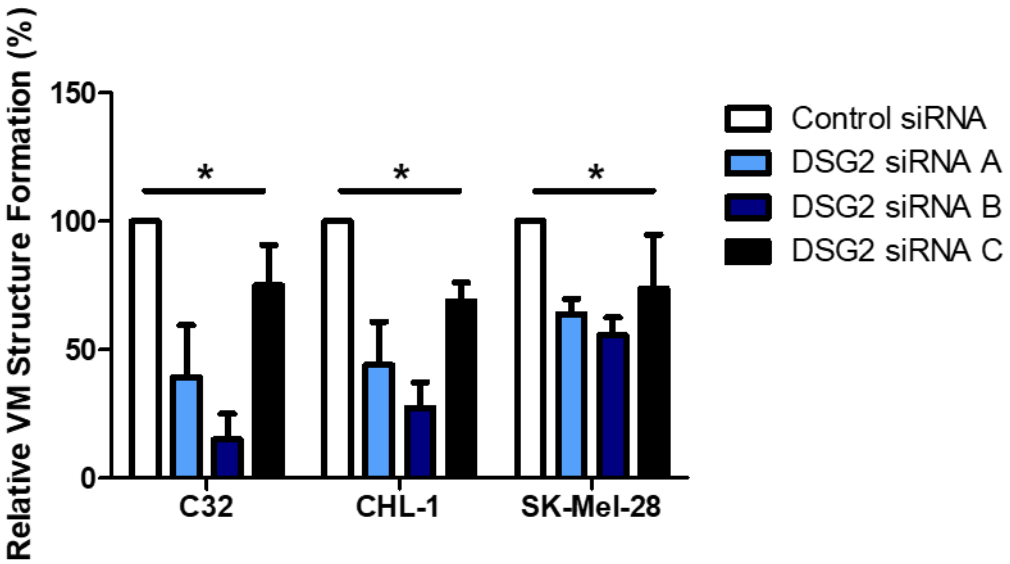

Figure 3.5. DSG2 knockdown leads to disruption of melanoma VM formation.

(A) C32, CHL-1 and SK-Mel-28 transfected with either a control siRNA or one of three siRNA targeting DSG2 were harvested and seeded onto Matrigel growth factor reduced basement membrane matrix. After 3-6 hours, multiple images across the whole well were taken using a 4x objective lens. Representative Matrigel images shown from n≥3 independent experiments. Scale bars= 200 µm. (B) Matrigel images taken across the whole well were merged and blinded. The number of VM structures formed, stringently defined as elongated structures extending from cell clusters formed by multiple cells in intimate association were quantified manually and presented as a fold change over that of control cells. Bar graph shows mean percentage of VM structure formation ± SEM for n≥3 independent experiments. * = $p < 0.05$, one way ANOVA.

To assess the mechanism by which DSG2 regulates VM, the effects of DSG2 knockdown on melanoma cell proliferation, cytoskeleton rearrangement, migration and cell-cell adhesion were assessed, as these are key processes which underlie vessel formation (reviewed in (Chung, Lee & Ferrara 2010)). As discussed in the introduction, DSG2 has also been found to regulate each of these processes in different cell types, although not necessarily in melanoma.

WST-1 assays were performed to assess the effects of DSG2 knockdown on cell proliferation. WST-1 is a tetrazolium salt that is cleaved by viable cells to form a soluble purple formazan dye that can be detected using a spectrophotometer, and is widely used as an indirect measure of proliferation. As demonstrated in Figure 3.6, for the majority of cell lines and siRNAs used, the relative absorbance values did not significantly differ between the control and DSG2 KD cells, indicating that DSG2 knockdown did not affect melanoma cell proliferation, at least over the short-term. There was however a significant downregulation of proliferation observed for CHL-1 and SK-Mel-28 cells transfected with DSG2 siRNA A. As will be addressed further in the discussion, given that this was only observed following transfection with one of the three DSG2 targeting siRNAs, the reduced proliferation observed on the CHL-1 and SK-Mel-28 was highly likely due to off-target effects. For this reason, DSG2 siRNA A was omitted from the subsequent assays.

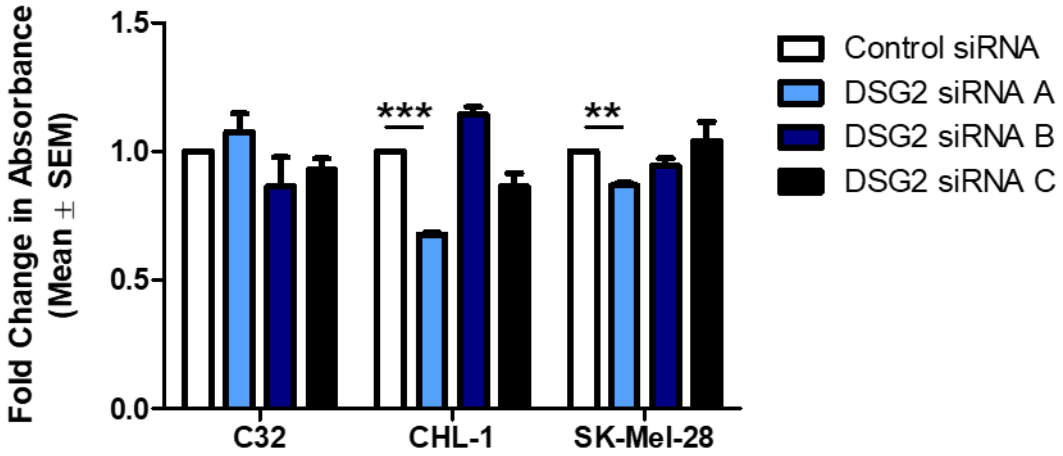

Figure 3.6. DSG2 knockdown does not affect melanoma cell proliferation.

C32, CHL-1 and SK-Mel-28 transfected with either a control siRNA or one of three siRNAs targeting DSG2 were seeded into 96 well plates. After 48-72 hours, WST-1 proliferation reagent was added into the wells. Following a 90-minute incubation, the absorbance values of the samples were measured using a spectrophotometer at 450 nm and presented as a fold change over that of control cells. Bar graphs show mean fold change in absorbance ± SEM for n=3 independent experiments. **= $p < 0.005$, ***= $p < 0.001$, two-tailed paired t-test.

To assess cytoskeletal changes following DSG2 knockdown, the transfected cells were subjected to immunofluorescence staining with both DSG2 and rhodamine phalloidin, a reagent that binds to F-actin. As briefly discussed in the introduction, F-actin is the building block of both stress fibres, which extend throughout the cell, and cortical fibres, which accumulate around the cell periphery (Prasain & Stevens 2009). Changes in the balance between stress fibres and cortical fibres affect cellular functions such as cell migration. As demonstrated in Figure 3.7, while the different cell lines had distinct stress fibre profiles and cell morphology under control conditions, these characteristics did not appear to change further with DSG2 knockdown. This suggests that DSG2 knockdown did not affect melanoma cell actin cytoskeleton structures.

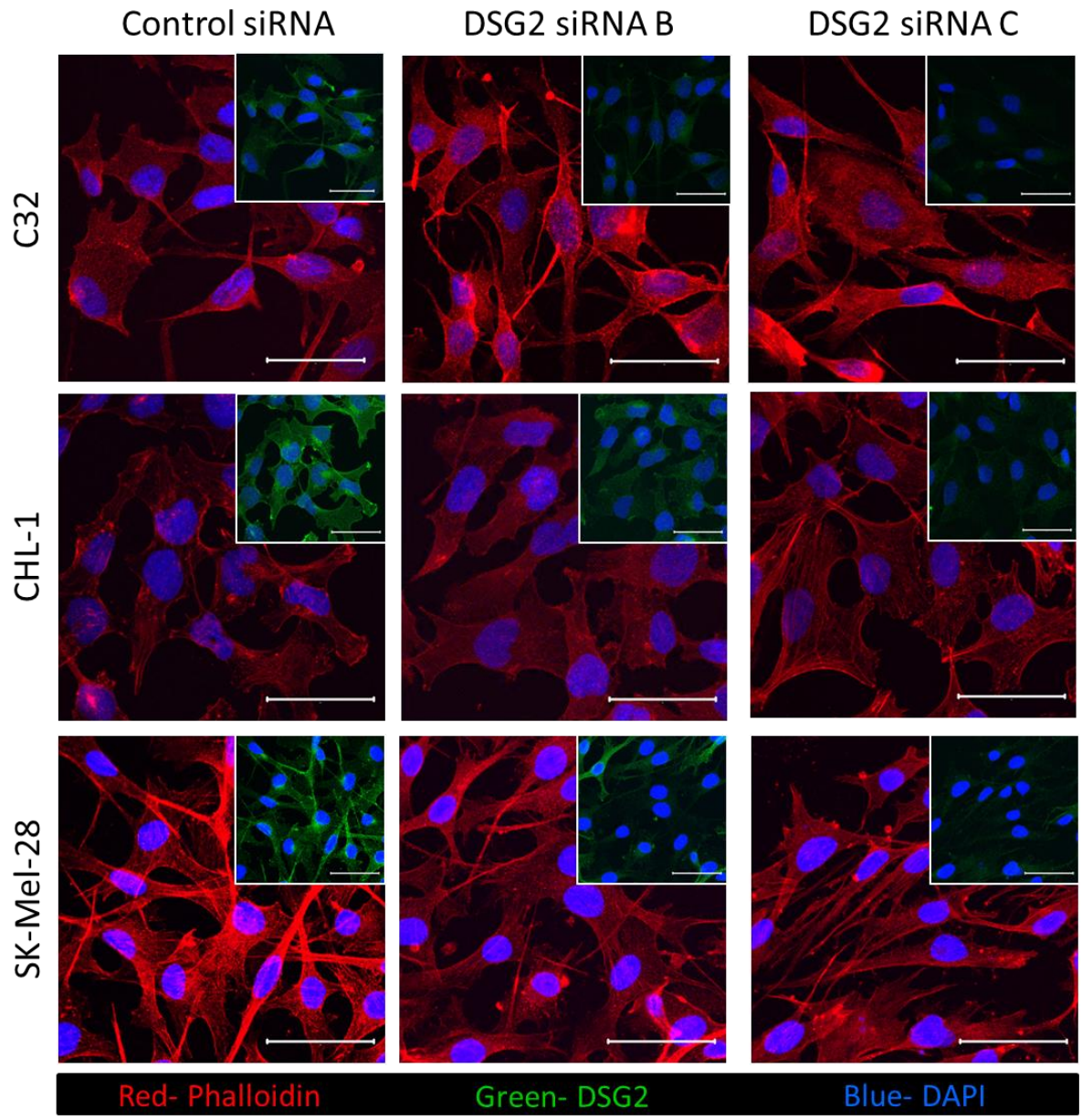

Figure 3.7. DSG2 knockdown does not alter melanoma cell actin cytoskeleton structure.

C32, CHL-1 and SK-Mel-28 cells transfected with either a control siRNA or one of two siRNAs targeting DSG2 were grown on coverslips, fixed and permeabilised. Immunofluorescence staining was performed with either an anti-desmoglein 2 or an isotype matched control, followed by a secondary Alexa Fluor 488 antibody and rhodamine phalloidin. Insets show DSG2 staining of cells. Representative images shown from n≥3 independent experiments. Scale bars= 50 µm.

Two approaches were taken to assess the effect of DGS2 knockdown on cell migration. The first approach was via xCELLigence assays (Figure 3.8). This method involves seeding transfected cells in serum free medium into the upper chamber of specialised CIM-16 plates, with the lower chamber filled with complete medium containing serum (Figure 3.8A). As the cells migrate across the serum gradient, they come into contact with the gold microelectrodes in between the chambers. This generates real time electrical impedance measurements which are represented as cell index values. An increase in cell index will then reflect an increase in cell migration. However, it is important to note that the impedance measurement is also confounded by other cellular properties, such as cell morphology and cell adhesiveness. As demonstrated in Figure 3.8B, when the assay was initially performed on CHL-1 cells, it was observed that DSG2 knockdown led to an increase in cell index, suggesting enhanced cell migration. However, while subsequent assays on the same cell line showed a similar trend, there was an overall lack of reproducibility of these assays as reflected in the massive error bars (Figure 3.8C). This was also observed when the transfected cells were serum starved overnight prior to the assay to synchronise the cell cycle and eliminate any potential differences in cell proliferation which would affect the impedance measurements (results not shown). When the assay was performed on the other two melanoma cell lines C32 (n=1) and SK-Mel-28 (n=2), there appeared to be no reproducible changes in cell migration with DSG2 knockdown (Figure 3.8C). While the presence of any inherent flaws within the experimental system itself could not be excluded due to the lack of a positive control, given the overall irreproducibility as well as the high cost of the consumable specialised gold plated plates required for the assay, no further xCELLigence assays were performed.

Scratch wound assays were then performed as an alternative approach to assess the effect of DSG2 knockdown on cell migration. Briefly, cells were seeded into 96 well plates in at least quintuplicates and allowed to grow into a confluent monolayer. Scratches of a fixed size were made across the cell monolayer with a WoundMaker^{TM} (Essen Bioscience), and the rate of wound closure as a reflective of cell migration was measured across time. As demonstrated in Figure 3.9, the rate of wound closure across 18 hours did not significantly differ between the control cells and DSG2 KD cells. Similar results were observed when the cells were pre-treated with mitomycin C prior to the introduction of the scratch to abolish any effects of differential cell proliferation rates on the rate of wound closure (results not shown). Together, these results indicated that DSG2 did not affect melanoma cell migration.

A)

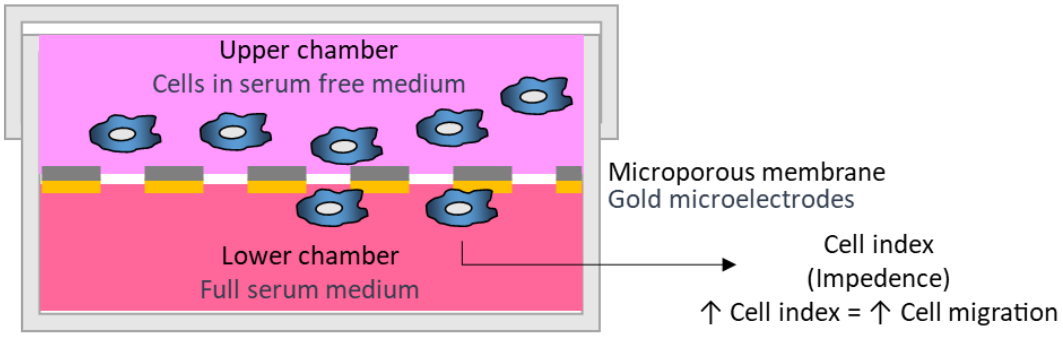
Upper chamber
Cells in serum free medium
Lower chamber
Full serum medium
Microporous membrane
Gold microelectrodes
Cell index
(Impedence)
↑ Cell index = ↑ Cell migration

B)

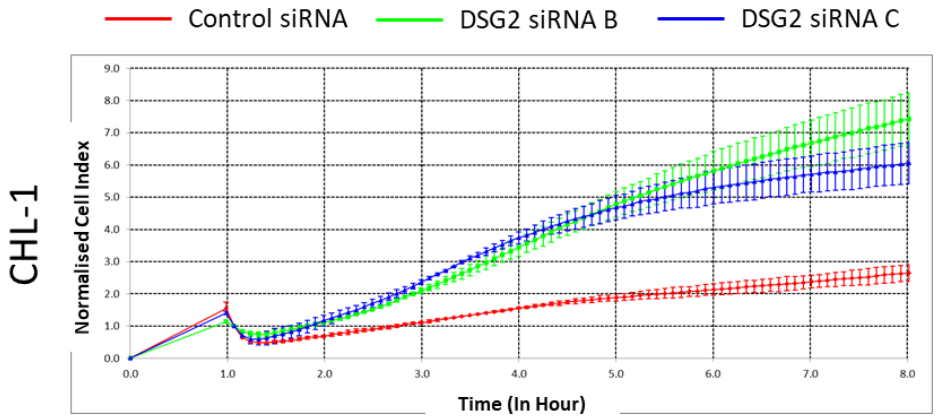
Control siRNA
DSG2 siRNA B
DSG2 siRNA C
CHL-1
Normalised Cell Index
Time (In Hour)

C)

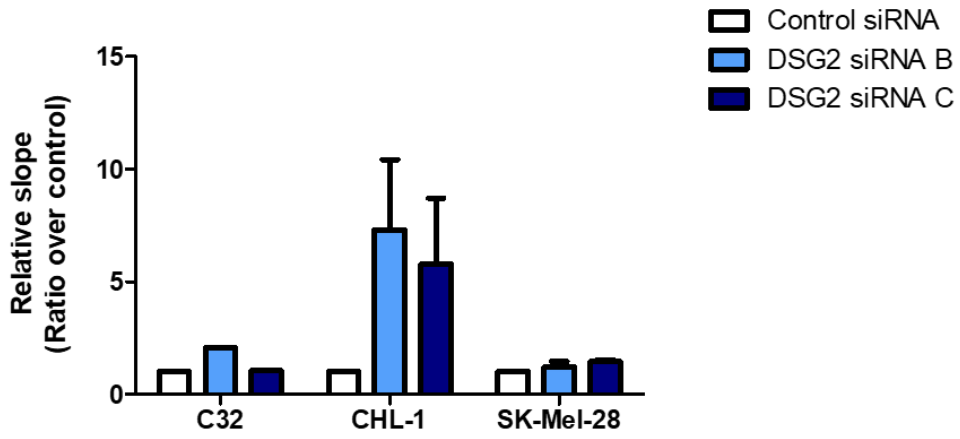
Control siRNA
DSG2 siRNA B
DSG2 siRNA C
Relative slope
(Ratio over control)
C32
CHL-1
SK-Mel-28

Figure 3.8. The xCELLigence assay does not allow for accurate measurement of melanoma cell migration.

(A) C32, CHL-1 and SK-Mel-28 transfected with either a control siRNA or one of two siRNAs targeting DSG2 were resuspended in serum free medium seeded into the upper chamber of a CIM-Plate 16, with the bottom chamber containing RF10 (medium with 10% FCS). Impedance measurements expressed as cell indices were taken at 5-minute intervals. (B) xCELLigence graph for CHL-1 showing normalised cell index against time (in hours) since start of assay; representative of n=3 experiments. (C) The slopes of the individual curves for the different treatments on the xCELLigence graph were quantified as an indication of the rate of migration. Bar graph shows mean relative slope as a ratio over control ± SEM (wherever applicable) for n=1 independent experiment for C32, n=3 independent experiments for CHL-1 and n=2 independent experiments for SK-Mel-28. Two-tailed paired t-test.

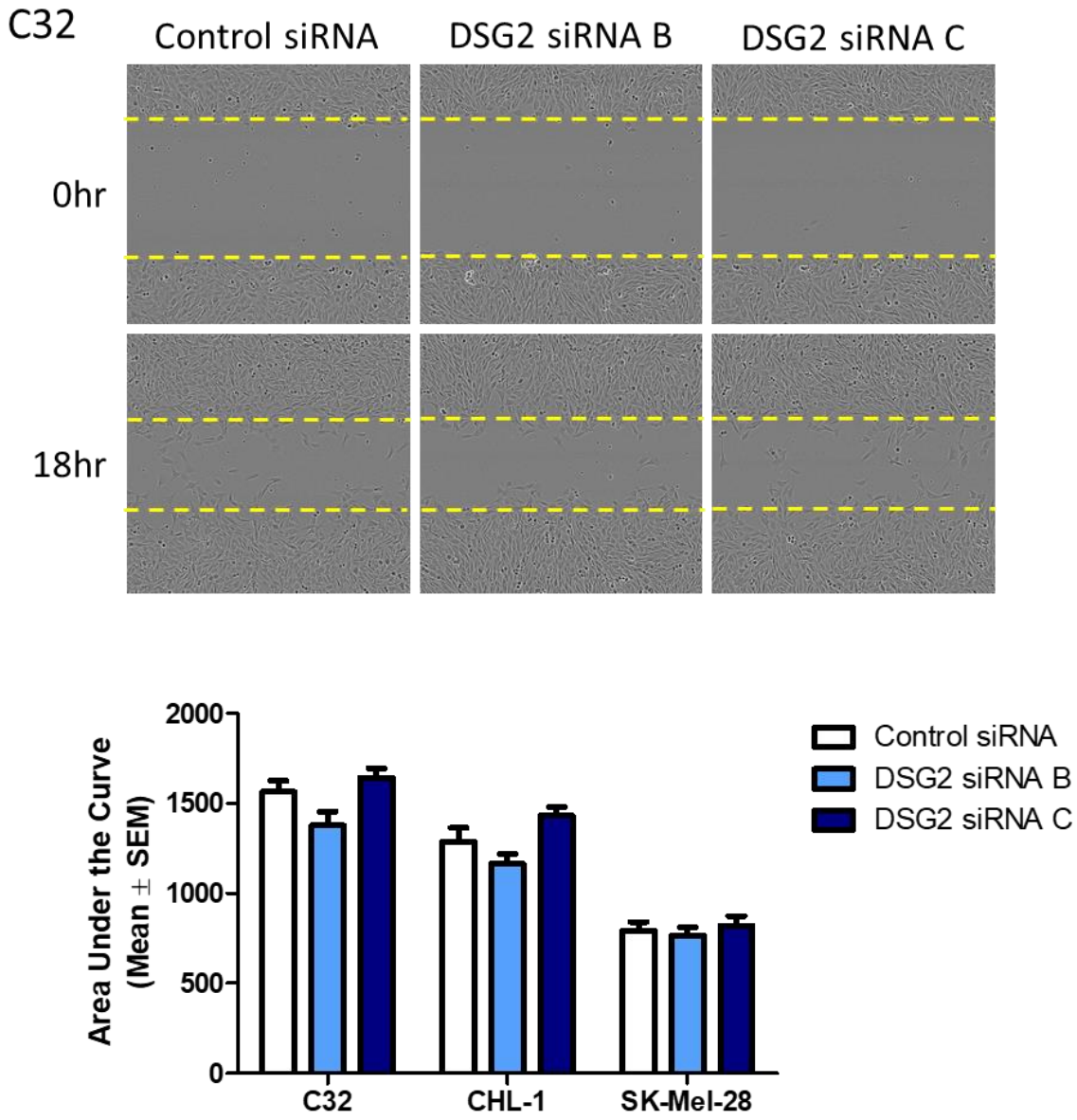

Figure 3.9. DSG2 knockdown does not affect melanoma cell migration.

C32, CHL-1 and SK-Mel-28 cells transfected with either a control siRNA or one of two siRNAs targeting DSG2 were seeded into 96 well plates and cultured to form a confluent monolayer. A scratch wound was introduced onto the monolayer and 10x images were taken every hour. Representative scratch wound images for C32 showing the scratch at 0 hours immediately after it was introduced and after 18 hours. The wound sizes across time for the individual treatments were plotted and the area under the curve was quantified as an indication of the rate of migration. Bar graph shows the mean area under the curve ± SEM for $n \geq 3$ experiments. Two-tailed paired t-test.

To assess the effects of DSG2 knockdown on cell-cell adhesion, adhesion assays were performed on the C32 cells. Briefly, as depicted in Figure 3.10A, a defined number of calcein AM-labelled transfected cells were added onto a confluent monolayer of cells transfected with the same siRNA and incubated at 37°C for 15 minutes under static conditions. The cells were then assembled onto a parallel plate flow chamber apparatus and rinsed with a constant flow of Hanks' Balanced Salt Solution (HBSS) at a shear stress of 2 dynes/cm^2 for 5 minutes to remove any cells that were not strongly bound. This method of rinsing was found to remove unbound cells in a more stringent and reproducible manner than could be achieved by manual rinsing with HBSS using a pipette (results not shown). As demonstrated in Figure 3.10B, while all the transfected C32 cells retained cell-cell adhesion, the DSG2 KD cells had significantly less cells bound to the monolayer compared to the control cells, indicating an impaired cell-cell adhesion with DSG2 knockdown. Due to time constraints, additional adhesion assays were not performed on the other two melanoma cell lines. Nonetheless, the results obtained on the C32 cell line highlights the importance of DSG2 in mediating melanoma cell-cell adhesion.

A)

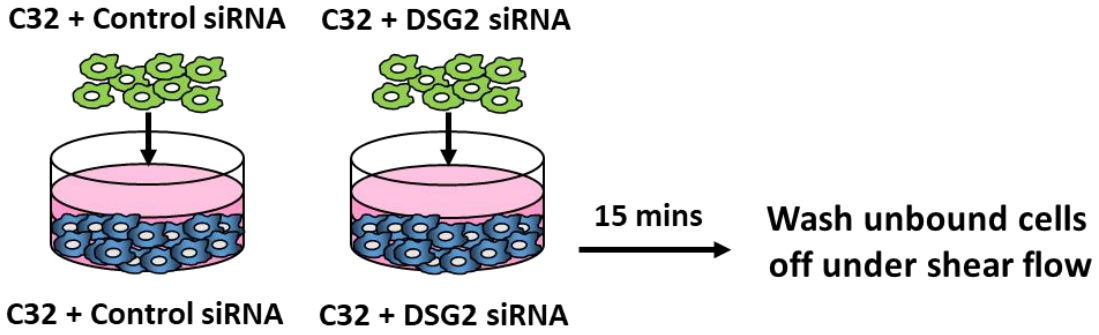
C32 + Control siRNA
C32 + DSG2 siRNA
15 mins
Wash unbound cells off under shear flow
C32 + Control siRNA
C32 + DSG2 siRNA

B)

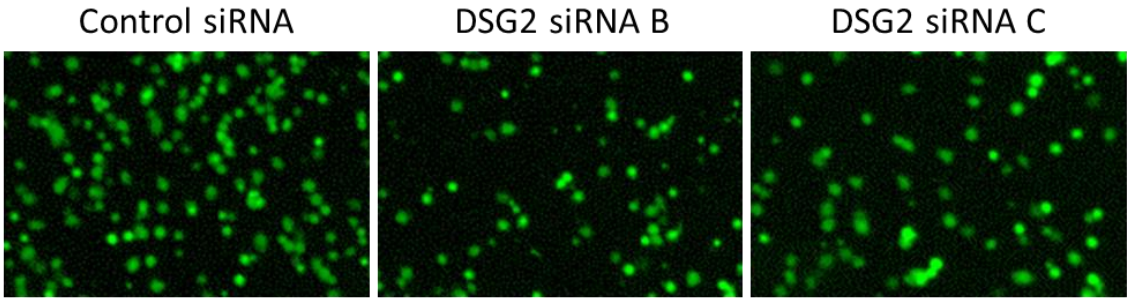
Control siRNA
DSG2 siRNA B
DSG2 siRNA C

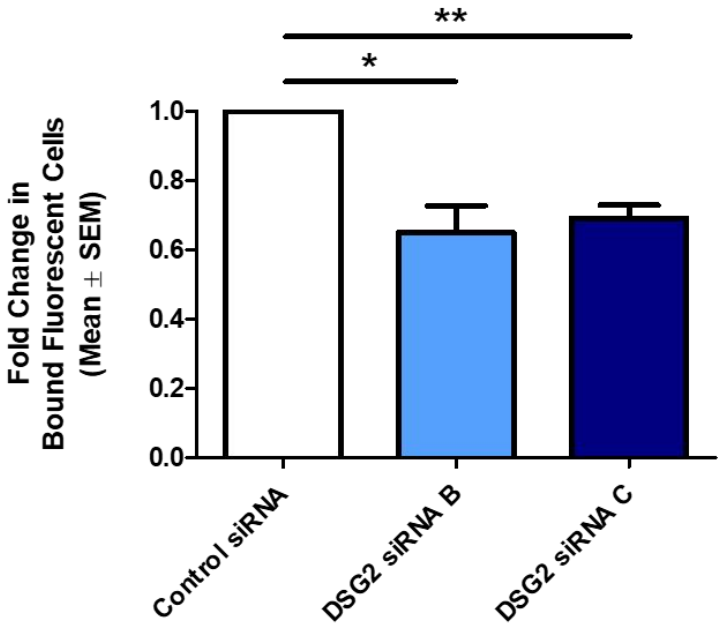
**
*
Fold Change in Bound Fluorescent Cells (Mean ± SEM)
1.0
0.8
0.6
0.4
0.2
0.0
Control siRNA
DSG2 siRNA B
DSG2 siRNA C

Figure 3.10. DSG2 knockdown impairs melanoma cell-cell adhesion.

(A) Transfected C32 cells were harvested, stained with calcein AM and then added onto a confluent monolayer of C32 cells transfected with the same siRNA. After a 15-minute incubation, any unbound cells were washed away with a HBSS flow at 2dynes/cm^2 using a parallel plate flow chamber setup. Fluorescent images for 4-5 fields of view were taken using an epifluorescent microscope with a 4x objective lens. (B) Representative fluorescent images showing adhered C32 for the different treatments for n=3 independent experiments. The number of adhered cells was quantified and presented relative to control cells. Bar graph shows mean fold change in bound fluorescent cells ± SEM for n=3 independent experiments. * = $p < 0.05$, ** = $p < 0.005$, two-tailed paired t-test.

As part of the study relevant to Chapter 4 of this thesis, RNA sequencing was performed on these three melanoma cell lines to examine differential gene expression between ambient (21% O_2) and hypoxic (0.5% O_2) culture conditions. The RNA sequencing results were also analysed to examine if *DSG2* expression was altered under hypoxic conditions (confirmation of hypoxia induction is shown in Figure 4.4 in Chapter 4). As demonstrated in Figure 3.11A, while *DSG2* gene expression remained unchanged following hypoxic stimulation for C32 and SK-Mel-28, it was significantly increased for CHL-1 cultured under 0.5% O_2 for both 3 and 7 days. This was similarly observed at the protein level when the cells were subjected to flow cytometry analysis to examine DSG2 expression (Figure 3.11B). Analysis of the promoter region of *DSG2* revealed that DSG2 has two putative hypoxic response elements (HRE) to which hypoxia inducible factors (HIF) could bind to and initiate transcription (Figure 3.12). However, given that the upregulation of DSG2 under hypoxia was only observed in one out of the three cell lines, there is also a possibility that its expression could be regulated by other molecules responsive to hypoxia rather than through direct regulation by HIF, and that these molecules are differentially expressed in the three cell lines.

Based on the literature, EGFR signalling, which is inducible under hypoxia, is involved in regulating DSG2 internalisation from the surface of the cell (Klessner et al. 2009; Wang, Y et al. 2012). The internalised DSG2 is then cleaved by ADAM proteins, including ADAM17. Further analysis of the RNA sequencing results however revealed a lack of *EGFR* expression (Figure 3.13A) and no significant changes in *ADAM17* expression (Figure 3.13B) in CHL-1 following hypoxia stimulation. Hypoxia stimulation of C32 and SK-Mel-28 also did not result in significant changes in *EGFR* and *ADAM17* expression, indicating that both *EGFR* and *ADAM17* gene expression was not regulated by hypoxia. However, it is important to assess the protein expression levels and activity levels of these molecules, which were not assessed here due to time constraints, as these are the players directly involved in regulating DSG2 internalisation and cleavage. Of note, HIF gene expression was not examined here as it has been well documented that HIF activity is regulated post-transcriptionally at the protein level and therefore cannot be accurately assessed at the mRNA level (Wenger et al. 1997).

Taken together, the findings of this Chapter demonstrate the role of DSG2 in regulating VM in melanoma cells through mediating cell-cell adhesion via homotypic DSG2 interactions. While DSG2 appeared to be upregulated in one melanoma cell line following hypoxic stimulation, the actual underlying mechanism regulating this effect remains to be elucidated.

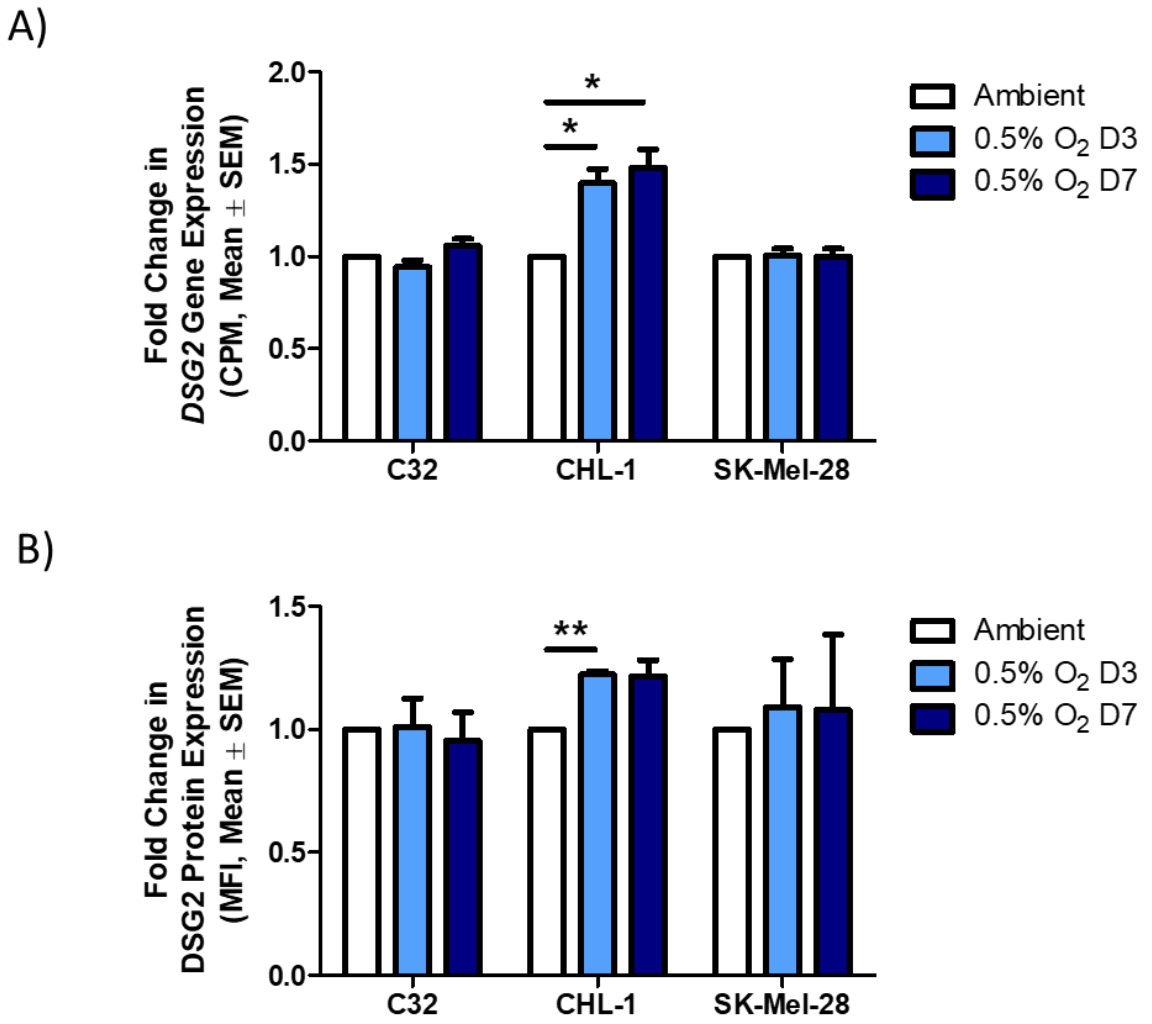

Figure 3.11. Pre-existing DSG2 expression levels on melanoma cells may be affected by hypoxia.

C32, CHL-1 and SK-Mel-28 cells were cultured under ambient (21% O_2) and hypoxic (0.5% O_2) conditions for 3 (D3) or 7 days (D7). (A) To examine gene expression of *DSG2*, total RNA was harvested from the cultured cells and subjected to RNA sequencing. Results were presented as a fold change of *DSG2* expression of cells cultured under 0.5% O_2 over that of cells cultured under ambient conditions. Bar graph shows mean fold change in *DSG2* gene expression (counts per million; CPM) ± SEM for n=3 independent samples. * = $p < 0.05$, two-tailed paired t-test. (B) To examine protein expression of DSG2, the cultured cells were stained with either an anti-DSG2 or an isotype matched control, followed by a secondary DyLight® 650 antibody and subjected to flow cytometric analysis. 7-AAD was included in the antibody mastermix to allow dead cells (7-AAD$^+$) to be gated out from analysis. The DSG2 protein expression was quantified by assessing the mean fluorescence intensity (MFI) and presented as a fold change of DSG2 expression of cells cultured under 0.5% O_2 over that of cells cultured under ambient conditions. Bar graph shows mean fold change in DSG2 protein expression (MFI) (normalised over isotype control) ± SEM for $n \geq 3$ independent experiments. ** = $p < 0.005$, two-tailed paired t-test.

>NG_007072.3 Homo sapiens desmoglein 2 (DSG2), RefSeqGene (LRG_397)on chromosome 18
CATTGCCATTTACGTGGGATAAAGGTTGTTTACTCCTAAAAGTACTGTGCGTGGCTTCTCCCCTCACAGGTCTCCCACACAGA
ACATTTTTGGCGTCACGAACAGGATCTGAAAGCGAAAGCATGCCATTTTCCACCACAAGGACCGGGCTGGGAGGTCCCCATAT
TCCGGGATGGGAACTCCCCAACTTCTCCTCCTTGGCCATTGAGTGGTCCAATGGAACTGGCCTTTGTGAAAATTGGGAATCTA
AATTAGTGCATTTTGAACCATTGGCTGTGCATGAGGTGCTGCAGGGAATCCCAGTTGGTAAAGTGGAAACTGAGGGAATTTAC
TGGCATGGATGGTGCTTGCTTACTGCTTATAAGTTAATGTGTCAAGATAGGAACAATAAAAATGTAAGCTGGAAAAGGAAAAT
GCTAATTTGATTTCCAAACTGGCCCTGGCCCAATGCCAGGCCTATGTCTTGATGGATCAGGCTCAAATCTATCAGCCTATTGC
TGAAAAGGCAGCTATTCAAGTGGCCCAGTCAGGGTAAAACTGAAGAACTAGTCAGCCAGGGATCAGAACAGGTAAAAACTCAG
CTCCTGTCTCAAGAATGGGAAATTAACCCCAGTAAAATTCAAGGACCTACACAAATTGTAAAATTTCTTGGCATCCTATGGAA
TGCAGGGAAATAGTCCATTTTACCAAAGGCTAAGCTAAAATACTAAAATGTGCAACCCCTACCATTAAAAAGGAGGCTCAGAA
ATTTATTGCCTTGTTTGGATTCTGGAGACATCATATTCCCCACTTGGGTGACATTTTACAACCTCTTCAGGCAGTCACTAGAA
AAGGCTATGACTTTCACTGGGGAGAGGAAGAGAGCATGGCTTCTGAACAAGTTAAACAAGTGGTGCAACTGGCCCTGGATTTA
TGGCCCATACAAGATGGACCAGTAGAACTGCAAGTAACTGTCCTAGATCAACATGCTAATTGGAGCCTCAGCCAGGAACAAGA
TAGGAAGAGGGTACCTTTGGGGTTTTGGACCTGGAAACTGCCAGAGGATGGCAAAGTTTATACACCTTTCTAGAAGCAATTGT
TAGCTTGCTATTGGGCTTTGCTGGAAATGGAGCACCTCTGCTTCAACCATGATATCTTTATGAGGCTTGAAATTCCTATTATG
ACTTGGGTCATGAGTTCCCCCAAAGCTCACCGGATAGGGCACACCCAAGAAAGTAGCATCATCAAATGGAAATGGTACATACA
AGACCAGGCTAAGCCAAAACCAAAGGGGGTATCACTTTTACATGAGGATATATACAAAACTTGCCAGCTCAGGAAACCACCAA
GCAAGTCCTACAGATAGGGAAGGAAACCTCCCCCGCCCAATGGGGCAAATCCTTTAAAGAACTAAGCCCAGAGGATCAGAAAC
ATGCTTGGTTTACTGATGGATCTACCAAATACATTGATGGGACCCGATGCTAGAAGGCCATGGCTCATAACCCTGTTAAAAAG
CATAAGCATTTCTGATGAAGGAAGGGGTGGGAGCAGCCAGCTGGCTGAACTAGTAGTGGTCCTCTGAGCTATTCAGGAGGAGG
CCAGAGGGATTTGCCACTTGAATACCAACTCTTGGTCAGTAGCAAATGTTCTTACCACCTGGATGCCCCAATGGCAACAAAAC
AAATGGTTAATTGGGAATGAAGAGGTTTGGGGTAAACAATACTGGGAAGATATCTGAATCCTGGCACACACTACCATTATCAC
TGTTTTCCATGTTGATGCTCATGCGTCTGTTTGCTCTTGACAGACTATTTCATCAGCAGGCAGATCAACAGGCCAAAATTTCC
ACCATAACTGCAAACTTGAATGTGGATGAATGGATTACAACATGTTCAAGACTTGCAATGAGAGGCTTTATAATGTATGGTGG
TATAATTGATAGTGCTTACCGGGGAGAGTTAAAGGTCATTTTATACAATACCACTCCAGATTCTTTTGCTATAAAACCTCAGA
TGCAGGTTGCTCAATTGTTAGTGGAACCTTGTCAGCAATTAACCCCTGAGGAAATCTGCCCCAACAGAGGCTACATGCAGAAC
TGGGGGATTCAGATCCTGGAGCCAAAATCCTGGAGCCAAAATATGGGTACAGCGTCCATCAGGTCCCACCCTTAAGACTGGTG
ACCTTGTAGCTATAGGAGCAGAAAATGAAGCACACTACAATTTCCTAAAGATGAAAAACAATATCATGTTCCCCTCTGTTTTT
GTTATCACATGGAATAACCTATCTACTAATGGTCAGCACCTGTGTCTTTGTGTCTGACGCCAAGATTAAATTCATCAACTGGG
TAGCCACCGCTGCAGAGGAAGCCAACCACAGTCAATGTTGGCTATGTGGGAATGAGCTACCTTGGAGAATCCTCCCTGCTAAC
ATTTCTGAATGACTATGTCGCTACCAATGGGACCACAACAACAACACTTGCAATCCAACCTGGACTTTCTTTGACCAAACCAA
GCCTTGGTACTCTGGGGTTTCTCCTGCCAGACAATTGTCAACACATGCTCCAAATCAACAACATTACCCCCAATGAAACACAA
TCTCTTTCCTACTTTTATAACACATTAGTACACTATGATTACAGTAACTCCATTGCTGTCCCCTGCGGGGCCCTCTGGGTATG
CGGATCCTATGGGTAGCGATACCTGCCCCCATATTGGATGGGGATATGCACTTGGGGGTGGCCATTAATTCCATTCACCATCC
GGGATAATATTCCCCTCCCCAGTAATCTAGATGCTTACAAACATCCCTGGTTAGAATGCATCCGACTCCGTAGGGGTGGTATC
CTATCACAGCATTCTCCCCTGCAGCTGATACAATCCTGCTTCAGCAACAAATTAAAACATTAAGCTCACTTCTAAGAAAAGCT
CTTAATGATAGTAGCACTGGATGTATGTTGTTATCAGATGAATTTGCTCAGCTATGTACTGTTGTGTTGCAAATGGAAAGGCA
TTAGATATGCTTACTGCAGCCCAAGGAGGGGTTTGCACCTTACTGCACTGGATGTTATGTGTATATCCCTGACAATTCTCACA
ATATTACTCTCCTTGCAAAGCCATGATGGGTGTGTTATTAATTTTGCTTTTAATTCTCCTGTGCTTACCCTGTATCTGTAATC
TCTATCAACTATGCCTTCCCCATGTATCTGTAGGGGTATTTTCCTGCGATTGAGTATCAGATTGAAGCCGAATGTGGAGGAAA
ACTTAAATATTAAATTTGAACTCAATTGAACATGGACACAAACAATGGCCACCAAGTCCCAGAACAGGTGGTGTGAGCCCCTT
GAGGAATTCATCGAGCGCTGTTTCAAATAAATCTCTATTTAAATTCCTATTTGTTAGTTATTGAAACACAACAGACAATCGCA
AACACAAGTTGACCTTTTTGTGTTCCTTGAGTCCAGTCGGGAAGGGCCCTTGTGACTGGGTCTCATGCCAAACAACTTGTTAC
GATAAGAGCTAGGGTCCCAGACCATGAGGAAACTTCATGAGAATCCTCTGTAGTCTGGTGAGTGTAGTGTCCGACTCTGGAGC
CCAGGCTGTTGCTTCCCGGTGTGGTGGTGAATCCTCCACAGTCTGGTGAGTGTACCTATAAATATATCTTTTCCTTCTCCCCT
TCCCATTGCAATTTGCTTATTATATCATTTGCTTATTATATCCGCGTTGCCATTTAATTGGGATAAAGGTTGTTTACCCTTAA
AAGTATGGTGTGTGTGTCTTTTCTTCTCCCCTTGCGCCTTTCTCGCACAGAACAATAGGCTCGTCCATTACTTTCAGTCGTTA
CATTTCTTGGAAGTTTCGTAATCCGGTGCTGATTCTAGTGTTTGGATGCCCATACTAAGTTTCTGCTTTTCAAGATGTCAATT
TAACATCTCACCTCGCAATCACGTTGTTCTAATTTTAACAATTATTTATTGAACCCTTAAGTTCTAGACACTGCAGAATGCTT
TACCTAAGATTTTCCAATTTCGTTCTCAAAACTTCCCCGTGCGTTGGTCGCTATTAACTCCATTTGACAGATCTGGAAACTGG
GGCCCAGAGAGGCTAGTCCAGGCCACTCAGCTAGTCACTCTTGGAGCGGGGCCTCTGATCTAGCTAGTGGTGTAATAGAAATT
GTAAATCATTTCAAAGAATATATATATTTCCCGTAACACCCTAGAGTTTTCTCCTAGCCCAAGAATTGTCCTTTTTGACCTCT
GGTGATTGTTTCTCCTTGAGCCAGATAAGCTGCAAACCTGTTGGAAGCAGTGAAGGGCCATAGGGAAGAGCAGCCTTTGGGGA
GACAGCCACCTGAAATTCTGCTCCACAACCTCCGCTCCAGGAGAGCGGGCCGAACGCACCGCGGTCGCAGCTTTCCTGAGGAC
ACGGGTCCCCATGTCACTAGCGACACCTGCGCTCCGGGCCCAAAGCACAATCACAAAGTGCGGGACCTTTGGGCGGTGCTGGG
CGGCCTGGCCCCGCAGCCACTGGGCCGGTTGGTCCCGCAGGACTCTGCTCCGTGGAGCTTTTGTCCTTGGGCCGGGGCCCTGC
GACCCGCGCTACCCAGGTCGAGCCCCGCCAGGAGGCTCCCTCCTCCCGCCATTCTCCAGAGAGTAGGGGGTCGGGAAGGAGAG
AACGGCGGGGCGGGGCCTGCCACCCACAGTCCCCAACCCAAGGACGTCACGGTCCCAGGTGCGAGTGCGAGCGGGCGGGAGTC
CACCCCGCGCCTCCCTCCTCTGCTGAACTCCCCACCTCTGTAAAAGCGGCCCGGGCCGGCCCCCGGCTCCATTTTCTCGCGGC
GGCCACACCTGGAGCCGCGCCTTTGGGTTGGGCTGGGCTGGGCCGCGCAACCGCCACGGGAAGACAGCCCTCGGGGCGGGGAG
GGAGAGGGTGGCCGGGCCGGGGGGAGGCCGGGGCCAGGGAGGAGCCGAGTGCGCGCTCGGGGCAGGCGGCGGCGCGGAGCGGT
GCGGCGGCGGGAGGCGGAGGCGAGGGTGCGATGGCGCGGAGCCCGGGACGCGCGTACGCCCTGCTGCTTCTCCTGGTAAGTGC
CGCAAGCGGGACAGGGGAGCCACCGCCGGGGAGGGCGTCGGTAGGCGAGGTCTAGACCTCGCGACCAGACTTGCCCGCCGCCC
TTGTGCGCGTTACCTGCCCGGCGCTCCTTCCTGC

Figure 3.12. The DSG2 promoter region has putative hypoxia response elements (HRE).

The promoter region of *DSG2* was interrogated for putative HRE (5'- (A/C)CGTG-3') consensus sites. These sites are highlighted above in yellow, while the start codon of the *DSG2* transcript (ATG) is highlighted in green.

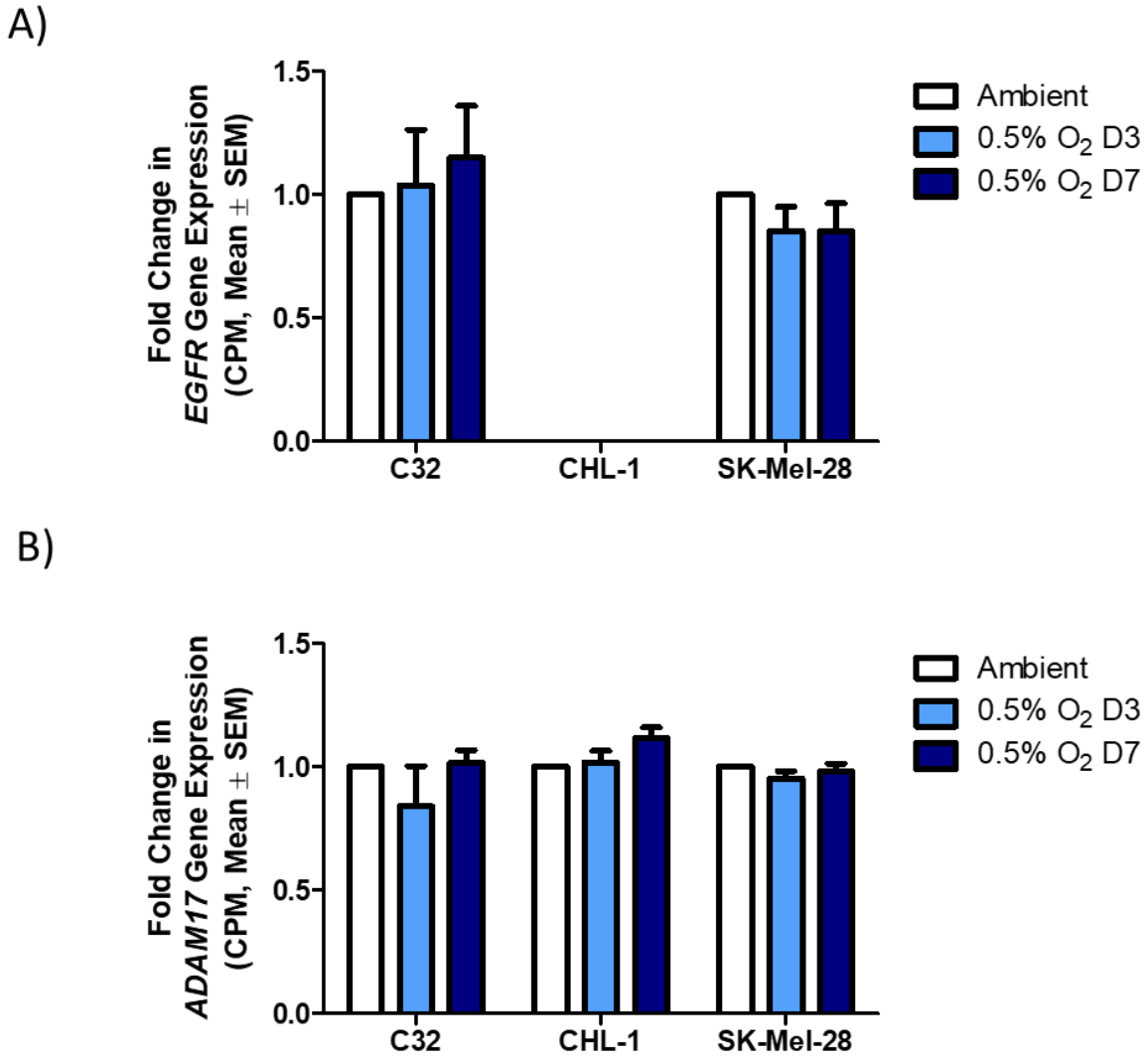

Figure 3.13. EGFR and ADAM17 gene expression levels are not affected by hypoxia.

C32, CHL-1 and SK-Mel-28 were cultured under ambient (21% O_2) and hypoxic conditions (0.5% O_2) for 3 (D3) or 7 days (D7). Total RNA was harvested from the cultured cells and subjected to RNA sequencing. (A) The RNA sequencing data was analysed to examine *EGFR* gene expression. Results were presented as a fold change of *EGFR* gene expression of cells cultured under 0.5% O_2 over that of cells cultured under ambient conditions. Bar graph shows mean fold change in *EGFR* gene expression (counts per million; CPM) ± SEM for n=3 independent samples. Two-tailed paired t-test. (B) The RNA sequencing data was also analysed to examine *ADAM17* gene expression. Results were presented as a fold change of *ADAM17* expression of cells cultured under 0.5% O_2 over that of cells cultured under ambient conditions. Bar graph shows mean fold change in *ADAM17* gene expression (counts per million; CPM) ± SEM for n=3 independent samples. Two-tailed paired t-test.

3.4. Discussion

DSG2 is a cadherin molecule that, since its discovery as a desmosomal cadherin, has now been implicated in other roles including proliferation, angiogenesis, migration and apoptosis (Brennan et al. 2007; Ebert et al. 2016; Kamekura et al. 2014; Overmiller et al. 2016; Peitsch et al. 2014). Here, a new role of DSG2 is described, where it regulates melanoma VM through direct cell-cell adhesion in a desmosome-independent manner.

In particular, the ability of $DSG2^+$ melanoma cell lines to form VM structures *in vitro* was affected following siRNA-mediated DSG2 knockdown. An interesting experiment to perform to complement this study is to identify $DSG2^-$ melanoma cell lines which are VM incompetent and overexpress DSG2 to examine if this enables the cells to undergo VM. However, given the large suite of other molecules that has been reported to regulate VM, there is a possibility that $DSG2^-$ melanoma cell lines can also undergo VM. Nonetheless, the findings from this study confirm the role of DSG2 in enabling VM in DSG2-expressing melanoma cells.

A limitation to the current *in vitro* approach of assessing VM is the lack of further confirmation that these structures formed on Matrigel contained a lumen and could be perfused. Indeed, it has been reported that while many cancer cell lines could rearrange and organise into network structures resembling that of VM when seeded on Matrigel, the networks formed by some of those cell lines actually lacked a hollow perfusable lumen upon further interrogation, thereby excluding them as real VM structures (Racordon et al. 2017). For this reason, it has been emphasised that additional validation approaches using microscopy and dye injection should be performed to confirm both the structural and functional properties of these networks (Racordon et al. 2017). Due to the lack of an optimised protocol (required for the processing of Matrigel for microscopy) as well as the unavailability of the appropriate equipment (required for the microinjection of dye), I could not address the concerns above to further validate *in vitro* that the networks formed by the $DSG2^+$ melanoma cells on Matrigel were real VM structures. PAS based staining was also not performed on the aforementioned networks. However, as will be presented in Chapter 5, when injected into mice to generate xenografts, the C32 cells were able to form $CD31^-$ PAS^+ VM structures with lumen containing blood cells, thereby confirming their VM competency *in vivo*.

Further to that, multiple cellular processes were examined to investigate the potential mechanisms by which DSG2 may regulate VM. In the majority of melanoma cell lines, DSG2 knockdown did not appear to affect cell proliferation. However, DSG2 siRNA A appeared to significantly reduce proliferation in CHL-1 and SK-Mel-28. While siRNAs are designed to achieve gene silencing by complete sequence matching with the target gene, it has also been reported that these siRNAs may bind in a mismatch manner with sequences in the 3' UTR of mRNAs, resulting in what is known as a microRNA-like off-target silencing effect (reviewed in (Jackson, AL & Linsley 2010)). This induces both target gene silencing as well as off-target effects in cells. One method to confirm the specificity of the gene silencing is to use multiple siRNAs of unique sequences that target the same RNA and compare the outcome of gene silencing, as has been performed in this study. Given that a reduction in cell proliferation was only seen with one of the three DSG2 siRNAs (DSG2 siRNA A) on two of the three cell lines, it was deduced that this effect was highly likely to be off-target. Further to that, CHL-1 cells transfected with DSG2 siRNA A underwent changes in cell morphology, something that was not observed with the other DSG2 targeting siRNAs on other cell lines (results not shown). Therefore, DSG2 siRNA A was excluded from subsequent experiments and it was concluded that DSG2 is not involved in regulating melanoma cell proliferation.

In addition, DSG2 knockdown did not appear to affect actin cytoskeleton structure in melanoma cells. As mentioned in the introduction of this Chapter, the balance between actin stress fibres and cortical stress fibres greatly influences multiple cellular processes, including cell migration. While an earlier study performed by our laboratory revealed changes in actin cytoskeleton rearrangement following DSG2 knockdown, this effect was observed in ECs (Ebert et al. 2016). Therefore, this difference in findings could be attributed to intrinsic differences between different cell types.

In line with the lack of changes in actin cytoskeleton rearrangement which can affect cell migration, scratch wound assays confirmed that DSG2 knockdown did not affect melanoma cell migration. This was however in contradiction with a previous study in which DSG2 knockdown increased melanoma cell migration (Peitsch et al. 2014). A potential reason that may explain this discrepancy is the difference in the approach taken to assess cell migration. The evidence for increased migration observed in the aforementioned study was detected in the presence of an externally introduced serum gradient established using Transwell assays, which could be attributed to differences in receptor expression towards a particular chemoattractant in the serum following DSG2 knockdown, even though this was not directly

assessed (Peitsch et al. 2014). This increased migration may therefore not be detected through scratch wound assays for two main reasons. Firstly, the chemoattractant may not be present at all or in sufficient amounts within the supernatant to induce migration. Secondly, such a gradient cannot be formed in a scratch wound assay as whatever chemoattractant present will be equally diffused within the medium due to the lack of a barrier.

In the present study, however, DSG2 knockdown did result in a significant reduction in melanoma cell-cell adhesion. This finding is somewhat surprising, as the role of DSG2 in mediating cell-cell adhesion has largely been demonstrated to occur through the interaction with other desmosomal cadherins to form desmosomes. However, it has been previously established that melanoma cells lack expression of other components involved in desmosome formation, and are not known to form desmosomes (Tan et al. 2016). This suggests that DSG2 can also undergo homotypic interactions to mediate cell-cell adhesion outside of desmosomes. Indeed, this has also been demonstrated in an earlier study performed by our laboratory on ECs (Ebert et al. 2016). Interestingly, melanoma cells, including C32, have been reported to express a plethora of adhesion molecules, including P-cadherin and N-cadherin (Schmitt et al. 2007), which can similarly mediate cell-cell adhesion through homotypic interactions. The observation that the downregulation of just one adhesion molecule (DSG2) amongst all the other adhesion molecules was sufficient to induce a significant inhibition of cell-cell adhesion highlights the importance of DSG2 in mediating this process.

While this study has demonstrated that DSG2 mediates VM through direct cell-cell adhesion, there is a potential of other mechanisms in play, in particular cell signalling through EGFR. As previously mentioned, a reduction in DSG2 expression in colon cancer cells led to the inhibition of EGFR signalling (Kamekura et al. 2014). Interestingly, EGFR signalling has been found to be involved in breast cancer VM (Lee, CH et al. 2014), whereby drug mediated inhibition of EGFR phosphorylation or shRNA knockdown of EGFR impaired VM *in vitro* (Lee, CH et al. 2014). While the role of EGFR signalling in melanoma VM is yet to be determined, given the close interaction of DSG2 and EGFR, it would be interesting to examine if the VM reduction observed following DSG2 knockdown could be dependent on EGFR signalling. Western blots could be performed to examine the expression and activation status of key molecules involved in the EGFR signalling pathway, such as p-EGFR, p-RAF, p-MEK, p-MAPK, as well as p-AKT (Brennan et al. 2007; Kamekura et al. 2014). This would reveal if there are any changes in this signalling pathway following DSG2 knockdown.

Further to that, DSG2 siRNA transfected melanoma cells could also be treated with EGF to examine if this restores the ability of the melanoma cells to undergo VM. If VM is restored following EGFR stimulation with EGF, this would suggest a role of EGFR signalling in mediating the impaired VM following DSG2 knockdown.

An investigation of the mechanisms that regulate DSG2 expression will be an interesting line of inquiry. Here, the potential role of hypoxia in regulating DSG2 is examined. The results showed that hypoxia upregulated DSG2 expression both at the RNA and protein levels in only one of the three cell lines. Examination of the promoter region of *DSG2* revealed that it has putative HREs to which HIF can bind and initiate *DSG2* transcription under hypoxic conditions. However, whether or not these HRE are functional needs to be validated through functional assays such as luciferase assays. Apart from direct regulation by HIF, there is also a possibility that DSG2 levels are indirectly regulated by other molecules that respond to hypoxia instead. While the RNA expression of EGFR, a molecule that is responsive to hypoxic stimulation, remained unaltered, it will be important in future studies to assess the actual activation and signalling of the pathway instead, as this is what triggers a functional outcome. Should the findings support the role of hypoxia in upregulating DSG2 expression, this would provide a logical mechanistic explanation which would fit with the notion that VM structures serve to enhance oxygen flow into the tumours. More specifically, hypoxia either directly or indirectly enhances DSG2 expression which subsequently promotes VM to increase vascularisation and promote tumour growth.

There are also other potential mechanisms that can regulate DSG2 expression apart from hypoxia. As mentioned in the introduction, work done by my colleagues and collaborators revealed that DSG2 is gradually downregulated as embryonic stem cells differentiated into melanocyte precursors and subsequently mature melanocytes, but is upregulated again in nevi, primary melanoma and metastatic melanoma (Tan et al. 2016). This suggests that DSG2 re-expression in melanoma may be a consequence of melanoma cells reverting into an embryonic phenotype, and therefore embryonic transcription factors may be involved in this re-expression process. Indeed, embryonic pathways are often found to be upregulated in melanoma and are associated with melanoma aggressiveness and VM (Topczewska et al. 2006). This speculation of DSG2 being regulated by embryonic pathways however warrants further investigation. In addition to that, it would also be interesting to expand our unpublished observations to examine the roles of KLF2/4 transcription factors in regulating Dsg2 expression (Jain and Bonder, unpublished).

Further to the *in vitro* findings presented here, the relevance of DSG2 in regulating melanoma VM has also been expanded to human melanoma patients by my colleagues and collaborators. As mentioned in the introduction of this Chapter, analysis of TCGA data revealed that DSG2 overexpression in melanoma is strongly correlated with reduced patient survival (Tan et al. 2016). More importantly, immunohistochemistry analysis on human melanoma samples confirmed that increased DSG2 expression was associated with increased VM (Tan et al. 2016). This links the relevance of the *in vitro* findings from this study to clinical observations, and further emphasises the importance of DSG2 in regulating VM.

Taken together, the findings of this study suggest the potential of targeting DSG2 as part of anti-VM therapy to reduce cancer progression. An issue of concern is the potential of side effects, as DSG2 is also expressed on epithelial tissues, whereby its downregulation has been found to result in loss of epithelial tissue integrity (Schlegel et al. 2010). More importantly, DSG2 is also key in desmosome formation in cardiomyocytes whereby impaired DSG2 binding resulted in significant defects in heart function (Pilichou et al. 2006). Therefore, it is crucial that the targeting of DSG2 as part of anti-VM therapy does not also affect vital normal tissue function. While examining the literature, it was found that antagonists of other cadherins have already been developed and used in clinical trials. In particular, ADH-1, an N-cadherin antagonist, has been used in phase I and II clinical trials for melanoma treatment (Beasley et al. 2009; Beasley et al. 2011). Systemic administration of this antagonist enhanced treatment response with no dose-limiting toxicities observed even though N-cadherin is also widely expressed on other tissues (Beasley et al. 2009; Beasley et al. 2011). This highlights the possibility of also targeting DSG2 as part of melanoma treatment with tolerable toxicities. Furthermore, there is a potential to minimise side effects with delivery methods which allow for directed homing to the tumour, such as directed delivery of DSG2 targeting siRNA through the use of nanoparticles (Davis et al. 2010). Alternatively, peptides blocking homotypic DSG2 binding, as validated in our previous study (Ebert et al. 2016), can also be used to minimise any potential microRNA-like off-target effects induced through the use of siRNA, although the optimal method of delivery remains to be elucidated.

Apart from direct targeting of DSG2, an alternative approach to downregulate DSG2 is through the targeting of the key factors regulating DSG2 expression. Depending on the factors identified, there is a potential of co-targeting multiple pathways through the inhibition of one factor. For example, should DSG2 expression be found to be regulated by embryonic transcription factors, then targeting these transcription factors may potentially allow for both

combined VM disruption due to DSG2 knockdown as well as a reduction in melanoma aggressiveness resistance development due to the loss of cell plasticity governed by these embryonic transcription factors (Hardy et al. 2010; Topczewska et al. 2006). Therefore, there is great benefit from further deciphering the mechanism underlying the regulation of DSG2 expression. Of note, it would also be interesting to examine if CVM-1118, the small molecule currently in clinical trials to target VM, could affect DSG2 expression (Tolcher et al. 2017). CVM-1118 has been found to target multiple signalling pathways, including Notch4/Nodal and VEGF signalling pathways (Hendrix, MJC et al. 2016). Whether or not DSG2 expression could be affected following CVM-1118 treatment may provide a hint as to which pathways may be involved in regulating DSG2 expression.

All the speculations discussed above can be further assessed in *in vivo* studies, which is beyond the scope of this thesis. While the *in vitro* results presented here highlight the role of DSG2 in VM, these findings can be further strengthened via performing xenograft studies to confirm that DSG2 KD melanoma cells do also have impaired VM capabilities *in vivo*. In accordance with this, my colleagues and collaborators are in the process of generating shRNA targeting DSG2 to allow for sustained DSG2 knockdown that is not achievable with siRNA. However, a caveat with this approach to bear in mind is that these stable DSG2 KD cells may upregulate alternative pathways to allow for compensation and hence masking the true effects of DSG2 KD. Alternatively, established DSG2-expressing melanoma xenografts can be treated with DSG2 targeting siRNAs delivered in nanoparticles to gain insight to both the effectiveness of this treatment and the potential side effects, as mice also express DSG2 that is highly homologous (76%) to human DSG2 (Mahoney et al. 2002). The role of DSG2 in mediating melanoma progression can also be addressed using an inducible mouse model. More specifically, xenografts could be generated using melanoma cells which are initially DSG2 negative. These melanoma cells would carry a plasmid where DSG2 expression is under the control of a tetracycline responsive operator, therefore allowing DSG2 expression to be induced on the melanoma cells following the administration of doxycycline. These would then allow us to understand if VM occurrence is a result of aberrant re-expression of DSG2 or rather aberrant re-expression of another factor that also induces DSG2 expression. Once identified, the key transcription factors which regulate DSG2 expression can also be targeted *in vivo* instead to inhibit DSG2 expression and subsequently VM occurrence.

An issue of concern for direct targeting DSG2 is the potential of therapeutic resistance, like that commonly observed in other targeted therapies. Given the plastic nature of VM-

competent cells, as well as the availability of other molecules that can govern VM as elaborated in Chapter 1, there is a potential for alternative pathways to be activated to re-enable VM. This is where the targeting of the upstream transcription factors regulating DSG2 expression may be a more feasible approach, although this speculation also requires further investigation. Furthermore, as VM vessels are often directly in contact with blood flow, loss of melanoma cell-cell adhesion following DSG2 knockdown could potentially promote the detachment of VM vessel lining melanoma cells into the blood flow and thereby exacerbate disease through promoting metastasis. This is another speculation that can be assessed in the aforementioned *in vivo* models. An alternative use of this finding perhaps is to utilise DSG2 as a biomarker. Given its significant association with both VM occurrence in melanoma as well as poor melanoma patient prognosis, DSG2 can be used as a prognostic biomarker (Tan et al. 2016). In addition to that, DSG2 can also be included to the list of biomarkers to detect VM vessels, and in turn utilise the VM vessels present as a potential route for leukocyte recruitment, which is a focus of the subsequent Chapters of this thesis.

In conclusion, a new non-canonical role of the cadherin DSG2 in regulating melanoma VM through cell-cell adhesion outside of desmosome formation is established in this Chapter. Further studies as described above are required to understand how this information can be utilised and translated into therapeutic applications.

Chapter 4. Function of Melanoma VM: Leukocyte Recruitment *in Vitro*

4.1. Introduction

4.1.1. *General Introduction*

While there is growing evidence around the occurrence and regulators of VM in melanoma, there is a lack of understanding of the function of VM. It is generally assumed that the function of VM vessels is similar to that of EC vessels, that is to enhance blood circulation into tumours for increased supply of nutrients and oxygen to promote tumour growth. However, blood vessels have additional roles, such as governing leukocyte recruitment. This Chapter focuses on deciphering the role of VM vessels in regulating leukocyte recruitment.

4.1.2. *Leukocyte Recruitment by EC Vessels*

The leukocyte recruitment cascade is a multistep process that is orchestrated by the interplay of complementary molecules on the endothelium and the leukocytes. The three key stages involved in this cascade are rolling, firm adhesion and transmigration, each facilitated by a variety of molecules (summarised in Table 4.1 and Table 4.2) (reviewed in (Ley et al. 2007)).

The first stage of the cascade is the tethering and rolling of leukocytes along the endothelium. This process involves interactions between selectins (E-selectin and P-selectin) and/or hyaluronic acid (HA)-bound CD44 on the endothelium with their counter ligands on the leukocytes. HA is an extracellular matrix glycosaminoglycan which is commonly bound to its receptor CD44 (Lesley et al. 2000). The binding of selectins and HA-bound CD44 to their counter ligands is a weak interaction with high disassociation rates such that leukocytes will lose their interaction with the vasculature and return to the circulation in the absence of stronger interactions. The expression of E-selectin, P- selectin and HA-bound CD44 can all be enhanced following inflammatory cytokine stimulation such as IL-1 and TNFα (Bevilacqua et al. 1987; Hattori et al. 1989; Nandi, Estess & Siegelman 2000).

The second stage of the leukocyte recruitment cascade is the firm adhesion of leukocytes on the endothelium. This process is mediated by the binding of a family of immunoglobulin superfamily adhesion molecules which include intercellular adhesion molecule-1 (ICAM-1), ICAM-2, vascular cell adhesion molecule-1 (VCAM-1) and mucosal addressin cell adhesion molecule-1 (MAdCAM-1) expressed by the endothelium to integrins on the leukocytes. These molecules provide a stronger adhesive interaction compared to that of selectins, and hence while they have also been reported to play a role in mediating leukocyte rolling (Berlin

et al. 1995; Salas et al. 2004), the main task of these adhesion molecules is to act as brakes to slow the rolling leukocytes to a point for complete adhesion on the endothelium. All four of these adhesion molecules are constitutively expressed at low levels on the endothelium, and can be strongly upregulated upon stimulation by the inflammatory cytokines IL-1 and TNFα, with the exception of ICAM-2 (McLaughlin et al. 1998; Steffen et al. 1996). This firm adhesion of leukocytes onto the endothelium is also regulated by chemokines which can be produced either endogenously by ECs or exogenously by surrounding cells (Ebnet et al. 1996). These chemokines are associated with glycosaminoglycans which anchor and present them on the luminal surface of the endothelium (reviewed in (Middleton et al. 2002)). The binding of chemokines to their receptors on the rolling leukocytes stimulate conformation changes on the integrins on the leukocytes, which then facilitates the subsequent high affinity binding to the immunoglobulin superfamily adhesion molecules resulting in firm adhesion (Detmers et al. 1990).

The third stage of the leukocyte recruitment cascade is the transmigration of leukocytes, which is mediated by junctional adhesion molecules (JAMs) and platelet/endothelial cell adhesion molecule-1 (PECAM-1; also known as CD31). Under normal resting conditions, these adhesion molecules are localised within EC cell-cell junctions where they maintain intercellular adhesion and cell polarity. Upon cytokine stimulation, the ECs dynamically direct these adhesion molecules away from the cell junctions and loosen up the intercellular space to allow for leukocyte transmigration (Keiper et al. 2005; Ostermann et al. 2002; Ozaki et al. 1999; Romer et al. 1995). The chemokine gradient in the underlying tissue then further directs the transmigrated leukocytes to specific sites.

Table 4.1. Endothelial cell adhesion molecules implicated in the leukocyte recruitment cascade and their respective receptors/ligands on leukocytes. Table adapted and modified from (Tan et al. 2017).

Step of leukocyte recruitment cascade	Adhesion molecule on endothelium	Counter receptor/ ligand on leukocytes	Counter receptor/ligand expression status on leukocyte subsets						Ref
			Naïve T cells	Memory T cells	Mono-cytes	Neutro-phils	NK cells	B cells	
Rolling	P-selectin	PSGL-1	✓	✓	✓	✓	✓	✓	(Laszik et al. 1996)
	E-selectin	PSGL-1	✓	✓	✓	✓	✓	✓	(Laszik et al. 1996)
		ESL-1	×	✓	✓	✓	✓	×	(Easton et al. 1993; Postigo et al. 1994)
	MAdCAM-1 / PNAd	L-selectin	✓	×	✓	✓	✓	✓	(Arbones et al. 1994; Tang, ML et al. 1998)
	CD44/HA	CD44	✓	✓	✓	✓	✓	✓	(Kremmidiotis & Zola 1995; Pure & Cuff 2001)
Firm adhesion	ICAM-1, ICAM-2	LFA-1 (CD11a/CD18; αLβ2 integrin)	✓	✓	✓	✓	✓	✓	(Arnaout 1990; Carrasco et al.)
		MAC-1 (CD11b/CD18; αMβ2 integrin)	×	×	✓	✓	✓	✓	(Arnaout 1990; Ghosn et al. 2008)
	VCAM-1	VLA-4 ($\alpha_4\beta_1$ integrin)	✓	✓	✓	×	✓	✓	(Kirveskari et al. 2000; Ryan et al. 1991)
		$\alpha_4\beta_7$ integrin	×	✓	×	×	×	✓	(Tang, ML et al. 1998)
	MAdCAM-1	$\alpha_4\beta_7$ integrin	×	✓	×	×	×	✓	(Tang, ML et al. 1998)
Transmig-ration	PECAM-1 (CD31)	PECAM-1	✓	×	✓	✓	✓	✓	(Jackson, DE et al. 2000)
	JAM-A	LFA-1 (CD11a/CD18; αLβ2 integrin)	✓	✓	✓	✓	✓	✓	(Arnaout 1990; Carrasco et al.)
	JAM-B	VLA-4 ($\alpha_4\beta_1$ integrin)	✓	✓	✓	×	✓	✓	(Kirveskari et al. 2000; Ryan et al. 1991)
	JAM-C	MAC-1 (CD11b/CD18; αMβ2 integrin)	×	×	✓	✓	✓	✓	(Arnaout 1990; Ghosn et al. 2008)

Table 4.2. List of chemokines currently demonstrated to recruit CD8$^+$ T cells, TAM, TAN and NK cells to melanoma, and their respective receptors on leukocytes. Table adapted and modified from (Tan et al. 2017).

Leukocyte population	Chemokine receptors	Cognate chemokines	Source of Data	References
CD8$^+$ T cells	CCR5	CCL3, CCL4, CCL5	Human clinical studies and murine models	(González-Martín et al. 2011)
	CXCR3	CXCL9, CXCL10, CXCL11	Human clinical studies and murine models	(Mikucki et al. 2015)
TAM	CCR2	CCL2	Murine models	(Gazzaniga et al. 2007; Nesbit et al. 2001)
TAN	CXCR1, CXCR2	CXCL1, CXCL2, CXCL6, CXCL8	Murine models	(Jablonska et al. 2014; Schaider et al. 2003; Van Coillie et al. 2001)
NK cells	CCR5	CCL3, CCL4, CCL5	Murine models	(Liu, C et al. 2008)
	CXCR3	CXCL9, CXCL10, CXCL11	Murine models	(Wendel et al. 2008; Wennerberg et al. 2015)

4.1.3. *Leukocyte Recruitment by Melanoma EC Vessels*

As demonstrated in Table 4.1 and Table 4.2, leukocytes only express a select range of ligands and receptors for the EC-expressed adhesion molecules and chemokines. Therefore, the adhesion molecule and chemokine profile of the endothelium is important in the selection of leukocyte subsets that are being recruited. In melanoma, it has often been reported that there is a reduction in P-selectin, E-selectin, ICAM-1 and VCAM-1 expression on tumour ECs compared to normal ECs as well as a reduction in CCL3, CCL4, CCL5, CXCL9, CXCL10 expression, which correlates with a reduction in $CD8^+$ T cells and NK cells (Harlin, H. et al. 2009; Weishaupt et al. 2007). On the other hand, an increase of CCL2, CXCL1, CXCL2, CXCL6 and CXCL8 within tumours compared to surrounding tissues has been associated with an increase in tumour associated macrophage (TAM) and tumour associated neutrophil (TAN) recruitment to murine melanoma tumours, although the adhesion molecules that govern the specific recruitment of TANs/TAMs remain to be elucidated (Gazzaniga et al. 2007; Jablonska et al. 2014; Nesbit et al. 2001; Schaider et al. 2003; Van Coillie et al. 2001). Two potential adhesion molecules which could mediate TAN and TAM recruitment are CD44 and PNAd, which are both elevated on tumour endothelium, although further investigation is required (Griffioen, Arjan W. et al. 1997; Martinet et al. 2011). Together, these changes in the endothelium facilitate the preferential recruitment of pro-tumourigenic leukocytes and help create an immune microenvironment that supports tumour growth.

In keeping with this notion, alterations of the adhesion molecule and chemokine profile on the endothelium following treatment has been documented to have a profound impact on the types of leukocytes that are recruited to a tumour. For example, restored ICAM-1 and VCAM-1 expression as well as enhanced CXCL9, CXCL10 and CXCL11 expression following anti-angiogenic therapy or low dose radiation have been found to enhance $CD8^+$ T cell recruitment (Ganss et al. 2002; Wu, X et al. 2016). On the other hand, inhibition of CCL2 or CXCR2 signalling has been documented to inhibit TAM and TAN recruitment (Gazzaniga et al. 2007; Tazzyman et al. 2011).

Interestingly, hypoxia has been found to be involved in the regulation of adhesion molecule expression on ECs. Long term culture of ECs under hypoxic (1% O_2) conditions rendered them insensitive to TNFα induction and inhibited VCAM-1 expression through a HIF-dependent mechanism (Cartee et al. 2012). Further to that, other studies have reported that ECs can also be rendered anergic following chronic stimulation with multiple factors such as

VEGF, bFGF, TGFβ and adenosine. *In vitro*, prolonged VEGF and bFGF exposure modified ECs epigenetically (Hellebrekers et al. 2006), resulting in suppressed adhesion molecule expression, even following the stimulation with the pro-inflammatory cytokine TNFα stimulation (Dirkx, AE et al. 2003). Similarly, *in vitro* treatment of IL-1α- or TNFα-activated ECs with TGFβ or adenosine was found to differentially downregulate P-selectin, E-selectin, ICAM-1 and VCAM-1 expression (Carlos 2001; Wang, L et al. 2011). Of note, these factors, which are often found to be upregulated in tumours, can be upregulated following hypoxia stimulation and can further feed into the activation of hypoxia-associated pathways (McMahon et al. 2006; Merighi et al. 2006). This highlights the importance of hypoxia in regulating adhesion molecule expression and provides a potential mechanism to explain the low adhesion molecule expression observed on ECs in melanoma.

In addition to adhesion molecules, hypoxia has also been found to play a role in regulating chemokine expression on ECs. An increase in CCL2 and CXCL8 expression in ECs was observed following hypoxic stimulation (Karakurum et al. 1994), which may in turn enhance the recruitment of CCR2 expressing TAM and CXCR1/2 expressing TAN. The effects of hypoxia on EC expression of CXCR3 signalling ligands key for $CD8^+$ T cell and NK cell recruitment remains to be elucidated. However, chemokines presented on the endothelium may also be acquired following endocytosis of chemokines produced by surrounding cells. Therefore, the mechanism underlying changes in EC expression of chemokines may also be related to overall changes in local chemokine expression independent of hypoxia stimulation on ECs.

4.2. Hypothesis and Aims

Interestingly, in addition to ECs, melanoma cells have also been reported to express various adhesion molecules and chemokines which are characteristic of ECs and are involved in regulating leukocyte recruitment. Some of these include CD44, ICAM-1, VCAM-1, JAM-C, PECAM-1, CCL2, CXCL8 and CXCL12 (Denton et al. 1992; Dietrich et al. 1997; Dunleavey et al. 2014; Harlin, Helena et al. 2009; Langer et al. 2011; Payne & Cornelius 2002). Notably, expression of the majority of these molecules has often been associated with increased melanoma aggressiveness and even VM occurrence (Denton et al. 1992; Dunleavey et al. 2014; Langer et al. 2011; Payne & Cornelius 2002). Given that leukocytes can also circulate through blood-perfused VM vessels where they can directly come in contact with these melanoma cells (Hillen, F. et al. 2008), it is tempting to speculate that these adhesion

molecules and chemokines also serve as ligands to facilitate leukocyte recruitment through VM vessels. Based on this, I hypothesised that **VM competent-melanoma cells can mediate leukocyte recruitment through adhesion molecules and chemokines characteristic of ECs.** The aims to address this hypothesis in this Chapter are to:

1) Examine the ability of leukocytes to roll, adhere and migrate across monolayers of VM-competent melanoma cells
2) Determine the expression of adhesion molecules and chemokines on VM-competent melanoma cell lines under normoxic and hypoxic conditions

It is expected that the ability of VM-competent melanoma cells to mediate leukocyte recruitment as well as the leukocyte subsets which can be recruited would correlate with the adhesion molecule and chemokine profile of these melanoma cells.

4.3. Results

Throughout this Chapter, experiments have been performed on the human melanoma cell lines C32, CHL-1 and SK-Mel-28, all of which have been confirmed to be VM-competent in Chapter 3. To allow for comparison with conventional ECs known to be involved in leukocyte recruitment, the transformed human bone marrow EC line TrHBMEC was included as a positive control. Wherever stated, TrHBMEC cells were treated with TNFα to stimulate adhesion molecule expression for leukocyte recruitment. On the other hand, the keratinocyte cell line HaCaT was included as an opposing comparator cell as keratinocytes are not known to recruit leukocytes.

Several functional assays were first performed to establish the concept that melanoma VM vessels may be involved in leukocyte recruitment. More specifically, parallel plate flow chamber assays were performed to assess leukocyte rolling and adhesion under physiologically relevant flow conditions, while Transwell assays were performed to assess leukocyte transmigration. These assays have been widely used to assess leukocyte recruitment by ECs *in vitro* (Allingham, van Buul & Burridge 2007; Sun, WY, Pitson & Bonder 2010) and have hence been adapted here to assess leukocyte recruitment by VM-competent melanoma cells *in vitro*. Note that while the actual EC/VM vessels are 3D structures, these *in vitro* assays were designed to be performed on 2D monolayers of ECs/VM-competent melanoma cells. This is a common technical limitation in the vascular biology field where the majority of leukocyte recruitment studies are performed on 2D EC monolayers due to the lack of easily accessible 3D *in vitro* systems. The implications of this will be addressed further in the discussion.

Parallel plate flow chamber assays were performed to assess the ability of leukocytes to roll and adhere on a confluent melanoma monolayer under shear flow conditions. Briefly, as demonstrated in Figure 4.1A, peripheral blood bulk mononuclear cells (MNC) pre-labelled with the fluorescent dye calcein AM were perfused across a confluent melanoma cell monolayer or a confluent TrHBMEC monolayer at a rate which creates a shear stress of 0.5dynes/cm^2. Parallel plate flow chamber assays have widely been used to assess leukocyte rolling and adhesion on ECs (dela Paz & D'Amore 2009; Sun, WY, Pitson & Bonder 2010) as the presence of a shear flow better recapitulates the recruitment process under physiologically relevant flow conditions. Further to that, a prior optimisation showed that this approach greatly reduced non-specific binding compared to leukocyte adhesion assays

performed under static conditions (results not shown). Of note, the shear stress within a blood vessel is directly influenced by the flow rate of blood, the viscosity of blood, and the size of blood vessels. Parallel plate flow chamber assays assessing leukocyte recruitment by ECs normally apply a shear stress of 2 dynes/cm^2 to recapitulate the shear stress at postcapillary venules where leukocyte recruitment occurs (dela Paz & D'Amore 2009; Sun, WY, Pitson & Bonder 2010). However, a lower shear stress of 0.5 dynes/cm^2 was used here instead to better recapitulate the physiological conditions in tumour blood vessels where a lower flow rate of blood is commonly reported (Jain 1988). As demonstrated in Figure 4.1B, fluorescence microscopy revealed that calcein AM-labelled MNC adhered on all three VM-competent melanoma cell lines. Similar results were observed on the EC line TrHBMEC, and greatly enhanced on TrHBMEC treated with TNFα. The negative control HaCaT cell line, however, had minimal adhered MNC.

The cells in the dishes (both the adhered MNC and melanoma/TrHBMEC/HaCaT monolayer) were then detached and subjected to flow cytometric analysis (see Appendix Figure B1 for gating strategy). The addition of a fixed volume of counting beads to each sample allowed for the determination of absolute cell numbers. As demonstrated in Figure 4.1C, there were very few adhered MNC recovered from the negative control HaCaT cells. On the other hand, the total numbers of adhered MNC bound on the VM-competent melanoma cell lines were at levels similar to untreated TrHBMEC. Unsurprisingly, TNFα-treated TrHBMEC had the most adhered MNC, and this was significantly higher than resting TrHBMEC.

The staining of the detached cells with multiple fluorescently labelled antibodies targeting leukocyte subset specific markers allowed for the characterisation of the specific phenotypes, in particular CD4$^+$ T cells, CD8$^+$ T cells, CD14$^+$ monocytes, CD16$^+$ NK cells and CD19$^+$ B cells. The MNC used for each assay (referred to as input cells) were also characterised to examine the initial proportion of each of the leukocyte subsets prior to the assay. This characterisation was not done for the HaCaT cells, as there were insufficient MNC bound. As shown in Figure 4.1D, the predominant leukocyte subset within the input cells was CD4$^+$ T cells, followed by CD14+ monocytes, CD8$^+$ T cells, CD16$^+$ NK cells and CD19$^+$ B cells, in keeping with the expected frequencies of these cell types in healthy blood. Compared to the input population, there was a significant reduction in CD4$^+$ T cell frequency and a trend towards an increased frequency of CD14$^+$ monocytes recovered from the TrHBMEC monolayer. This suggests that TrHBMEC cells preferentially bind monocytes and show limited binding of CD4$^+$ T cells. When the TrHBMEC were pre-treated with TNFα, there was

a significant reduction in both $CD4^+$ T cell and $CD19^+$ B cell frequency compared to the input population, as well as a more pronounced trend towards an increased $CD14^+$ monocyte adhesion compared to the untreated TrHBMEC, although this was not statistically significant ($p = 0.3519$). Interestingly, the three melanoma cell lines exhibited different leukocyte binding profiles. The overall profile of the leukocyte subsets bound on the C32 melanoma cells was similar to the resting TrHBMEC monolayer, where a significant reduction in $CD4^+$ T cell frequency and a slight trend towards enhanced $CD14^+$ monocyte frequency was observed compared to the input population. CHL-1 cells had a leukocyte binding profile similar to that of the TNFα-treated TrHBMEC, characterised by a further enhancement of $CD14^+$ monocyte adhesion. On the other hand, the cells recovered from SK-Mel-28 monolayers displayed a similar profile to that of the input cells, which may reflect a non-biased adhesion of the leukocytes. Apart from the aforementioned differences in $CD4^+$ T cell and $CD14^+$ monocyte binding, the overall binding of $CD8^+$ T cells and $CD16^+$ NK cells were similar across the three melanoma cell lines although there appeared to be a trend towards less $CD19^+$ B cell binding on the CHL-1 cells.

A)

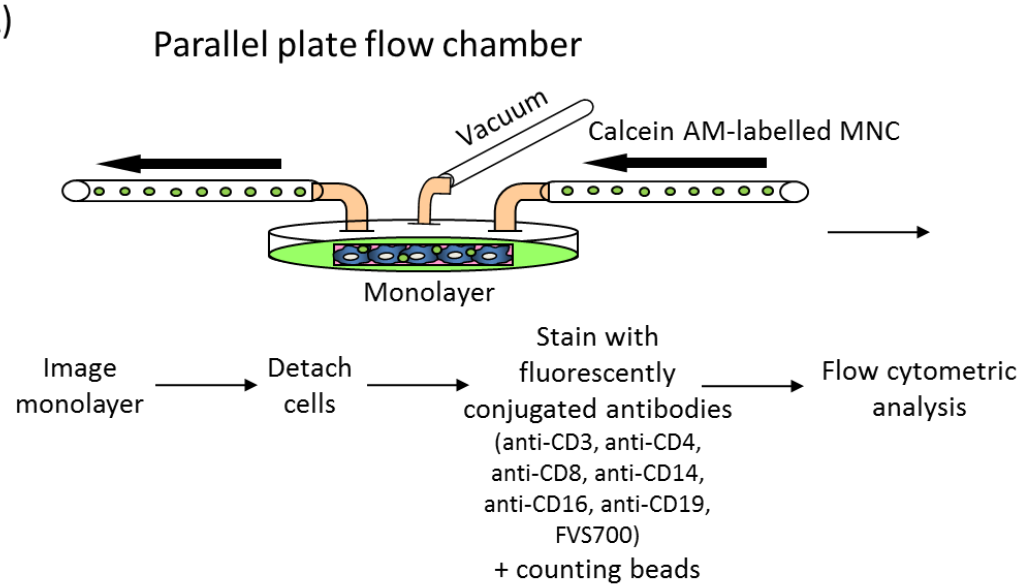
Parallel plate flow chamber
Vacuum
Calcein AM-labelled MNC
Monolayer
Image monolayer
Detach cells
Stain with fluorescently conjugated antibodies (anti-CD3, anti-CD4, anti-CD8, anti-CD14, anti-CD16, anti-CD19, FVS700) + counting beads
Flow cytometric analysis

B)

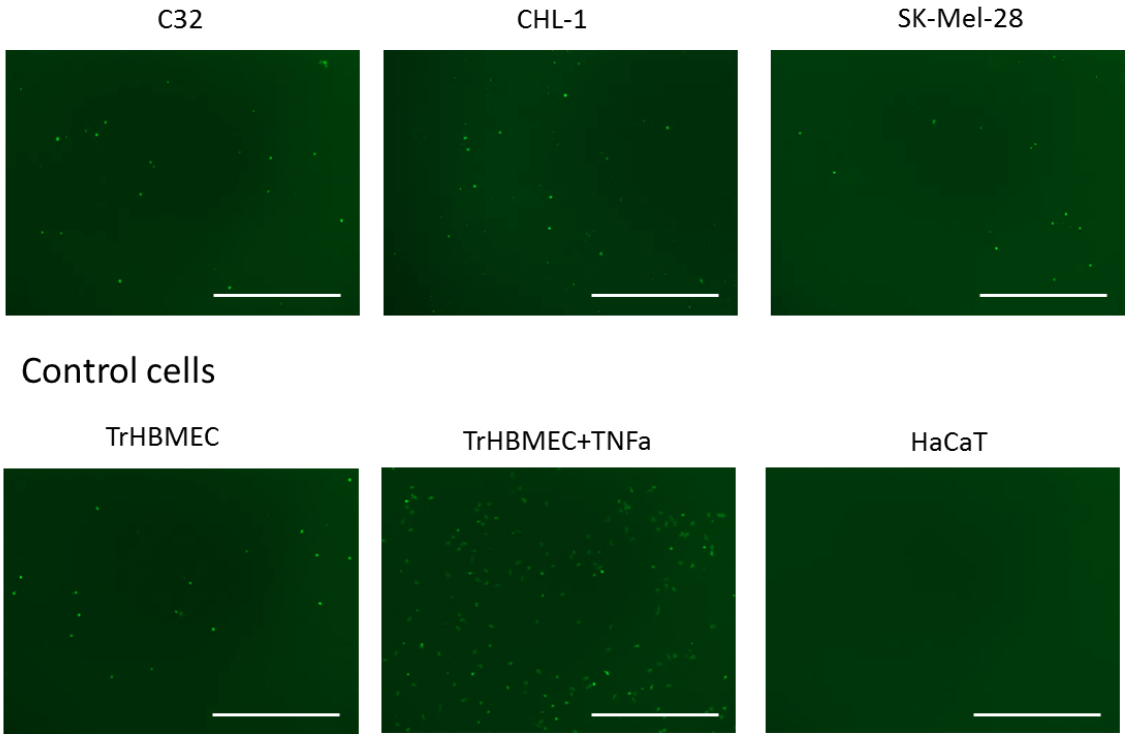
VM-competent melanoma cells
C32
CHL-1
SK-Mel-28
Control cells
TrHBMEC
TrHBMEC+TNFa
HaCaT

C)

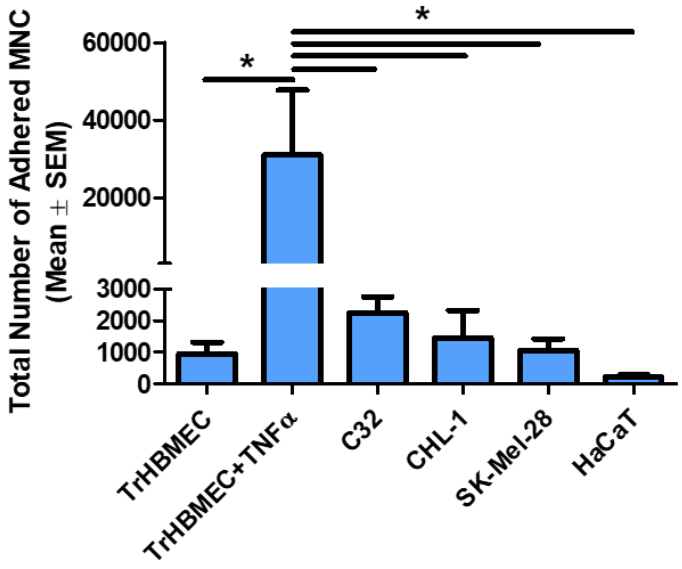
Total Number of Adhered MNC
(Mean ± SEM)
60000
40000
20000
3000
2000
1000
0
*
*
TrHBMEC
TrHBMEC+TNFα
C32
CHL-1
SK-Mel-28
HaCaT

D)

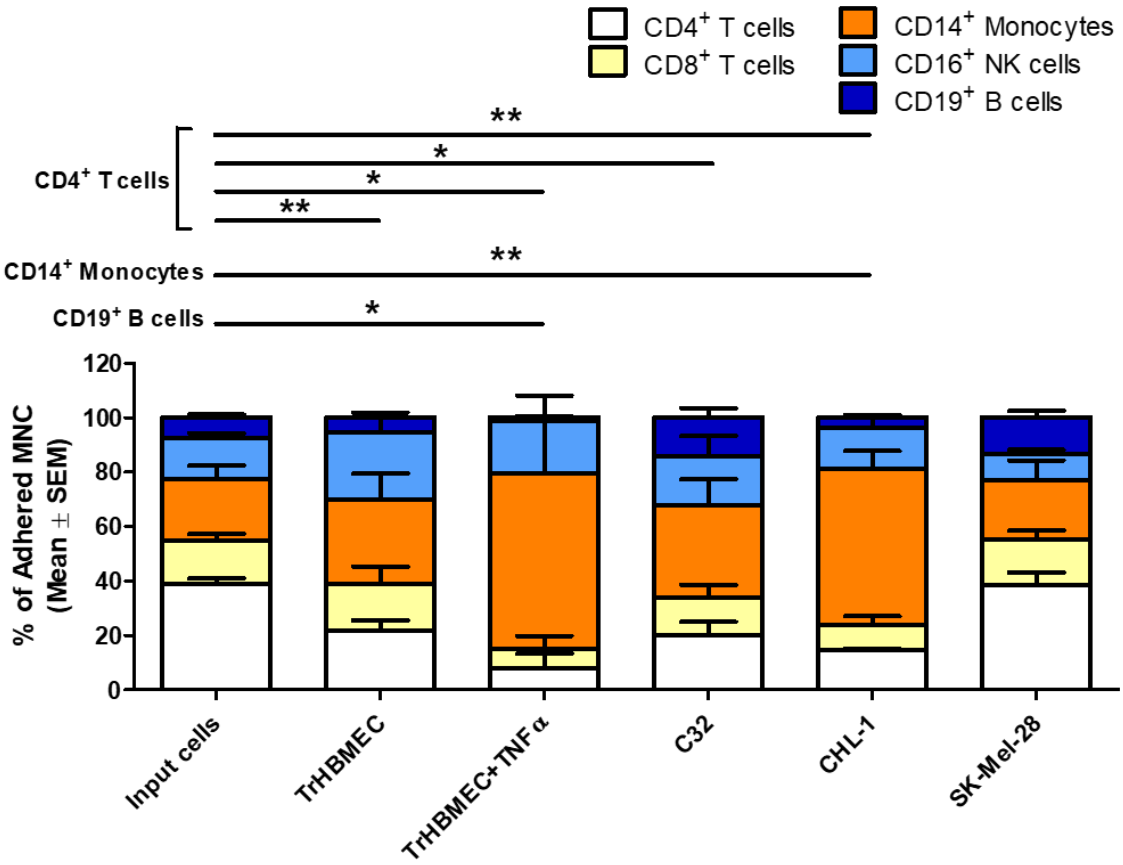
CD4+ T cells
CD8+ T cells
CD14+ Monocytes
CD16+ NK cells
CD19+ B cells
CD4+ T cells
**
*
*
**
CD14+ Monocytes
**
CD19+ B cells
*
% of Adhered MNC
(Mean ± SEM)
120
100
80
60
40
20
0
Input cells
TrHBMEC
TrHBMEC+TNFα
C32
CHL-1
SK-Mel-28

Figure 4.1. Leukocytes can roll and adhere on a VM-competent melanoma cell monolayer.

(A) The VM-competent melanoma cell lines C32, CHL-1 and SK-Mel-28, the EC line TrHBMEC and the keratinocyte cell line HaCaT were cultured on dishes until a confluent monolayer was formed. Calcein AM-labelled peripheral blood bulk mononuclear cells ($8x10^6$) were flowed across the cell monolayer at a defined shear stress of 0.5 dynes/cm^2. Any unbound cells were rinsed off. The adhered cells were imaged, and then harvested and stained with multiple fluorescently labelled antibodies targeting leukocyte subset specific surface markers to examine the phenotype of the adhered MNC via flow cytometry. FVS700 was included in the antibody mastermix to allow dead cells ($FVS700^+$) to be gated out from analysis. A standard number of counting beads was also added to the stained samples prior to flow cytometric analysis to allow for the determination of absolute MNC numbers. (B) Fluorescence microscopy images taken using a 4x objective showing the adhesion of calcein AM-labelled MNC on the various cell monolayers prior to detachment for flow cytometric analysis, representative of n=3-5 independent MNC donors. Scale bars = 400 μm. (C) The total number of adhered MNC was deduced following flow cytometric analysis using counting beads. Bar graph shows the mean total number of adhered MNC on different cell monolayers ± SEM with n=3-5 independent MNC donors. * = $p< 0.05$, one way ANOVA with Bonferroni's Multiple Comparison Test. (D) The phenotype of the adhered MNC was characterised using antibodies. Bar graph shows the mean percentage of different leukocyte subsets within the total population of adhered MNC on different cell monolayers ± SEM with n=3-5 independent MNC donors. * = $p< 0.05$, * = $p< 0.005$, two-tailed paired t-test compared to the input population.

Transwell assays were performed to assess the ability of leukocytes to migrate across a confluent melanoma monolayer (Figure 4.2A). Prior to the addition of MNC, the cell monolayer was first stained with calcein-AM to visualise the morphology of the monolayer (Figure 4.2B). Any monolayers with visible gaps between cells were excluded from the assay. Furthermore, the permeability of the cell monolayers was examined (Figure 4.2C). Briefly, a suspension of 2000kDa FITC-labelled dextran in PBS was added to the top chamber of the Transwells and fluorescence intensity of the medium was measured in the bottom chamber after a 15-minute incubation. This assesses the amount of FITC-dextran that had freely diffused across the cell monolayer, thereby reflecting the permeability of the cell monolayer. The majority of studies in the literature utilise 40-70 kDa FITC-labelled dextran to assess changes in EC monolayer permeability following treatment (Gavard & Gutkind 2006; Ikeda et al. 1999; Utoguchi et al. 1995; Wojciak-Stothard et al. 2001). However, these molecules are much smaller than the average leukocyte size which is between 6-8 µm (Downey et al. 1990) (70 kDa dextran= 14 nm in diameter, (Choi et al. 2010)). Therefore, I sought to utilise FITC-labelled dextran of a larger size that would better reflect the size of leukocytes to assess the permeability of untreated cell monolayers. Despite this attempt, the largest FITC-labelled dextran available for purchase was 2000 kDa which only correlated to approximately 54.4nm in diameter (Choi et al. 2010) but was nevertheless used here. As shown in Figure 4.2C, control wells containing no cell monolayer had significantly higher permeability compared to wells containing monolayers, as expected. In comparison to the EC line TrHBMEC, the melanoma cell lines C32, CHL-1 and SK-Mel-28 appeared to be more permeable. Nonetheless, these melanoma cell monolayers still acted as effective barriers when compared to the no monolayer control. On the other hand, the keratinocyte cell line HaCaT exhibited very limited permeability, as expected for keratinocytes whose primary function is maintenance of a biological barrier.

As depicted in Figure 4.2A, initial Transwell assays were performed using fetal bovine serum (FBS) gradients, as FBS contains a broad range of factors which have leukocyte chemoattractant activities. MNC resuspended in medium containing 0.1% FBS were seeded into the top chamber of the Transwell and allowed to migrate across an FBS gradient created by the addition of medium containing 10% FBS in the bottom chamber. Any non-FBS specific migration was also accounted for with the inclusion of control Transwells containing medium with 0.1% FBS in the bottom chamber. After 3 hours, the MNCs in the bottom chamber were collected and subjected to flow cytometry analysis for phenotyping. Similar to

the flow cytometry analysis for the parallel plate flow chamber assays, counting beads were included to determine the total number of migrated MNC (see Appendix Figure B1 for gating strategy).

As shown in Figure 4.2D, there was a significant increase in the total number of migrated MNC across Transwells with no monolayer or containing a monolayer of TrHBMEC cells in the presence of a FBS gradient. This difference in total cell number was not observed with the melanoma cell lines or HaCaT cells. Further analysis was performed to calculate the chemotactic differential value for the different leukocyte subsets. The chemotactic differential is the difference between the number of cells that have migrated across Transwells with 10% FBS in the lower chamber and the number of cells that have migrated across Transwells with 0.1% FBS in the lower chamber. This method of analysis was chosen over a migration index (ratio of migrated cells) as it has been previously published to provide a more accurate quantification of chemoattractant specific migration (Repo, Leirisalo & Kosunen 1981). As a rule of thumb, the difference between 0.1% and 0.1% will always be 0, and therefore, a chemotactic differential for 10% FBS that is significantly higher than 0 reflects the presence of FBS-directed migration.

As shown in Figure 4.2E, in the absence of a monolayer, all the assessed leukocyte subsets ($CD4^+$ T cells, $CD8^+$ T cells, $CD14^+$ monocytes, $CD16^+$ NK cells and $CD19^+$ B cells) demonstrated a trend in ability to respond and migrate specifically across an FBS gradient (compared to no gradient). Notably, in the presence of any cell monolayer, the overall migration of $CD8^+$ T cells was inhibited. The overall migration of $CD4^+$ T cells, $CD16^+$ NK cells and $CD19^+$ B cells in the presence of an FBS gradient was also impaired for most cell monolayers, with the exception of TrHBMEC and SK-Mel-28 monolayers. Interestingly, $CD14^+$ monocytes remained responsive to the FBS gradient and were able to migrate across all cell monolayers, including the three melanoma cell lines.

A)

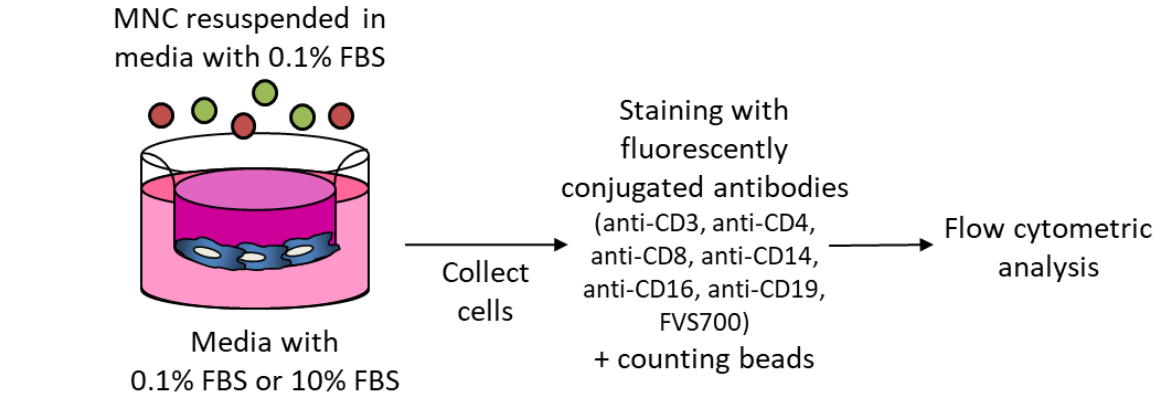
MNC resuspended in media with 0.1% FBS
Media with 0.1% FBS or 10% FBS
Collect cells
Staining with fluorescently conjugated antibodies (anti-CD3, anti-CD4, anti-CD8, anti-CD14, anti-CD16, anti-CD19, FVS700) + counting beads
Flow cytometric analysis

B)

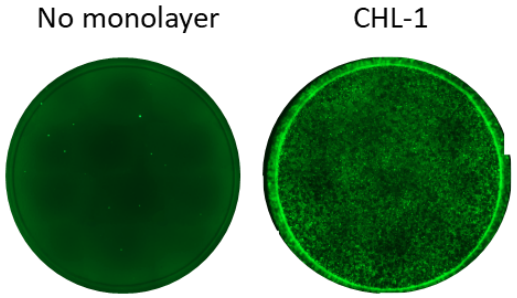
No monolayer
CHL-1

C)

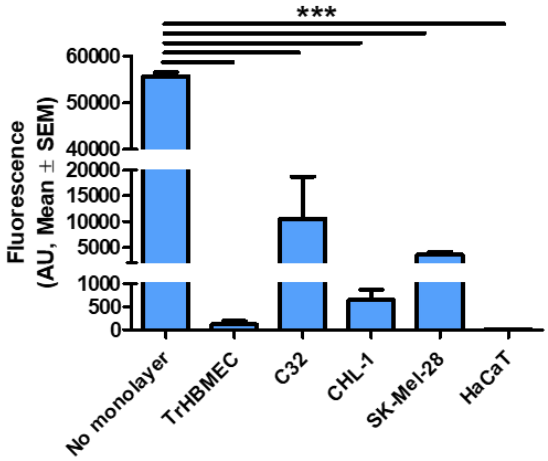
***
Fluorescence (AU, Mean ± SEM)
60000
50000
40000
20000
15000
10000
5000
1000
500
0
No monolayer
TrHBMEC
C32
CHL-1
SK-Mel-28
HaCaT

D)

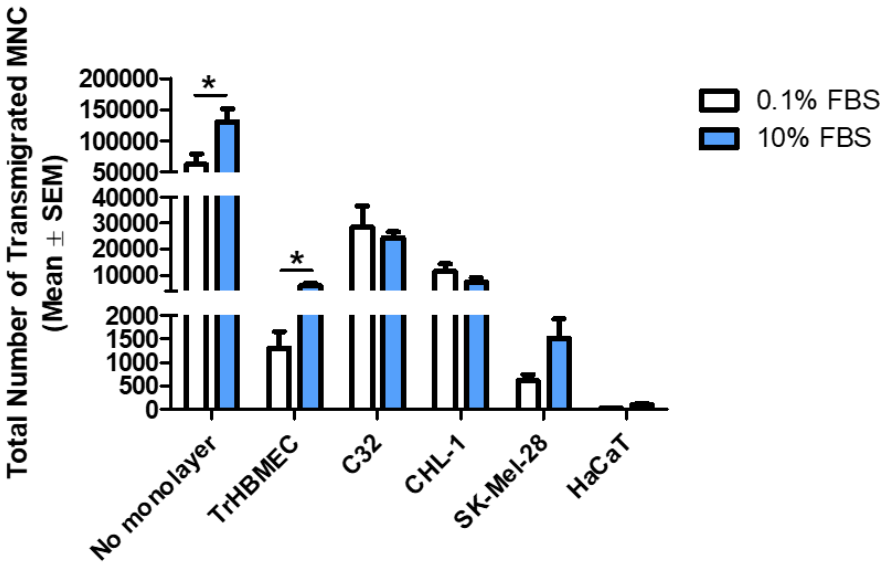
Total Number of Transmigrated MNC (Mean ± SEM)
200000
150000
100000
50000
40000
30000
20000
10000
2000
1500
1000
500
0
*
*
0.1% FBS
10% FBS
No monolayer
TrHBMEC
C32
CHL-1
SK-Mel-28
HaCaT

E)

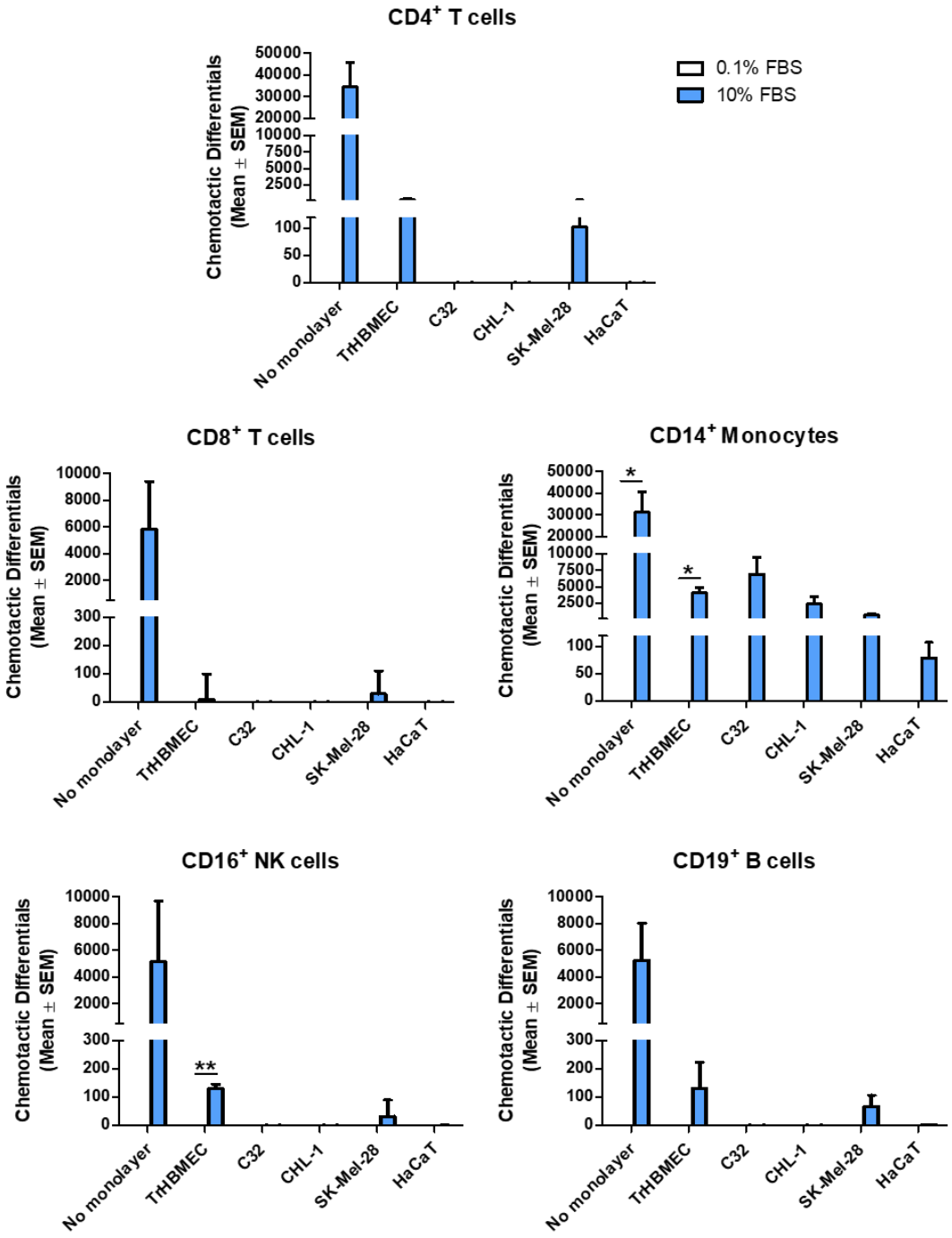
CD4+ T cells
0.1% FBS
10% FBS
Chemotactic Differentials (Mean ± SEM)
50000
40000
30000
20000
10000
7500
5000
2500
100
50
0
No monolayer
TrHBMEC
C32
CHL-1
SK-Mel-28
HaCaT
CD8+ T cells
10000
8000
6000
4000
2000
300
200
100
0
CD14+ Monocytes
*
*
CD16+ NK cells
**
CD19+ B cells

Figure 4.2. Some leukocyte subsets can transmigrate across a melanoma monolayer in response to an FBS gradient.

(A) The VM-competent melanoma cell lines C32, CHL-1 and SK-Mel-28, the EC line TrHBMEC and the keratinocyte cell line HaCaT were cultured on Transwells until a confluent monolayer was formed. MNC resuspended in medium containing 0.1% FBS were added onto the top chamber, while the bottom chamber was filled with medium containing 0.1% FBS or 10% FBS. After 3 hours, the cells in the bottom chamber were collected and stained with multiple fluorescently labelled antibodies targeting leukocyte subset specific surface markers to examine the phenotype of the transmigrated MNC via flow cytometry. FVS700 was included in the antibody mastermix to allow dead cells ($FVS700^+$) to be gated out from analysis. A standard number of counting beads was also added to the stained samples prior to flow cytometric analysis to allow for the determination of absolute MNC numbers. (B) Prior to the addition of MNC, the morphology of the cell monolayers was assessed via calcein AM staining. Representative images showing staining for Transwells with no monolayer and CHL-1 with $n \geq 3$ independent experiments. (C) Prior to the addition of MNC, the permeability of the cell monolayers was assessed by adding 2000 kDa FITC-labelled dextran to the top chamber, and measuring the fluorescence intensity of the medium in the bottom chamber following a 15-minute incubation. Bar graph shows the mean fluorescence in arbitrary units for each of the different monolayers ± SEM pooled from n=3 independent experiments. *** = $p < 0.0001$, one-way ANOVA with Bonferroni's Multiple Comparison Test. (D) The total number of transmigrated MNC was deduced following flow cytometric analysis using counting beads. Bar graph shows the mean total number of transmigrated MNC for all the different cell monolayers ± SEM from n= 4 independent MNC donors. * = $p < 0.05$, two-tailed paired t-test. (E) The phenotype of the transmigrated MNC was characterised using antibodies. Chemotactic differentials were obtained via subtracting the number of cells which have transmigrated across 0.1% FBS from the number of cells which have transmigrated across 10% FBS. Bar graphs show the mean chemotactic differentials for the different leukocyte subsets for each of the cell monolayers ± SEM with n= 4 independent MNC donors. * = $p < 0.05$, ** = $p < 0.005$, two-tailed paired t-test.

Subsequent Transwell assays were repeated with CXCL12, which has known chemotactic activities on both lymphocytes and monocytes (Ancuta et al. 2003; Hara-Chikuma et al. 2012), and has been described to be expressed in patient melanoma samples (Harlin, H. et al. 2009) (Figure 4.3A). As demonstrated in Figure 4.3B, initial optimisation of various concentrations of CXCL12 in the absence of a cell monolayer showed a dose dependent increase of both monocyte and lymphocyte transmigration. To achieve maximal leukocyte transmigration, 100 ng/ml of CXCL12 was selected for subsequent Transwell assays.

When the Transwell assay was repeated with 100 ng/ml of CXCL12, there was a significant increase in the total number of migrated MNC across all the cell monolayers, except for the HaCaT cell line (Figure 4.3C). Detailed analysis of the chemotactic differential confirmed that all of the different leukocyte populations migrated across TrHBMEC and the VM-competent melanoma cell lines towards CXCL12 (Figure 4.3D). This was observed at a much lower level on the negative control HaCaT cells.

A)

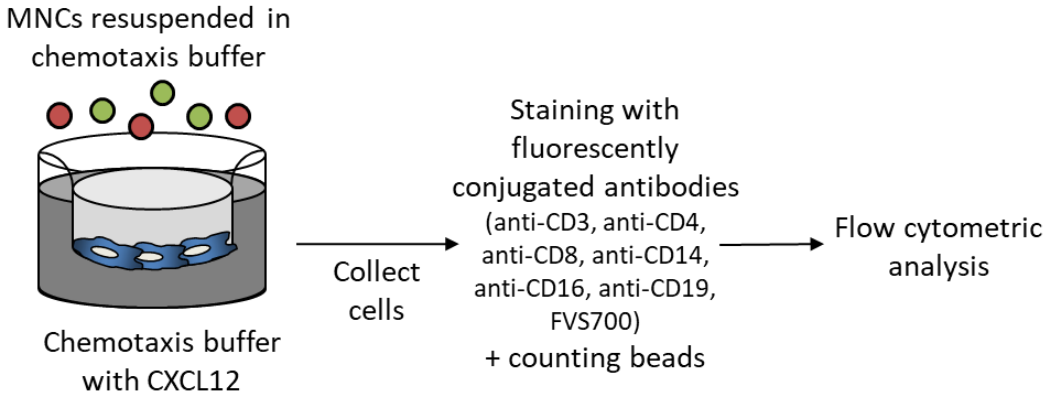
MNCs resuspended in chemotaxis buffer
Chemotaxis buffer with CXCL12
Collect cells
Staining with fluorescently conjugated antibodies
(anti-CD3, anti-CD4, anti-CD8, anti-CD14, anti-CD16, anti-CD19, FVS700)
+ counting beads
Flow cytometric analysis

B)

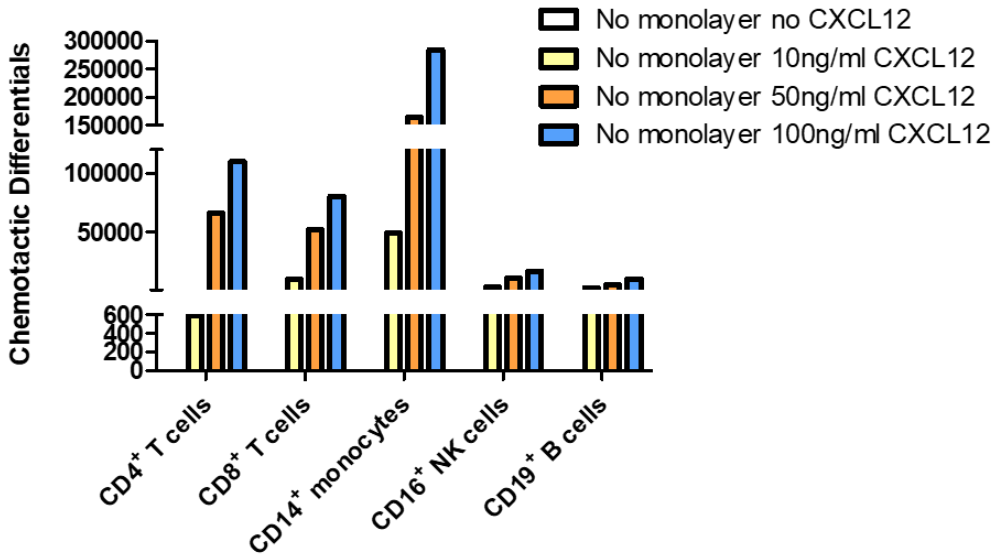
No monolayer no CXCL12
No monolayer 10ng/ml CXCL12
No monolayer 50ng/ml CXCL12
No monolayer 100ng/ml CXCL12
Chemotactic Differentials
300000
250000
200000
150000
100000
50000
600
400
200
0
CD4+ T cells
CD8+ T cells
CD14+ monocytes
CD16+ NK cells
CD19+ B cells

C)

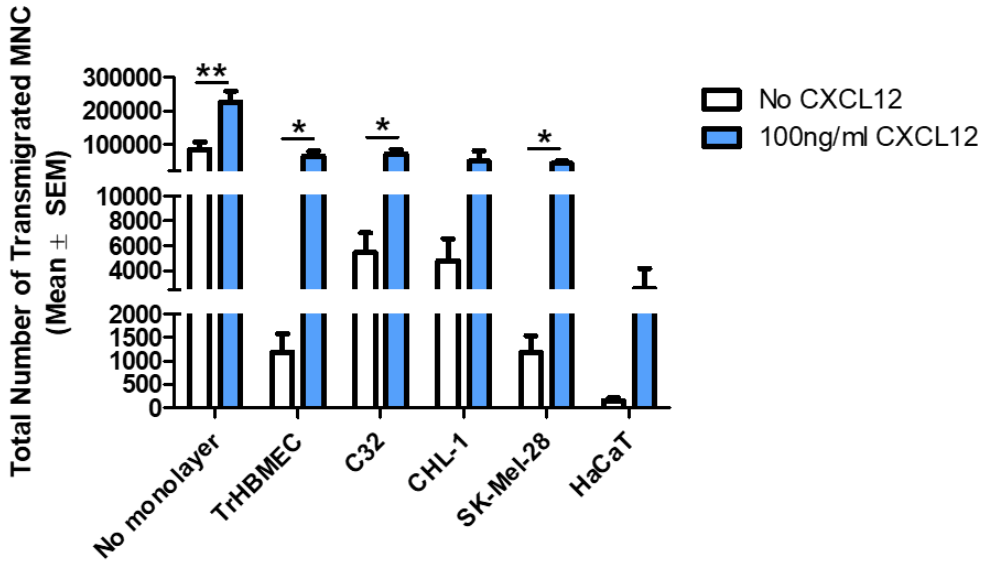
No CXCL12
100ng/ml CXCL12
Total Number of Transmigrated MNC (Mean ± SEM)
300000
200000
100000
10000
8000
6000
4000
2000
1500
1000
500
0
**
*
*
*
No monolayer
TrHBMEC
C32
CHL-1
SK-Mel-28
HaCaT

D)

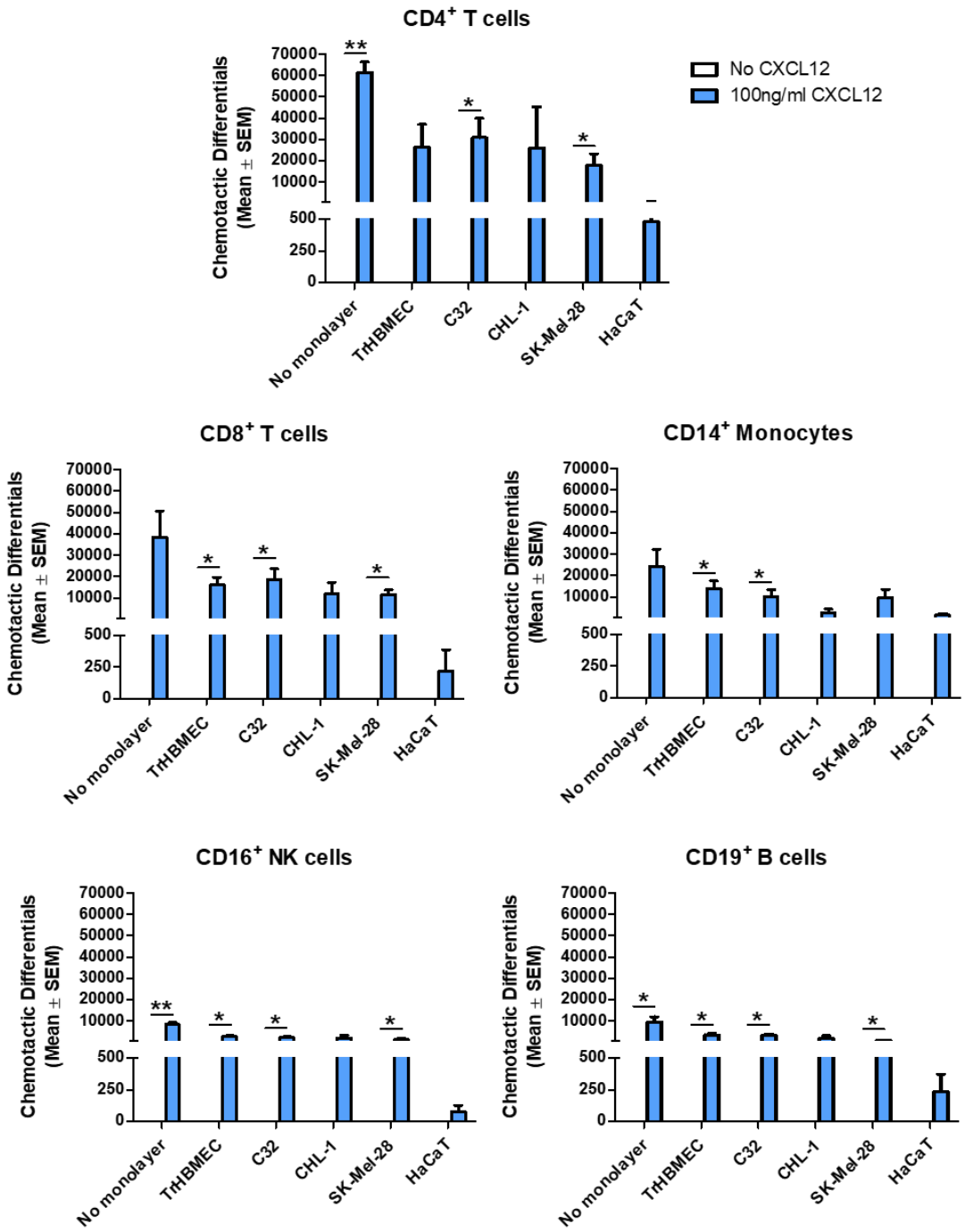
CD4+ T cells
CD8+ T cells
CD14+ Monocytes
CD16+ NK cells
CD19+ B cells
Chemotactic Differentials (Mean ± SEM)
No CXCL12
100ng/ml CXCL12
70000
60000
50000
40000
30000
20000
10000
500
250
0
**
*
No monolayer
TrHBMEC
C32
CHL-1
SK-Mel-28
HaCaT

Figure 4.3. Leukocytes can transmigrate across a melanoma monolayer in response to a CXCL12 gradient.

(A) The VM-competent melanoma cell lines C32, CHL-1 and SK-Mel-28, the EC line TrHBMEC and the keratinocyte cell line HaCaT were cultured on Transwells until a confluent monolayer was formed. MNC resuspended in chemotaxis buffer were added onto the top chamber, while the bottom chamber was filled with either chemotaxis buffer alone or chemotaxis buffer containing CXCL12. After 3 hours, the cells in the bottom chamber were collected and stained with multiple fluorescently labelled antibodies targeting leukocyte subset specific surface markers to examine the phenotype of the transmigrated MNC via flow cytometry. FVS700 was included in the antibody mastermix to allow dead cells ($FVS700^{+}$) to be gated out from analysis. A standard number of counting beads was also added to the stained samples prior to flow cytometric analysis to allow for the determination of absolute MNC numbers. (B) An optimisation was first performed with three different concentrations of CXCL12 to identify the CXCL12 concentration which allowed for maximal MNC transmigration. Bar graph shows the chemotactic differential for all the different leukocyte populations in the absence of a monolayer across the different concentrations of CXCL12 for n=1 independent MNC donor. (C) The total number of transmigrated MNC was deduced following flow cytometric analysis using counting beads. Bar graph shows the mean total number of transmigrated MNC for all the different cell monolayers ± SEM from n= 4 independent MNC donors. * = $p< 0.05$, ** = $p< 0.005$, two-tailed paired t-test. (D) The phenotype of the transmigrated MNC was characterised using antibodies. Chemotactic differentials were obtained via subtracting the number of cells which have transmigrated across no CXCL12 from the number of cells which have transmigrated across 100 ng/ml CXCL12. Bar graphs show the mean chemotactic differentials for the different leukocyte subsets for each of the cell monolayers ± SEM with n=3- 4 independent MNC donors. * = $p< 0.05$, ** = $p< 0.005$, two-tailed paired t-test.

Having established that leukocytes can indeed adhere on and migrate across a monolayer of VM-competent melanoma cells, the subsequent aim was to identify the potential adhesion molecules and chemokines involved in these processes. As discussed earlier in the introduction, the literature suggests that hypoxia plays a role in affecting adhesion molecule expression by ECs. This can occur through HIF-dependent regulation of gene transcription (Cartee et al. 2012) as well as through an increase in the angiogenic factors VEGF and bFGF, which leads to decreased levels of selectin and ICAM expression, and in turn correlates with decreased $CD8^+$ T cell infiltration (Dirkx, AE et al. 2003). Therefore hypoxic conditions were included to examine if this change in oxygen levels would also impact adhesion molecule and chemokine expression on melanoma cells.

Firstly, culture conditions that would best induce a hypoxic response were determined. This was performed by culturing the melanoma cell lines C32, CHL-1 and SK-Mel-28 in hypoxic chambers containing either 3% O_2 or 0.5% O_2 for 3, 7 or 14 days, or under ambient conditions (21% O_2) in a standard incubator. The cells were subjected to qPCR to assess expression of the hypoxia responsive genes *ANGPLT4*, *ANKRD37*, *ADM*, and *SLC2A1* (Benita et al. 2009; Hu et al. 2003; Kubo et al. 2016). These genes were selected following an *in silico* analysis of publically available data (Gene Expression Omnibus Accession ID GSE53012) by our laboratory (Olbryt et al. 2014). Briefly, Olbryt and colleagues cultured three separate cancer cell lines (melanoma, prostate, ovarian) under ambient (21% O_2), chronic (1% O_2 for 3 days) and cycling hypoxia (21% O_2 and 1% O_2 for 3 days) conditions, and then examined the global gene expression profile of these cells under the different culture conditions (Olbryt et al. 2014). Their findings suggested cell line-dependent variabilities in gene expression in response to hypoxia (Olbryt et al. 2014). Accordingly, we sought to identify the top four hypoxia responsive genes that were highly upregulated across the three cell lines to minimise the impact of variabilities that might arise from the use of different cell lines. Therefore, the published data was further interrogated by our laboratory and this led to the identification of the genes *ANGPLT4*, *ANKRD37*, *ADM*, and *SLC2A1* which were upregulated across the three separate cancer cell lines. Subsequent study of the literature confirmed that these genes were indeed hypoxia responsive genes (Benita et al. 2009; Hu et al. 2003; Kubo et al. 2016) and were hence used as markers for hypoxic stimulation. As demonstrated in Figure 4.4A, there appeared to still be cell line-specific variabilities in expression of the aforementioned genes under 0.5% O_2 or 3% O_2 stimulation. Nonetheless, in comparison to ambient conditions, there was an overall trend towards enhanced expression of

these genes in the melanoma cells cultured under 0.5% O_2, with statistical significance achieved for *ANKRD37* for C32 and CHL-1 for both 3 days and 7 days. On the other hand, in comparison to the cells cultured under 0.5% O_2, there was a trend towards decreased hypoxia responsive gene expression in cells cultured under 3% O_2, although statistical comparison could not be performed between these two conditions as the qPCR was only performed twice for the 3% O_2 condition. This suggested that the 0.5% O_2 condition could be more successful in stimulating a hypoxic response in the melanoma cell lines and hence was selected for subsequent assays.

One key limitation of this initial assessment was that all the cells cultured under hypoxic conditions were simultaneously harvested in a large batch. Hence, the cells were exposed to normoxic conditions for short periods of time (approximately 1 hour) during the harvesting process, which may allow for the recovery of these genes to normoxic levels. Therefore, for subsequent experiments using genome-wide RNA sequencing, the cells were harvested in small batches and kept on ice to minimise the potential effects of re-exposure to normoxia. When RNA sequencing was performed on the melanoma cells cultured under ambient or 0.5% O_2 conditions for 3 or 7 days and harvested in small batches, there was an overall upregulation of all of these genes as expected (Figure 4.4B). Note that *ANGPLT4* expression was not detected on the SK-Mel-28 for unknown reasons. In addition to that, four other hypoxia responsive genes *BNIP3*, *ENO1*, *LDHA* and *PGK1* (Hu et al. 2003; Zheng et al. 2016) were interrogated and were found to be significantly upregulated when the cells were cultured under 0.5% O_2 conditions, thereby further confirming that 0.5% O_2 culture conditions for either 3 or 7 days induced a hypoxic response in these cells.

A)

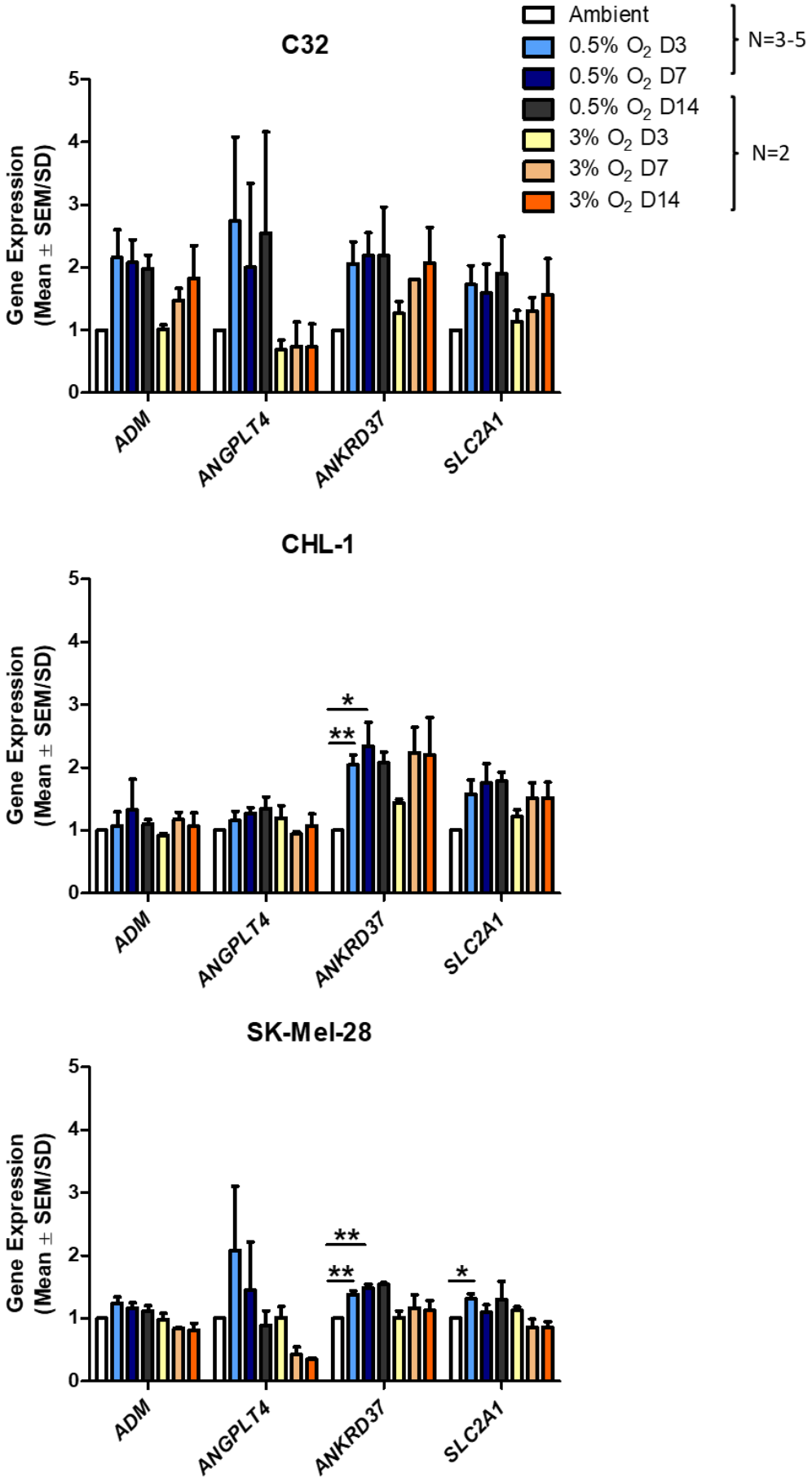
C32
Ambient
0.5% O2 D3
0.5% O2 D7
0.5% O2 D14
3% O2 D3
3% O2 D7
3% O2 D14
N=3-5
N=2
Gene Expression (Mean ± SEM/SD)
0
1
2
3
4
5
ADM
ANGPLT4
ANKRD37
SLC2A1
CHL-1
*
**
SK-Mel-28
**
**
*

B)

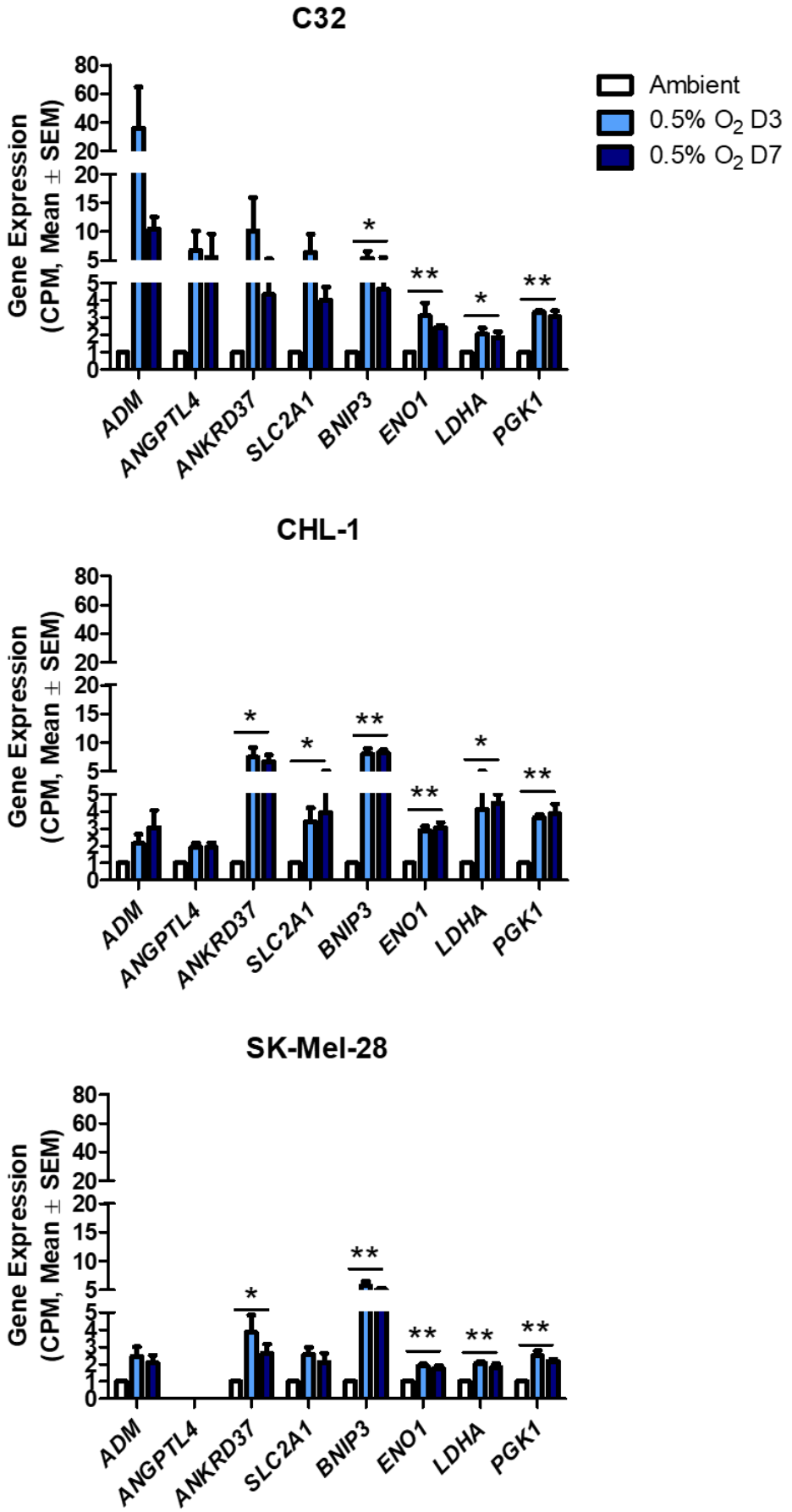
C32
Ambient
0.5% O2 D3
0.5% O2 D7
Gene Expression
(CPM, Mean ± SEM)
ADM
ANGPTL4
ANKRD37
SLC2A1
BNIP3
ENO1
LDHA
PGK1
CHL-1
SK-Mel-28

Figure 4.4. 0.5% O_2 culture conditions stimulate the expression of hypoxia responsive genes in C32, CHL-1 and SK-Mel-28.

(A) The VM-competent melanoma cell lines C32, CHL-1 and SK-Mel-28 were cultured under ambient (21% O_2), 0.5% O_2 or 3% O_2 conditions for 3, 7 or 14 days. RNA was harvested from the cells, and qPCR was performed to examine the induction of hypoxia through the expression of hypoxia responsive genes *ADM*, *ANGPLT4*, *ANKRD37* and *SLC2A1*. Bar graphs show mean fold change of gene expression over ambient ± SEM (for 0.5 % O_2 culture conditions) or SD (for 3 % O_2 culture conditions) with n=2-5. * = $p< 0.05$, ** = $p< 0.005$, two-tailed paired t-test. (B) C32, CHL-1 and SK-Mel-28 were cultured under ambient (21% O_2) or 0.5% O_2 conditions for 3 or 7 days. RNA was harvested from the cells, and RNA sequencing was performed. The expression levels of multiple hypoxia responsive genes were examined to confirm the induction of hypoxia. Bar graphs show mean fold change of gene expression over ambient ± SEM with n=3. * = $p< 0.05$, ** = $p< 0.005$, one way repeated measures ANOVA with Bonferroni's Multiple Comparison Test.

Next, to examine if the 0.5% O_2 hypoxic conditions could also stimulate changes in adhesion molecule expression by ECs, as described in the literature (Cartee et al. 2012), resting TrHBMEC were cultured in 0.5% O_2 for both 3 and 7 days and then subjected to flow cytometry analysis. Unexpectedly, there were very minimal changes in adhesion molecule expression between TrHBMEC cultured under ambient and 0.5% O_2 conditions (Figure 4.5A). Even though there appeared to be a statistically significant downregulation of CD44 and ICAM-1 expression upon quantification (Figure 4.5B), this reduction is unlikely to be physiologically relevant. Parallel plate flow chamber assays performed on these cells revealed no changes in the total number of bound cells between TrHBMEC cultured under ambient and 0.5% O_2 for 3 days (Figure 4.5C), thereby confirming that as expected, the lack of adhesion molecule expression changes under hypoxic conditions did not result in changes in leukocyte adhesion. The possible reasons contributing to this will be addressed in the discussion.

A)

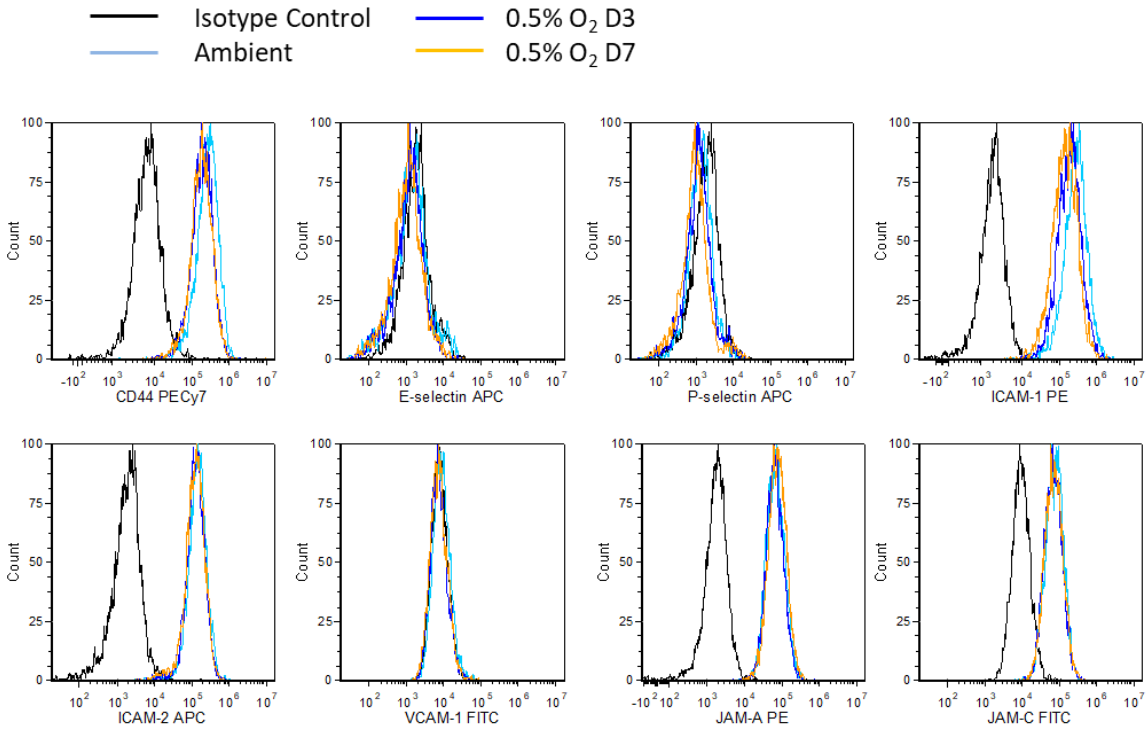
Isotype Control
Ambient
0.5% O2 D3
0.5% O2 D7
Count
CD44 PECy7
E-selectin APC
P-selectin APC
ICAM-1 PE
ICAM-2 APC
VCAM-1 FITC
JAM-A PE
JAM-C FITC

B)

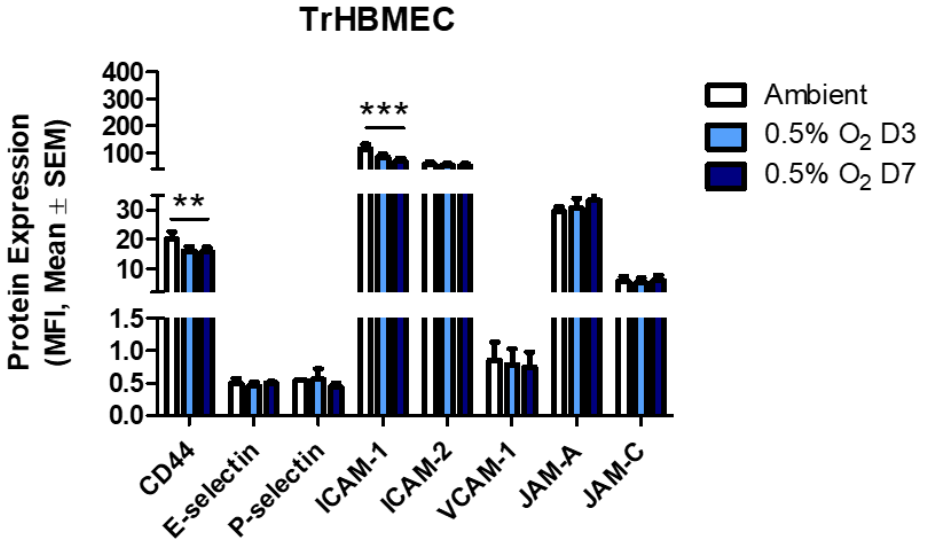
TrHBMEC
Protein Expression
(MFI, Mean ± SEM)
Ambient
0.5% O2 D3
0.5% O2 D7
**
***
CD44
E-selectin
P-selectin
ICAM-1
ICAM-2
VCAM-1
JAM-A
JAM-C

C)

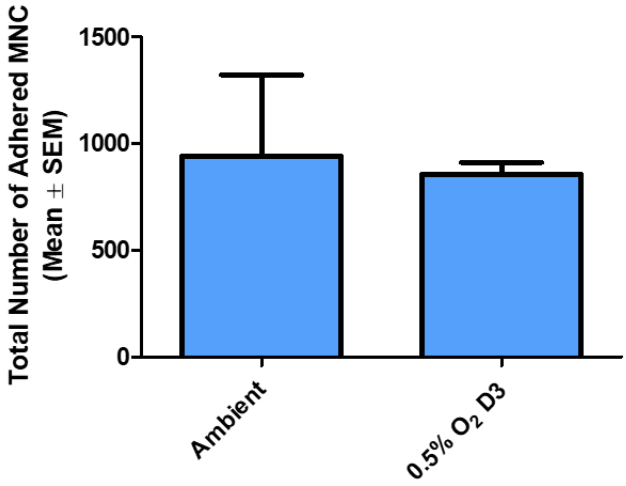

Figure 4.5. TrHBMEC do not show altered adhesion molecule expression or reduced leukocyte adhesion after culture in 0.5% O_2.

TrHBMEC were cultured under ambient (21% O_2) and hypoxic (0.5% O_2) conditions for 3 (D3) or 7 days (D7). To examine surface protein expression of adhesion molecules, the cultured cells were harvested and stained with multiple fluorescently labelled antibodies targeting specific adhesion molecules and subjected to flow cytometric analysis. 7-AAD was included in the antibody mastermix to allow dead cells (7-AAD$^+$) to be gated out from analysis. (A) Representative histograms showing adhesion molecule expression on TrHBMEC cells under ambient, 0.5% O_2 for 3 days (D3) and 0.5% O_2 for 7 days (D7) for n=3 independent experiments. (B) Mean adhesion molecule protein expression (MFI) (normalised over isotype control) ± SEM, pooled from n=3 independent experiments. ** = p< 0.005, *** = p< 0.0005, one way Repeated Measures ANOVA with Bonferroni's Multiple Comparison Test. (C) TrHBMEC were cultured under either ambient (21% O_2) or 0.5% O_2 conditions for 3 days on dishes until a confluent monolayer was formed. Calcein AM-labelled MNC ($8x10^6$) were flowed across the cell monolayer at a defined shear stress of 0.5 dynes/cm^2. Any unbound cells were rinsed off, and the adhered cells were harvested and subjected to flow cytometric analysis with the addition of a standard number of counting beads to determine absolute cell numbers. Bar graph shows total number of adhered MNC ± SEM, pooled from n=3-5 independent MNC donors.

To obtain a non-biased global understanding of adhesion molecule and chemokine gene expression by the melanoma cell lines, total RNA was collected from cells cultured under ambient, 0.5% O_2 for 3 and 7 days, and subjected to RNA sequencing. Following stringent filtering to remove both duplicate entries and low level noise genes (with CPM expression values of under 1 for the triplicates), the filtered data was normalised with an algorithm and the results were narrowed down to a concise list of genes which were expressed by the cells under the different culture conditions. As demonstrated in Figure 4.6, the results show that melanoma cells express genes for several adhesion molecules that are characteristic of ECs and are involved in leukocyte recruitment. More specifically, all three melanoma cell lines expressed mRNA for at least one adhesion molecule required for each step of the leukocyte recruitment process, namely *CD44* for leukocyte rolling, *ICAM1* for leukocyte adhesion as well as *F11R* and *JAM3* required for leukocyte transmigration, with the exception of CHL-1 which lacked *ICAM1* expression. Apart from a modest but statistically significant downregulation in *CD44* expression by CHL-1, expression levels of the aforementioned genes remained largely unchanged following hypoxia (Figure 4.6).

Next, the protein expression of these adhesion molecules on the cell surface was assessed using flow cytometric analysis (Figure 4.7). The results confirmed the expression of CD44, ICAM-1, JAM-A and JAM-C on the surface of the melanoma cells at levels that correlated with their gene expression levels. Even though CHL-1 lacked *ICAM1* gene expression, ICAM-1 protein was detected on the cell surface (Figure 4.7). The overall protein expression of these adhesion molecules remained unchanged under hypoxic stimulation. While there appeared to be a statistically significant downregulation of JAM-A and JAM-C expression on CHL-1 upon quantification (Figure 4.7B), this reduction is very slight and unlikely to be physiologically relevant. Together, the results indicate that VM-competent melanoma cells are equipped with a full suite of adhesion molecules which would allow them to promote leukocyte rolling, adhesion and transmigration.

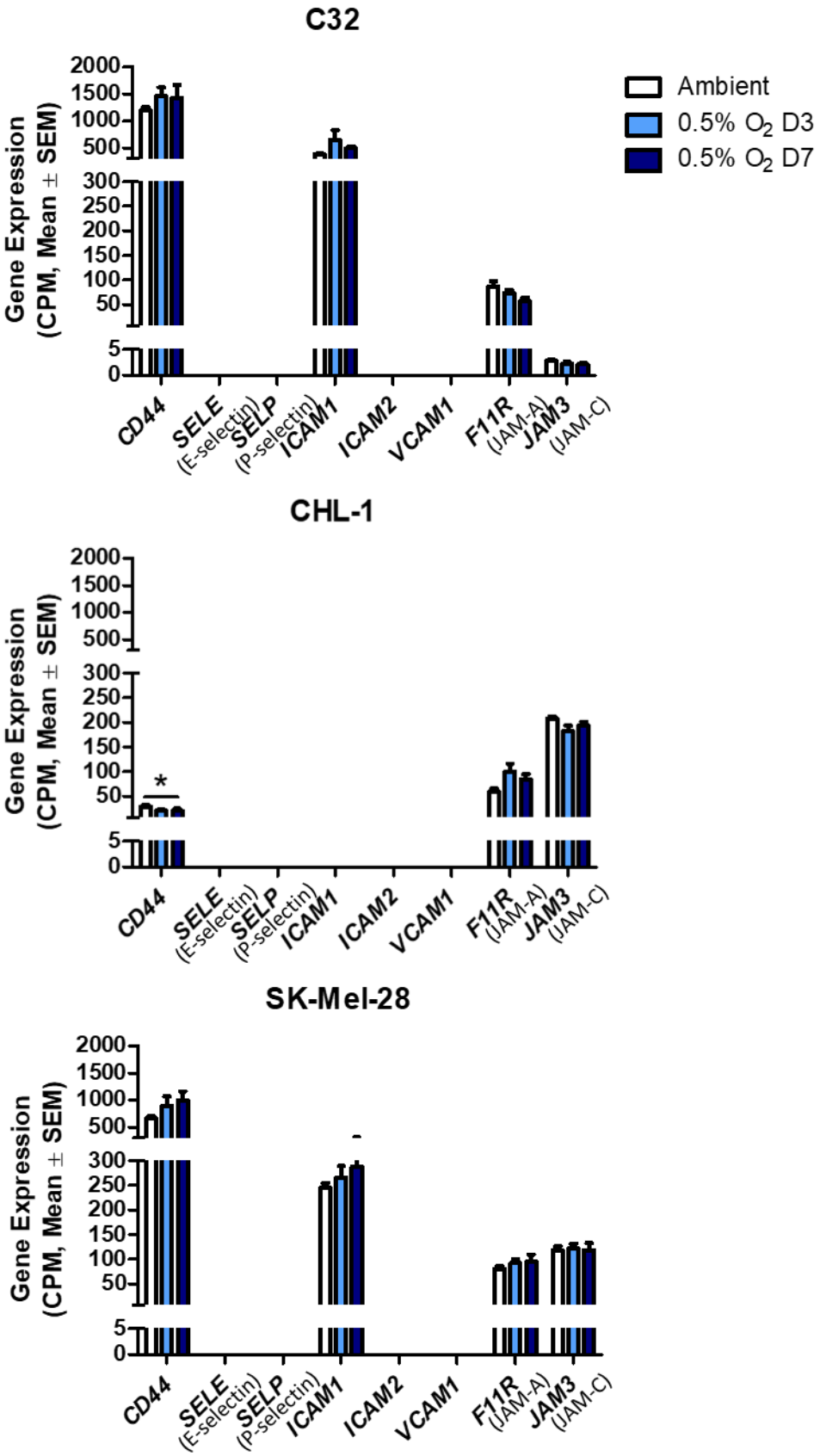
C32
Ambient
0.5% O2 D3
0.5% O2 D7
Gene Expression
(CPM, Mean ± SEM)
2000
1500
1000
500
300
250
200
150
100
50
5
0
CD44
SELE (E-selectin)
SELP (P-selectin)
ICAM1
ICAM2
VCAM1
F11R (JAM-A)
JAM3 (JAM-C)
CHL-1
*
SK-Mel-28

Figure 4.6. C32, CHL-1 and SK-Mel-28 express mRNA for adhesion molecules characteristic of endothelial cells under both ambient and hypoxic conditions.

C32, CHL-1 and SK-Mel-28 were cultured under ambient (21% O_2) and hypoxic (0.5% O_2) conditions for 3 (D3) or 7 days (D7). To examine gene expression of various adhesion molecules, total RNA was harvested from the cultured cells and subjected to RNA sequencing. Bar graphs shows mean adhesion molecule gene expression (counts per million, CPM) ± SEM, with n=3 independent samples. ** = $p< 0.005$, one way Repeated Measures ANOVA with Bonferroni's Multiple Comparison Test.

A)

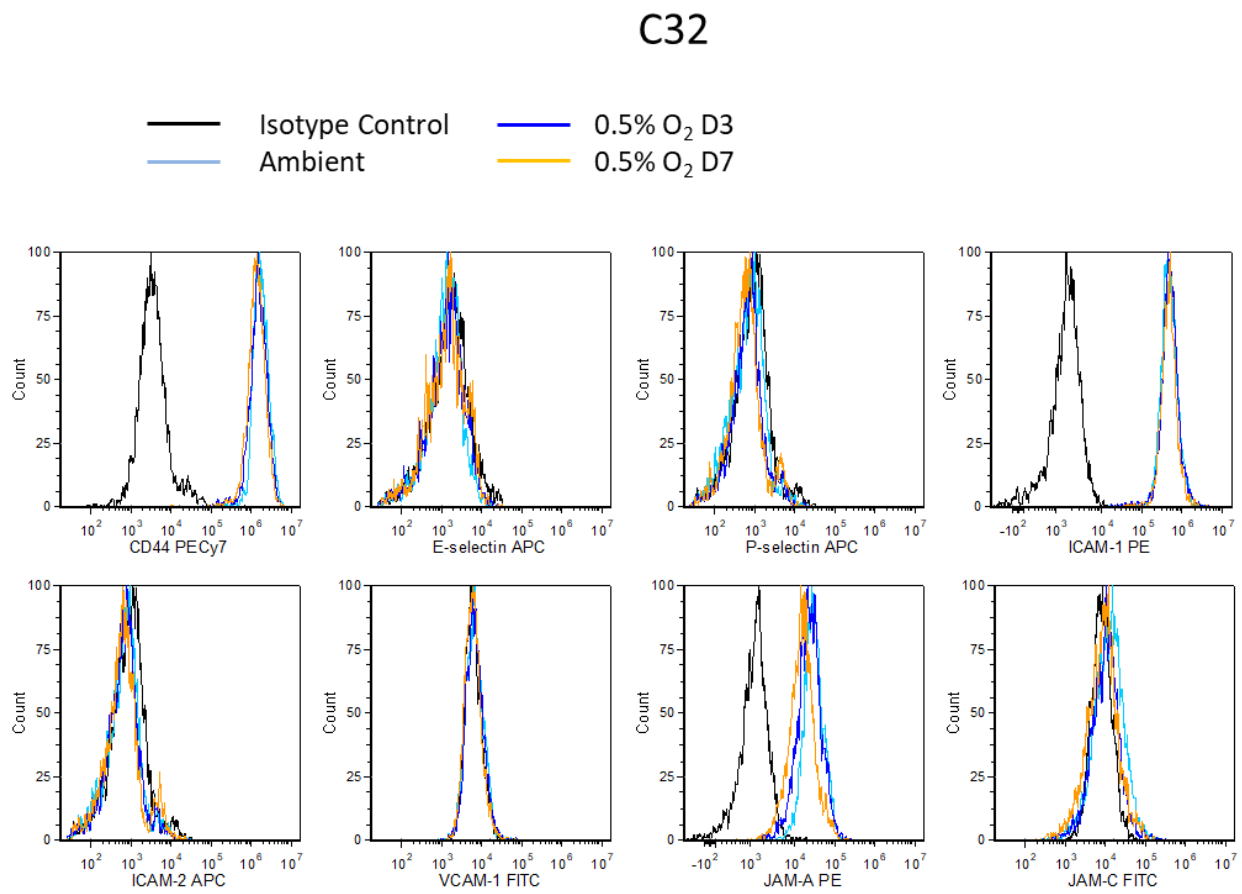
C32
Isotype Control
Ambient
0.5% O2 D3
0.5% O2 D7
Count
CD44 PECy7
E-selectin APC
P-selectin APC
ICAM-1 PE
ICAM-2 APC
VCAM-1 FITC
JAM-A PE
JAM-C FITC

B)

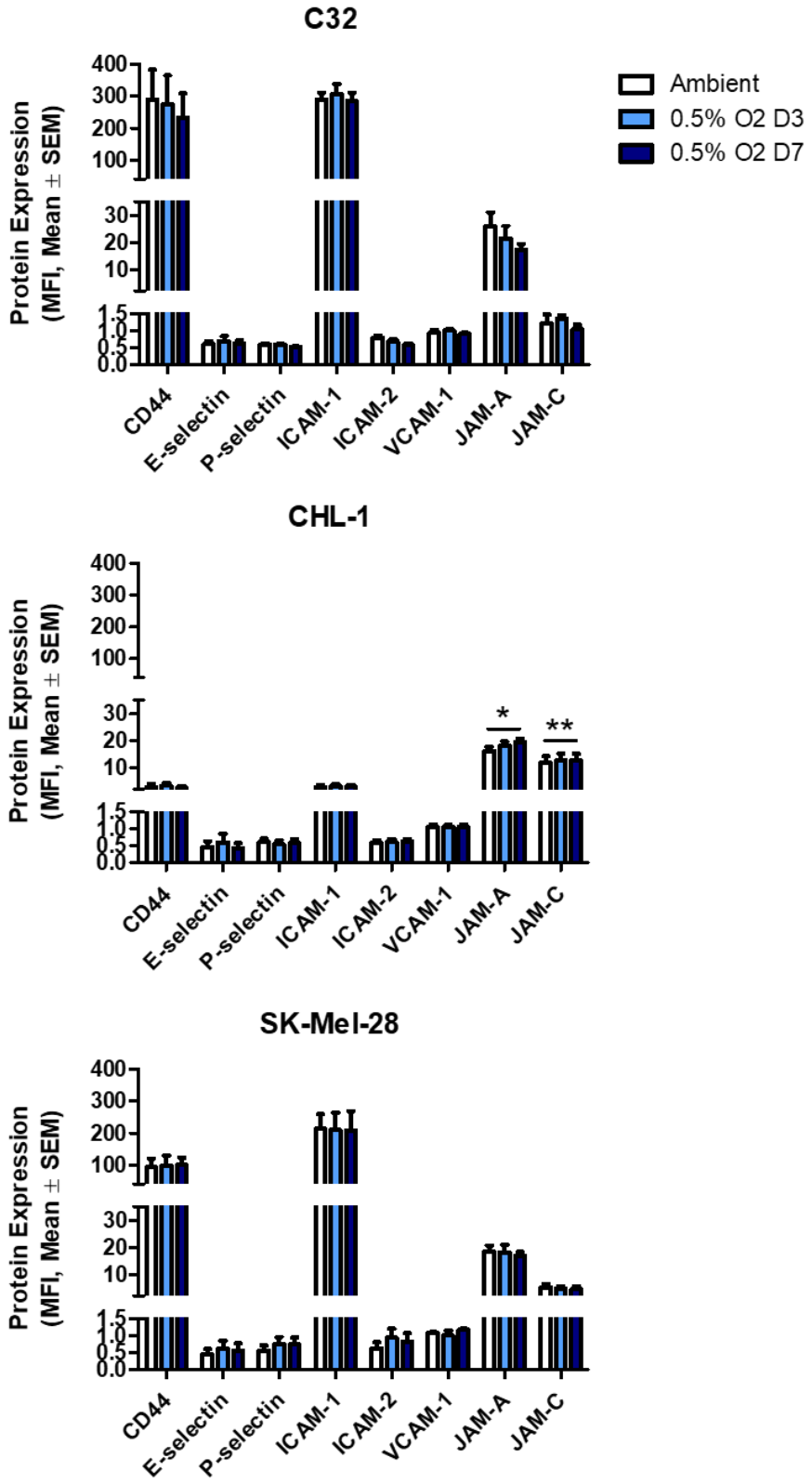
C32
Ambient
0.5% O2 D3
0.5% O2 D7
Protein Expression
(MFI, Mean ± SEM)
400
300
200
100
30
20
10
1.5
1.0
0.5
0.0
CD44
E-selectin
P-selectin
ICAM-1
ICAM-2
VCAM-1
JAM-A
JAM-C
CHL-1
*
**
SK-Mel-28

Figure 4.7. C32, CHL-1 and SK-Mel-28 express adhesion molecules characteristic of endothelial cells on the cell surface under both ambient and hypoxic conditions.

C32, CHL-1 and SK-Mel-28 were cultured under ambient (21% O_2) and hypoxic conditions (0.5% O_2) for 3 (D3) or 7 days (D7). To examine surface protein expression of adhesion molecules, the cultured cells were harvested and stained with multiple fluorescently labelled antibodies targeting specific adhesion molecules and subjected to flow cytometric analysis. 7-AAD was included in the antibody mastermix to allow dead cells (7-AAD^+) to be gated out from analysis. (A) Representative histograms showing adhesion molecule expression on C32 cells cultured under ambient, 0.5% O_2 for 3 days (D3) and 0.5% O_2 for 7 days (D7) for n=3 independent experiments. (B) The adhesion molecule protein expression was quantified by assessing the mean fluorescence intensity (MFI). Bar graphs show mean adhesion molecule protein expression (MFI) (normalised over isotype control) ± SEM, with n=3 independent experiments. * = $p< 0.05$, ** = $p< 0.005$, one way Repeated Measures ANOVA with Bonferroni's Multiple Comparison Test.

Having characterised the adhesion molecule profile of these VM-competent melanoma cells, subsequent blocking assays were performed to determine if these adhesion molecules contributed to the leukocyte rolling and adhesion observed in Figure 4.1. More specifically, parallel plate flow chamber assays were undertaken with the C32 melanoma monolayer pre-treated with an ICAM-1 blocking antibody. As the final readout of this assay relies on characterising the leukocytes which are adhered onto the monolayer, ICAM-1 was chosen as a blocking target due to its important role in mediating leukocyte adhesion. As demonstrated in Figure 4.8A, in comparison to the untreated C32 melanoma cells, the addition of the IgG1 control antibody led to an unexpected reduction of adhesion of these cells. The blocking of ICAM-1 on C32 melanoma cells however resulted in a greater reduction in $CD4^+$ T cell, $CD8^+$ T cell and $CD19^+$ B cell adhesion compared to both the untreated and control mIgG1 conditions (Figure 4.8A). In contrast and unexpectedly, blocking ICAM-1 on the control cell line TrHBMEC revealed an opposite trend, with minimal reduction of $CD4^+$ T cell, $CD8^+$ T cell and $CD19^+$ B cell adhesion (Figure 4.8A). There was also a striking increase in $CD14^+$ monocyte binding on TrHBMEC with ICAM-1 blocking (Figure 4.8A). This unexpected finding on the TrHBMEC highlighted the need for further optimisation of the study. As monocytes are known to express Fc receptors (FcR) as part of their surveillance function (Liu, Y et al. 2005), binding of the anti-ICAM-1 antibody onto the TrHBMEC monolayer may have provided Fc regions available for binding by the monocytes via their FcR, leading to the enhanced monocyte binding observed. To eliminate this, the MNC used for the subsequent experiment were pre-treated with human IgG to block any free FcR on the MNC. As shown in Figure 4.8B, hIgG1 treatment did not reduce the number of monocytes bound on ICAM-1 treated TrHBMEC compared to their untreated counterparts, suggesting that the unexpected binding of monocytes may be due to reasons unrelated to FcR function. Due to time constraints, no further optimisation or experiments were performed to confirm that ICAM-1 is responsible for the adhesion of MNC subsets to ECs or melanoma cells.

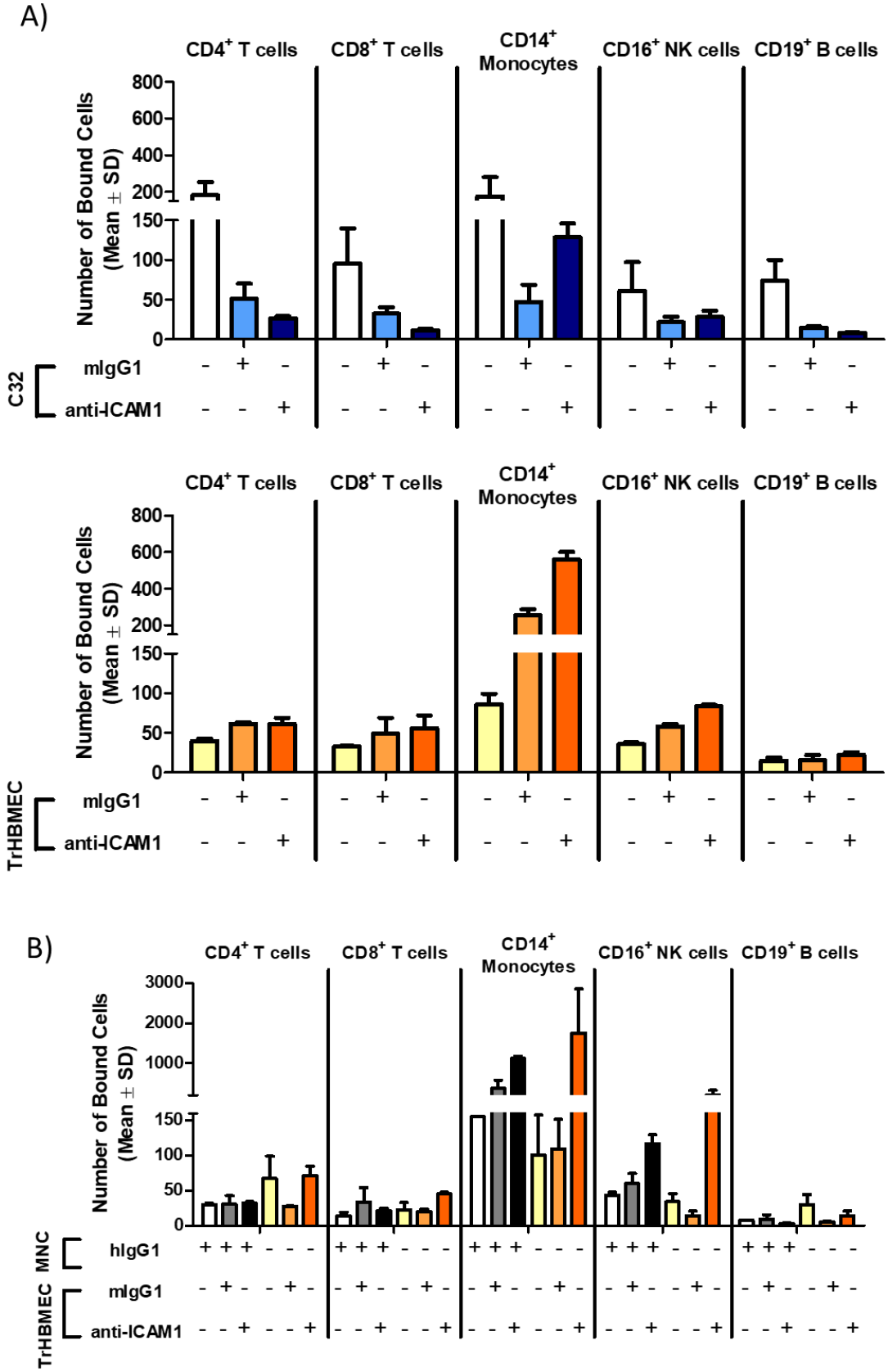
A)
CD4+ T cells
CD8+ T cells
CD14+ Monocytes
CD16+ NK cells
CD19+ B cells
Number of Bound Cells (Mean ± SD)
800
600
400
200
150
100
50
0
C32
mIgG1
anti-ICAM1
TrHBMEC
B)
3000
2000
1000
MNC
hIgG1

Figure 4.8. The effect of blocking ICAM-1 on leukocyte adhesion to melanoma cells could not be assessed.

C32 and TrHBMEC were cultured under ambient conditions on dishes until a confluent monolayer was formed. The monolayers were treated with either a mIgG1 isotype control or ICAM-1 blocking antibody for 1 hour at 37°C. Later, $8x10^6$ calcein AM-labelled MNC were flowed across the monolayer at a defined shear stress of 0.5 dynes/cm^2. Any unbound cells were rinsed off, and the adhered cells were harvested and stained with multiple fluorescently labelled antibodies targeting leukocyte subset specific surface markers to examine the phenotype of the adhered MNC via flow cytometry. FVS700 was included in the antibody mastermix to allow dead cells ($FVS700^+$) to be gated out from the analysis. A standard number of counting beads was also added to the stained samples prior to flow cytometric analysis to allow for the determination of absolute MNC numbers. (A) Bar graph shows mean number of bound cells (technical duplicates) ± SD for n=1 MNC donor. (B) The experiment as described above was repeated on TrHBMEC, with the additional treatment of MNCs with hIgG1 for at least 1 hour on ice to block Fc receptors. Bar graph shows mean number of bound cells (technical duplicates) ± SD for n=1 independent MNC donor.

In addition to adhesion molecules, chemokines also play a crucial role in regulating leukocyte recruitment. The RNA sequencing data obtained from melanoma cells cultured under ambient conditions or 0.5% O_2 for 3 days or 7 days was further interrogated with the aforementioned criteria to identify chemokines which were expressed on the gene level in these cell lines. The chemokines expressed by each of the melanoma cell lines are presented in Figure 4.9. Some of the chemokines were commonly expressed across all three cell lines, including *CX3CL1*, *CXCL16*, *CCL28* and *CCL5*. In addition, some cell lines also expressed several other chemokine and chemotactic cytokine genes, such as *MDK*, *IL16*, *CXCL12* and *CXCL1*. The gene expression levels of these chemokines remained largely unchanged under hypoxia stimulation, with the exception of a significant increase in *CXCL16* expression on C32 and *CCL28* on CHL-1 respectively, as well as a significant decrease in *CXCL12* expression on CHL-1 and *CX3CL1* on SK-Mel-28 respectively following hypoxic culture.

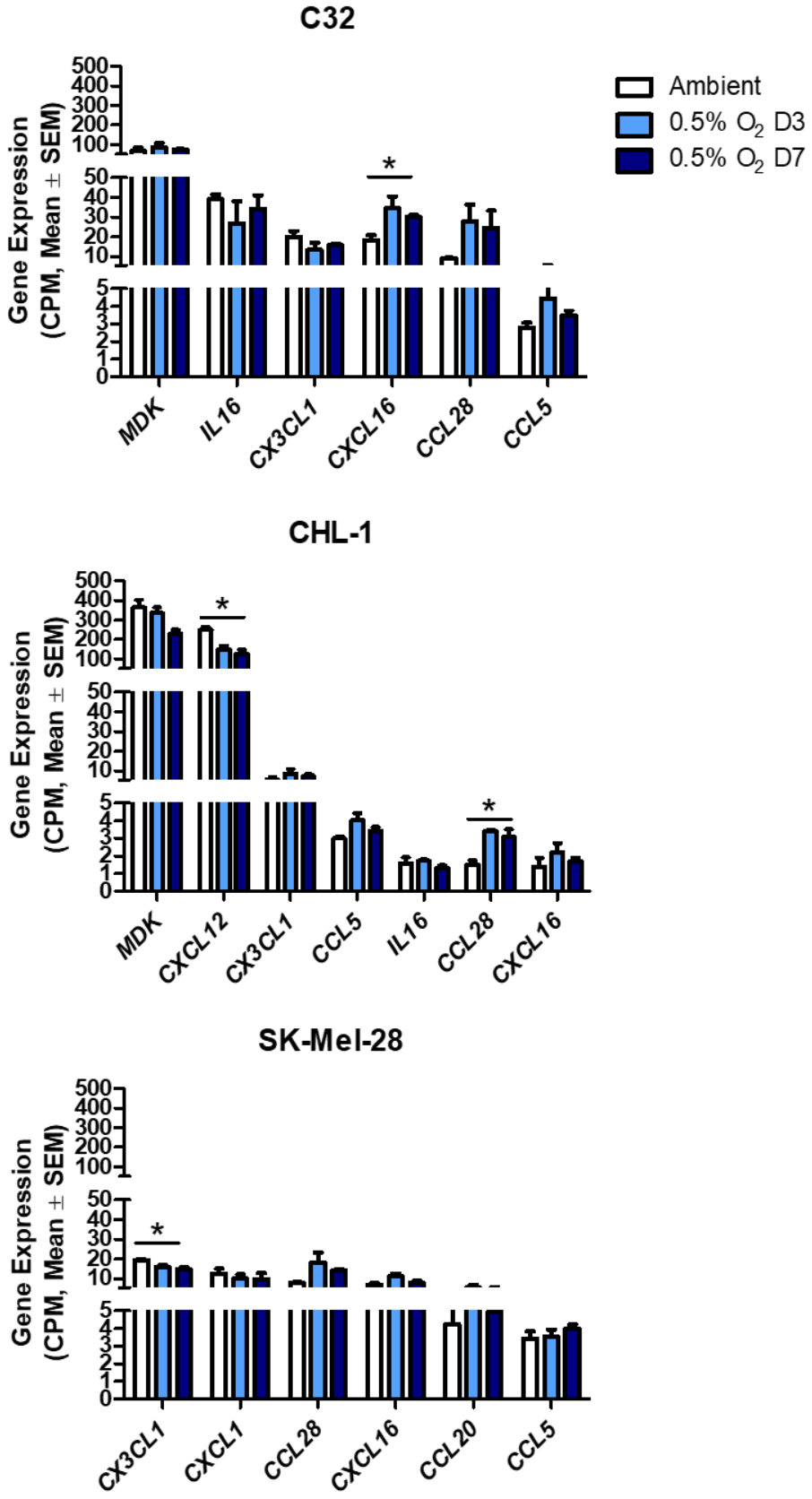
C32
Gene Expression (CPM, Mean ± SEM)
Ambient
0.5% O2 D3
0.5% O2 D7
MDK
IL16
CX3CL1
CXCL16
CCL28
CCL5
CHL-1
MDK
CXCL12
CX3CL1
CCL5
IL16
CCL28
CXCL16
SK-Mel-28
CX3CL1
CXCL1
CCL28
CXCL16
CCL20
CCL5

Figure 4.9. C32, CHL-1 and SK-Mel-28 express mRNA for chemokines under both ambient and hypoxic conditions.

C32, CHL-1 and SK-Mel-28 were cultured under ambient (21% O_2) and hypoxic (0.5% O_2) conditions for 3 (D3) or 7 days (D7). To examine gene expression of various chemokines, total RNA was harvested from the cultured cells and subjected to RNA sequencing. Bar graphs show mean chemokine gene expression (counts per million, CPM) ± SEM, with n=3 independent samples. * = $p< 0.05$, ** = $p< 0.005$, one way Repeated Measures ANOVA with Bonferroni's Multiple Comparison Test.

To confirm expression of chemokines at the protein level, melanoma cell culture supernatants were analysed using a commercially available chemokine array. Briefly, melanoma cells were grown at 100% confluency in 10ml of culture medium in a 175 cm^2 flask for 3 days until the supernatant was collected. The collected supernatant was mixed with detection antibodies and the mix was then added onto a membrane blotted with capture antibodies. The captured chemokines were then detected via chemiluminescence. An array performed with the melanoma cell culture medium RF10 alone revealed that cell culture medium contained low but detectable levels of CXCL12 (Figure 4.10A). In comparison, there were many more chemokine spots detected on the membrane blotted with melanoma cell culture supernatants, indicating that these chemokines were secreted by the melanoma cells and were not originally present in the culture medium (Figure 4.10A).

To confirm expression of chemokines above background and RF10 levels, the intensity of each spot was quantified using densitometry analysis and normalised over background and over that of RF10. As shown in Figure 4.10B, supernatant from C32 contained low levels of CXCL8, CXCL16, CX3CL1 and midkine. CHL-1 supernatant contained high levels of CXCL12 and midkine, as well as lower levels of CXCL16 and CX3CL1. SK-Mel-28 supernatant contained high levels of CXCL8, and lower levels of CCL3, CCL4, CCL20, CXCL1, CXCL7, CXCL16, CX3CL1 and midkine. Interestingly, some of these chemokines or chemotactic cytokines (e.g. CXCL8 for C32 and SK-Mel-28; CCL3, CCL4, CXCL7 and midkine for SK-Mel-28) were not identified in the RNA sequencing (Figure 4.9) and yet were present at detectable levels in the supernatant. Similarly, while CCL28 was detected at high levels at the RNA level for all three melanoma cell lines (Figure 4.9), it was barely detectable at the protein level (Figure 4.10). In addition, minimal changes in chemokine expression were observed with hypoxia, although additional experiments are required to provide the confidence/power for statistical analysis.

A)

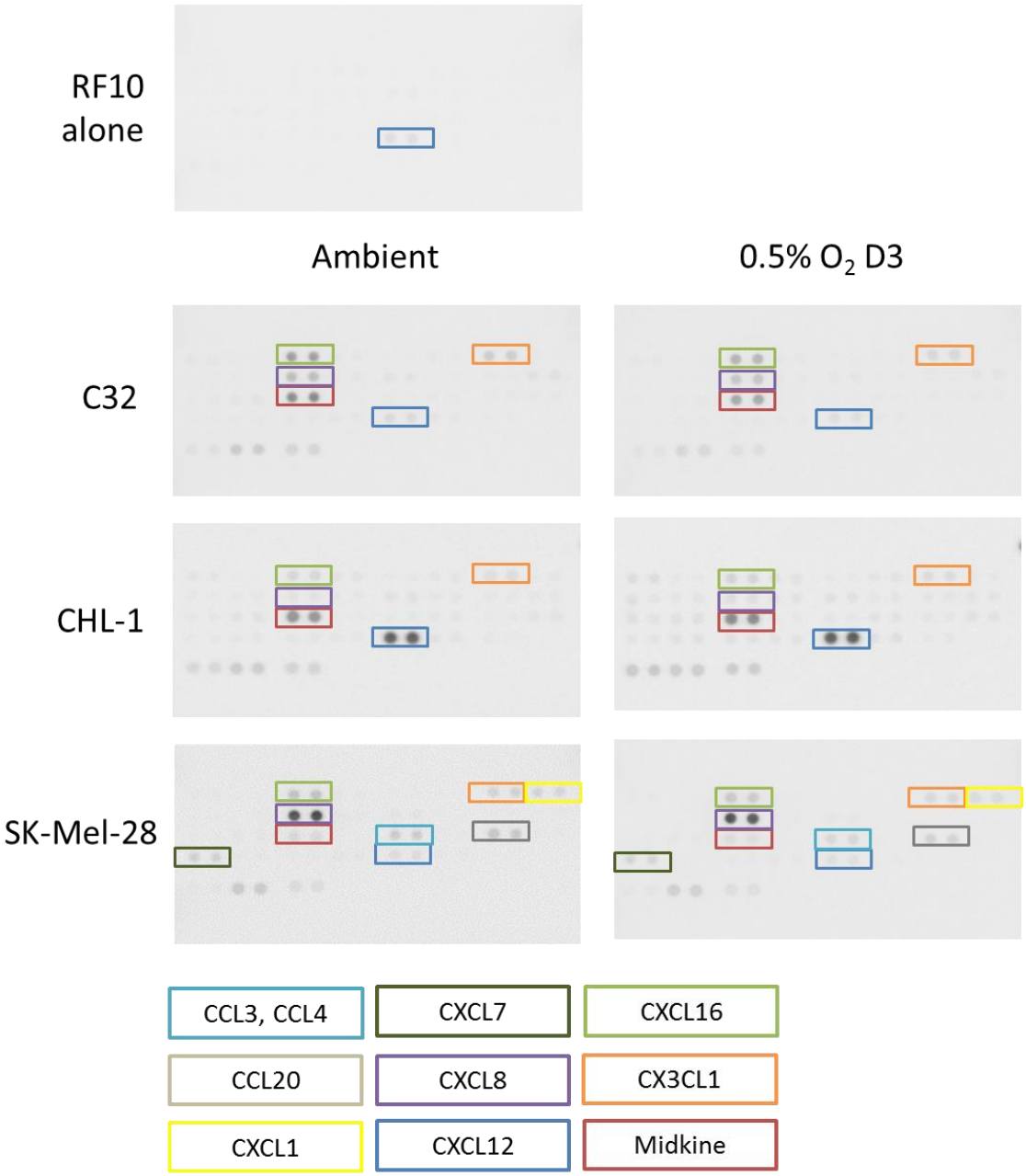
RF10 alone
Ambient
0.5% O_2 D3
C32
CHL-1
SK-Mel-28
CCL3, CCL4
CXCL7
CXCL16
CCL20
CXCL8
CX3CL1
CXCL1
CXCL12
Midkine

B)

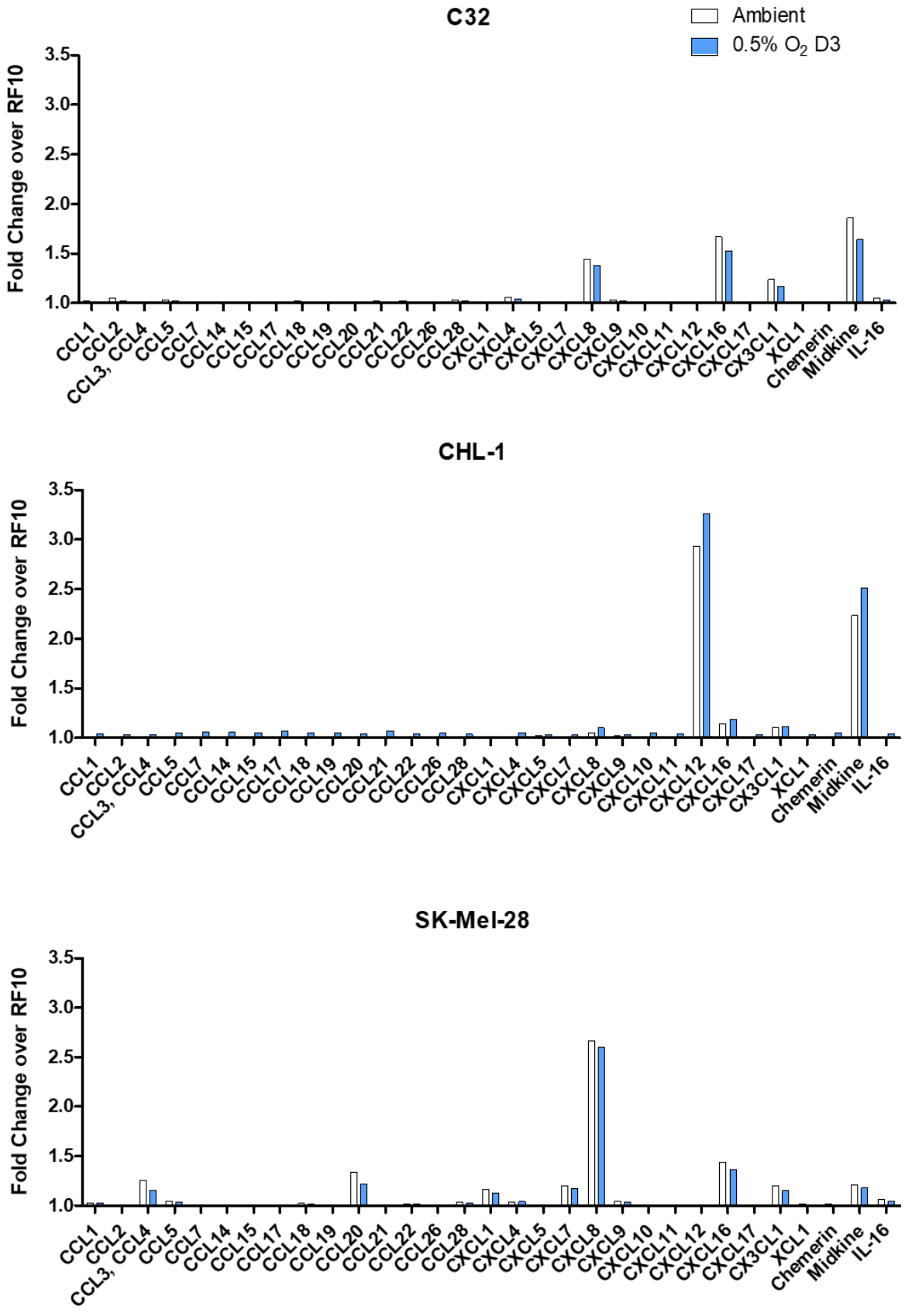
C32
Ambient
0.5% O2 D3
Fold Change over RF10
3.5
3.0
2.5
2.0
1.5
1.0
CCL1
CCL2
CCL3, CCL4
CCL5
CCL7
CCL14
CCL15
CCL17
CCL18
CCL19
CCL20
CCL21
CCL22
CCL26
CCL28
CXCL1
CXCL4
CXCL5
CXCL7
CXCL8
CXCL9
CXCL10
CXCL11
CXCL12
CXCL16
CXCL17
CX3CL1
XCL1
Chemerin
Midkine
IL-16
CHL-1
Fold Change over RF10
SK-Mel-28
Fold Change over RF10

Figure 4.10. C32, CHL-1 and SK-Mel-28 secrete chemokines into the supernatant under both ambient and hypoxic conditions.

C32, CHL-1 and SK-Mel-28 melanoma cells were cultured under ambient (21% O_2) and hypoxic (0.5% O_2) conditions for 3 days (D3). To examine protein expression of chemokines, the cell culture supernatant was collected, filtered and subjected to analysis with a commercially available chemokine array. (A) For dots that were readily visible on the membrane, the duplicate dots that correspond to different chemokines were boxed and represented with different colours. (B) The pixel intensity of the duplicate dots and of the background (random area on the blot with no capture antibodies blotted) were quantified using Image Quant. The pixel intensity of the duplicate dots on the membranes incubated with melanoma cell culture supernatant was then corrected by subtracting the average of the background values, and then represented as a fold change over the pixel intensity of the corresponding dots over RF10 alone. Bar graphs show fold change of corrected pixel intensity over RF10 alone with n=1 experiment.

Some of the known roles of these chemokines in regulating leukocyte recruitment under both cancer and inflammatory conditions are summarised in Table 4.3. In particular, while some of the chemokines can mediate $CD8^+$ T cell (such as CXCL16, CXCL12, CX3CL1, CCL3, CCL5) and NK cell (such as CXCL8, CXCL12, CX3CL1, CCL3, CCL4) recruitment, the majority of these chemokines also had overlapping roles in the recruitment of monocytes (such as CXCL8, CXCL12, CX3CL1, CXCL7, CCL3, CCL4, CXCL1) and neutrophils (such as CXCL8, midkine, CXCL12, CX3CL1, CXCL7, CXCL1). Note that these general chemotactic effects were described under inflammatory conditions and other cancer types, and their specific roles in mediating leukocyte recruitment to melanoma warrants further investigations. While extensive work had been performed to characterise the chemokine profile of the aforementioned melanoma cell lines, RNA sequencing and chemokine arrays were not similarly performed on the TrHBMEC line. Therefore the chemokine profile of this control EC line and how it compares with the melanoma cell lines remain to be elucidated.

Table 4.3. Summary of the known roles of the various chemokines and chemotactic cytokines secreted by the melanoma cells, their corresponding receptors, the leukocyte subsets expressing these receptors and the disease model whereby the recruitment of the respective leukocyte subsets were demonstrated.

Chemokine/ chemotactic cytokine	Receptor	Cells expressing receptor	Disease model	References
CXCL16	CXCR6 (only known receptor)	$CD8^+$ T cells	Recruitment of $CD8^+$ T cells in inflammatory models	(Kim, CH et al. 2001; Nakayama et al. 2003)
CXCL8	CXCR1 CXCR2	NK cells	CXCL8 recruitment of NK cells to inflamed tissues	(Chuang et al. 2006)
		Monocytes	CXCL8 enhanced monocyte adhesion to endothelium *in vitro*	(Gerszten et al. 1999)
		Neutrophils	Enhanced neutrophil recruitment in CXCL8 overexpressing human melanoma xenografts	(Schaider et al. 2003)
Midkine		Neutrophil	Adhesion of neutrophils through β2 integrin in acute inflammation	(Weckbach et al. 2014)
CXCL12	CXCR4	$CD8^+$ T cells	Regulation of $CD8^+$ T cell recruitment to B16 melanoma	(Vianello et al. 2006)
		NK cells	Trafficking of mice NK cells	(Bernardini et al. 2008)
		Monocytes	Recruitment of monocytes in multiple myeloma	(Beider et al. 2014)
		Neutrophils	Neutrophil recruitment in acute lung injury	(Petty et al. 2007)
		Tregs	Treg recruitment in breast cancer	(Yan et al. 2011)
CX3CL1	CX3CR1	T cells	Infiltration of $CD3^+$ T cells into lungs overexpressing CX3CL1 expression following smoke exposure	(McComb et al. 2008)
		NK cells	Adhesion of NK cells to CX3CL1 expressing endothelium *in vitro*	(Robinson, LA et al. 2003)
		Monocytes	*In vitro* recruitment of monocytes; Infiltration of macrophages into lungs overexpressing CX3CL1 exposure following smoke exposure	(Ancuta et al. 2003) (McComb et al. 2008)
CXCL7	CXCR2	Monocytes	Colocalisation of macrophages and CXCL7 in inflamed synovial tissue	(Yeo et al. 2015)
		Neutrophils	Neutrophil adhesion and transmigration on HUVEC *in vitro*	(Schenk et al. 2002)
CCL3,CCL4	CCR5	$CD8^+$ T cells	CCL3 and CCL4 preferentially expressed in tumours containing T cells	(Harlin, H. et al. 2009)
		NK cells	Trafficking of mice NK cells	(Bernardini et al. 2008)
		Monocytes	*In vitro* recruitment of monocytes; reduced macrophage accumulation in lung metastasis in CCL3 deficient mice	(Ancuta et al. 2003) (Wu, Y et al. 2008)
CCL20	CCR6	Tregs	Recruitment of Tregs in hepatocellular carcinoma and colorectal cancer	(Chen, KJ et al. 2011) (Liu, J et al. 2011)
		B cells	B cell chemotaxis	(Krzysiek et al. 2000)
		Th17	Recruitment of Th17 cells inflamed joints in rheumatoid arthritis	(Yu, Lou & He 2015) (Hirota et al. 2007)

CXCL1	CXCR2	Monocytes	Enhanced CXCL1 and marcrophage recruitment after arterial ligation to promote arterogenesis in mice	(Vries et al. 2015)
		Neutrophils	Recruitment of neutrophils to B16-F10 melanoma	(Jablonska et al. 2014)

To examine if the adhesion molecule and chemokine expression profile of these cell lines were relevant to human disease, *in silico* analysis of The Cancer Genome Atlas (TCGA) melanoma dataset ('Genomic Classification of Cutaneous Melanoma' 2015) was undertaken by a laboratory member (Mr Brenton Ebert) to examine gene expression of the aforementioned adhesion molecules and chemokines. As demonstrated in Figure 4.11, the adhesion molecules *CD44*, *ICAM1*, *F11R (*JAM-A), *JAM3* (JAM-C) and chemokines expressed on the melanoma cell lines were also detected in human melanoma samples, although there was a larger level of variation in chemokine expression compared to the expression of adhesion molecules. As TCGA gene expression analysis was performed from whole tumour samples which are heterogenous and contain a small proportion of ECs, a correlation study was performed to examine if the detected expression of adhesion molecules and chemokines was associated with ECs. The gene expression levels of the various adhesion molecules and chemokines were compared against endomucin (*EMCN*), a key marker of ECs that is not known to be co-expressed on melanoma cells (Kuhn et al. 2002), as well as microphthalmia-associated transcription factor (*MITF*), a key marker of melanoma cells that is not known to be co-expressed on ECs (Garraway et al. 2005). Interestingly, of all the genes examined, the expression of *JAM3* (JAM-C), *PPBP* (CXCL7) and *CXCL12* were significantly positively correlated with *EMCN* expression (Figure 4.12A), but happen to be significantly negatively correlated with *MITF* expression (Figure 4.12B). This suggested that there is a possibility of ECs contributing to the detection of these molecules in Figure 4.11, although the correlation coefficients are quite small. Conversely, the expression of *CD44*, *F11R* (JAM-A), *CCL28* and *IL16* were significantly positively correlated with *MITF* expression (Figure 4.12B), but significantly negatively correlated with *EMCN* expression (Figure 4.12A). This suggests that the expression of these molecules is largely contributed by melanoma cells and not ECs, at least in this cohort of patients, although again the correlation coefficients are quite low. It would be interesting to examine the actual protein levels of these adhesion molecules and chemokines on patient melanoma cells, as it is the protein that is physically involved in leukocyte recruitment.

Taken together, the findings of this Chapter suggest that VM-competent melanoma cell lines express numerous adhesion molecules and chemokines which equip them with the ability to promote leukocyte rolling, adhesion and transmigration.

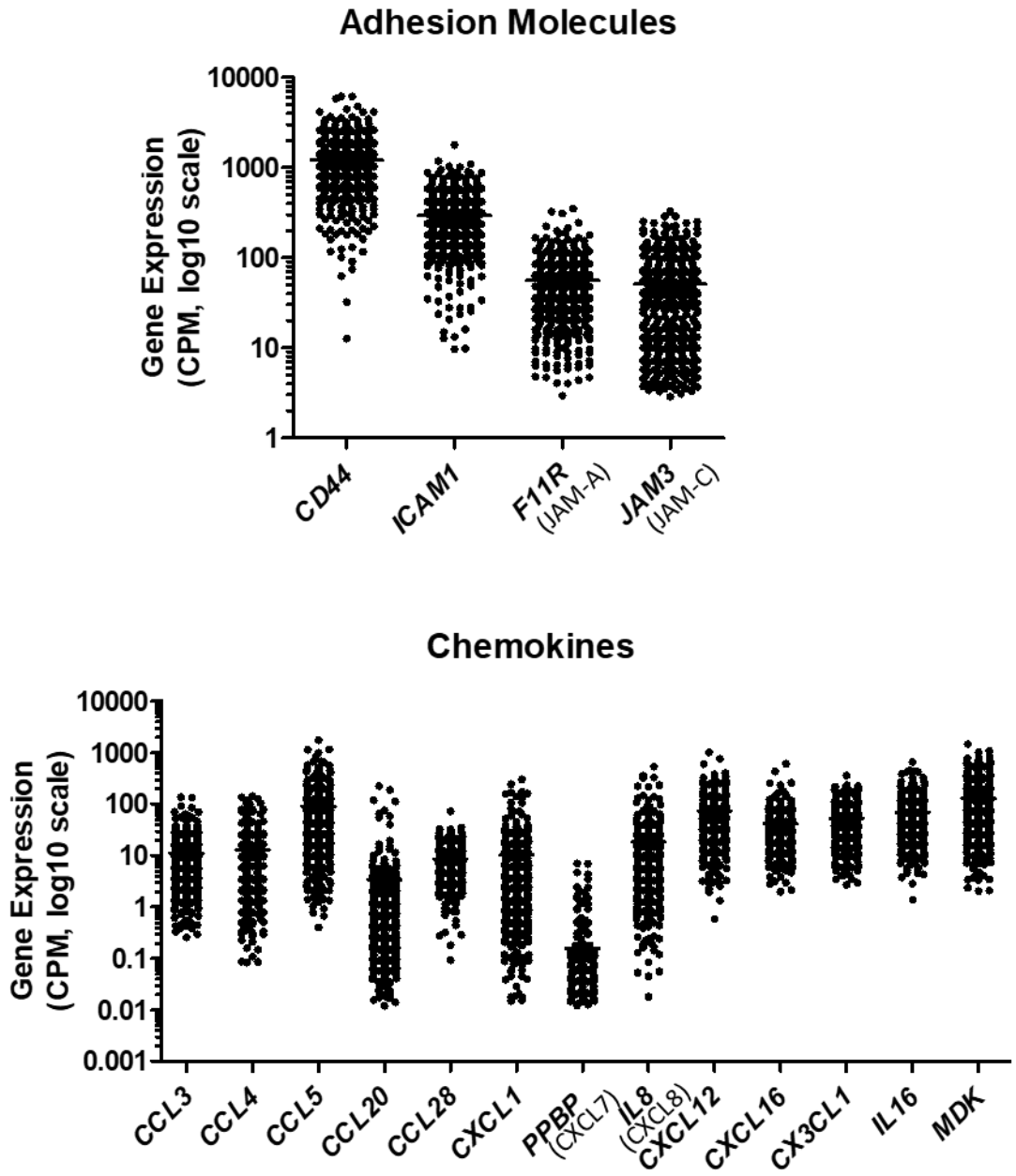

Figure 4.11. The adhesion molecules and chemokines expressed in melanoma cell lines C32, CHL-1 and SK-Mel-28 are also expressed at the RNA level in human melanoma samples.

Analysis was performed on The Cancer Genome Atlas (TCGA) melanoma dataset to examine expression of adhesion molecules and chemokines. Plots show the gene expression (CPM, log10 scale) of the different adhesion molecules and chemokines for n= 427 samples.

A)

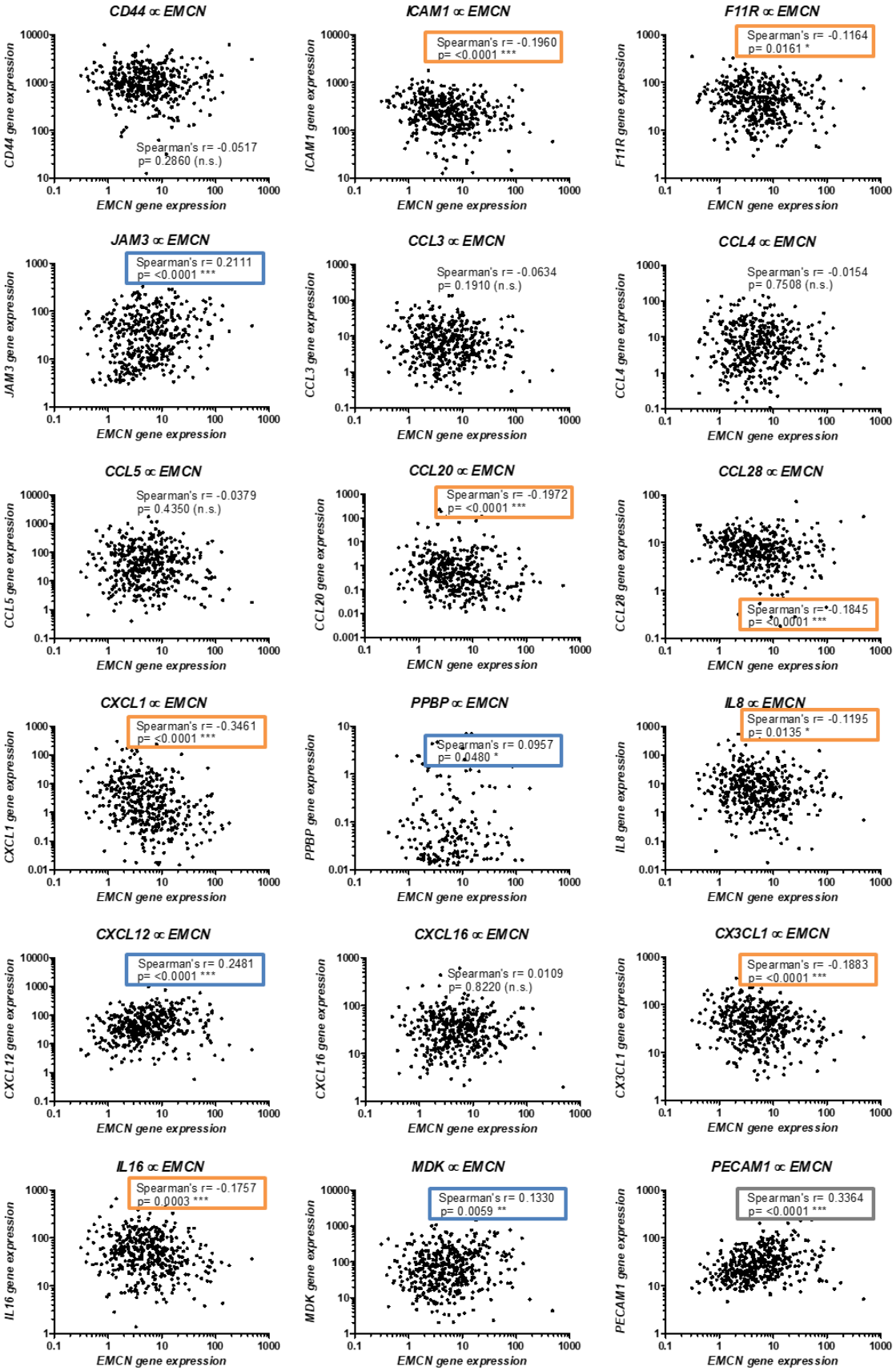
CD44 ∝ EMCN
Spearman's r= -0.0517
p= 0.2860 (n.s.)
ICAM1 ∝ EMCN
Spearman's r= -0.1960
p= <0.0001 ***
F11R ∝ EMCN
Spearman's r= -0.1164
p= 0.0161 *
JAM3 ∝ EMCN
Spearman's r= 0.2111
p= <0.0001 ***
CCL3 ∝ EMCN
Spearman's r= -0.0634
p= 0.1910 (n.s.)
CCL4 ∝ EMCN
Spearman's r= -0.0154
p= 0.7508 (n.s.)
CCL5 ∝ EMCN
Spearman's r= -0.0379
p= 0.4350 (n.s.)
CCL20 ∝ EMCN
Spearman's r= -0.1972
p= <0.0001 ***
CCL28 ∝ EMCN
Spearman's r= -0.1845
p= <0.0001 ***
CXCL1 ∝ EMCN
Spearman's r= -0.3461
p= <0.0001 ***
PPBP ∝ EMCN
Spearman's r= 0.0957
p= 0.0480 *
IL8 ∝ EMCN
Spearman's r= -0.1195
p= 0.0135 *
CXCL12 ∝ EMCN
Spearman's r= 0.2481
p= <0.0001 ***
CXCL16 ∝ EMCN
Spearman's r= 0.0109
p= 0.8220 (n.s.)
CX3CL1 ∝ EMCN
Spearman's r= -0.1883
p= <0.0001 ***
IL16 ∝ EMCN
Spearman's r= -0.1757
p= 0.0003 ***
MDK ∝ EMCN
Spearman's r= 0.1330
p= 0.0059 **
PECAM1 ∝ EMCN
Spearman's r= 0.3364
p= <0.0001 ***
EMCN gene expression

B)

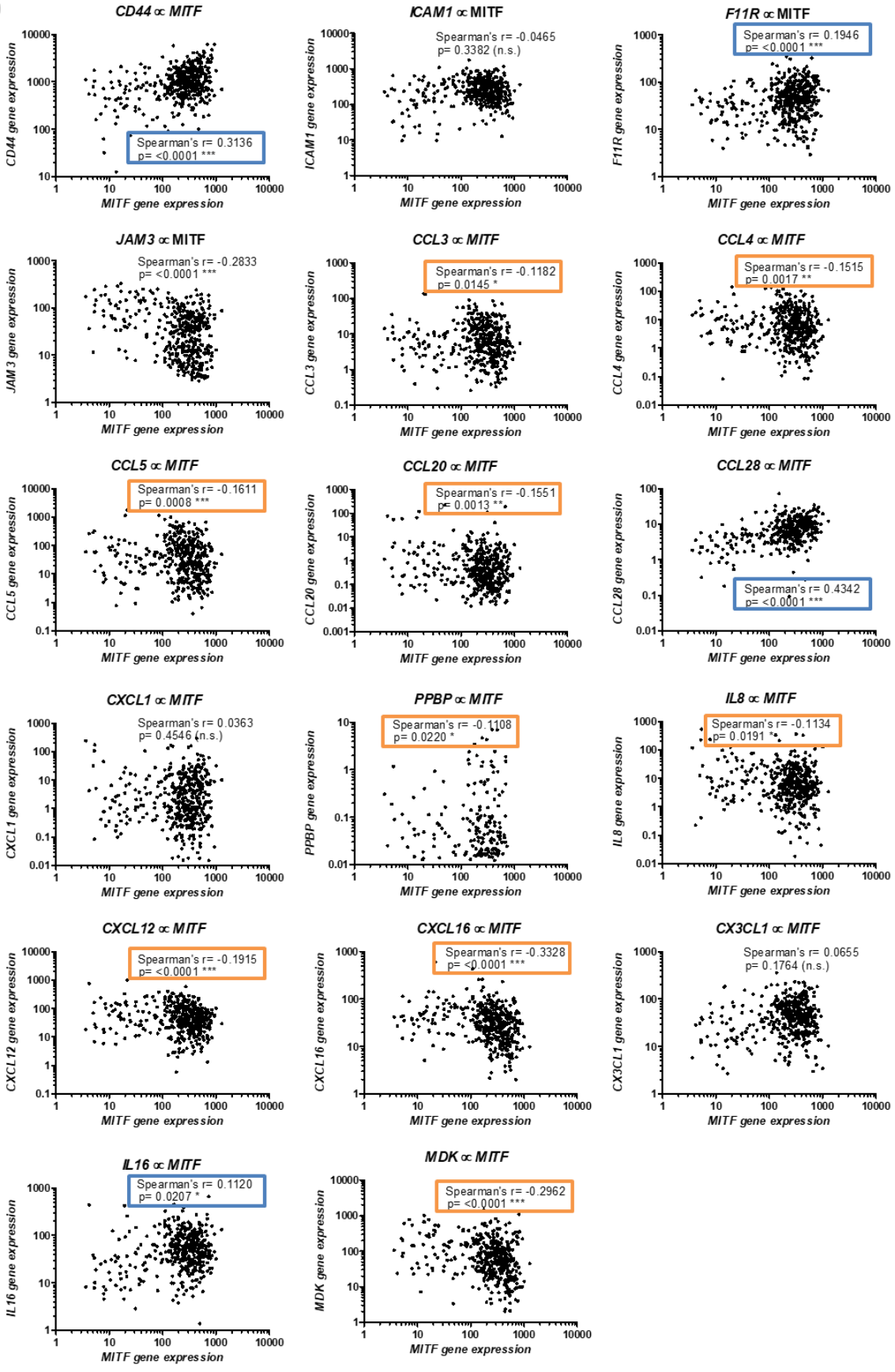
CD44 ∝ MITF
Spearman's r= 0.3136
p= <0.0001 ***
CD44 gene expression
MITF gene expression
ICAM1 ∝ MITF
Spearman's r= -0.0465
p= 0.3382 (n.s.)
ICAM1 gene expression
MITF gene expression
F11R ∝ MITF
Spearman's r= 0.1946
p= <0.0001 ***
F11R gene expression
MITF gene expression
JAM3 ∝ MITF
Spearman's r= -0.2833
p= <0.0001 ***
JAM3 gene expression
MITF gene expression
CCL3 ∝ MITF
Spearman's r= -0.1182
p= 0.0145 *
CCL3 gene expression
MITF gene expression
CCL4 ∝ MITF
Spearman's r= -0.1515
p= 0.0017 **
CCL4 gene expression
MITF gene expression
CCL5 ∝ MITF
Spearman's r= -0.1611
p= 0.0008 ***
CCL5 gene expression
MITF gene expression
CCL20 ∝ MITF
Spearman's r= -0.1551
p= 0.0013 **
CCL20 gene expression
MITF gene expression
CCL28 ∝ MITF
Spearman's r= 0.4342
p= <0.0001 ***
CCL28 gene expression
MITF gene expression
CXCL1 ∝ MITF
Spearman's r= 0.0363
p= 0.4546 (n.s.)
CXCL1 gene expression
MITF gene expression
PPBP ∝ MITF
Spearman's r= -0.1108
p= 0.0220 *
PPBP gene expression
MITF gene expression
IL8 ∝ MITF
Spearman's r= -0.1134
p= 0.0191 *
IL8 gene expression
MITF gene expression
CXCL12 ∝ MITF
Spearman's r= -0.1915
p= <0.0001 ***
CXCL12 gene expression
MITF gene expression
CXCL16 ∝ MITF
Spearman's r= -0.3328
p= <0.0001 ***
CXCL16 gene expression
MITF gene expression
CX3CL1 ∝ MITF
Spearman's r= 0.0655
p= 0.1764 (n.s.)
CX3CL1 gene expression
MITF gene expression
IL16 ∝ MITF
Spearman's r= 0.1120
p= 0.0207 *
IL16 gene expression
MITF gene expression
MDK ∝ MITF
Spearman's r= -0.2962
p= <0.0001 ***
MDK gene expression
MITF gene expression

Figure 4.12. The expression of adhesion molecules and chemokines in the TCGA dataset may be attributed to both ECs and melanoma cells.

(A) To examine the correlation of adhesion molecule and chemokine expression with EC frequency, the expression values of these genes were plotted against *EMCN*, the gene that encodes for endomucin, an EC specific marker. A correlation analysis was performed with the Spearman's r and p value listed on the individual graphs. Blue boxes indicate genes that were significantly positively correlated with *EMCN* expression, while orange boxes indicate genes that were significantly negatively correlated with *EMCN* expression. The correlation of *EMCN* and *PECAM1*, which encodes for CD31, another EC specific marker was included as a control (grey box). (B) To examine the correlation of the adhesion molecules and chemokines with melanoma cells, the expression values of these genes were plotted against *MITF*, the gene that encodes for microphthalmia-associated transcription factor, a melanoma specific marker. A correlation analysis was performed with the Spearman's r and p value listed on the individual graphs. Blue boxes indicate genes that were significantly positively correlated with *MITF* expression, while orange boxes indicate genes that were significantly negatively correlated with *MITF* expression.

4.4. Discussion

It is well established that the leukocyte composition within a tumour greatly dictates disease fate and outcome. In particular, an abundance of functional anti-tumourigenic leukocytes such as $CD8^+$ T cells and NK cells can lead to tumour regression, whereas an abundance of pro-tumourigenic leukocytes such as TAM, TAN and Tregs promotes tumour growth (Tan et al. 2017). However, our current understanding of the pathways of leukocyte entry into the tumour microenvironment is largely limited to conventional blood vessels that are lined entirely by ECs. While VM vessels have been reported to conduct blood and carry leukocytes (Hillen, F. et al. 2008), the notion of them directly recruiting leukocytes has never been examined. This work presents exciting data supporting a novel concept that VM-competent melanoma cells can actively recruit leukocyte subsets.

The findings were obtained through functional assays including parallel plate flow chamber assays and Transwell assays to assess leukocyte rolling, adhesion and transmigration across VM-competent melanoma cells, as well as RNA sequencing, flow cytometric analysis and chemokine arrays to characterise the adhesion molecule and chemokine profile of these melanoma cells. To facilitate discussion, a summary of the key findings on the three VM-competent melanoma cell lines are provided in Table 4.4.

Table 4.4. Summary of key findings on the three VM-competent melanoma cells

	Parallel plate flow chamber assay (Leukocyte rolling and adhesion)	Transwell assay (Leukocyte transmigration)		FITC-dextran permea-bility	Adhesion molecule expression (protein)	Chemokine expression (protein)
		FBS gradient	**CXCL12 gradient**			
SK-Mel-28	- Binds all leukocyte subsets assessed - No preferential binding	Transmigrated leukocyte subsets: - $CD4^+$ T cells - $CD14^+$ monocytes	All leukocyte subsets assessed transmigrated	C32 > SK-Mel-28 > CHL-1	CD44 $^{+++}$ ICAM-1 $^{+++}$ JAM-A $^{++}$ JAM-C $^{+}$	CXCL8 $^{++}$ CCL3,4 $^{+}$ CCL20 $^{+}$ CXCL1 $^{+}$ CXCL16 $^{+}$ CX3CL1 $^{+}$ Midkine $^{+}$
C32	- Binds all leukocyte subsets assessed - Some preferential binding of $CD14^+$ monocytes (similar to TrHBMEC)	Transmigrated leukocyte subsets: - $CD14^+$ monocytes	All leukocyte subsets assessed transmigrated		CD44 $^{+++}$ ICAM-1 $^{+++}$ JAM-A $^{++}$ JAM-C $^{+}$	CXCL8 $^{+}$ CXCL16 $^{+}$ CX3CL1 $^{+}$ Midkine $^{+}$
CHL-1	- Binds all leukocyte subsets assessed - Enhanced preferential binding of $CD14^+$ monocytes (similar to TNFα-treated TrHBMEC)	Transmigrated leukocyte subsets: - $CD14^+$ monocytes	All leukocyte subsets assessed transmigrated		CD44 $^{+}$ ICAM-1 $^{+}$ JAM-A $^{++}$ JAM-C $^{++}$	CXCL12 $^{++}$ Midkine $^{++}$

As demonstrated in Table 4.4, all three VM-competent melanoma cell lines were able to promote adhesion of all the different leukocyte subsets assessed. This matched well with the adhesion molecule profile of the VM-competent melanoma cells, as all these leukocytes express the respective counter-receptors for CD44 (CD44) and ICAM-1 (LFA-1/MAC-1) on the melanoma cells. Similarly, the adhered leukocytes also expressed the respective receptors for the chemokines expressed by the melanoma cells (such as $CD8^+$ T cell binding to CXCL16 through CXCR6; T cell, $CD14^+$ monocyte and $CD16^+$ NK cell binding to CX3CL1 through CX3CR1, $CD19^+$ B cell binding to CCL20 through CCR6), thereby explaining their ability to adhere on the melanoma cells. However, the current adhesion molecule and chemokine profile may not be sufficient to explain the preferential adhesion of monocytes. In particular, CHL-1 cells which exhibited the lowest level of ICAM-1 expression had the most monocytes bound among the three VM-competent melanoma cell lines used. This suggests that there may be other molecules involved in mediating this adhesion of monocytes. One approach of assessing this is to identify adhesion molecules which are differentially expressed across the three melanoma cell lines and are particularly upregulated on CHL-1. Ideally, the counter-receptors for these adhesion molecules would also only be expressed on monocytes and not on other leukocyte subsets to maintain the monocyte specific recruitment. Some possible candidates include *ICAM3* and *ICAM4*, which can bind to CD11c/CD18 and CD11d/CD18 expressed exclusively on monocytes (Uotila, Aatonen & Gahmberg 2013; Yakubenko, Yadav & Ugarova 2006). Further interrogation of the RNA sequencing data however revealed that all three melanoma cell lines did not express *ICAM4*, while the expression of *ICAM3* was similar across the three melanoma cell lines, although the protein levels remain to be elucidated (results not shown). Alternatively, the enhanced monocyte binding to CHL-1 cells could also be due to differential expression of chemokines, which are important in mediating leukocyte adhesion via activation of integrins (Montresor et al. 2012). Indeed, chemokine arrays demonstrate enhanced CXCL12 expression by CHL-1 compared to the other two melanoma cell lines. CXCL12 however is also involved in the recruitment of other leukocyte subsets apart from monocytes. Given the similarities in leukocyte binding profile between CHL-1 and TNFα-treated TrHBMEC, an alternative approach could be to examine the adhesion molecule and chemokine expression profile of the TNFα-treated TrHBMEC to identify potential candidates which may explain the enhanced monocyte adhesion. This is an area that warrants further investigation.

In addition to that, the overall ability of the VM-competent melanoma cell lines to promote transmigration of all the different leukocyte subsets also matched well with their adhesion molecule profile, as all of these leukocytes express the respective counter-receptors for JAM (LFA-1/MAC-1) on the melanoma cells. The role of melanoma cell secreted chemokines in regulating leukocyte transmigration however could not be assessed using the current approach as artificial chemoattractant gradients (FBS/CXCL12) were utilised instead of melanoma cell culture supernatant. One important cellular feature that may affect the permissiveness of the different cell monolayers to support leukocyte transmigration is the permeability of the monolayer. Indeed, the melanoma cell monolayers appeared to be more permeable than the TrHBMEC monolayer as reflected by the FITC-dextran permeability assay. This however could be an indication of the inherent feature of melanoma cells, and may reflect the leakiness of VM vessels *in vivo*, although this has not been assessed before. Nonetheless, the enhanced leukocyte transmigration following the addition of FBS and CXCL12 confirmed that this process was chemoattractant dependent too.

Having established the potential role of VM-competent melanoma cells in mediating leukocyte recruitment, it is tempting to compare it to the leukocyte recruitment capabilities of ECs. For this reason, the EC line TrHBMEC was included throughout the study as a comparator cell. Indeed, the total number of adhered and transmigrated leukocytes for the melanoma cell lines was similar to that of resting TrHBMEC. Furthermore, the composition of the adhered leukocytes for C32 as well as the composition of the transmigrated leukocytes for all three melanoma cells lines across a CXCL12 gradient were similar to that of TrHBMEC too. This suggests that these VM-competent melanoma cells can behave like unstimulated TrHBMEC.

However, it has been well documented that tumour ECs have different properties to that of normal healthy ECs. Of particular relevance to this study, tumour ECs are found to be anergic following chronic stimulation by hypoxia (Cartee et al. 2012) as well as pro-angiogenic factors such as VEGF and bFGF (Dirkx, AE et al. 2003; Weishaupt et al. 2007). This in turn results in a reduction in P-selectin, E-selectin, ICAM-1 and VCAM-1 expression and subsequently affects leukocyte recruitment (Cartee et al. 2012; Dirkx, AE et al. 2003; Weishaupt et al. 2007). In fact, this has been proposed to be one of the key mechanisms underlying the impaired $CD8^+$ T cell recruitment observed in melanoma tumours (Dirkx, AE et al. 2003; Weishaupt et al. 2007).

Due to the complicated process required to obtain tumour ECs from fresh tumours, I sought to mimic tumour conditions by exposing the TrHBMEC to hypoxic conditions. Unfortunately, the selected culture condition (0.5% O_2) did not result in a downregulation of adhesion molecule on TrHBMEC and a reduction in cell adhesion like that described in the literature (Cartee et al. 2012; Weishaupt et al. 2007). There are several reasons that could explain this. Firstly, the EC lines used in the literature (mainly primary human umbilical vein derived EC (HUVEC)) were different to the immortalised EC line used in this study (Griffioen, A. W. et al. 1996; Hellebrekers et al. 2006). It has been reported that different EC lines could respond differently to inflammatory cytokine stimuli resulting in different adhesion molecule expression (Haraldsen et al. 1996). Therefore, it is possible that the bone marrow derived TrHBMEC used in this study would have responded differently towards the 0.5% O_2 stimulation. Indeed, while the selected culture condition (0.5% O_2) had been extensively validated to stimulate hypoxic reactions within the melanoma cells, this was not similarly validated on the EC. Secondly, the approach of recapitulating the tumour environment is also different. As opposed to the short term hypoxic stimulation utilised in this study, the two main approaches to mimic tumour conditions *in vitro* in the literature are long term hypoxic stimulation in a specialised hypoxic glovebox (Cartee et al. 2012) and direct treatment with substantial amounts of the pro-angiogenic factors VEGF and bFGF (10ng/ml) (Griffioen, A. W. et al. 1996; Hellebrekers et al. 2006), which were both able to reduce adhesion molecule expression on EC. While the use of a hypoxic glovebox was not possible due to the lack of this specialised equipment, subsequent studies can be repeated with direct VEGF and bFGF treatment. This will at least assist in providing a minimum required amount of VEGF and bFGF for adhesion molecule reduction, which was likely not achievable through the short term culture of TrHBMEC alone as it relies solely on the ECs to generate these factors. As a reference, another published study demonstrated that supernatant collected from HUVEC cultured under 2% O_2 for 24 hours at $5x10^5$ cells in 2 ml of medium only contained less than 5pg/ml of VEGF (Lee, Y-A et al. 2014). This is a lot less than that utilised in the aforementioned studies as well as that within the tumour, where the average concentration of VEGF was found to be 54ng/ml (Kut, Mac Gabhann & Popel 2007). Should subsequent *in vitro* assays be repeated using TrHBMEC directly treated with VEGF as a comparator cell, then the melanoma cells should also be similarly treated with these angiogenic factors to examine if this would also stimulate changes in adhesion molecule and chemokine expression. For the aforementioned reasons, the leukocyte recruitment capabilities of these VM-

competent melanoma cells could only be directly compared with normal ECs but not the more physiologically relevant tumour conditioned ECs.

Further to that, the keratinocyte cell line HaCaT cells were also included as a negative comparator cell population as they are not known to be directly involved in the recruitment of leukocytes from blood. Perhaps unsurprisingly, these cells barely bound any MNC as demonstrated from the parallel plate flow chamber assays. Further to that, there was also lack of MNC transmigration as shown in the Transwell assays. While the latter observation is mostly likely due to the lack of permeability, these findings also suggest that HaCaT lack the necessary receptors required for MNC interaction, although this remains to be confirmed on the protein level. More importantly, this further highlights that the adhesion of MNC to both melanoma cells and TrHBMEC as well as the transmigration is a specific process mediated by the interactions between adhesion molecules/chemokines and their counter-receptors.

Throughout the process of deciphering this novel phenomenon, there were several technical limitations that were encountered (in addition to the EC limitation as discussed above). While these could not all be addressed in this study due to time constraints, they are discussed below as they will provide critical directions in subsequent studies which aim to expand this novel field.

Firstly, the current roles of adhesion molecules and chemokines in mediating the recruitment of leukocytes on VM-competent melanoma cells are largely correlational. While they matched with the types of leukocytes which were recruited, the actual functional roles of these molecules were not assessed. In an attempt to determine whether ICAM-1 played a functional role in the leukocyte recruitment process, parallel plate flow chamber assays were conducted with an ICAM-1 blocking antibody. However, the results obtained from the control TrHBMEC cells revealed an unexpected increase in leukocyte binding with ICAM-1 blocking, indicating a need to further optimise the assay. Subsequent approaches taken however did not appear to alleviate the issue, and the underlying reason for this unexpected binding remained unknown. Functional assays with blocking antibodies targeting other adhesion molecules and chemokines were also not performed due to time constraints. Therefore, it is important to address this in future experiments. An alternative approach to antibody blocking is through siRNA or shRNA mediated silencing of adhesion molecule or chemokine expression. These approaches however have their own limitations (as previously discussed in Chapter 3) and will also require detailed optimisation. Further to that, the roles

of melanoma cell secreted chemokines should also be examined by repeating the Transwell assays with melanoma cell culture supernatant as a chemoattractant with or without chemokine blocking strategies.

Secondly, this current study only focused on the characterisation of the expression of a conventional list of adhesion molecules and chemokines on the VM-competent melanoma cells. More specifically, the adhesion molecules assessed are the conventional ones widely reported in the literature to mediate leukocyte recruitment, while the chemokines assessed were limited to the conventional ones detectable through the commercially available chemokine array. Undoubtedly, this has proven to be a useful starting point. However, as discussed above, the enhanced adhesion of $CD14^+$ monocytes on the CHL-1 melanoma cells with the least ICAM-1 expression suggested the possibility of other perhaps non-conventional adhesion molecules in mediating this process. This has also been suggested in the literature for EC vessels in tumours. As previously described in Chapter 1, while monocytes, neutrophils and Tregs are also typically recruited via adhesion molecules such as P-selectin, E-selectin, ICAM-1 and VCAM-1, the downregulation of these molecules on tumour ECs does not appear to correlate with decreased monocyte or neutrophil infiltration (Ahmadzadeh et al. 2008; Hillen, Femke et al. 2008). Further to that, the specific enhanced transmigration of $CD14^+$ monocytes observed across an FBS gradient suggested that there could be other chemoattractants apart from the conventional chemokines within the FBS. Indeed, apart from the CXCL12 detected in RF10 via chemokine arrays, FBS is also known to contain VEGF and bFGF, which have both been shown to induce monocyte recruitment (Zittermann & Issekutz 2006). These factors can also be secreted by melanoma cells (Rofstad & Halsør 2000) but will not be detected through the chemokine arrays due to the lack of the corresponding capture and detection antibodies. Therefore, it is crucial to expand the study in the future to identify other adhesion molecules and chemoattractants which may regulate the leukocyte recruitment process. A potential approach of doing this is to further interrogate the RNA sequencing results obtained in this study to identify potential candidates. For example, the RNA sequencing results also demonstrated that all three melanoma cell lines expressed *VEGFA* that was upregulated following hypoxic stimulation (results not shown). However, it is also crucial to validate these findings at the protein level. The importance of this is highlighted in the chemokine results, where not all of the chemokines expressed at the mRNA level (such as CCL28) were detected at the protein level when assessed using the chemokine array. Similarly, not all chemokines detected in the chemokine array (such as

CXCL8 for C32; CCL3, CCL4, CXCL7 and midkine for SK-Mel-28) were detected at high levels in the RNA sequencing. The former observation is likely to be due to post-transcriptional control of chemokine production and stability (reviewed in (Mortier, Van Damme & Proost 2012)). Therefore, there may be chemokine mRNAs that have been degraded prior to translation and secretion, and are not detected in supernatant. On the other hand, the latter observation may be an indication of the affinities of the antibodies used in the chemokine array. More specifically, these antibodies may have high binding affinities and hence are capable of detecting low levels of proteins produced from small amounts of mRNA transcripts. Therefore, it is critical to validate all RNA findings at the protein level, as it is the proteins that are directly interacting with the leukocytes and regulating their recruitment.

Thirdly, this *in vitro* study is performed on 2D melanoma cell monolayers while the actual VM structures are 3D when *in vivo*. This is a common limitation in the vascular biology field, as the majority of leukocyte recruitment studies are all performed on 2D EC monolayers. While there are complex *in vitro* 3D systems available, they are financially and technically challenging to set up and are currently only specialised to a few laboratories worldwide (such as the Hughes Lab at the University of California). However, it is known that cells can alter gene and protein expression following interaction with the extracellular matrix (Demou & Hendrix 2008; Edmondson et al. 2014). Therefore, there is a potential that the adhesion molecule and chemokine expression profile of the melanoma cells may change when they are in VM structures. Currently, the most widely used model for assessing vessel formation *in vitro* is through the short term culture of cells on a thick layer of gelatinous Matrigel (refer to Matrigel tube formation assays performed in Chapter 3 where these melanoma cell lines were first characterised to be VM-competent). Therefore, subsequent assays could be performed with a layer of Matrigel to recapitulate these conditions, although it would have to be a thin coating rather than a thick gel to be technically feasible for the current functional assays.

The fourth point relates to the importance of shear stress in affecting leukocyte recruitment. The importance of shear stress in affecting adhesion molecule profile has been acknowledged in the literature (Cockcroft et al. 2009) and has been recapitulated here in the parallel plate flow chamber assays. However, the current setup only allows for short term flow at a specified flow rate which generates a specified shear stress. This is different to the conditions within a tumour, where there are changes of blood flow rate within different areas of the tumour (reviewed in (Jain 1988)). Changes in flow rates subsequently affect the viscosity of blood (Lominadze & McHedlishvili 1999). These two factors in turn affect the shear stress

experienced by the vessels. Therefore, an alternative approach is to utilise optimised pumps which allow for long term oscillating flow of fluids across the cell monolayer, like that achievable with an Ibidi pump (Cockcroft et al. 2009). This may better recapitulate physiological conditions within the tumour. In addition, transmigration assays may also be performed in the presence of a shear flow using specialised setups to better recapitulate leukocyte recruitment under physiological conditions (Kwasny et al. 2011).

Lastly, this study has assessed the function of VM-competent melanoma cells in the recruitment of different leukocyte subsets, namely $CD4^+$ T cells, $CD8^+$ T cells, $CD14^+$ monocytes, $CD16^+$ NK cells and $CD19^+$ B cells, which all play a role in regulating melanoma progression (reviewed in (Tan et al. 2017)). In addition to these subsets, other leukocyte subsets also play an important role in regulating melanoma progression, such as neutrophils and Tregs (reviewed in (Tan et al. 2017)). The ability of VM-competent melanoma cells to recruit these cell types could not be assessed in this study and is largely due to the approach chosen to isolate MNC. This happens because the use of gradient centrifugation to isolate MNC sediments neutrophils together with the red blood cells and hence they were not collected for use in my assays. Furthermore, the lack of enrichment steps to select Tregs results in inadequate numbers required for the assays, as these cells only make up to less than 1% of the whole leukocyte population in whole blood. Given the importance of these leukocyte populations in dictating disease progression (reviewed in (Tan et al. 2017)), it will be important to include these cell types in subsequent assays to examine if they too can be recruited through VM vessels. It is however tempting to speculate from the current findings of this study that neutrophils and Tregs can also be recruited through VM vessels. More specifically, as indicated in Table 4.1, both leukocyte subsets express the counter-receptors (CD44, LFA-1) for the adhesion molecules expressed on the melanoma cells (CD44, ICAM-1, JAM-A, JAM-C). Further to that, as indicated in Table 4.3, these melanoma cells also secreted chemokines such as CXCL8, CXCL12 and CCL20 which have been shown to recruit neutrophils and Tregs respectively. Nonetheless, these speculations are currently correlative assumptions and are not necessarily specific to melanoma. Therefore, subsequent functional assays with blocking approaches are warranted to confirm if these leukocyte subsets can indeed be recruited via VM vessels through the interaction with these adhesion molecules and chemokines.

Despite the limitations of this study, it provides new knowledge that profoundly expands our understanding of leukocyte recruitment in tumours, where VM vessels may preferentially

recruit monocytes. More specifically, parallel plate flow chamber assays demonstrated that wherever present, there was an enhanced frequency of monocytes on the melanoma cells compared to the input population, indicating enhanced monocyte adhesion. These monocytes were also actively allowed to transmigrate across the melanoma cells in response to a chemoattractant gradient. Overall, this preferential recruitment of monocytes corresponded well with the adhesion molecule profile of the melanoma cells, where the expression of CD44, ICAM-1 and JAM would allow for the adhesion and migration of monocytes which express the counter-receptors CD44, LFA-1 and MAC-1 (Table 4.1), although there were hints towards the presence of alternative adhesion molecules mediating monocyte adhesion. The identity of these alternative adhesion molecules however remain to be elucidated. While the roles of melanoma cell derived chemokines in mediating monocyte recruitment were not directly assessed in this study, the melanoma cell lines expressed a broad range of chemokines such as CXCL7, CXCL8, CXCL12 and CX3CL1 which have been shown in other studies to be monocyte attracting. More importantly, unlike the ECs reported in the literature, the expression of these adhesion molecules and chemokines was not affected by hypoxia, at least in the short term culture in this study. This suggests that VM vessels may also perform similarly within a hypoxic tumour environment. Conversely, this route would be expected to be non-permissive to $CD8^+$ T cells even with the expression of the full suite of adhesion molecules, as VM vessels would lack the critical $CD8^+$ T cell attracting (CXCR3-signalling) chemokines CXCL9, CXCL10 and CXCL11 (Mikucki et al. 2015). Together, this suggests that VM vessels may aid in the progression of melanoma through the recruitment of monocytes which are often pro-tumourigenic (Torisu et al. 2000; Varney, Michelle L, Johansson & Singh 2005).

Taken together, my results highlight great value in studying the VM leukocyte recruitment process in an *in vivo* setting, which allows for the majority of the aforementioned limitations to be addressed. In particular, the melanoma cells will be able to grow and form tumours, and their ability to recruit leukocytes via actual 3D VM structures can be assessed. In addition to that, the ability of VM vessels in mediating this process can be directly compared with tumour ECs, which will form leakier vessels than normal ECs. As the melanoma cells will experience interactions with the extracellular matrix as well as exposure to hypoxia and angiogenic factors, the impact of these factors on adhesion molecule and chemokine expression of these VM-competent cells can also be assessed. There is also a potential to decipher the mechanisms underlying these observations through further antibody mediated

blocking or shRNA mediated downregulation of adhesion molecule and chemokine expression. The establishment of a mouse model to examine leukocyte recruitment through VM vessels will be the focus of the final Chapter of this thesis.

One question of interest which has arisen out of this study is whether or not VM-incompetent cells can also participate in the leukocyte recruitment process. Indeed, this study has focused on characterising the leukocyte recruitment capability of VM-competent melanoma cell lines, but not all melanoma cell lines are VM-competent. However, when translating leukocyte recruitment into an *in vivo* situation, it is crucial for the melanoma cells to have the ability to form vascular structures first in order to be able to conduct blood and be in contact with leukocytes circulating in the bloodstream. Therefore, any VM-incompetent melanoma cells would unlikely be involved in leukocyte recruitment *in vivo*. This is the main reason why VM-competent melanoma cells were the focus of the *in vitro* assays. One interesting observation however, is that preliminary parallel plate flow chamber assays performed by colleagues in the laboratory comparing VM-competent and VM-incompetent melanoma cell lines demonstrated a positive correlation between VM competency and the number of bound leukocytes (results not shown). This is perhaps not surprising, as VM-competent melanoma cells have been reported to have different features compared to VM-incompetent cells (Demou & Hendrix 2008). For example, owing to their plasticity, VM-competent melanoma cells were found to express higher levels of pro-angiogenic genes compared to their VM-incompetent counterparts (Demou & Hendrix 2008). It is worth noting that perhaps the acquisition of VM competency is a dynamic process (Demou & Hendrix 2008) and what we are capturing in this study is but a snapshot of the later stages after initially VM-incompetent melanoma cells have evolved to gain VM competency. Therefore, it would be interesting to know if this leukocyte recruitment capability is acquired following the acquisition of VM competency, and compare it between VM-incompetent and VM-competent cells. More specifically, given the importance of adhesion molecules and chemokines in mediating leukocyte recruitment, the relationship between VM competency and adhesion molecule/chemokine expression would be an interesting line of enquiry. One potential approach of assessing this is by comparing the adhesion molecule and chemokine profile of $DSG2^+$ VM-competent melanoma cells to that of their DSG2 KD counterparts, which have been established in Chapter 3 to have impaired VM competency.

There are multiple implications of this study in future research and therapy. In particular, the findings of this study may alter our research on patient samples. While leukocytes have often

been detected within VM vessels in human melanoma samples through IHC (Tan et al. 2016), the precise phenotypes of these leukocytes remain unknown. Having established the potential importance of VM vessels in leukocyte recruitment here, it would be worthwhile to examine the phenotype of these leukocytes within the VM vessels as well as the surrounding tissues across different depths in the tumour. This information could be used to (i) confirm their association with VM vessels, (ii) understand how well they infiltrate into the tumour via VM vessels by correlating their distance from VM vessels as well as correlating the frequency of VM vessels with the frequencies of particular leukocyte types, and (iii) examine their phenotype and functional states (for example, activation status of $CD8^+$ T cells, M1/M2 markers on monocytes/macrophages).

It is also tempting to suggest that this information could be used to shape and design therapies, in particular CAR-T cell therapy. One key advantage of CAR-T cell therapy is the ability to engineer T cells to express specific receptors in addition to the CAR molecule which directs their specificity. For our purpose, these cells could be engineered to express receptors to monocyte or neutrophil attracting chemokines that are upregulated in the tumours (such as CXCL8, CXCL12, CXCL7, CXCL1). With this, these cells which are already equipped with the right ligands for adhesion molecules on the VM vessels (i.e. CD44 to facilitate CD44 binding, as well as LFA-1 to facilitate ICAM-1 and JAM-A binding), will also have the right receptors (such as CXCR1 and CXCR2 externally engineered into the cells) to be responsive to the chemokines on the VM vessels, thereby allowing them to be recruited through these vessels. This may negate the need to introduce additional therapies to stimulate adhesion molecule expression on ECs as these are associated with severe toxicities such as adrenal insufficiency that can result in liver failure (Wu, X et al. 2016).

In summary, this study has uncovered a novel role of VM vessels in mediating leukocyte recruitment, which is made possible with the expression of various leukocyte-recruiting adhesion molecules and chemokines. Current evidence prompts the speculation that of all the leukocyte subsets assessed, VM vessels may preferentially recruit monocytes, since two out of three melanoma cell lines assessed displayed a distinct preference for monocyte adhesion over other leukocyte subsets. This monocyte recruitment could be mediated through interaction with the adhesion molecules CD44, ICAM-1 and JAM, as well as the monocyte-attracting CXCL7, CXCL8, CXCL12 and CX3CL1, although there are also hints towards a role for other adhesion molecules and chemokines not characterised in this current study.

This study will form an important foundation to support further studies investigating the recruitment of leukocytes through VM vessels.

Chapter 5. Function of Melanoma VM: Leukocyte Recruitment *in Vivo*

5.1. Introduction

5.1.1. *General Introduction*

While work done in Chapter 4 has demonstrated that VM-competent melanoma cell monolayers can actively participate in leukocyte recruitment *in vitro*, it is important to assess this in an *in vivo* setting. As discussed in the previous Chapter, the use of an *in vivo* model would allow us to examine whether or not leukocyte recruitment can occur within 3D VM vessels which are under the physiological influence of the extracellular matrix, angiogenic factors and irregular shear stress. This Chapter focuses on establishing a mouse model to examine leukocyte recruitment through VM vessels in real time *in vivo*, in particular through the use of 2 photon intravital microscopy.

5.1.2. *Strengths and Limitations of Intravital Microscopy*

All biological processes within the body, including leukocyte recruitment, are dynamic. There are multiple approaches which can be used to understand these processes. One approach is via intravital microscopy that involves imaging of tissues in living animals. Alternatively, immunohistochemistry/immunofluorescence and flow cytometric analysis which involve analysing samples harvested from humanely killed animals can also be used. Some of the strengths and technical limitations of intravital microscopy in relation to immunohistochemistry/immunofluorescence and flow cytometry analysis will be discussed below.

One of the key strengths of intravital microscopy is the ability to visualise dynamic interactions in real time longitudinally. For example, intravital microscopy of an inflammatory model of the cremaster muscle revealed that myeloid cells arrive at inflammatory sites in waves, with neutrophils arriving first followed by monocytes within the first 4 hours of inflammation (Zuchtriegel et al. 2016). While this information can also be obtained through snapshots via immunohistochemical or immunofluorescence analysis of tissue sections, and has also been confirmed in B16 melanoma tumours through flow cytometry analysis (Headley et al. 2016), the use of intravital microscopy negates the need of progressively killing multiple animals to obtain this information across time. Moreover, intravital microscopy makes it possible to image the same tissue within the same mouse across time, and this has been utilised by one research group to track the development of cancer metastasis, from the initial interaction of cancer cells with leukocytes within the blood

through to the colonisation and development of metastatic sites (Tanaka et al. 2014). Furthermore, the ability to image continuously using intravital microscopy alleviates the likelihood of missing important interactions in between snapshots like that obtained through immunohistochemistry/immunofluorescence and flow cytometric analysis

Another key strength of intravital microscopy is the ability to visualise interactions within a tissue in its native physiological form. For example, the interactions of leukocytes with the blood vessel can be visualised within vessel structures which retain both their physiological structure as well as key features such as flow of blood which is crucial in mediating such interactions. This also enables the examination of direction of flow and migration. The minimal amount of tissue manipulation required also reduces the likelihood of introducing artefacts. On the other hand, the dissociation of tissue samples into single cell suspension for flow cytometry completely destroys the architecture of the tissue. While the overall structure of the tissue is retained to a larger extent using immunohistochemistry/immunofluorescence analysis, the need for lengthy and sometimes aggressive tissue processing procedures may still introduce damage and artefacts to the tissue. For example, it has been observed that within the same tumour tissue, blood vessels visualised using immunohistochemical analysis had a significantly smaller diameter compared to those visualised using intravital microscopy, and this is consistent across both mouse and human tissues (Fisher et al. 2016). Given the importance of blood vessel diameter in determining various properties such as blood pressure and blood flow, differences observed in this regard would likely lead to differences in the conclusions of the study.

Despite the aforementioned strengths, there are still limitations with current intravital microscopy technology. Perhaps one of the biggest technical limitations is the amount of penetrance which can be achieved using different lasers. Single photon confocal lasers can only achieve a depth of 100 µm, while two photon lasers, which are generally used for intravital microscopy, allow deeper penetration of the tissue at a depth of 1mm (reviewed in (Ustione & Piston 2011)). This in turn limits the visualisation to structures that are within 1mm from the tissue surface, but not anything deeper unless additional surgical preparations are performed to remove the upper layer of tissue (Mizrahi et al. 2004). Alternatively, imaging probes can be directly inserted into the tissue to allow for deeper imaging (Levene et al. 2004). These procedures may however result in damage to the tissue of interest. Therefore, it is crucial to take the thickness and location of the tissue into account while using intravital microscopy. On the other hand, the ability to section tumour tissues for

immunohistochemical/immunofluorescence analysis allows for the examination of structures that are embedded within the deeper layers of the tissue.

Taken together, while intravital microscopy is useful to examine the real time interactions of leukocytes with blood vessels within their physiological environment, this approach is currently limited to imaging vessels which are closer to the surface of the tumour.

5.1.3. *Intravital Microscopy on VM Vessels*

To the best of my knowledge, there is currently only one publication showing intravital microscopy analysis of VM vessels (Hillen, F. et al. 2008). The need for special setups to distinguish between conventional EC-lined blood vessels and tumour cell-lined VM vessels could contribute to the lack of progress in this area. In the aforementioned publication, a specific strain of mice, Balb/c nude Tie2-GFP was used. This strain was derived following the backcrossing of Balb/c nude mice to FVB/N-Tie2-GFP mice for over 10 generations (Hillen, F. et al. 2008). The expression of GFP under the control of the endothelial-specific receptor tyrosine kinase (Tie-2) promoter allows for ECs to express GFP, thereby labelling all EC-lined blood vessels fluorescent green. On the other hand, VM vessels within subcutaneous tumour xenografts would be non-fluorescent. Intravital microscopy following intravenous injection of fluorescent dye confirmed the perfusion of both fluorescent green EC vessels and non-fluorescent EC vessels. More importantly, fluorescently labelled leukocytes were seen to circulate in both of these vessel types, confirming the involvement of VM vessels in leukocyte circulation. However, whether or not leukocytes were recruited through these non-fluorescent VM vessels into the tumour was not assessed in that study.

5.2. Hypothesis and Aims

While the Balb/c nude Tie2-GFP mice utilised for intravital microscopy in the aforementioned study (Hillen, F. et al. 2008) are available for purchase commercially, there is a high cost associated. Therefore, we sought to establish an alternative mouse model that would allow us to study this process. The aim of this Chapter is to establish a mouse model for intravital microscopy examination of VM vessels.

It is expected that this model would enable VM vessels to be distinguished from EC vessels in tumours *in vivo* and allow for their interaction with leukocytes to be imaged in real time.

5.3. Results

Of the three VM-competent human melanoma cell lines used in the previous Chapter, C32 melanoma cells were used for the *in vivo* studies. This was because a pilot study had already been performed in the laboratory to optimise the dosage and timing to generate C32 subcutaneous xenograft tumours. As part of this pilot study, C32 cells were also examined if they could form VM vessels *in vivo*. Briefly, $2x10^6$ C32 cells were subcutaneously injected into the flanks of NOD/SCID mice and the resulting tumours were collected at day 17. The tumours were then sectioned for immunohistochemical analysis using anti-CD31 antibody that stains ECs brown and Periodic Acid Schiff (PAS) that stains basement membrane components pink. As demonstrated in Figure 5.1, immunohistochemical analysis of the tumours confirmed the presence of both $CD31^+$ PAS^+ EC-lined vessels and $CD31^-$ PAS^+ VM vessels. $CD31^+$ PAS^+ EC-lined vessels appeared to be localised around the tumour periphery, while the $CD31^-$ PAS^+ VM vessels appeared to be distributed within deeper areas of the tumour. The number of VM vessels and EC vessels were also examined from tumours collected from day 10, day 12 and day 17. When presented as a ratio of VM vessels to EC vessels, the ratio was found to be 0:22 at day 10, 1:4 at day 12 and 1:1.4 at day 17, suggesting an increase in VM vessels with increasing C32 tumour size. Together, these findings confirmed that C32 cells could form VM vessels *in vivo*.

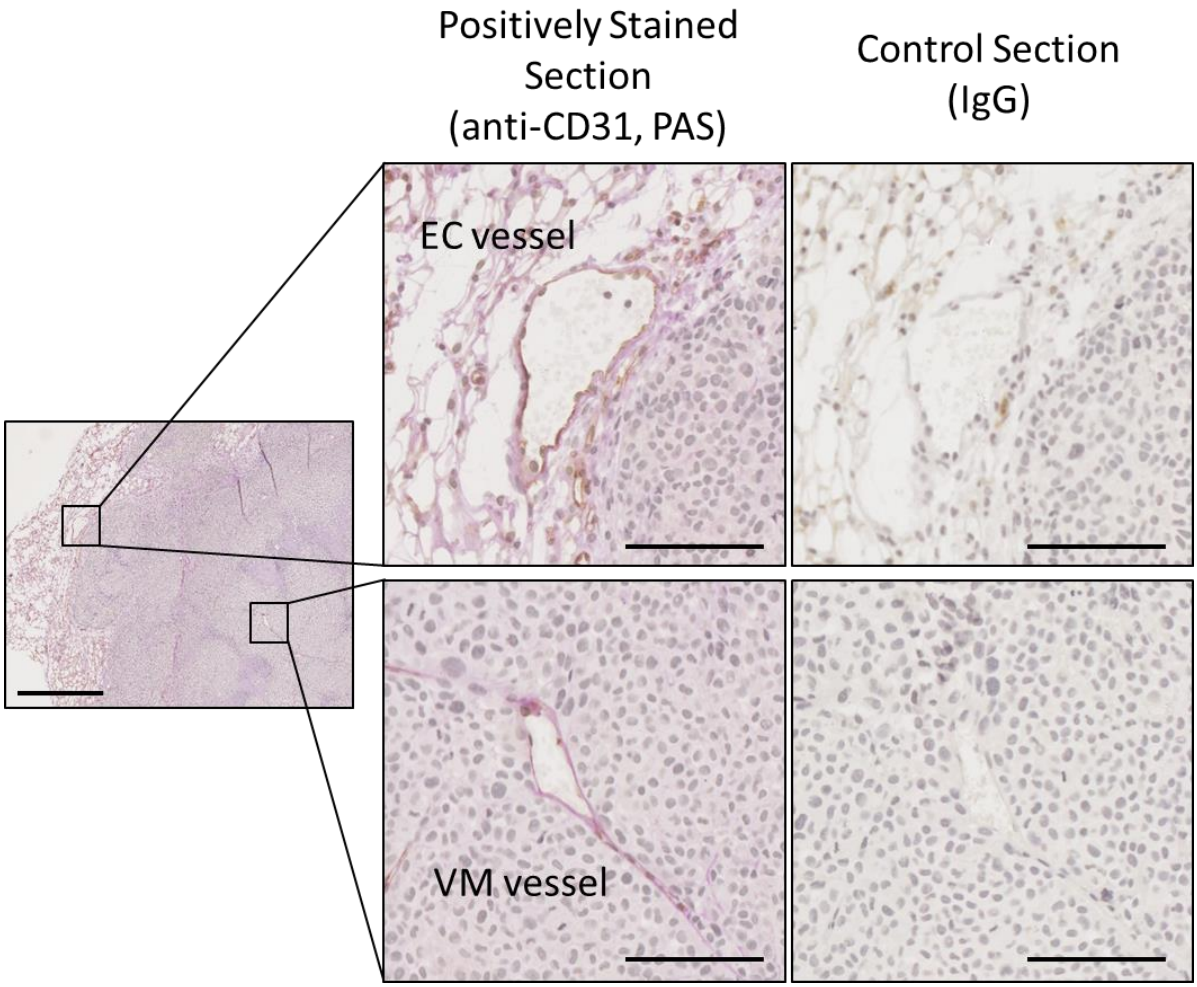

Figure 5.1. C32 human melanoma cells which are VM-competent in vitro are also VM-competent in vivo. (Combined effort between Ms Kay Khine Myo Min and myself to generate xenografts, immunohistochemistry results kindly provided by Ms Kay Khine Myo Min)

C32 cells (2 x 10^6) were injected subcutaneously into the flanks of NOD/SCID mice. The tumours formed were measured and harvested across different time points. The harvested tumours were fixed in formalin, embedded in paraffin and cut into 5 µm sections. Immunohistochemical analysis was performed on the sections. Briefly, sections were stained with anti-CD31 (stains ECs brown) and then counterstained with Periodic Acid Schiff (PAS; stains basement membrane pink) and haematoxylin (stains nuclei purple). Sections stained with an isotype matched antibody and counterstained with haematoxylin were included as controls. Representative immunohistochemistry images shown for n=1 tumour harvested on Day 17. Scale bar on tumour = 500 µm, scale bars on zoomed in vessels = 100 µm.

With this current setup, while normal EC-lined vessels and tumour cell-lined VM vessels could be distinguished through immunohistochemical analysis of harvested tumours, this would not be possible in real time in living mice using intravital microscopy. The approach taken to overcome this was to generate C32 cells which stably express GFP and use these modified cells to create tumours in mice. With this approach, all the tumour cell-lined VM vessels would appear fluorescently green, while the EC vessels would lack the green fluorescence.

To achieve this, C32 melanoma cells were transduced with a lentiviral vector encoding the GFP marker (MSCV-GFP-T2A-Luc). The transduced cells were expanded and then sorted via flow cytometry to select for cells that expressed GFP at high levels. These sorted cells were then further expanded to obtain sufficient cell numbers required to generate the xenografts. As demonstrated in Figure 5.2A, these sorted cells (henceforth referred to as C32-GFP) were confirmed to be fluorescently green when viewed under a fluorescent microscope. Matrigel tube formation assays performed on these C32-GFP cells confirmed that similar to their non-transduced counterparts (Chapter 3, Figure 3.3), these cells were able to rearrange and organise into networks of elongated VM structures extending from cell clusters formed by multiple cells in intimate association (Figure 5.2B). In addition, flow cytometric analysis performed on these C32-GFP cells confirmed that these cells had similar adhesion molecule expression profiles to that of their non-transduced counterparts as described in Chapter 4. More specifically, they expressed the adhesion molecules CD44 (required for leukocyte rolling), ICAM-1 (required for leukocyte adhesion) and JAM-A (required for leukocyte transmigration) at levels similar to that of non-transduced C32 cells (Figure 5.2C; compare to Figure 4.7 for non-transduced C32). These findings confirmed that the C32-GFP cells retained their VM competency and adhesion molecule expression, two critical features which are key to the investigations in this Chapter.

A)

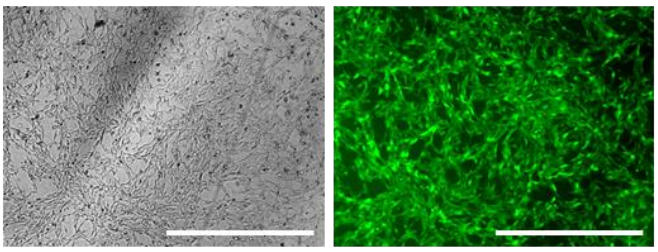

B)

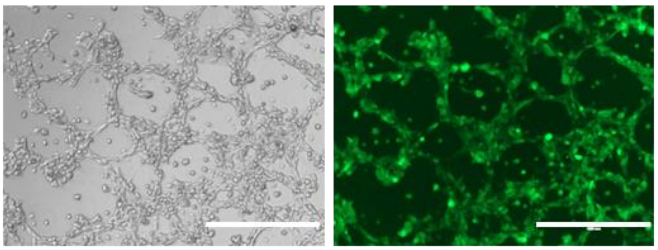

C)

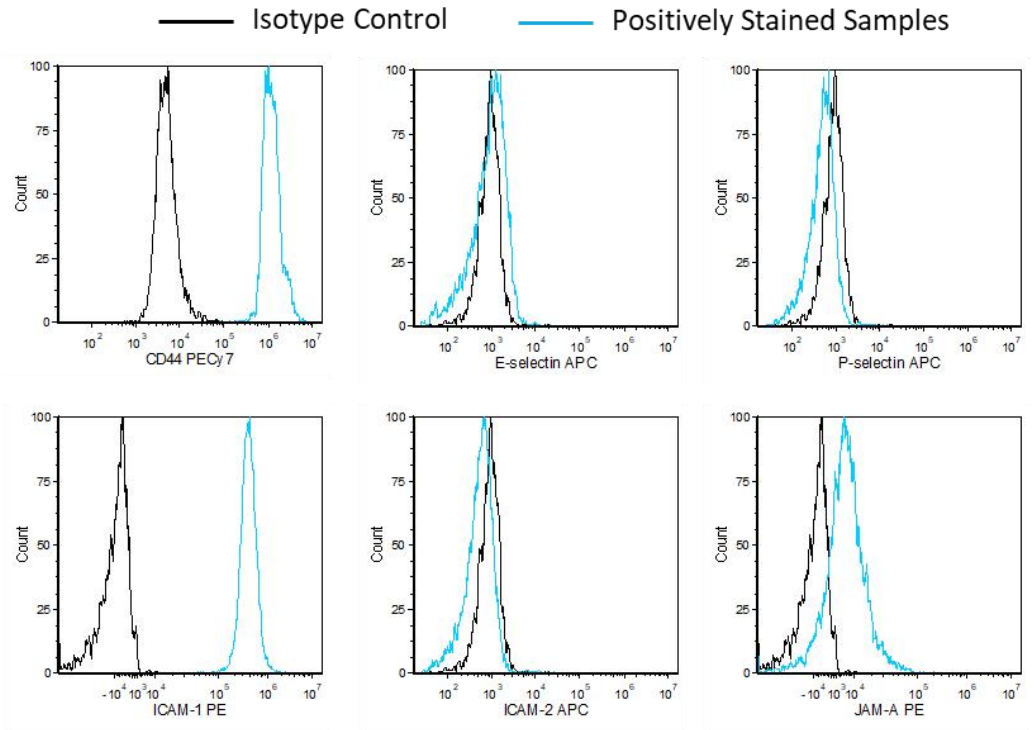
Isotype Control
Positively Stained Samples
Count
CD44 PECy7
E-selectin APC
P-selectin APC
ICAM-1 PE
ICAM-2 APC
JAM-A PE

Figure 5.2. C32 human melanoma cells transduced to stably express GFP retain VM-competency and adhesion molecule expression in vitro.

C32 melanoma cells were transduced with a lentiviral vector to enforce stable expression of GFP. The transduced cells were expanded and sorted via flow cytometry to select for cells that highly expressed GFP. (A) C32-GFP cells growing on tissue culture plastic were routinely examined under a fluorescence microscopy to confirm GFP expression. Representative phase contrast (left) and fluorescent (right) images shown. Scale bar = 200 μm. (B) To assess their VM competency *in vitro*, C32-GFP cells were harvested and seeded onto Matrigel® growth factor reduced basement membrane matrix. After 3-6 hours, images across the whole well were taken using a 4x objective lens. Representative phase contrast (left) and fluorescent (right) images shown for n=2 independent experiments. Scale bar = 400 μm. (C) To examine surface protein expression of adhesion molecules, C32-GFP cells were harvested and stained with multiple fluorescently labelled antibodies targeting specific adhesion molecules and subjected to flow cytometric analysis. 7-AAD was included in the antibody mastermix to allow dead cells (7-AAD$^+$) to be gated out from analysis. Representative histograms showing adhesion molecule expression on C32-GFP cells for n=2 independent experiments.

A schematic diagram detailing the model setup is shown in Figure 5.3A. To generate C32-GFP xenografts for intravital microscopy, $2x10^6$ C32-GFP cells were subcutaneously injected into the flanks of nu/nu mice. Of note, nu/nu mice were used here instead of the NOD/SCID strain used for the initial optimisation of non-transduced C32 xenografts as the lack of hair on the nude mice will aid in the imaging and visualisation of the subcutaneous C32-GFP tumours. The weight of the mice was monitored daily, and tumour sizes were measured using callipers. After the tumours had reached a size of 1 cm^3, the mice were subjected to intravital microscopy. As mentioned before, owing to the expression of GFP, the C32-GFP lined VM vessels would appear fluorescently green. Murine EC-lined blood vessels were highlighted through the retro-orbital injection of DyLight® 594 *Lycipersicon esculentum* agglutinin (tomato lectin). Tomato lectin is a protein derived from tomato that recognises and binds to specific carbohydrate moieties which are also present on the surface of ECs and hence has been widely used to identify EC vessels (Kobayashi, Y et al. 2014; Robertson et al. 2015). In this study, the use of DyLight® 594 tomato lectin will allow for the EC-lined blood vessels to appear fluorescently red. Approximately 10-15 minutes later, MNC pre-stained with CellTracker™ Blue CMAC (7-amino-4-chloromethylcoumarin) were injected intravenously through the tail vein and the movements of these blue cells within the tumour blood vessels were visualised in real time.

Using the one-photon Argon Laser at 488 nm, we were able to visualise the fluorescently green C32-GFP tumours (Figure 5.3B). Conduit structures resembling blood vessels could be seen extending throughout the tumour. When the one-photon DPSS 561-10 laser at 561 nm was used, these same structures appeared to be lined with fluorescently labelled red cells (Figure 5.3B). As tomato lectin is well published to be taken up by EC (Robertson et al. 2015), it was deduced that these vessels were likely to be conventional EC-lined vessels. While using these two lasers to visualise multiple fields of views on the tumour surface, we were unable to find fluorescently green vessels which were not also lined with fluorescently labelled red cells. Unfortunately, during the period of the experiment, the two-photon laser had malfunctioned and was not performing optimally. For this reason, we could not visualise deeper into the tumour to search for such vessels. Further to that, as our microscope setup requires the use of the same two-photon laser to provide the excitation required to visualise CellTracker™ Blue CMAC, we were also unable to visualise the injected MNC pre-stained with CellTracker™ Blue CMAC within the blood vessels.

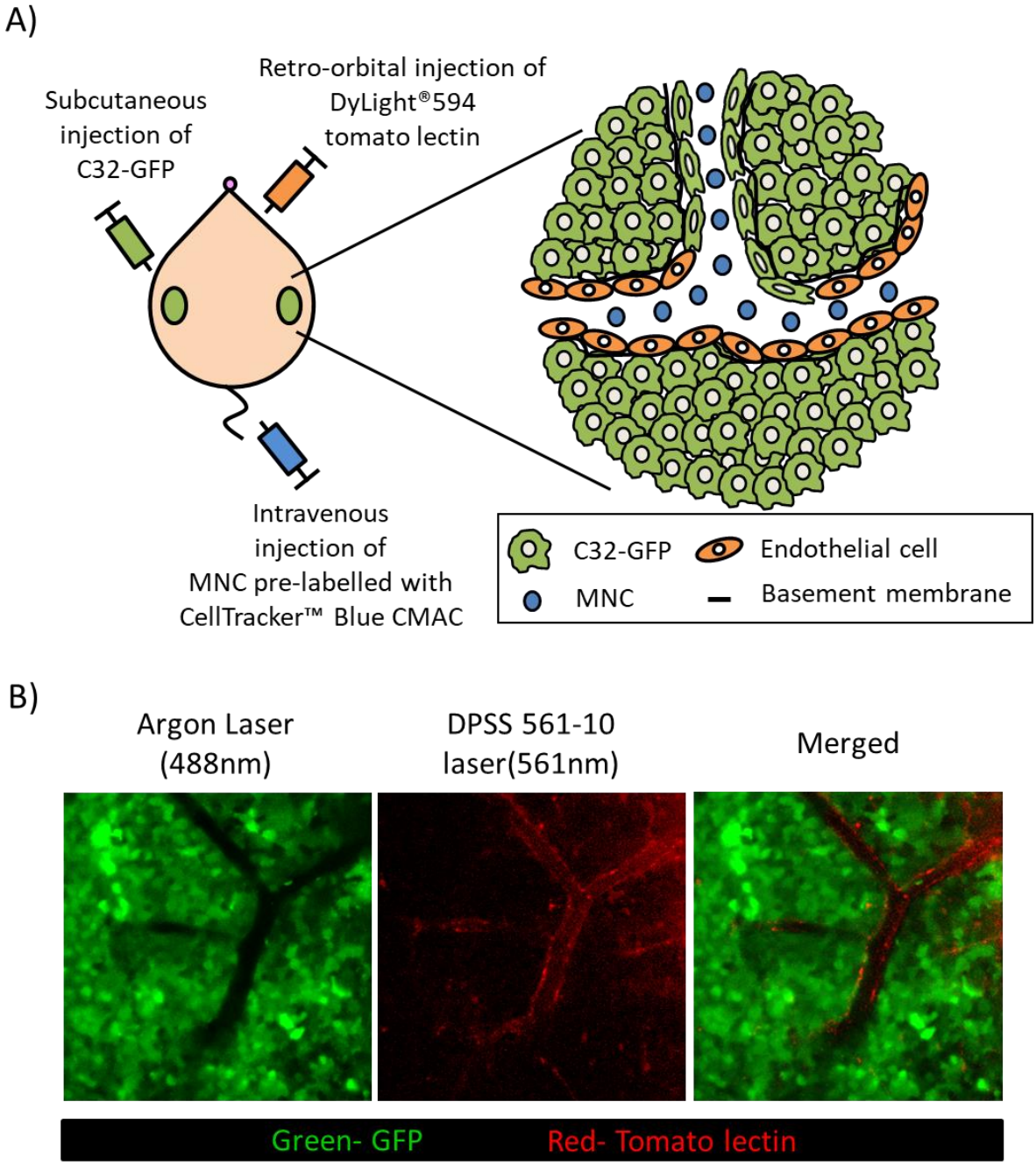

Figure 5.3. Setup of mouse model for examination of leukocyte recruitment via VM vessels. (Group effort co-ordinated by myself but with input from Associate Professor Claudine Bonder, Dr Eli Moore, Ms Michaelia Cockshell and Ms Kay Khine Myo Min)

(A) Schematic diagram of intravital microscopy experimental setup. C32-GFP cells were injected subcutaneously into both flanks of 6-8 week old female nu/nu mice. Tumours were allowed to grow to 1cm^3, at which time intravital microscopy was performed. DyLight® 594 tomato lectin (100 µl) was injected retro-orbitally and 5x10^6 MNC pre-labelled with CellTracker™ Blue CMAC were injected intravenously through the tail vein. (B) Confocal images of the fluorescently green C32-GFP tumours were taken using the one-photon Argon Laser at 488 nm, while the one-photon DPSS 561-10 laser was used at 561 nm to image the fluorescently red DyLight® 594$^+$ EC-lined blood vessels.

One question that arose during the intravital microscopy imaging was the ability of C32-GFP cells to bind to tomato lectin. While melanoma cell lines and patient tissue have been described in the literature to bind to a variety of lectins (Monastirli et al. 2000; Romani, Schuler & Fritsch 1983), these lectins bind to specific carbohydrate structures which are different to that recognised by tomato lectin (Kobayashi, Y et al. 2014). Therefore, unlike ECs, the ability of melanoma cells to bind to tomato lectin is unknown. To assess this, DyLight® 594 tomato lectin was added to C32-GFP cells grown on coverslips. As demonstrated in Figure 5.4, C32-GFP cells which were incubated in DyLight® 594 tomato lectin fluoresced upon excitation at 561 nm, indicating their binding to DyLight® 594 tomato lectin. This was absent when DyLight® 594 tomato lectin was not added onto the cells. This indicated that the use of tomato lectin was unsuitable for the purpose of distinguishing EC vessels and VM vessels *in vivo*, as both the ECs and melanoma cells lining these vessels bind to tomato lectin readily.

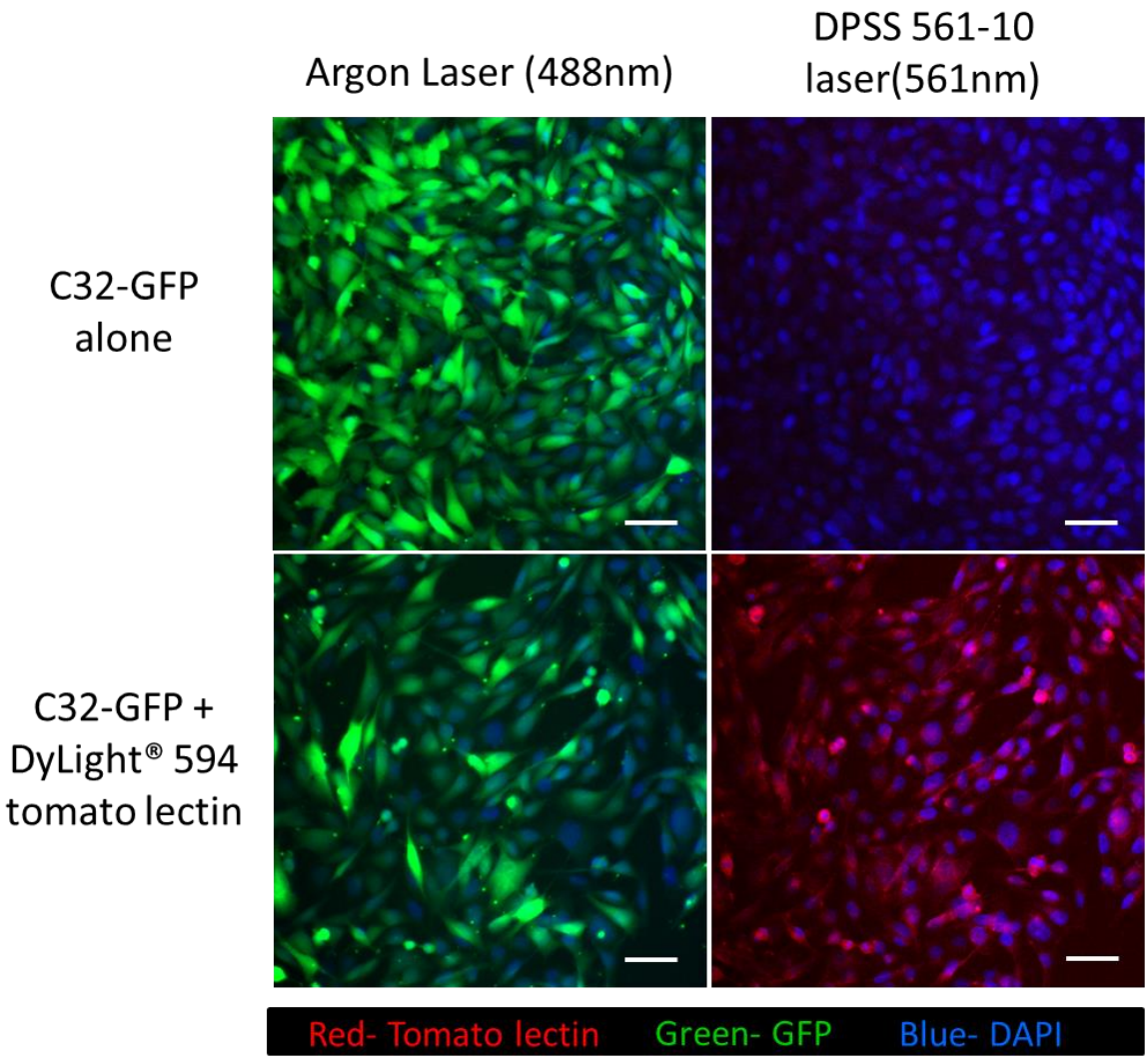

Figure 5.4. C32-GFP cells can bind to DyLight® 594 tomato lectin.

To examine if C32-GFP can bind to tomato lectin, tomato lectin was added to C32-GFP cells grown on coverslips. Coverslips with C32-GFP cells alone were also included as a control. Confocal images of the fluorescently green C32-GFP cells were taken using the one-photon Argon Laser at 488 nm, while the one-photon DPSS 561-10 laser was used at 561 nm to image the fluorescently red cells which had bound to DyLight® 594 tomato lectin. Scale bar = 50 µm.

To make the best use of the tumour xenografts which were already generated, I sought to perform analysis on the tumours using alternative approaches. In particular, I wanted to confirm that the injected MNC pre-stained with CellTracker™ Blue CMAC could still be detected in the tumour even though we were unable to visualise them under the microscope due to the faulty laser. Briefly, MNC pre-stained with CellTracker™ Blue CMAC were injected intravenously through the tail vein. After 20 minutes, the mice were humanely killed. The tumours were excised and dissociated into single cell suspensions via a combination of enzymatic digestion and mechanical dissociation using the commercially available Human Tumour Dissociation Kit and gentleMACS™ Octo Dissociator with Heaters (Miltenyi Biotec). The cell suspensions were then labelled with fluorescently labelled antibodies targeting leukocyte subset-specific markers (CD4, CD8 and CD14) and subjected to flow cytometric analysis.

The gating strategy and results for the flow cytometric analysis are detailed in Figure 5.5. When analysing the data, a FSC/SSC gate was first made based on the injected MNC population to gate all of the MNC population (Figure 5.5A). The viable cells within the MNC population were then selected (FVS700-) and these cells were confirmed to be positively stained with the CellTracker™ Blue CMAC. The same MNC gate was then placed on the FSC/SSC plot for the cell samples obtained from a mouse that did not receive the MNC injection (Figure 5.5B). This allows us to examine if there would be tumour cells which would also fall into the same MNC gate and may confound further analysis. As demonstrated in the FSC/SSC and FVS700/SSC plot, there were indeed viable tumour cells that were present in the same MNC gate. Similar to the analysis shown in Figure 5.5A, the gated tumour cells were presented on a CellTracker™ Blue CMAC/SSC plot. As this sample was known to lack the CellTracker™ Blue CMAC cell population, the gate meant to mark the CellTracker™ Blue CMAC$^+$ cells could be placed accurately at the edge of the tumour cell population to exclude the tumour cells from the analysis. Similarly, subsequent gates designed to mark the CD4$^+$, CD8$^+$ and CD14$^+$ cell populations respectively within the CellTracker™ Blue CMAC$^+$ cells were also set at the edge of the tumour cell population to exclude these cells.

These gates were then used to analyse the results for the tumour cell suspensions obtained from mice which had received the MNC injection (Figure 5.5C). As demonstrated in Figure 5.5C, these tumours contained a small population of viable CellTracker™ Blue CMAC$^+$ cells which was absent in the cell samples from a mouse lacking the injection, indicating the

presence of these cells within the tumour. Further analysis revealed that these viable CellTracker™ Blue CMAC^{+} cells expressed CD8, but not CD4 or CD14 (Figure 5.5C). These results confirm that the injected CellTracker™ Blue CMAC labelled MNC could indeed be detected within the tumour.

A)

CellTracker™ Blue labelled MNC

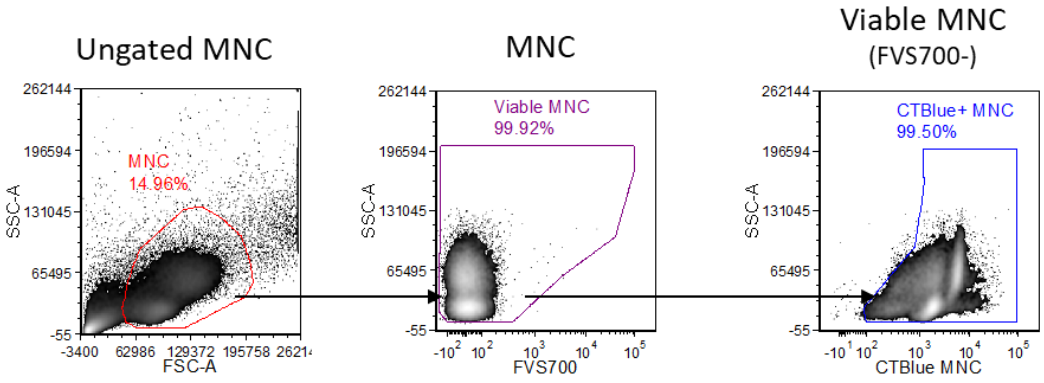

B)

C32-GFP tumour alone

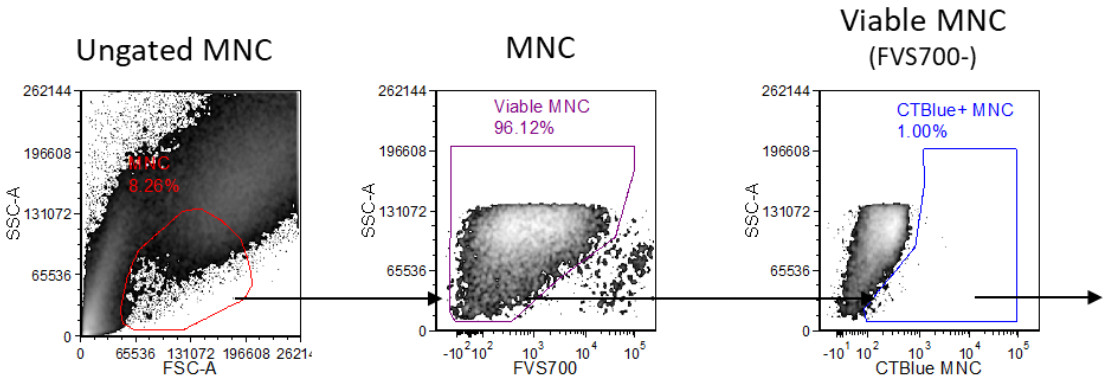

CellTracker™ Blue CMAC+ MNC

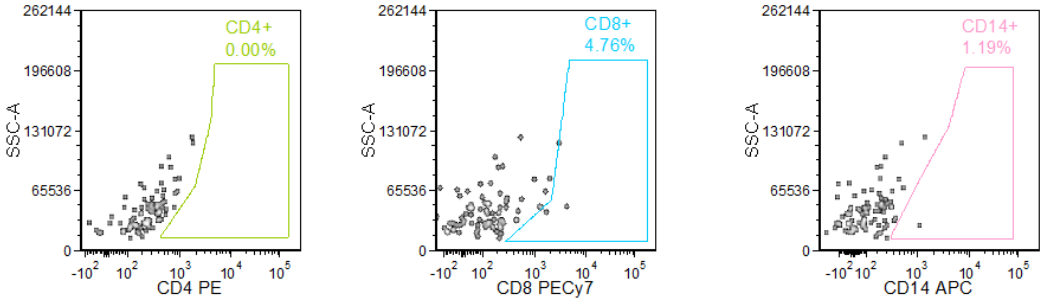

C)

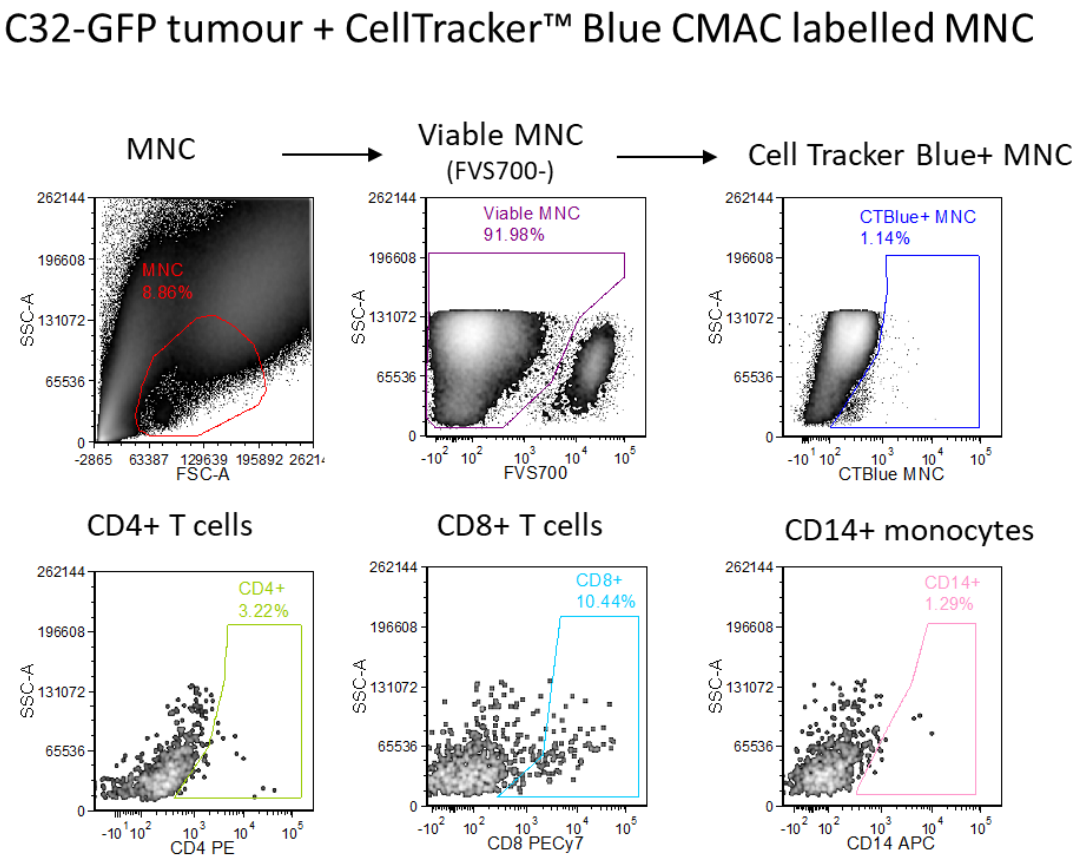

Figure 5.5. Intravenously injected CellTracker™ Blue CMAC labelled MNC can be detected in excised C32-GFP tumours.

MNC ($5x10^6$) pre-labelled with CellTracker™ Blue CMAC were injected intravenously through the tail vein of mice bearing duplicate C32-GFP tumours (one on each flank). After 20 minutes, tumours were excised and dissociated into single cell suspensions. As a control, a tumour was also excised from one mouse that did not receive MNC. The dissociated tumour suspensions were stained with fluorescently labelled antibodies targeting surface markers of various leukocyte subsets, and subjected to flow cytometric analysis. Fixable Viability Stain 700 (FVS700) was included in the antibody mastermix to allow dead cells ($FVS700^+$) to be gated out from analysis. Representative scatter plots shown for n=1 independent MNC donor, n=1 tumour excised from 1 mouse that did not receive MNC injection and n=4 tumours excised from 2 mice which received MNC injection.

Further to that, the cell suspensions were also stained with fluorescently tagged antibodies targeting various adhesion molecules to examine the expression of these molecules through flow cytometry. As demonstrated in Figure 5.6, the C32-GFP cells retained expression of CD44, ICAM-1 and JAM-A required for leukocyte recruitment *in vivo*. This suggested that these C32-GFP cells might still retain their leukocyte recruitment capabilities *in vivo*.

In addition to generating cell suspensions for flow cytometric analysis, tumours were also harvested, fixed in formalin and embedded in paraffin to be used for immunohistochemical analysis. Due to time constraints, this analysis was not performed as part of this study.

Taken together, the results demonstrate the ability to visualise conventional EC vessels in a C32-GFP tumour through the use of intravital microscopy. While VM vessels and injected MNC were unable to be visualised due to the faulty two photon laser, the presence of injected MNC within the tumours was confirmed via flow cytometric analysis. Further to that, C32-GFP cells also retained adhesion molecule expression *in vivo*, hinting at their potential in mediating leukocyte recruitment.

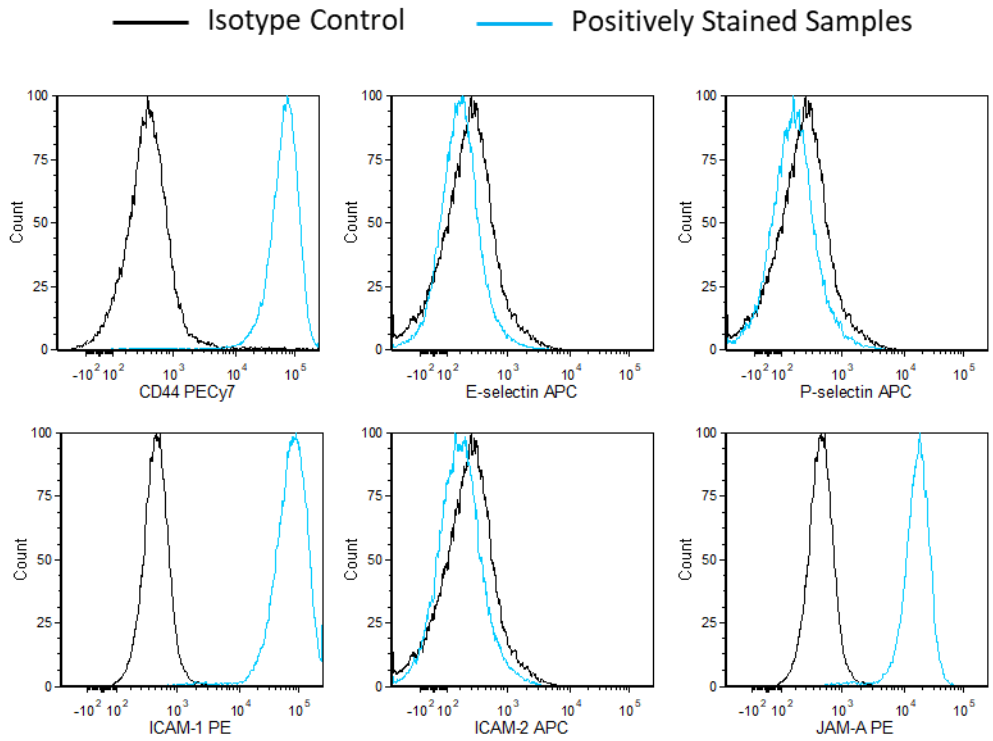

Figure 5.6. Excised C32-GFP tumours retain expression of adhesion molecules required for leukocyte recruitment.

MNC ($5x10^6$) pre-labelled with CellTracker™ Blue CMAC were injected intravenously through the tail vein of mice bearing C32-GFP tumours. After 20 minutes, tumours were excised and dissociated into single cell suspensions. The cell suspensions were stained with multiple fluorescently labelled antibodies targeting specific adhesion molecules, and subjected to flow cytometric analysis. Fixable Viability Stain 700 (FVS700) was included in the antibody mastermix to allow dead cells ($FVS700^+$) to be gated out from analysis. Representative histograms showing adhesion molecule expression for n=4 tumours excised from 2 mice.

5.4. Discussion

The leukocyte composition within a tumour is critical in dictating tumour fate. This composition in turn is shaped by the ability of the leukocytes to migrate from the blood circulation across the blood vessels into the tumour. The current understanding in the literature of this recruitment process is largely limited to EC-lined blood vessels. However, it has been established in the previous Chapter that melanoma cell-lined VM vessels can also play a role in this recruitment process *in vitro*. This Chapter presents the approaches taken to establish a mouse model to examine this process *in vivo* in real time through intravital microscopy.

Due to both time and financial constraints, we opted to use a different approach to that of the only study that has reported the detection of leukocytes within VM vessels in the literature. While Hillen and colleagues made this observation through tumours with fluorescently green EC-lined vessels (Hillen, F. et al. 2008), we sought to utilise tumours with fluorescently green VM vessels instead. Unfortunately, while the initial plan to differentiate EC-lined vessels in our model was with the use of DyLight® 594 tomato lectin, which readily binds to murine EC, subsequent experiments performed confirmed that melanoma cells could bind to this lectin too. Therefore, we could not conclusively determine if the vessel structures detected in Figure 5.3B were EC vessels or VM vessels. Nonetheless, based on our understanding of the limited penetrance of single-photon lasers and the distribution of vessels within these tumours, it is likely that the vessel structures shown in Figure 5.3B were EC vessels. More specifically, as mentioned in the introduction, one key limitation of the single photon lasers is their shallower penetrance and hence they can only be used to visualise vessels on the surface of the tumour. According to the pilot study performed on the C32 melanoma cells, while EC vessels were present on the surface of the tumour, the majority of VM vessels were located deeper within the tumour (Figure 5.1). This highlights the importance of utilising the two photon laser to acquire deeper penetration into the tumour to locate these vessels. Unfortunately, this approach was hampered by the two photon laser unexpectedly malfunctioning during these experiments. Therefore, the presence and location of these VM vessels remain to be elucidated.

Flow cytometric analysis performed on single cell suspensions derived from dissociated tumours confirmed the presence of a small population of CellTracker™ Blue CMAC MNC within the tumours of mice which had received the injection of these cells. This was

otherwise absent in mice lacking injection of MNC. Even though the population of CellTracker™ Blue CMAC MNC detected was small, this was not unexpected, as the bulk of the cell suspension would be made up of tumour cells. Further to that, intravenous injection of $5x10^6$ CellTracker™ Blue CMAC MNC would lead to the dispersion and circulation of the cells throughout the whole body as opposed to localised catheter injection into the tumour, thereby explaining the small number of CellTracker™ Blue CMAC MNC detected within the tumour. While the results demonstrate that these MNC could be detected in the tumour, they does not provide information on the spatial distribution of these cells. More specifically, this approach does not allow us to know if these cells were still in circulation in the blood vessels or if they had already transmigrated across the blood vessels into the tumour tissue.

The flow cytometric analysis also confirmed the expression of CD44, ICAM-1 and JAM-A, key adhesion molecules required for leukocyte recruitment, on the surface of the bulk C32-GFP tumours. This approach does not allow us to identify the C32-GFP cells lining the VM vessels from the bulk of the tumour and examine their adhesion molecule expression. However, considering the strong and uniform nature in which these molecules were expressed by the tumour cell population, it is reasonable to speculate that VM vessel-lining cells would also maintain similar adhesion molecule expression.

To maximise the amount of information we can obtain from this current study, we will address the aforementioned limitations in future studies using immunohistochemical analysis of the formalin fixed paraffin embedded tumour tissues. Briefly, serial tumour sections will be co-stained with PAS (stains basement membrane) and anti-CD31 (stains ECs); PAS and anti-GFP (stains C32-GFP); PAS and anti-CD44/ICAM-1/JAM-A; as well as PAS and human-specific CD45 (stains leukocytes). These staining approaches conducted on serial sections will allow us to identify VM vessels as PAS^+ $CD31^-$ GFP^+ vessels and examine their distribution within the tumour. The adhesion molecule expression profile of these VM vessels can also be assessed with the inclusion of anti-CD44/ICAM-1/JAM-A, which can further confirm their potential in leukocyte recruitment. The localisation of $CD45^+$ leukocytes in relation to these vessels can also be assessed. Further to that, the phenotype of the leukocytes can also be characterised with the use of antibodies targeting subset specific markers.

While I was unable to fully achieve the aim of establishing a mouse model to examine leukocyte recruitment via VM vessels within the scope of this study, the current work has provided important information on the strengths and technical limitations of the current setup.

Moving forward, there are multiple strategies that we can utilise to improve this model. Firstly, the location of the VM vessels within the tumour is critical. As mentioned in the introduction, while the use of a two photon laser would allow for deeper penetration than what could be achieved using single photon lasers, it is still limited to a depth of 1 mm (Ustione & Piston 2011). Therefore, the availability of VM vessels closer to the surface of the tumour would greatly aid imaging. A potential approach to achieve this could be the pre-treatment of smaller tumours with anti-VEGFA. Based on our observations in the pilot study (results not shown), VM vessels began to appear at Day 10 post tumour cell injection when the tumours were around 25 mm^3, but became more abundant at later stages after the tumours have grown past ~60 mm^3 (Day 12 post tumour cell injection). It has been documented in the literature that the use of anti-VEGF – aimed to inhibit conventional vessel formation – paradoxically stimulates the occurrence of VM (Schnegg et al. 2015). Therefore, the use of anti-VEGF on smaller tumours may enhance the occurrence of VM and increase their abundance on the surface of the tumour, allowing for easier imaging. Secondly, alternative approaches should be used to differentiate EC vessels and VM vessels. One possible approach is through the use of fluorescently conjugated anti-mouse CD31 antibodies, which are specific to the EC marker CD31. Preliminary flow cytometry analysis on C32 cells demonstrated the lack of CD31 expression on these cells (results not shown), therefore highlighting the feasibility of this approach over tomato lectin binding. Thirdly, alternative dyes which are brighter can also be used to stain the MNC. For example, CellTracker™ Blue CMAC can be replaced with CellTrace Violet, which has the same emission and excitation spectrum to that of CellTracker™ Blue CMAC but stains cells brighter. This may aid in the visualisation of these cells within the tumour tissue. Nonetheless, the availability of an optimally operating two photon laser will be the underlying key to driving the development of this model. Of note, the microscope has now been repaired and hence will be available for future studies.

Ultimately, the established model will be used to examine the ability of VM vessels to recruit leukocytes into tumours. In this preliminary study, freshly isolated bulk MNC had been utilised to examine if there were any leukocytes at all which could interact with the VM vessels. Subsequent studies can be performed with pre-isolated leukocyte subsets to examine their interaction with the VM structures. These pre-isolated leukocytes can also be further stimulated as required to promote tumour directed migration. For example, while pre-isolated monocytes will be fluorescently labelled and injected without any further treatment (Sidibe et

al. 2018), $CD8^+$ T cells will be activated with CD3 and CD28 beads prior to fluorescent labelling and injection (Breart et al. 2008). These pre-isolated leukocytes can also be stained with different dyes, mixed and injected intravenously into the mice to examine if there is preferential recruitment of any specific leukocyte subset across VM vessels. In addition, this model can be further used to identify the adhesion molecules and chemokines involved in mediating leukocyte recruitment through VM vessels. This can be assessed through the use of antibody-mediated blocking of adhesion molecule and chemokine function or shRNA-mediated downregulation of adhesion molecule and chemokine expression on the melanoma cells. This model can also be extended to examine the likelihood of drug delivery and perfusion of nanoparticles through VM vessels, an area of interest that has been widely studied in conventional EC-lined vessels (Murphy, EA et al. 2008).

In conclusion, this Chapter details the steps taken to establish a cost-efficient model to enable the examination of leukocyte recruitment in VM vessels. Despite the inability to directly visualise such interactions due to technical issues, the results obtained are promising in showing that this is a feasible model.

Chapter 6. Final Discussion

The importance of conventional EC vessels in cancer biology has been long recognised. As one of the major transportation routes within the body, EC vessels play important roles in the distribution of nutrients and oxygen, trafficking of leukocytes and delivery of drugs. Therefore, their significance extends from affecting melanoma progression to melanoma treatment. It is commonly recognised that solid tumours cannot grow beyond $1mm^3$ without expansion of the pre-existing vasculature (Gimbrone et al. 1972), and an increase in tumour vascularity is correlated with increased tumour thickness and ulceration as well as decreased patient survival in melanoma (Kashani-Sabet et al. 2002) and many other cancers (Weidner et al. 1991). Physical abnormalities such as irregular tortuousness and enhanced leakiness in these tumour EC vessels significantly hinder drug delivery (Stylianopoulos & Jain 2013). Furthermore, as discussed in detail in previous Chapters, changes in adhesion molecule and chemokine profile on ECs greatly affects leukocyte recruitment.

This knowledge of EC vessels has enabled us to both optimise current treatment designs and develop novel treatment approaches. Anti-angiogenics were first designed to target tumour vascularity to inhibit tumour growth (reviewed in (Goel et al. 2011)). The lack of clinical success however has led to the repurposing of these drugs for vascular normalisation to correct for various physical abnormalities. This can be achieved through the administration of lower doses of anti-angiogenics (Huang, Y et al. 2012) or is present within a specific window of time following administration of high doses of anti-angiogenics (Winkler et al. 2004). This correction has in turn led to improved drug delivery (Stylianopoulos & Jain 2013). Further to that, vascular normalisation also leads to changes in adhesion molecule and chemokine expression on the ECs which allow for better recruitment of anti-tumourigenic leukocytes (Dirkx, AEM et al. 2006). Understanding the adhesion molecule and chemokine profile required for enhanced leukocyte recruitment has also led to the development of CAR-T cells equipped with receptors towards the overexpressed chemokines to enhance recruitment (Peng et al. 2010).

An alternative form of vascularisation that has gained growing interest in recent years is VM. In contrast to our wealth of knowledge of EC vessels, VM vessels are relatively less understood. Nonetheless, our current understanding of VM vessels clearly demonstrates a close relationship with EC vessels, with both similarities and differences to allow for complementarity. Similar to EC vessels, VM vessels are conduit structures which can be actively perfused with blood (Dunleavey et al. 2014; Hillen, F. et al. 2008; Ruf et al. 2003). Increased VM is associated with increased disease metastasis and aggressiveness

(Wagenblast et al. 2015). Similar to EC vessels, blocking VM vessel formation *in vivo* decreased tumour growth (Francescone et al. 2012; Misra, Bajaj & Kale 2012). Studies performed to understand the regulation of VM revealed some overlap with molecules that regulate EC vessel formation (Hendrix, MJ et al. 2001; Vartanian et al. 2011). However, the use of anti-angiogenics does not simultaneously target these VM vessels. Instead, it led to enhanced expansion of VM competent tumour cells (Dunleavey et al. 2014) and promoted the occurrence of VM (Schnegg et al. 2015), suggesting that these VM vessels played complementary roles with EC vessels. This difference in responsiveness towards anti-angiogenics could be attributed to the ability of plastic cancer cells to initiate VM through other molecules. For example, while anti-VEGF inhibited the growth of VEGF-dependent B16-F10 tumour cells lacking CD31 expression, it enhanced the expansion of $CD31^+$ tumour cells that were capable of undergoing VM independent of VEGF (Dunleavey et al. 2014). Together, these findings highlight both the importance of VM as an alternative form of vascularisation complementary to EC vessels and the effects of this in mediating disease progression. However, there remains a big gap in our understanding of VM. In particular, the functional roles of VM vessels in drug delivery and leukocyte recruitment remain largely un-investigated.

This thesis presents novel data which demonstrates that VM vessels possess two additional properties which are similar to that of EC vessels. Firstly, VM vessels are found to be regulated by DSG2, a cadherin molecule that we (Ebert et al. 2016) and others (Giusti et al. 2013) have recently reported to also regulate EC vessels. siRNA-mediated DSG2 knockdown was found to impair the ability of $DSG2^+$ human melanoma cell lines to form VM structures *in vitro*. Subsequent assays deciphering the underlying mechanism of this observation revealed a downregulation of DSG2 homotypic cell-cell adhesion following DSG2 knockdown. Preliminary data acquired from RNA sequencing, flow cytometric analysis and *in silico* analysis suggested the potential of hypoxia in regulating DSG2 expression, although the actual pathways and molecules involved remain to be elucidated.

Secondly, similar to EC vessels, VM vessels can actively participate in leukocyte recruitment, at least *in vitro*. Note that the concept of VM vessels recruiting leukocytes has also recently been raised by other researchers (Sackstein, Schatton & Barthel 2017). This is made possible due to the expression of adhesion molecules and chemokines characteristic of EC. Unlike the expression of adhesion molecules and chemokines on ECs, the expression of adhesion molecules and chemokines on the melanoma cells appeared to be largely unaffected by

hypoxic stimulation. The expression of these adhesion molecules was also retained on melanoma cells obtained from excised xenografts. This highlights the potential of VM vessels to participate in leukocyte recruitment *in vivo*, although this remains to be elucidated.

The significance of these individual findings in our understanding of VM as well as the key research questions following these findings have been addressed in detail in the respective Chapters. Briefly, additional research is required to extend the role of DSG2 in VM *in vitro* into *in vivo* studies, and the key molecules regulating DSG2 expression remain to be elucidated. Similarly, additional work is required to expand on the preliminary work done to establish a cost efficient model to examine the ability of VM vessels to recruit leukocytes *in vivo*. This final discussion will focus on linking these two findings together, raise future research questions and suggest potential applications based on the findings of these research questions.

A key question to arise from this work is if DSG2 plays a role in regulating leukocyte recruitment through VM vessels. This could potentially occur through several mechanisms. Firstly, it has been demonstrated in EC vessels that VE-cadherin is involved in mediating the recruitment of neutrophils. More specifically, antibody mediated inhibition of homotypic VE-cadherin binding resulted in increased vascular permeability and increased neutrophil recruitment through EC vessels *in vivo* (Gotsch et al. 1997). DSG2 has also been found to participate in EC homotypic adhesion, and a lack of DSG2 resulted in increased vascular permeability (Ebert et al. 2016). Hence, it would be interesting to examine if DSG2 could also play a similar role in VM vessels by regulating leukocyte recruitment through changes in vessel permeability. Secondly, an alternative mechanism of DSG2 in regulating leukocyte recruitment is its potential as an adhesion molecule expressed within the vessel lumen to allow for direct binding of counter ligands on leukocytes. Interestingly, the *DSC2* gene, which encodes for DSC2 known to bind heterotypically to DSG2 as part of desmosome formation, has been found to be expressed on monocytes (Frankenberger et al. 2012), and unpublished findings from our own group have shown the *DSC2* gene to be expressed by both monocytes and neutrophils. While its protein expression remains to be elucidated, this highlights a potential of DSG2 to be directly involved in monocyte and neutrophil recruitment through VM vessels.

Depending on the outcome of the research questions above, there can be multiple potential applications for therapy. The basis however is that VM vessels are indeed involved in

leukocyte recruitment *in vivo*, which then allows them to be utilised as an additional route for the entry of anti-tumour leukocyte populations, such as chimeric antigen receptor (CAR)-T cells. As previously described in Chapter 1, CAR-T cells are autologous $CD8^+$ T cells that have been engineered to express synthetic receptors with extracellular domains specific to tumour antigens and intracellular domains transducing $CD8^+$ T cell activating signals. Owing to their enhanced tumour recognition and eradication properties, CAR-T cells have been highly successful in achieving cure for haematological cancers and have been approved for the treatment of acute lymphoblastic leukaemia. Their effectiveness in solid cancers including melanoma however is currently low, partly due to the presence of a physical blood vessel barrier which can block the entry of CAR-T cells into the tumour microenvironment. Melanoma cell lines, at least the ones used in this study, appeared to consistently express CD44, ICAM-1 and JAM *in vitro*, albeit at different levels. Further to that, melanoma cells obtained from excised xenografts also retained CD44, ICAM-1 and JAM expression. Should these be consistently present on *in vivo* tumours and patient samples, this makes VM vessels a more attractive route of leukocyte entry for CAR-T cells, as EC vessels often lack a full suite of adhesion molecules required for leukocyte recruitment. This could potentially explain the preferential recruitment of TAM and TAN which should also be reliant on similar adhesion molecules for recruitment but remain recruited even with the lack of such adhesion molecules on EC vessels. Therefore, CAR-T cells only need to be engineered to express the receptors corresponding to the chemokines which are overexpressed in the tumour. Unlike the adhesion molecules which are consistently expressed across the three different $DSG2^+$ melanoma cell lines, the expression of chemokines and chemotactic cytokines appeared to be cell-line dependent. For example, midkine was found to be secreted the most by C32 cells, CXCL12 was found to be secreted the most by CHL-1 cells, while CXCL8 was found to be secreted the most by SK-Mel-28 cells. This highlights the need to characterise the chemokine profile of a tumour prior to the design of the CAR-T cells to achieve optimal tumour homing.

If DSG2 is found to play a role in regulating leukocyte recruitment through VM vessels via changes in vessel permeability, then there is the potential of developing therapeutics to block homotypic DSG2 interactions to enhance leukocyte recruitment, as has been done previously for VE-cadherin (Gotsch et al. 1997). This can be achieved through multiple approaches, including antibodies such as that used for VE-cadherin blocking (Gotsch et al. 1997) or peptides like that used for N-cadherin blocking (Beasley et al. 2009; Beasley et al. 2011). Alternatively, siRNAs can also be used to inhibit DSG2 expression, with additional

packaging and modifications required to prevent degradation and ensure tumour directed delivery (Davis et al. 2010). As DSG2 is also involved in regulating both angiogenesis and VM, and blocking DSG2 can achieve both anti-angiogenic (Ebert et al. 2016) and anti-VM (Chapter 3; (Tan et al. 2016)) effects at least *in vitro*, it is tempting to speculate that this approach may target these three arms (vessel permeability, angiogenesis and VM) simultaneously. However, drawing from our knowledge of how anti-angiogenics can select for alternative pathways to reactivate vessel formation, using DSG2-blocking drugs at high doses is likely to also result in resistance. Therefore, it may be more optimal to utilise these agents at a lower dosage like that previously demonstrated for anti-angiogenics such as anti-VEGFR2 (Huang, Y et al. 2012) which would be both sufficient to block homotypic DSG2 interaction and induce a vascular normalising effect. It would also be interesting to assess if VM vessels can also be physically normalised similar to EC vessels, or if DSG2-blocking drugs can induce changes in adhesion molecule and chemokine expression on VM vessels when utilised as a vascular normalising agent.

If DSG2 is found to be involved in monocyte or neutrophil recruitment through VM vessels via direct DSG2-DSC2 interactions, it highlights the potential of using DSG2 or DSC2 as a molecule to promote recruitment of CAR-T cells into the tumour. One potential issue of concern is the recruitment of these CAR-T cells through EC vessels that are lined with ECs expressing DSG2 into non-tumour tissues. Indeed, immunohistochemical and immunofluorescence analysis performed on a human tissue microarray by our group has shown that DSG2 can be expressed heterogeneously on ECs lining both arteries and veins in normal and tumour tissues (Ebert et al. 2016). Normal tissues however may not necessarily express the same chemokines like that of the tumour tissues to which the CAR-T cells are able to bind to through their engineered chemokine receptors. Furthermore, CAR T- cells are engineered to target tumour specific antigens which should not be expressed in normal tissues. These speculations suggest that CAR-T cells designed to be recruited via DSG2/DSC2 interactions might not necessarily be recruited through DSG2 expressing EC vessels due to the lack of the corresponding chemokines, and if they are recruited into non-tumour tissues, they may not be able to exert their cytotoxic activity due to the lack of tumour specific antigens. Nonetheless, such assumptions should be further addressed through *in vivo* studies.

While this study currently focuses on understanding VM in melanoma, the knowledge acquired is applicable to other cancers too. VM is present in many other solid cancer types, including breast cancer, prostate cancer and glioblastoma (Yang et al. 2016). While CAR-T

cells have demonstrated great success in haematological cancers, the effectiveness of this approach in solid cancers is limited by issues such as the presence of a vessel barrier. The ability to direct these CAR-T cells though VM vessels, which carry a full suite of adhesion molecules and are likely enhanced in cancers at more aggressive stages where other conventional treatments have failed, may greatly improve the success rates in solid cancers.

In summary, this thesis presents novel findings on the regulation (by DSG2) and function (leukocyte recruitment) of VM in melanoma. While further research is still required to answer several critical questions, the findings of this thesis will form an important foundation for subsequent studies aimed towards better deciphering these processes and ultimately may lead to the development of more effective cancer therapies.

Appendix A. Summary of RNA Sequencing Statistics

Table A1. Summary of reads and alignment rates of RNA sequencing performed on the melanoma cell lines C32, CHL-1 and SK-Mel-28 cultured under ambient (21% O_2) and hypoxic (0.5% O_2) conditions for 3 (D3) and 7 days (D7).

Sample	Sequencing Run	Processed Reads	Reads After Trimming	Reads Mapped	Alignment Rate (%)	Merged Reads Mapped	Merged Alignment Rate (%)
C32_1_05_O2_D3	1	15,984,242	15,930,945	15,259,996	95.8	31,103,088	96.4
C32_1_05_O2_D3	2	16,388,663	16,342,716	15,843,092	96.9		
C32_1_05_O2_D7	1	16,674,136	16,603,522	15,986,553	96.3	32,742,122	96.9
C32_1_05_O2_D7	2	17,246,524	17,184,401	16,755,569	97.5		
C32_1_Ambient	1	16,266,552	16,177,811	15,572,513	96.3	31,798,638	96.8
C32_1_Ambient	2	16,734,210	16,652,431	16,226,125	97.4		
C32_2_05_O2_D3	1	17,767,177	17,707,186	17,041,015	96.2	34,945,795	96.9
C32_2_05_O2_D3	2	18,420,532	18,368,999	17,904,780	97.5		
C32_2_05_O2_D7	1	15,214,826	15,169,248	14,598,480	96.2	29,967,006	96.9
C32_2_05_O2_D7	2	15,804,280	15,766,677	15,368,526	97.5		
C32_2_Ambient	1	17,217,896	17,158,400	16,546,914	96.4	33,931,239	97.0
C32_2_Ambient	2	17,860,753	17,809,556	17,384,325	97.6		
C32_3_05_O2_D3	1	18,741,787	18,673,742	17,977,931	96.3	36,725,076	96.9
C32_3_05_O2_D3	2	19,289,910	19,231,674	18,747,145	97.5		
C32_3_05_O2_D7	1	17,689,433	17,622,039	16,975,427	96.3	34,677,706	96.9
C32_3_05_O2_D7	2	18,221,949	18,161,840	17,702,279	97.5		
C32_3_Ambient	1	21,936,991	21,852,900	21,037,076	96.3	43,209,410	96.9
C32_3_Ambient	2	22,805,826	22,734,165	22,172,334	97.5		
CHL-1_1_05_O2_D3	1	19,250,867	19,173,012	18,475,851	96.4	37,839,581	97.0
CHL-1_1_05_O2_D3	2	19,912,118	19,843,930	19,363,730	97.6		
CHL-1_1_05_O2_D7	1	15,691,279	15,623,926	15,038,378	96.3	30,851,459	96.9
CHL-1_1_05_O2_D7	2	16,284,598	16,223,320	15,813,081	97.5		
CHL-1_1_Ambient	1	18,947,933	18,879,822	18,217,829	96.5	37,273,456	97.1
CHL-1_1_Ambient	2	19,573,913	19,514,254	19,055,627	97.6		
CHL-1_2_05_O2_D3	1	19,903,354	19,828,538	19,093,715	96.3	39,172,738	96.9
CHL-1_2_05_O2_D3	2	20,647,896	20,583,985	20,079,023	97.5		
CHL-1_2_05_O2_D7	1	37,368,803	37,239,254	35,881,744	96.4	73,840,401	97.0
CHL-1_2_05_O2_D7	2	38,988,653	38,878,514	37,958,657	97.6		
CHL-1_2_Ambient	1	13,271,740	13,226,041	12,753,980	96.4	26,169,284	97.0
CHL-1_2_Ambient	2	13,775,771	13,737,680	13,415,304	97.7		
CHL-1_3_05_O2_D3	1	18,364,068	18,296,328	17,629,427	96.4	35,978,996	96.9
CHL-1_3_05_O2_D3	2	18,875,947	18,815,844	18,349,569	97.5		
CHL-1_3_05_O2_D7	1	19,435,440	19,367,612	18,706,186	96.6	38,285,459	97.2
CHL-1_3_05_O2_D7	2	20,091,894	20,032,717	19,579,273	97.7		
CHL-1_3_Ambient	1	16,237,663	16,179,711	15,580,583	96.3	32,086,027	96.9
CHL-1_3_Ambient	2	16,967,671	16,917,237	16,505,444	97.6		
SK-Mel-28_1_05_O2_D3	1	16,703,025	16,641,654	16,037,046	96.4	32,891,662	97.0
SK-Mel-28_1_05_O2_D3	2	17,321,591	17,268,765	16,854,616	97.6		
SK-Mel-28_1_05_O2_D7	1	16,379,397	16,328,062	15,709,448	96.2	32,396,067	96.9
SK-Mel-28_1_05_O2_D7	2	17,155,521	17,112,936	16,686,619	97.5		
SK-Mel-28_1_Ambient	1	19,217,507	19,154,288	18,469,840	96.4	37,880,355	97.0
SK-Mel-28_1_Ambient	2	19,934,305	19,881,006	19,410,515	97.6		
SK-Mel-28_2_05_O2_D3	1	15,182,145	15,124,892	14,578,573	96.4	29,941,850	97.0
SK-Mel-28_2_05_O2_D3	2	15,790,993	15,740,901	15,363,277	97.6		
SK-Mel-28_2_05_O2_D7	1	15,810,191	15,753,690	15,172,735	96.3	31,145,567	96.9
SK-Mel-28_2_05_O2_D7	2	16,427,664	16,378,945	15,972,832	97.5		
SK-Mel-28_2_Ambient	1	17,120,368	17,061,446	16,443,426	96.4	33,743,778	97.0
SK-Mel-28_2_Ambient	2	17,775,511	17,725,533	17,300,352	97.6		
SK-Mel-28_3_05_O2_D3	1	19,904,695	19,826,991	19,077,984	96.2	39,088,545	96.8
SK-Mel-28_3_05_O2_D3	2	20,597,812	20,530,343	20,010,561	97.5		
SK-Mel-28_3_05_O2_D7	1	14,819,167	14,770,124	14,216,322	96.3	29,332,076	96.9
SK-Mel-28_3_05_O2_D7	2	15,534,449	15,493,508	15,115,754	97.6		
SK-Mel-28_3_Ambient	1	20,357,437	20,275,208	19,538,318	96.4	39,987,331	96.9
SK-Mel-28_3_Ambient	2	21,039,808	20,967,920	20,449,013	97.5		

Appendix B. Gating Strategy for Flow Cytometric Phenotyping of Mononuclear Cells

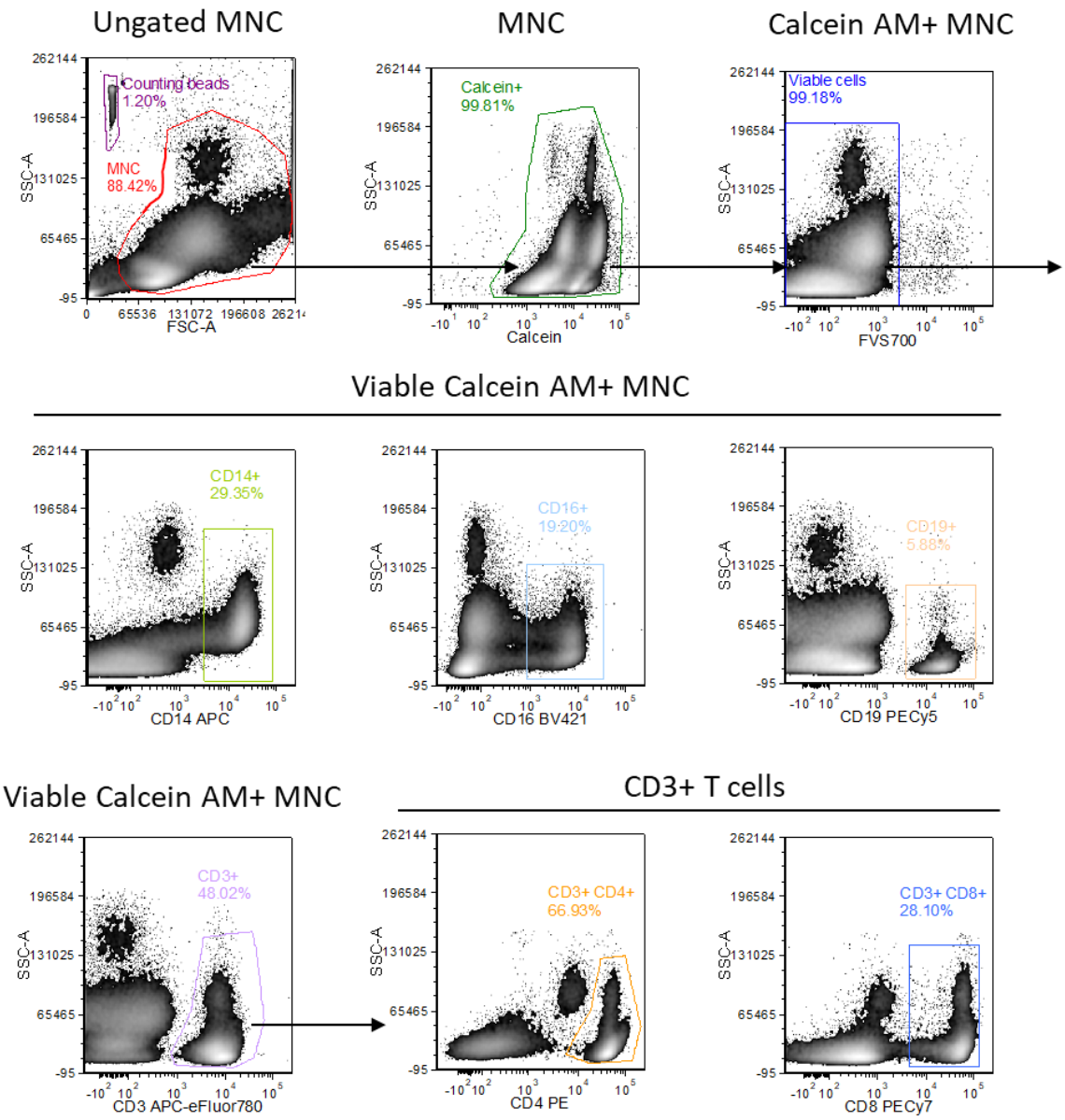

Figure B1. Gating strategy for flow cytometric phenotyping of MNC from parallel plate flow chamber and Transwell assays.

For flow cytometric results obtained from the parallel plate flow chamber assay, counting beads and MNC were first gated respectively on a FSC/SSC plot. The gated MNCs were then displayed on a calcein AM/SSC scatter plot and the calcein AM^+ MNCs were gated. The calcein AM^+ MNCs were then displayed on a FVS700/SSC scatter plot where the viable calcein AM^+ MNCs ($FVS700^-$) were gated. Within this population, the individual $CD14^+$ monocytes, $CD16^+$ NK cells, $CD19^+$ B cells, $CD3^+$ $CD4^+$ T cells and $CD3^+$ $CD8^+$ T cells were gated. The number of cells within each gate were then normalised to the number of counting beads using the following formula (number of gated cells/ (number of gated counting beads/total number of counting beads added to sample)) to obtain the absolute cell numbers for each respective population. Note that a similar gating strategy was used for phenotyping of MNC for the Transwell assays, with the only exclusion of the calcein AM^+ MNC gating step as the MNCs used for the Transwell assays had not been pre-labelled with calcein AM.

References

Ahmadzadeh, M, Felipe-Silva, A, Heemskerk, B, Powell, DJ, Wunderlich, JR, Merino, MJ & Rosenberg, SA 2008, 'FOXP3 expression accurately defines the population of intratumoral regulatory T cells that selectively accumulate in metastatic melanoma lesions', *Blood*, vol. 112, no. 13, pp. 4953-4960.

Akbani, R, Akdemir, Kadir C, Aksoy, BA, Albert, M, Ally, A, Amin, Samirkumar B, Arachchi, H, Arora, A, Auman, JT, Ayala, B, Baboud, J, Balasundaram, M, Balu, S, Barnabas, N, Bartlett, J, Bartlett, P, Bastian, Boris C, Baylin, Stephen B, Behera, M, Belyaev, D, Benz, C, Bernard, B, Beroukhim, R, Bir, N, Black, Aaron D, Bodenheimer, T, Boice, L, Boland, Genevieve M, Bono, R, Bootwalla, Moiz S, Bosenberg, M, Bowen, J, Bowlby, R, Bristow, Christopher A, Brockway-Lunardi, L, Brooks, D, Brzezinski, J, Bshara, W, Buda, E, Burns, William R, Butterfield, Yaron SN, Button, M, Calderone, T, Cappellini, Giancarlo A, Carter, C, Carter, Scott L, Cherney, L, Cherniack, Andrew D, Chevalier, A, Chin, L, Cho, J, Cho, Raymond J, Choi, Y-L, Chu, A, Chudamani, S, Cibulskis, K, Ciriello, G, Clarke, A, Coons, S, Cope, L, Crain, D, Curley, E, Danilova, L, D'Atri, S, Davidsen, T, Davies, Michael A, Delman, Keith A, Demchok, John A, Deng, Qixia A, Deribe, Yonathan L, Dhalla, N, Dhir, R, DiCara, D, Dinikin, M, Dubina, M, Ebrom, JS, Egea, S, Eley, G, Engel, J, Eschbacher, Jennifer M, Fedosenko, Konstantin V, Felau, I, Fennell, T, Ferguson, Martin L, Fisher, S, Flaherty, Keith T, Frazer, S, Frick, J, Fulidou, V, Gabriel, Stacey B, Gao, J, Gardner, J, Garraway, Levi A, Gastier-Foster, Julie M, Gaudioso, C, Gehlenborg, N, Genovese, G, Gerken, M, Gershenwald, Jeffrey E, Getz, G, Gomez-Fernandez, C, Gribbin, T, Grimsby, J, Gross, B, Guin, R, Gutschner, T, Hadjipanayis, A, Halaban, R, Hanf, B, Haussler, D, Haydu, Lauren E, Hayes, DN, Hayward, Nicholas K, Heiman, David I, Herbert, L, Herman, James G, Hersey, P, Hoadley, Katherine A, Hodis, E, Holt, Robert A, Hoon, Dave S, Hoppough, S, Hoyle, Alan P, Huang, Franklin W, Huang, M, Huang, S, Hutter, Carolyn M, Ibbs, M, Iype, L, Jacobsen, A, Jakrot, V, Janning, A, Jeck, William R, Jefferys, Stuart R, Jensen, Mark A, Jones, Corbin D, Jones, Steven JM, Ju, Z, Kakavand, H, Kang, H, Kefford, Richard F, Khuri, Fadlo R, Kim, J, Kirkwood, John M, Klode, J, Korkut, A, Korski, K, Krauthammer, M, Kucherlapati, R, Kwong, Lawrence N, Kycler, W, Ladanyi, M, Lai, Phillip H, Laird, Peter W, Lander, E, Lawrence, Michael S, Lazar, Alexander J, Łaźniak, R, Lee, D, Lee, Jeffrey E, Lee, J, Lee, K, Lee, S, Lee, W, Leporowska, E, Leraas, Kristen M, Li, Haiyan I, Lichtenberg, Tara M, Lichtenstein, L, Lin, P, Ling, S, Liu, J, Liu, O, Liu, W, Long, Georgina V, Lu, Y, Ma, S, Ma, Y, Mackiewicz, A, Mahadeshwar, Harshad S, Malke, J, Mallery, D, Manikhas, Georgy M, Mann, Graham J, Marra, Marco A, Matejka, B, Mayo, M, Mehrabi, S, Meng, S, Meyerson, M, Mieczkowski, Piotr A, Miller, John P, Miller, Martin L, Mills, Gordon B, Moiseenko, F, Moore, Richard A, Morris, S, Morrison, C, Morton, D, Moschos, S, Mose, Lisle E, Muller, Florian L, Mungall, Andrew J, Murawa, D, Murawa, P, Murray, Bradley A, Nezi, L, Ng, S, Nicholson, D, Noble, Michael S, Osunkoya, A, Owonikoko, Taofeek K, Ozenberger, Bradley A, Pagani, E, Paklina, Oxana V, Pantazi, A, Parfenov, M, Parfitt, J, Park, Peter J, Park, W-Y, Parker, Joel S, Passarelli, F, Penny, R, Perou, Charles M, Pihl, Todd D, Potapova, O, Prieto, Victor G, Protopopov, A, Quinn, Michael J, Radenbaugh, A, Rai, K, Ramalingam, Suresh S, Raman, Ayush T, Ramirez, Nilsa C, Ramirez, R, Rao, U, Rathmell, WK, Ren, X, Reynolds, Sheila M, Roach, J, Robertson, AG, Ross, Merrick I, Roszik, J, Russo, G, Saksena, G, Saller, C, Samuels, Y, Sander, C, Sander, C, Sandusky, G, Santoso, N, Saul, M, Saw, Robyn P, Schadendorf, D, Schein, Jacqueline E, Schultz, N, Schumacher, Steven E, Schwallier, C, Scolyer, Richard A, Seidman, J, Sekhar, Pedamallu C, Sekhon, Harmanjatinder S, Senbabaoglu, Y, Seth, S, Shannon, Kerwin F, Sharpe, S, Sharpless, Norman E, Shaw, Kenna RM, Shelton, C, Shelton, T, Shen, R, Sheth, M, Shi, Y, Shiau, Carolyn J, Shmulevich, I, Sica, Gabriel L, Simons, Janae V, Sinha, R, Sipahimalani, P, Sofia, Heidi J, Soloway, Matthew G, Song, X, Sougnez, C, Spillane, Andrew J, Spychała, A, Stretch, Jonathan R, Stuart, J, Suchorska, Wiktoria M, Sucker, A, Sumer, SO, Sun, Y, Synott, M, Tabak, B, Tabler, Teresa R, Tam, A, Tan, D, Tang, J, Tarnuzzer, R, Tarvin, K, Tatka, H, Taylor, Barry S, Teresiak, M, Thiessen, N, Thompson, John F, Thorne, L, Thorsson, V, Trent, Jeffrey M, Triche, Timothy J, Jr., Tsai, Kenneth Y, Tsou, P,

Van Den Berg, David J, Van Allen, Eliezer M, Veluvolu, U, Verhaak, Roeland G, Voet, D, Voronina, O, Walter, V, Walton, Jessica S, Wan, Y, Wang, Y, Wang, Z, Waring, S, Watson, Ian R, Weinhold, N, Weinstein, John N, Weisenberger, Daniel J, White, P, Wilkerson, Matthew D, Wilmott, James S, Wise, L, Wiznerowicz, M, Woodman, Scott E, Wu, C-J, Wu, C-C, Wu, J, Wu, Y, Xi, R, Xu, Andrew W, Yang, D, Yang, L, Yang, L, Zack, Travis I, Zenklusen, Jean C, Zhang, H, Zhang, J, Zhang, W, Zhao, X, Zhu, J, Zhu, K, Zimmer, L, Zmuda, E & Zou, L 'Genomic Classification of Cutaneous Melanoma', *Cell*, vol. 161, no. 7, pp. 1681-1696.

Aken, BL, Ayling, S, Barrell, D, Clarke, L, Curwen, V, Fairley, S, Fernandez Banet, J, Billis, K, Garcia Giron, C, Hourlier, T, Howe, K, Kahari, A, Kokocinski, F, Martin, FJ, Murphy, DN, Nag, R, Ruffier, M, Schuster, M, Tang, YA, Vogel, JH, White, S, Zadissa, A, Flicek, P & Searle, SM 2016, 'The Ensembl gene annotation system', *Database (Oxford)*, vol. 2016.

Allingham, MJ, van Buul, JD & Burridge, K 2007, 'ICAM-1-Mediated, Src- and Pyk2-Dependent Vascular Endothelial Cadherin Tyrosine Phosphorylation Is Required for Leukocyte Transendothelial Migration', *The Journal of Immunology*, vol. 179, no. 6, pp. 4053-4064.

Amin, A, Lawson, DH, Salama, AKS, Koon, HB, Guthrie, T, Thomas, SS, O'Day, SJ, Shaheen, MF, Zhang, B, Francis, S & Hodi, FS 2016, 'Phase II study of vemurafenib followed by ipilimumab in patients with previously untreated BRAF-mutated metastatic melanoma', *Journal for immunotherapy of cancer*, vol. 4.

Ancuta, P, Rao, R, Moses, A, Mehle, A, Shaw, SK, Luscinskas, FW & Gabuzda, D 2003, 'Fractalkine Preferentially Mediates Arrest and Migration of CD16+ Monocytes', *The Journal of experimental medicine*, vol. 197, no. 12, pp. 1701-1707.

Anders, S, Pyl, PT & Huber, W 2015, 'HTSeq—a Python framework to work with high-throughput sequencing data', *Bioinformatics*, vol. 31, no. 2, pp. 166-169.

Antony, PA, Piccirillo, CA, Akpinarli, A, Finkelstein, SE, Speiss, PJ, Surman, DR, Palmer, DC, Chan, CC, Klebanoff, CA, Overwijk, WW, Rosenberg, SA & Restifo, NP 2005, 'CD8+ T cell immunity against a tumor/self-antigen is augmented by CD4+ T helper cells and hindered by naturally occurring T regulatory cells', *Journal of Immunology*, vol. 174, no. 5, pp. 2591-2601.

Arbones, ML, Ord, DC, Ley, K, Ratech, H, Maynard-Curry, C, Otten, G, Capon, DJ & Tedder, TF 1994, 'Lymphocyte homing and leukocyte rolling and migration are impaired in L-selectin-deficient mice', *Immunity*, vol. 1, no. 4, pp. 247-260.

Arnaout, MA 1990, 'Structure and function of the leukocyte adhesion molecules CD11/CD18', *Blood*, vol. 75, no. 5, pp. 1037-1050.

Ballas, ZK, Buchta, CM, Rosean, TR, Heusel, JW & Shey, MR 2013, 'Role of NK Cell Subsets in Organ-Specific Murine Melanoma Metastasis', *PloS one*, vol. 8, no. 6, p. e65599.

Beasley, GM, McMahon, N, Sanders, G, Augustine, CK, Selim, MA, Peterson, B, Norris, R, Peters, WP, Ross, MI & Tyler, DS 2009, 'A phase 1 study of systemic ADH-1 in combination with melphalan via isolated limb infusion in patients with locally advanced in-transit malignant melanoma', *Cancer*, vol. 115, no. 20, pp. 4766-4774.

Beasley, GM, Riboh, JC, Augustine, CK, Zager, JS, Hochwald, SN, Grobmyer, SR, Peterson, B, Royal, R, Ross, MI & Tyler, DS 2011, 'Prospective multicenter phase II trial of systemic ADH-1 in combination with melphalan via isolated limb infusion in patients with advanced extremity melanoma', *Journal of Clinical Oncology*, vol. 29, no. 9, pp. 1210-1215.

Bedognetti, D, Spivey, TL, Zhao, Y, Uccellini, L, Tomei, S, Dudley, ME, Ascierto, ML, De Giorgi, V, Liu, Q, Delogu, LG, Sommariva, M, Sertoli, MR, Simon, R, Wang, E, Rosenberg, SA & Marincola, FM 2013, 'CXCR3/CCR5 pathways in metastatic melanoma patients treated with adoptive therapy and interleukin-2', *British journal of cancer*, vol. 109, no. 9, pp. 2412-2423.

Beider, K, Bitner, H, Leiba, M, Gutwein, O, Koren-Michowitz, M, Ostrovsky, O, Abraham, M, Wald, H, Galun, E & Peled, A 2014, 'Multiple myeloma cells recruit tumor-supportive macrophages through the CXCR4/CXCL12 axis and promote their polarization toward the M2 phenotype', *Oncotarget*, vol. 5, no. 22, p. 11283.

Benita, Y, Kikuchi, H, Smith, AD, Zhang, MQ, Chung, DC & Xavier, RJ 2009, 'An integrative genomics approach identifies Hypoxia Inducible Factor-1 (HIF-1)-target genes that form the core response to hypoxia', *Nucleic Acids Research*, vol. 37, no. 14, pp. 4587-4602.

Berlin, C, Bargatze, RF, Campbell, JJ, von Andrian, UH, Szabo, MC, Hasslen, SR, Nelson, RD, Berg, EL, Erlandsen, SL & Butcher, EC 1995, 'alpha 4 integrins mediate lymphocyte attachment and rolling under physiologic flow', *Cell*, vol. 80, no. 3, pp. 413-422.

Bernardini, G, Sciume, G, Bosisio, D, Morrone, S, Sozzani, S & Santoni, A 2008, 'CCL3 and CXCL12 regulate trafficking of mouse bone marrow NK cell subsets', *Blood*, vol. 111, no. 7, pp. 3626-3634.

Bevilacqua, MP, Pober, JS, Mendrick, DL, Cotran, RS & Gimbrone, MA, Jr. 1987, 'Identification of an inducible endothelial-leukocyte adhesion molecule', *Proceedings of the National Academy of Sciences of the United States of America*, vol. 84, no. 24, pp. 9238-9242.

Biswas, SK & Mantovani, A 2010, 'Macrophage plasticity and interaction with lymphocyte subsets: cancer as a paradigm', *Nature Immunology*, vol. 11, no. 10, pp. 889-896.

Bjoern, J, Juul Nitschke, N, Zeeberg Iversen, T, Schmidt, H, Fode, K & Svane, IM 2016, 'Immunological correlates of treatment and response in stage IV malignant melanoma patients treated with Ipilimumab', *Oncoimmunology*, vol. 5, no. 4, p. e1100788.

Blattner, C, Fleming, V, Weber, R, Himmelhan, B, Altevogt, P, Gebhardt, C, Schulze, TJ, Razon, H, Hawila, E, Wildbaum, G, Utikal, J, Karin, N & Umansky, V 2018, 'CCR5(+) Myeloid-Derived Suppressor Cells Are Enriched and Activated in Melanoma Lesions', *Cancer Res*, vol. 78, no. 1, pp. 157-167.

Boyman, O, Cho, JH & Sprent, J 2010, 'The role of interleukin-2 in memory CD8 cell differentiation', *Adv Exp Med Biol*, vol. 684, pp. 28-41.

Breart, B, Lemaître, F, Celli, S & Bousso, P 2008, 'Two-photon imaging of intratumoral CD8+ T cell cytotoxic activity during adoptive T cell therapy in mice', *The Journal of clinical investigation,* vol. 118, no. 4, pp. 1390-1397.

Brennan, D, Hu, Y, Joubeh, S, Choi, YW, Whitaker-Menezes, D, O'Brien, T, Uitto, J, Rodeck, U & Mahoney, MG 2007, 'Suprabasal Dsg2 expression in transgenic mouse skin confers a hyperproliferative and apoptosis-resistant phenotype to keratinocytes', *Journal of Cell Science,* vol. 120, no. Pt 5, pp. 758-771.

Brody, JR, Costantino, CL, Berger, AC, Sato, T, Lisanti, MP, Yeo, CJ, Emmons, RV & Witkiewicz, AK 2009, 'Expression of indoleamine 2,3-dioxygenase in metastatic malignant melanoma recruits regulatory T cells to avoid immune detection and affects survival', *Cell Cycle,* vol. 8, no. 12, pp. 1930-1934.

Brooke, MA, Nitoiu, D & Kelsell, DP 2012, 'Cell-cell connectivity: desmosomes and disease', *The Journal of pathology,* vol. 226, no. 2, pp. 158-171.

Buckanovich, RJ, Facciabene, A, Kim, S, Benencia, F, Sasaroli, D, Balint, K, Katsaros, D, O'Brien-Jenkins, A, Gimotty, PA & Coukos, G 2008, 'Endothelin B receptor mediates the endothelial barrier to T cell homing to tumors and disables immune therapy', *Nature medicine,* vol. 14, no. 1, pp. 28-36.

Carlos, TM 2001, 'Leukocyte recruitment at sites of tumor: dissonant orchestration', *Journal of Leukocyte Biology,* vol. 70, no. 2, pp. 171-184.

Carrasco, YR, Fleire, SJ, Cameron, T, Dustin, ML & Batista, FD 'LFA-1/ICAM-1 Interaction Lowers the Threshold of B Cell Activation by Facilitating B Cell Adhesion and Synapse Formation', *Immunity,* vol. 20, no. 5, pp. 589-599.

Cartee, TV, White, KJ, Newton-West, M & Swerlick, RA 2012, 'Hypoxia and hypoxia mimetics inhibit TNF-dependent VCAM1 induction in the 5A32 endothelial cell line via a hypoxia inducible factor dependent mechanism', *J Dermatol Sci,* vol. 65, no. 2, pp. 86-94.

Cavallaro, U, Liebner, S & Dejana, E 2006, 'Endothelial cadherins and tumor angiogenesis', *Experimental Cell Research,* vol. 312, no. 5, pp. 659-667.

Cha, E, Klinger, M, Hou, Y, Cummings, C, Ribas, A, Faham, M & Fong, L 2014, 'Improved survival with T cell clonotype stability after anti-CTLA-4 treatment in cancer patients', *Science Translational Medicine,* vol. 6, no. 238, p. 238ra270.

Chen, KJ, Lin, SZ, Zhou, L, Xie, HY, Zhou, WH, Taki-Eldin, A & Zheng, SS 2011, 'Selective recruitment of regulatory T cell through CCR6-CCL20 in hepatocellular carcinoma fosters tumor progression and predicts poor prognosis', *PloS one,* vol. 6, no. 9, p. e24671.

Chen, L 2004, 'Co-inhibitory molecules of the B7-CD28 family in the control of T-cell immunity', *Nature Reviews Immunology,* vol. 4, no. 5, pp. 336-347.

Chen, W, Jin, W, Hardegen, N, Lei, KJ, Li, L, Marinos, N, McGrady, G & Wahl, SM 2003, 'Conversion of peripheral CD4+CD25- naive T cells to CD4+CD25+ regulatory T cells by TGF-beta induction of transcription factor Foxp3', *The Journal of experimental medicine*, vol. 198, no. 12, pp. 1875-1886.

Chen, Y, McCarthy, D, Robinson, M & Smyth, GK 2014, 'edgeR: differential expression analysis of digital gene expression data User's Guide', *Available online a t: https://www. genomatix. de/online_help/help_regionminer/edgeR. pdf*.

Choi, JJ, Wang, S, Tung, Y-S, Morrison, B & Konofagou, EE 2010, 'Molecules of various pharmacologically-relevant sizes can cross the ultrasound-induced blood-brain barrier opening in vivo', *Ultrasound in medicine & biology*, vol. 36, no. 1, pp. 58-67.

Chuang, Y-H, Lian, Z-X, Tsuneyama, K, Chiang, B-L, Ansari, AA, Coppel, RL & Eric Gershwin, M 2006, 'Increased killing activity and decreased cytokine production in NK cells in patients with primary biliary cirrhosis', *Journal of Autoimmunity*, vol. 26, no. 4, pp. 232-240.

Chung, AS, Lee, J & Ferrara, N 2010, 'Targeting the tumour vasculature: insights from physiological angiogenesis', *Nature Reviews Cancer*, vol. 10, no. 7, pp. 505-514.

Clancy-Thompson, E, Perekslis, TJ, Croteau, W, Alexander, MP, Chabanet, TB, Turk, MJ, Huang, YH & Mullins, DW 2015, 'Melanoma Induces, and Adenosine Suppresses, CXCR3-Cognate Chemokine Production and T-cell Infiltration of Lungs Bearing Metastatic-like Disease', *Cancer Immunology Research*, vol. 3, no. 8, pp. 956-967.

Cockcroft, NY, Oke, O, Cunningham, F, Bishop, E, Fearon, IM, Zantl, R & Gaca, MD 2009, 'An in vitro perfusion system to examine the responses of endothelial cells to simulated flow and inflammatory stimulation', *Alternatives to Laboratory Animals*, vol. 37, no. 6, pp. 657-669.

Cooper, ZA, Juneja, VR, Sage, PT, Frederick, DT, Piris, A, Mitra, D, Lo, JA, Hodi, FS, Freeman, GJ & Bosenberg, MW 2014, 'Response to BRAF inhibition in melanoma is enhanced when combined with immune checkpoint blockade', *Cancer Immunology Research*, vol. 2, no. 7, pp. 643-654.

Corey, DM, Rinkevich, Y & Weissman, IL 2016, 'Dynamic Patterns of Clonal Evolution in Tumor Vasculature Underlie Alterations in Lymphocyte-Endothelial Recognition to Foster Tumor Immune Escape', *Cancer research*, vol. 76, no. 6, pp. 1348-1353.

Crawford, A, Macleod, M, Schumacher, T, Corlett, L & Gray, D 2006, 'Primary T cell expansion and differentiation in vivo requires antigen presentation by B cells', *Journal of Immunology*, vol. 176, no. 6, pp. 3498-3506.

Crosby, CV, Fleming, PA, Argraves, WS, Corada, M, Zanetta, L, Dejana, E & Drake, CJ 2005, 'VE-cadherin is not required for the formation of nascent blood vessels but acts to prevent their disassembly', *Blood*, vol. 105, no. 7, pp. 2771-2776.

Curran, MA, Montalvo, W, Yagita, H & Allison, JP 2010, 'PD-1 and CTLA-4 combination blockade expands infiltrating T cells and reduces regulatory T and myeloid cells within B16 melanoma tumors', *Proceedings of the National Academy of Sciences*, vol. 107, no. 9, pp. 4275-4280.

Dankort, D, Curley, DP, Cartlidge, RA, Nelson, B, Karnezis, AN, Damsky Jr, WE, You, MJ, DePinho, RA, McMahon, M & Bosenberg, M 2009, 'BrafV600E cooperates with Pten loss to induce metastatic melanoma', *Nat Genet*, vol. 41, no. 5, pp. 544-552.

Davies, H, Bignell, GR, Cox, C, Stephens, P, Edkins, S, Clegg, S, Teague, J, Woffendin, H, Garnett, MJ, Bottomley, W, Davis, N, Dicks, E, Ewing, R, Floyd, Y, Gray, K, Hall, S, Hawes, R, Hughes, J, Kosmidou, V, Menzies, A, Mould, C, Parker, A, Stevens, C, Watt, S, Hooper, S, Wilson, R, Jayatilake, H, Gusterson, BA, Cooper, C, Shipley, J, Hargrave, D, Pritchard-Jones, K, Maitland, N, Chenevix-Trench, G, Riggins, GJ, Bigner, DD, Palmieri, G, Cossu, A, Flanagan, A, Nicholson, A, Ho, JWC, Leung, SY, Yuen, ST, Weber, BL, Seigler, HF, Darrow, TL, Paterson, H, Marais, R, Marshall, CJ, Wooster, R, Stratton, MR & Futreal, PA 2002, 'Mutations of the BRAF gene in human cancer', *Nature*, vol. 417, no. 6892, pp. 949-954.

Davis, ME, Zuckerman, JE, Choi, CHJ, Seligson, D, Tolcher, A, Alabi, CA, Yen, Y, Heidel, JD & Ribas, A 2010, 'Evidence of RNAi in humans from systemically administered siRNA via targeted nanoparticles', *Nature*, vol. 464, no. 7291, pp. 1067-1070.

de Coana, YP, Wolodarski, M, Poschke, I, Yoshimoto, Y, Yang, Y, Nystrom, M, Edback, U, Brage, SE, Lundqvist, A, Masucci, GV, Hansson, J & Kiessling, R 2017, 'Ipilimumab treatment decreases monocytic MDSCs and increases CD8 effector memory T cells in long-term survivors with advanced melanoma', *Oncotarget*, vol. 8, no. 13, pp. 21539-21553.

dela Paz, NG & D'Amore, PA 2009, 'Arterial versus venous endothelial cells', *Cell Tissue Res*, vol. 335, no. 1, pp. 5-16.

Delva, E, Tucker, DK & Kowalczyk, AP 2009, 'The Desmosome', *Cold Spring Harbor Perspectives in Biology*, vol. 1, no. 2, p. a002543.

Demou, ZN & Hendrix, MJC 2008, 'Microgenomics Profile the Endogenous Angiogenic Phenotype in Subpopulations of Aggressive Melanoma', *Journal of cellular biochemistry*, vol. 105, no. 2, pp. 562-573.

Denton, KJ, Stretch, JR, Gatter, KC & Harris, AL 1992, 'A study of adhesion molecules as markers of progression in malignant melanoma', *The Journal of pathology*, vol. 167, no. 2, pp. 187-191.

Detmers, PA, Lo, SK, Olsen-Egbert, E, Walz, A, Baggiolini, M & Cohn, ZA 1990, 'Neutrophil-activating protein 1/interleukin 8 stimulates the binding activity of the leukocyte adhesion receptor CD11b/CD18 on human neutrophils', *The Journal of experimental medicine*, vol. 171, no. 4, pp. 1155-1162.

Di Giacomo, AM, Ascierto, PA, Pilla, L, Santinami, M, Ferrucci, PF, Giannarelli, D, Marasco, A, Rivoltini, L, Simeone, E, Nicoletti, SVL, Fonsatti, E, Annesi, D, Queirolo, P, Testori, A, Ridolfi, R, Parmiani, G & Maio, M 2012, 'Ipilimumab and fotemustine in patients with advanced melanoma

(NIBIT-M1): an open-label, single-arm phase 2 trial', *The Lancet Oncology,* vol. 13, no. 9, pp. 879-886.

Dietrich, A, Tanczos, E, Vanscheidt, W, Schopf, E & Simon, JC 1997, 'High CD44 surface expression on primary tumours of malignant melanoma correlates with increased metastatic risk and reduced survival', *European Journal of Cancer,* vol. 33, no. 6, pp. 926-930.

DiLillo, DJ, Yanaba, K & Tedder, TF 2010, 'B Cells Are Required for Optimal CD4(+) and CD8(+) T Cell Tumor Immunity: Therapeutic B Cell Depletion Enhances B16 Melanoma Growth in Mice', *Journal of Immunology,* vol. 184, no. 7, pp. 4006-4016.

Dirkx, AE, Oude Egbrink, MG, Kuijpers, MJ, van der Niet, ST, Heijnen, VV, Bouma-ter Steege, JC, Wagstaff, J & Griffioen, AW 2003, 'Tumor angiogenesis modulates leukocyte-vessel wall interactions in vivo by reducing endothelial adhesion molecule expression', *Cancer research,* vol. 63, no. 9, pp. 2322-2329.

Dirkx, AEM, oude Egbrink, MGA, Castermans, K, van der Schaft, DWJ, Thijssen, VLJL, Dings, RPM, Kwee, L, Mayo, KH, Wagstaff, J, ter Steege, JCAB- & Griffioen, AW 2006, 'Anti-angiogenesis therapy can overcome endothelial cell anergy and promote leukocyte-endothelium interactions and infiltration in tumors', *Faseb Journal,* vol. 20, no. 6, pp. 621-630.

Downey, GP, Doherty, DE, Schwab, B, 3rd, Elson, EL, Henson, PM & Worthen, GS 1990, 'Retention of leukocytes in capillaries: role of cell size and deformability', *Journal of Applied Physiology,* vol. 69, no. 5, pp. 1767-1778.

Dunleavey, JM, Xiao, L, Thompson, J, Kim, MM, Shields, JM, Shelton, SE, Irvin, DM, Brings, VE, Ollila, DW, Brekken, RA, Dayton, PA, Melero-Martin, JM & Dudley, AC 2014, 'Vascular channels formed by subpopulations of PECAM1+ melanoma cells', *Nature communications,* vol. 5, p. 5200.

Durig, J, Schmucker, U & Duhrsen, U 2001, 'Differential expression of chemokine receptors in B cell malignancies', *Leukemia,* vol. 15, no. 5, pp. 752-756.

Easton, E, Schiphorst, W, van Drunen, E, van der Schoot, C & van den Eijnden, D 1993, 'Human myeloid alpha 3-fucosyltransferase is involved in the expression of the sialyl-Lewis(x) determinant, a ligand for E- and P-selectin', *Blood,* vol. 81, no. 11, pp. 2978-2986.

Ebert, LM, Tan, LY, Johan, MZ, Min, KK, Cockshell, MP, Parham, KA, Betterman, KL, Szeto, P, Boyle, S, Silva, L, Peng, A, Zhang, Y, Ruszkiewicz, A, Zannettino, AC, Gronthos, S, Koblar, S, Harvey, NL, Lopez, AF, Shackleton, M & Bonder, CS 2016, 'A non-canonical role for desmoglein-2 in endothelial cells: implications for neoangiogenesis', *Angiogenesis,* vol. 19, no. 4, pp. 463-486.

Ebnet, K, Kaldjian, EP, Anderson, AO & Shaw, S 1996, 'Orchestrated information transfer underlying leukocyte endothelial interactions', *Annual review of immunology,* vol. 14, pp. 155-177.

Edmondson, R, Broglie, JJ, Adcock, AF & Yang, L 2014, 'Three-Dimensional Cell Culture Systems and Their Applications in Drug Discovery and Cell-Based Biosensors', *Assay and Drug Development Technologies,* vol. 12, no. 4, pp. 207-218.

Erdag, G, Schaefer, JT, Smolkin, ME, Deacon, DH, Shea, SM, Dengel, LT, Patterson, JW & Slingluff, CL, Jr. 2012, 'Immunotype and immunohistologic characteristics of tumor-infiltrating immune cells are associated with clinical outcome in metastatic melanoma', *Cancer research*, vol. 72, no. 5, pp. 1070-1080.

Eshkind, L, Tian, Q, Schmidt, A, Franke, WW, Windoffer, R & Leube, RE 2002, 'Loss of desmoglein 2 suggests essential functions for early embryonic development and proliferation of embryonal stem cells', *Eur J Cell Biol*, vol. 81, no. 11, pp. 592-598.

Ferrari de Andrade, L, Ngiow, SF, Stannard, K, Rusakiewicz, S, Kalimutho, M, Khanna, KK, Tey, SK, Takeda, K, Zitvogel, L, Martinet, L & Smyth, MJ 2014, 'Natural killer cells are essential for the ability of BRAF inhibitors to control BRAFV600E-mutant metastatic melanoma', *Cancer research*, vol. 74, no. 24, pp. 7298-7308.

Fisher, DT, Muhitch, JB, Kim, M, Doyen, KC, Bogner, PN, Evans, SS & Skitzki, JJ 2016, 'Intraoperative intravital microscopy permits the study of human tumour vessels', *Nature communications*, vol. 7.

Francescone Iii, RA, Faibish, M & Shao, R 2011, 'A Matrigel-Based Tube Formation Assay to Assess the Vasculogenic Activity of Tumor Cells', *Journal of Visualized Experiments : JoVE*, no. 55, p. 3040.

Francescone, R, Scully, S, Bentley, B, Yan, W, Taylor, SL, Oh, D, Moral, L & Shao, R 2012, 'Glioblastoma-derived tumor cells induce vasculogenic mimicry through Flk-1 protein activation', *Journal of Biological Chemistry*, vol. 287, no. 29, pp. 24821-24831.

Frankenberger, M, Hofer, TPJ, Marei, A, Dayyani, F, Schewe, S, Strasser, C, Aldraihim, A, Stanzel, F, Lang, R, Hoffmann, R, Costa, OPd, Buch, T & Ziegler-Heitbrock, L 2012, 'Transcript profiling of CD16-positive monocytes reveals a unique molecular fingerprint', *European journal of immunology*, vol. 42, no. 4, pp. 957-974.

Fregni, G, Messaoudene, M, Fourmentraux-Neves, E, Mazouz-Dorval, S, Chanal, J, Maubec, E, Marinho, E, Scheer-Senyarich, I, Cremer, I, Avril, MF & Caignard, A 2013, 'Phenotypic and functional characteristics of blood natural killer cells from melanoma patients at different clinical stages', *PloS one*, vol. 8, no. 10, p. e76928.

Fridlender, ZG, Sun, J, Kim, S, Kapoor, V, Cheng, G, Ling, L, Worthen, GS & Albelda, SM 2009, 'Polarization of tumor-associated neutrophil phenotype by TGF-β:"N1" versus "N2" TAN', *Cancer cell*, vol. 16, no. 3, pp. 183-194.

Fridman, WH, Pagès, F, Sautès-Fridman, C & Galon, J 2012, 'The immune contexture in human tumours: impact on clinical outcome', *Nature Reviews Cancer*, vol. 12, no. 4, pp. 298-306.

Ganss, R, Ryschich, E, Klar, E, Arnold, B & Hämmerling, GJ 2002, 'Combination of T-cell therapy and trigger of inflammation induces remodeling of the vasculature and tumor eradication', *Cancer research*, vol. 62, no. 5, pp. 1462-1470.

Garg, K, Maurer, M, Griss, J, Bruggen, MC, Wolf, IH, Wagner, C, Willi, N, Mertz, KD & Wagner, SN 2016, 'Tumor-associated B cells in cutaneous primary melanoma and improved clinical outcome', *Human pathology*, vol. 54, pp. 157-164.

Gargett, T, Yu, W, Dotti, G, Yvon, ES, Christo, SN, Hayball, JD, Lewis, ID, Brenner, MK & Brown, MP 2016, 'GD2-specific CAR T Cells Undergo Potent Activation and Deletion Following Antigen Encounter but can be Protected From Activation-induced Cell Death by PD-1 Blockade', *Molecular Therapy*, vol. 24, no. 6, pp. 1135-1149.

Garraway, LA, Widlund, HR, Rubin, MA, Getz, G, Berger, AJ, Ramaswamy, S, Beroukhim, R, Milner, DA, Granter, SR, Du, J, Lee, C, Wagner, SN, Li, C, Golub, TR, Rimm, DL, Meyerson, ML, Fisher, DE & Sellers, WR 2005, 'Integrative genomic analyses identify MITF as a lineage survival oncogene amplified in malignant melanoma', *Nature*, vol. 436, no. 7047, pp. 117-122.

Gavard, J & Gutkind, JS 2006, 'VEGF controls endothelial-cell permeability by promoting the beta-arrestin-dependent endocytosis of VE-cadherin', *Nat Cell Biol*, vol. 8, no. 11, pp. 1223-1234.

Gazzaniga, S, Bravo, AI, Guglielmotti, A, van Rooijen, N, Maschi, F, Vecchi, A, Mantovani, A, Mordoh, J & Wainstok, R 2007, 'Targeting tumor-associated macrophages and inhibition of MCP-1 reduce angiogenesis and tumor growth in a human melanoma xenograft', *Journal of Investigative Dermatology*, vol. 127, no. 8, pp. 2031-2041.

'Genomic Classification of Cutaneous Melanoma' 2015, *Cell*, vol. 161, no. 7, pp. 1681-1696.

Gerszten, RE, Garcia-Zepeda, EA, Lim, Y-C & Yoshida, M 1999, 'MCP-1 and IL-8 trigger firm adhesion of monocytes to vascular endothelium under flow conditions', *Nature*, vol. 398, no. 6729, p. 718.

Ghosn, EEB, Yang, Y, Tung, J, Herzenberg, LA & Herzenberg, LA 2008, 'CD11b expression distinguishes sequential stages of peritoneal B-1 development', *Proceedings of the National Academy of Sciences*, vol. 105, no. 13, pp. 5195-5200.

Giacomo, AMD, Annesi, D, Ascierto, PA, Calabrò, L, Chiarion-Sileni, V, Danielli, R, Vecchio, MD, Ferraresi, V, Ferrucci, PF, Fonsatti, E, Guida, M, Giannarelli, D, Guidoboni, M, Mandalà, M, Quaglino, P, Queirolo, P, Maccalli, C, Parmiani, G & Maio, M 2015, 'A randomized, phase III study of fotemustine versus the combination of fotemustine and ipilimumab or the combination of ipilimumab and nivolumab in patients with metastatic melanoma with brain metastasis: the NIBIT-M2 trial', *Journal of Clinical Oncology*, vol. 33, no. 15_suppl, pp. TPS9090-TPS9090.

Gimbrone, MA, Leapman, SB, Cotran, RS & Folkman, J 1972, 'TUMOR DORMANCY IN VIVO BY PREVENTION OF NEOVASCULARIZATION', *The Journal of experimental medicine*, vol. 136, no. 2, pp. 261-276.

Giusti, B, Margheri, F, Rossi, L, Lapini, I, Magi, A, Serratì, S, Chilla, A, Laurenzana, A, Magnelli, L & Calorini, L 2013, 'Desmoglein-2-integrin Beta-8 interaction regulates actin assembly in endothelial cells: deregulation in systemic sclerosis', *PloS one*, vol. 8, no. 7, p. e68117.

Goel, S, Duda, DG, Xu, L, Munn, LL, Boucher, Y, Fukumura, D & Jain, RK 2011, 'Normalization of the Vasculature for Treatment of Cancer and Other Diseases', *Physiological Reviews*, vol. 91, no. 3, pp. 1071-1121.

González-Martín, A, Gómez, L, Lustgarten, J, Mira, E & Mañes, S 2011, 'Maximal T Cell–Mediated Antitumor Responses Rely upon CCR5 Expression in Both CD4+ and CD8+ T Cells', *Cancer research*, vol. 71, no. 16, pp. 5455-5466.

Gotsch, U, Borges, E, Bosse, R, Boggemeyer, E, Simon, M, Mossmann, H & Vestweber, D 1997, 'VE-cadherin antibody accelerates neutrophil recruitment in vivo', *Journal of Cell Science*, vol. 110 (Pt 5), pp. 583-588.

Griffioen, AW, Damen, CA, Martinotti, S, Blijham, GH & Groenewegen, G 1996, 'Endothelial intercellular adhesion molecule-1 expression is suppressed in human malignancies: the role of angiogenic factors', *Cancer research*, vol. 56, no. 5, pp. 1111-1117.

Griffioen, AW, Coenen, MJH, Damen, CA, Hellwig, SMM, H.J. van Weering, D, Vooys, W, Blijham, GH & Groenewegen, G 1997, 'CD44 Is Involved in Tumor Angiogenesis; an Activation Antigen on Human Endothelial Cells', *Blood*, vol. 90, no. 3, pp. 1150-1159.

Guldberg, P, thor Straten, P, Birck, A, Ahrenkiel, V, Kirkin, AF & Zeuthen, J 1997, 'Disruption of the MMAC1/PTEN Gene by Deletion or Mutation Is a Frequent Event in Malignant Melanoma', *Cancer research*, vol. 57, no. 17, pp. 3660-3663.

Hara-Chikuma, M, Chikuma, S, Sugiyama, Y, Kabashima, K, Verkman, AS, Inoue, S & Miyachi, Y 2012, 'Chemokine-dependent T cell migration requires aquaporin-3–mediated hydrogen peroxide uptake', *The Journal of experimental medicine*, vol. 209, no. 10, pp. 1743-1752.

Haraldsen, G, Kvale, D, Lien, B, Farstad, IN & Brandtzaeg, P 1996, 'Cytokine-regulated expression of E-selectin, intercellular adhesion molecule-1 (ICAM-1), and vascular cell adhesion molecule-1 (VCAM-1) in human microvascular endothelial cells', *The Journal of Immunology*, vol. 156, no. 7, pp. 2558-2565.

Hardy, KM, Kirschmann, DA, Seftor, EA, Margaryan, NV, Postovit, LM, Strizzi, L & Hendrix, MJ 2010, 'Regulation of the embryonic morphogen Nodal by Notch4 facilitates manifestation of the aggressive melanoma phenotype', *Cancer research*, vol. 70, no. 24, pp. 10340-10350.

Harlin, H, Meng, Y, Peterson, AC, Zha, Y, Tretiakova, M, Slingluff, C, McKee, M & Gajewski, TF 2009, 'Chemokine expression in melanoma metastases associated with CD8+ T-cell recruitment', *Cancer research*, vol. 69, no. 7, pp. 3077-3085.

Harlin, H, Meng, Y, Peterson, AC, Zha, Y, Tretiakova, M, Slingluff, C, McKee, M & Gajewski, TF 2009, 'Chemokine expression in melanoma metastases associated with CD8+ T-cell recruitment', *Cancer research*, vol. 69, no. 7, pp. 3077-3085.

Hattori, R, Hamilton, KK, Fugate, RD, McEver, RP & Sims, PJ 1989, 'Stimulated secretion of endothelial von Willebrand factor is accompanied by rapid redistribution to the cell surface of the

intracellular granule membrane protein GMP-140', *The Journal of Biological Chemistry*, vol. 264, no. 14, pp. 7768-7771.

Headley, MB, Bins, A, Nip, A, Roberts, EW, Looney, MR, Gerard, A & Krummel, MF 2016, 'Visualization of immediate immune responses to pioneer metastatic cells in the lung', *Nature*, vol. 531, no. 7595, pp. 513-517.

Helfrich, I & Schadendorf, D 2011, 'Blood vessel maturation, vascular phenotype and angiogenic potential in malignant melanoma: One step forward for overcoming anti-angiogenic drug resistance?', *Molecular Oncology*, vol. 5, no. 2, pp. 137-149.

Hellebrekers, DM, Castermans, K, Vire, E, Dings, RP, Hoebers, NT, Mayo, KH, Oude Egbrink, MG, Molema, G, Fuks, F, van Engeland, M & Griffioen, AW 2006, 'Epigenetic regulation of tumor endothelial cell anergy: silencing of intercellular adhesion molecule-1 by histone modifications', *Cancer research*, vol. 66, no. 22, pp. 10770-10777.

Hellström, M, Phng, L-K, Hofmann, JJ, Wallgard, E, Coultas, L, Lindblom, P, Alva, J, Nilsson, A-K, Karlsson, L & Gaiano, N 2007, 'Dll4 signalling through Notch1 regulates formation of tip cells during angiogenesis', *Nature*, vol. 445, no. 7129, pp. 776-780.

Hendrix, MJ, Seftor, EA, Meltzer, PS, Gardner, LM, Hess, AR, Kirschmann, DA, Schatteman, GC & Seftor, RE 2001, 'Expression and functional significance of VE-cadherin in aggressive human melanoma cells: role in vasculogenic mimicry', *Proceedings of the National Academy of Sciences of the United States of America*, vol. 98, no. 14, pp. 8018-8023.

Hendrix, MJ, Seftor, RE, Seftor, EA, Gruman, LM, Lee, LM, Nickoloff, BJ, Miele, L, Sheriff, DD & Schatteman, GC 2002, 'Transendothelial function of human metastatic melanoma cells: role of the microenvironment in cell-fate determination', *Cancer research*, vol. 62, no. 3, pp. 665-668.

Hendrix, MJ, Seftor, EA, Hess, AR & Seftor, RE 2003, 'Vasculogenic mimicry and tumour-cell plasticity: lessons from melanoma', *Nature Reviews Cancer*, vol. 3, no. 6, pp. 411-421.

Hendrix, MJC, Seftor, EA, Seftor, REB, Chao, J-T, Chien, D-S & Chu, Y-W 2016, 'Tumor cell vascular mimicry: Novel targeting opportunity in melanoma', *Pharmacol Ther*, vol. 159, pp. 83-92.

Hess, AR, Seftor, EA, Seftor, RE & Hendrix, MJ 2003, 'Phosphoinositide 3-kinase regulates membrane Type 1-matrix metalloproteinase (MMP) and MMP-2 activity during melanoma cell vasculogenic mimicry', *Cancer research*, vol. 63, no. 16, pp. 4757-4762.

Hess, AR, Seftor, EA, Gruman, LM, Kinch, MS, Seftor, RE & Hendrix, MJ 2006, 'VE-cadherin regulates EphA2 in aggressive melanoma cells through a novel signaling pathway: implications for vasculogenic mimicry', *Cancer Biol Ther*, vol. 5, no. 2, pp. 228-233.

Hillen, F, Baeten, CI, van de Winkel, A, Creytens, D, van der Schaft, DW, Winnepenninckx, V & Griffioen, AW 2008, 'Leukocyte infiltration and tumor cell plasticity are parameters of aggressiveness in primary cutaneous melanoma', *Cancer Immunology, Immunotherapy*, vol. 57, no. 1, pp. 97-106.

Hillen, F, Kaijzel, EL, Castermans, K, oude Egbrink, MG, Lowik, CW & Griffioen, AW 2008, 'A transgenic Tie2-GFP athymic mouse model; a tool for vascular biology in xenograft tumors', *Biochemical and biophysical research communications*, vol. 368, no. 2, pp. 364-367.

Hino, R, Kabashima, K, Kato, Y, Yagi, H, Nakamura, M, Honjo, T, Okazaki, T & Tokura, Y 2010, 'Tumor cell expression of programmed cell death-1 ligand 1 is a prognostic factor for malignant melanoma', *Cancer*, vol. 116, no. 7, pp. 1757-1766.

Hipp, S, Walch, A, Schuster, T, Losko, S, Laux, H, Bolton, T, Höfler, H & Becker, K-F 2009, 'Activation of epidermal growth factor receptor results in Snail protein but not mRNA overexpression in endometrial cancer', *Journal of Cellular and Molecular Medicine*, vol. 13, no. 9b, pp. 3858-3867.

Hirota, K, Yoshitomi, H, Hashimoto, M, Maeda, S, Teradaira, S, Sugimoto, N, Yamaguchi, T, Nomura, T, Ito, H & Nakamura, T 2007, 'Preferential recruitment of CCR6-expressing Th17 cells to inflamed joints via CCL20 in rheumatoid arthritis and its animal model', *Journal of Experimental Medicine*, vol. 204, no. 12, pp. 2803-2812.

Hodis, E, Watson, IR, Kryukov, GV, Arold, ST, Imielinski, M, Theurillat, JP, Nickerson, E, Auclair, D, Li, L, Place, C, Dicara, D, Ramos, AH, Lawrence, MS, Cibulskis, K, Sivachenko, A, Voet, D, Saksena, G, Stransky, N, Onofrio, RC, Winckler, W, Ardlie, K, Wagle, N, Wargo, J, Chong, K, Morton, DL, Stemke-Hale, K, Chen, G, Noble, M, Meyerson, M, Ladbury, JE, Davies, MA, Gershenwald, JE, Wagner, SN, Hoon, DS, Schadendorf, D, Lander, ES, Gabriel, SB, Getz, G, Garraway, LA & Chin, L 2012, 'A landscape of driver mutations in melanoma', *Cell*, vol. 150, no. 2, pp. 251-263.

Hoeflich, KP, Merchant, M, Orr, C, Chan, J, Den Otter, D, Berry, L, Kasman, I, Koeppen, H, Rice, K, Yang, N-Y, Engst, S, Johnston, S, Friedman, LS & Belvin, M 2012, 'Intermittent Administration of MEK Inhibitor GDC-0973 plus PI3K Inhibitor GDC-0941 Triggers Robust Apoptosis and Tumor Growth Inhibition', *Cancer research*, vol. 72, no. 1, pp. 210-219.

Hong, M, Puaux, A-L, Huang, C, Loumagne, L, Tow, C, Mackay, C, Kato, M, Prévost-Blondel, A, Avril, M-F, Nardin, A & Abastado, J-P 2011, 'Chemotherapy Induces Intratumoral Expression of Chemokines in Cutaneous Melanoma, Favoring T-cell Infiltration and Tumor Control', *Cancer research*, vol. 71, no. 22, pp. 6997-7009.

Hu, C-J, Wang, L-Y, Chodosh, LA, Keith, B & Simon, MC 2003, 'Differential Roles of Hypoxia-Inducible Factor 1α (HIF-1α) and HIF-2α in Hypoxic Gene Regulation', *Molecular and Cellular Biology*, vol. 23, no. 24, pp. 9361-9374.

Huang, B, Pan, P-Y, Li, Q, Sato, AI, Levy, DE, Bromberg, J, Divino, CM & Chen, S-H 2006, 'Gr-1⁺CD115⁺ Immature Myeloid Suppressor Cells Mediate the Development of Tumor-Induced T Regulatory Cells and T-Cell Anergy in Tumor-Bearing Host', *Cancer research*, vol. 66, no. 2, pp. 1123-1131.

Huang, H, Langenkamp, E, Georganaki, M, Loskog, A, Fuchs, PF, Dieterich, LC, Kreuger, J & Dimberg, A 2015, 'VEGF suppresses T-lymphocyte infiltration in the tumor microenvironment through inhibition of NF-κB-induced endothelial activation', *Faseb Journal*, vol. 29, no. 1, pp. 227-238.

Huang, Y, Yuan, J, Righi, E, Kamoun, WS, Ancukiewicz, M, Nezivar, J, Santosuosso, M, Martin, JD, Martin, MR, Vianello, F, Leblanc, P, Munn, LL, Huang, P, Duda, DG, Fukumura, D, Jain, RK & Poznansky, MC 2012, 'Vascular normalizing doses of antiangiogenic treatment reprogram the immunosuppressive tumor microenvironment and enhance immunotherapy', *Proceedings of the National Academy of Sciences*, vol. 109, no. 43, pp. 17561-17566.

Iannone, R, Miele, L, Maiolino, P, Pinto, A & Morello, S 2014, 'Adenosine limits the therapeutic effectiveness of anti-CTLA4 mAb in a mouse melanoma model', *Am J Cancer Res*, vol. 4, no. 2, pp. 172-181.

Ikeda, K, Utoguchi, N, Makimoto, H, Mizuguchi, H, Nakagawa, S & Mayumi, T 1999, 'Different reactions of aortic and venular endothelial cell monolayers to histamine on macromolecular permeability: role of cAMP, cytosolic Ca2+ and F-actin', *Inflammation*, vol. 23, no. 1, pp. 87-97.

Jablonska, J, Wu, CF, Andzinski, L, Leschner, S & Weiss, S 2014, 'CXCR2-mediated tumor-associated neutrophil recruitment is regulated by IFN-β', *International Journal of Cancer*, vol. 134, no. 6, pp. 1346-1358.

Jackson, AL & Linsley, PS 2010, 'Recognizing and avoiding siRNA off-target effects for target identification and therapeutic application', *Nature Reviews Drug Discovery*, vol. 9, no. 1, pp. 57-67.

Jackson, DE, Gully, LM, Henshall, TL, Mardell, CE & Macardle, PJ 2000, 'Platelet endothelial cell adhesion molecule-1 (PECAM-1/CD31) is associated with a naive B-cell phenotype in human tonsils', *Tissue Antigens*, vol. 56, no. 2, pp. 105-116.

Jain, RK 1988, 'Determinants of tumor blood flow: a review', *Cancer research*, vol. 48, no. 10, pp. 2641-2658.

Jakob, JA, Bassett, RL, Jr., Ng, CS, Curry, JL, Joseph, RW, Alvarado, GC, Rohlfs, ML, Richard, J, Gershenwald, JE, Kim, KB, Lazar, AJ, Hwu, P & Davies, MA 2012, 'NRAS mutation status is an independent prognostic factor in metastatic melanoma', *Cancer*, vol. 118, no. 16, pp. 4014-4023.

Jensen, MM, Jørgensen, JT, Binderup, T & Kjær, A 2008, 'Tumor volume in subcutaneous mouse xenografts measured by microCT is more accurate and reproducible than determined by (18)F-FDG-microPET or external caliper', *BMC Medical Imaging*, vol. 8, pp. 16-16.

Jensen, TO, Schmidt, H, Møller, HJ, Donskov, F, Høyer, M, Sjoegren, P, Christensen, IJ & Steiniche, T 2012, 'Intratumoral neutrophils and plasmacytoid dendritic cells indicate poor prognosis and are associated with pSTAT3 expression in AJCC stage I/II melanoma', *Cancer*, vol. 118, no. 9, pp. 2476-2485.

Ji, R-R, Chasalow, SD, Wang, L, Hamid, O, Schmidt, H, Cogswell, J, Alaparthy, S, Berman, D, Jure-Kunkel, M, Siemers, NO, Jackson, JR & Shahabi, V 2012, 'An immune-active tumor microenvironment favors clinical response to ipilimumab', *Cancer Immunology, Immunotherapy*, vol. 61, no. 7, pp. 1019-1031.

Jordan, KR, Amaria, RN, Ramirez, O, Callihan, EB, Gao, D, Borakove, M, Manthey, E, Borges, VF & McCarter, MD 2013, 'Myeloid-derived suppressor cells are associated with disease progression and decreased overall survival in advanced-stage melanoma patients', *Cancer Immunology, Immunotherapy*, vol. 62, no. 11, pp. 1711-1722.

Kamekura, R, Kolegraff, K, Nava, P, Hilgarth, R, Feng, M, Parkos, C & Nusrat, A 2014, 'Loss of the desmosomal cadherin desmoglein-2 suppresses colon cancer cell proliferation through EGFR signaling', *Oncogene*, vol. 33, no. 36, pp. 4531-4536.

Karakurum, M, Shreeniwas, R, Chen, J, Pinsky, D, Yan, SD, Anderson, M, Sunouchi, K, Major, J, Hamilton, T, Kuwabara, K & et al. 1994, 'Hypoxic induction of interleukin-8 gene expression in human endothelial cells', *The Journal of clinical investigation*, vol. 93, no. 4, pp. 1564-1570.

Kashani-Sabet, M, Sagebiel, RW, Ferreira, CMM, Nosrati, M & III, JRM 2002, 'Tumor Vascularity in the Prognostic Assessment of Primary Cutaneous Melanoma', *Journal of Clinical Oncology*, vol. 20, no. 7, pp. 1826-1831.

Keiper, T, Al-Fakhri, N, Chavakis, E, Athanasopoulos, AN, Isermann, B, Herzog, S, Saffrich, R, Hersemeyer, K, Bohle, RM, Haendeler, J, Preissner, KT, Santoso, S & Chavakis, T 2005, 'The role of junctional adhesion molecule-C (JAM-C) in oxidized LDL-mediated leukocyte recruitment', *Faseb Journal*, vol. 19, no. 14, pp. 2078-2080.

Kim, CH, Kunkel, EJ, Boisvert, J, Johnston, B, Campbell, JJ, Genovese, MC, Greenberg, HB & Butcher, EC 2001, 'Bonzo/CXCR6 expression defines type 1-polarized T-cell subsets with extralymphoid tissue homing potential', *The Journal of clinical investigation*, vol. 107, no. 5, pp. 595-601.

Kim, D, Pertea, G, Trapnell, C, Pimentel, H, Kelley, R & Salzberg, SL 2013, 'TopHat2: accurate alignment of transcriptomes in the presence of insertions, deletions and gene fusions', *Genome Biology*, vol. 14, no. 4, p. R36.

Kirveskari, J, Bono, P, Granfors, K, Leirisalo-Repo, M, Jalkanen, S & Salmi, M 2000, 'Expression of α4-integrins on human neutrophils', *Journal of Leukocyte Biology*, vol. 68, no. 2, pp. 243-250.

Klarquist, J, Tobin, K, Farhangi Oskuei, P, Henning, SW, Fernandez, MF, Dellacecca, ER, Navarro, FC, Eby, JM, Chatterjee, S, Mehrotra, S, Clark, JI & Le Poole, IC 2016, 'Ccl22 Diverts T Regulatory Cells and Controls the Growth of Melanoma', *Cancer research*, vol. 76, no. 21, pp. 6230-6240.

Klessner, JL, Desai, BV, Amargo, EV, Getsios, S & Green, KJ 2009, 'EGFR and ADAMs cooperate to regulate shedding and endocytic trafficking of the desmosomal cadherin desmoglein 2', *Molecular Biology of the Cell*, vol. 20, no. 1, pp. 328-337.

Klug, F, Prakash, H, Huber, Peter E, Seibel, T, Bender, N, Halama, N, Pfirschke, C, Voss, Ralf H, Timke, C, Umansky, L, Klapproth, K, Schäkel, K, Garbi, N, Jäger, D, Weitz, J, Schmitz-Winnenthal, H, Hämmerling, Günter J & Beckhove, P 2013, 'Low-Dose Irradiation Programs Macrophage Differentiation to an iNOS+/M1 Phenotype that Orchestrates Effective T Cell Immunotherapy', *Cancer cell*, vol. 24, no. 5, pp. 589-602.

Kobayashi, T, Hamaguchi, Y, Hasegawa, M, Fujimoto, M, Takehara, K & Matsushita, T 2014, 'B cells promote tumor immunity against B16F10 melanoma', *Am J Pathol*, vol. 184, no. 11, pp. 3120-3129.

Kobayashi, Y, Tateno, H, Ogawa, H, Yamamoto, K & Hirabayashi, J 2014, 'Comprehensive List of Lectins: Origins, Natures, and Carbohydrate Specificities', in J Hirabayashi (ed), *Lectins: Methods and Protocols*, Springer New York, New York, NY, pp. 555-577.

Konerding, MA, Steinberg, F, van Ackern, C, Budach, V & Streffer, C 1992, 'Vascular patterns of tumors: scanning and transmission electron microscopic studies on human xenografts', *Strahlentherapie und Onkologie*, vol. 168, no. 8, pp. 444-452.

Kremmidiotis, G & Zola, H 1995, 'Changes in CD44 expression during B cell differentiation in the human tonsil', *Cellular immunology*, vol. 161, no. 2, pp. 147-157.

Krusche, CA, Holthofer, B, Hofe, V, van de Sandt, AM, Eshkind, L, Bockamp, E, Merx, MW, Kant, S, Windoffer, R & Leube, RE 2011, 'Desmoglein 2 mutant mice develop cardiac fibrosis and dilation', *Basic Res Cardiol*, vol. 106, no. 4, pp. 617-633.

Krzysiek, R, Lefevre, EA, Bernard, J, Foussat, A, Galanaud, P, Louache, F & Richard, Y 2000, 'Regulation of CCR6 chemokine receptor expression and responsiveness to macrophage inflammatory protein-3α/CCL20 in human B cells', *Blood*, vol. 96, no. 7, pp. 2338-2345.

Kubo, H, Kitajima, Y, Kai, K, Nakamura, JUN, Miyake, S, Yanagihara, K, Morito, K, Tanaka, T, Shida, M & Noshiro, H 2016, 'Regulation and clinical significance of the hypoxia-induced expression of ANGPTL4 in gastric cancer', *Oncology Letters*, vol. 11, no. 2, pp. 1026-1034.

Kuhn, A, Brachtendorf, G, Kurth, F, Sonntag, M, Samulowitz, U, Metze, D & Vestweber, D 2002, 'Expression of endomucin, a novel endothelial sialomucin, in normal and diseased human skin', *The Journal of Investigative Dermatology*, vol. 119, no. 6, pp. 1388-1393.

Kume, K, Haraguchi, M, Hijioka, H, Ishida, T, Miyawaki, A, Nakamura, N & Ozawa, M 2013, 'The transcription factor Snail enhanced the degradation of E-cadherin and desmoglein 2 in oral squamous cell carcinoma cells', *Biochemical and biophysical research communications*, vol. 430, no. 3, pp. 889-894.

Kut, C, Mac Gabhann, F & Popel, AS 2007, 'Where is VEGF in the body? A meta-analysis of VEGF distribution in cancer', *British journal of cancer*, vol. 97, no. 7, pp. 978-985.

Kwasny, D, Kiilerich-Pedersen, K, Moresco, J, Dimaki, M, Rozlosnik, N & Svendsen, WE 2011, 'Microfluidic device to study cell transmigration under physiological shear stress conditions', *Biomed Microdevices*, vol. 13, no. 5, pp. 899-907.

Ladányi, A, Somlai, B, Gilde, K, Fejös, Z, Gaudi, I & Tímár, J 2004, 'T-Cell Activation Marker Expression on Tumor-Infiltrating Lymphocytes As Prognostic Factor in Cutaneous Malignant Melanoma', *Clinical Cancer Research*, vol. 10, no. 2, pp. 521-530.

Lampugnani, MG, Zanetti, A, Corada, M, Takahashi, T, Balconi, G, Breviario, F, Orsenigo, F, Cattelino, A, Kemler, R, Daniel, TO & Dejana, E 2003, 'Contact inhibition of VEGF-induced proliferation requires vascular endothelial cadherin, β-catenin, and the phosphatase DEP-1/CD148', *The Journal of Cell Biology*, vol. 161, no. 4, pp. 793-804.

Langer, HF, Orlova, VV, Xie, C, Kaul, S, Schneider, D, Lonsdorf, AS, Fahrleitner, M, Choi, EY, Dutoit, V, Pellegrini, M, Grossklaus, S, Nawroth, PP, Baretton, G, Santoso, S, Hwang, ST, Arnold, B & Chavakis, T 2011, 'A Novel Function of Junctional Adhesion Molecule-C in Mediating Melanoma Cell Metastasis', *Cancer research*, vol. 71, no. 12, pp. 4096-4105.

Larkin, J, Chiarion-Sileni, V, Gonzalez, R, Grob, JJ, Cowey, CL, Lao, CD, Schadendorf, D, Dummer, R, Smylie, M, Rutkowski, P, Ferrucci, PF, Hill, A, Wagstaff, J, Carlino, MS, Haanen, JB, Maio, M, Marquez-Rodas, I, McArthur, GA, Ascierto, PA, Long, GV, Callahan, MK, Postow, MA, Grossmann, K, Sznol, M, Dreno, B, Bastholt, L, Yang, A, Rollin, LM, Horak, C, Hodi, FS & Wolchok, JD 2015, 'Combined Nivolumab and Ipilimumab or Monotherapy in Untreated Melanoma', *The New England Journal of Medicine*, vol. 373, no. 1, pp. 23-34.

Laszik, Z, Jansen, PJ, Cummings, RD, Tedder, TF, McEver, RP & Moore, KL 1996, 'P-selectin glycoprotein ligand-1 is broadly expressed in cells of myeloid, lymphoid, and dendritic lineage and in some nonhematopoietic cells', *Blood*, vol. 88, no. 8, pp. 3010-3021.

Lee, CH, Wu, YT, Hsieh, HC, Yu, Y, Yu, AL & Chang, WW 2014, 'Epidermal growth factor/heat shock protein 27 pathway regulates vasculogenic mimicry activity of breast cancer stem/progenitor cells', *Biochimie*, vol. 104, pp. 117-126.

Lee, Y-A, Ji, H-I, Lee, S-H, Hong, S-J, Yang, H-I, Chul Yoo, M & Kim, KS 2014, 'The role of adiponectin in the production of IL-6, IL-8, VEGF and MMPs in human endothelial cells and osteoblasts: implications for arthritic joints', *Experimental & Molecular Medicine*, vol. 46, p. e72.

Lesley, J, Hascall, VC, Tammi, M & Hyman, R 2000, 'Hyaluronan Binding by Cell Surface CD44', *Journal of Biological Chemistry*, vol. 275, no. 35, pp. 26967-26975.

Lesokhin, AM, Hohl, TM, Kitano, S, Cortez, C, Hirschhorn-Cymerman, D, Avogadri, F, Rizzuto, GA, Lazarus, JJ, Pamer, EG & Houghton, AN 2012, 'Monocytic CCR2+ myeloid-derived suppressor cells promote immune escape by limiting activated CD8 T-cell infiltration into the tumor microenvironment', *Cancer research*, vol. 72, no. 4, pp. 876-886.

Levene, MJ, Dombeck, DA, Kasischke, KA, Molloy, RP & Webb, WW 2004, 'In Vivo Multiphoton Microscopy of Deep Brain Tissue', *Journal of Neurophysiology*, vol. 91, no. 4, pp. 1908-1912.

Ley, K, Laudanna, C, Cybulsky, MI & Nourshargh, S 2007, 'Getting to the site of inflammation: the leukocyte adhesion cascade updated', *Nature Reviews Immunology*, vol. 7, no. 9, pp. 678-689.

Liu, C, Lou, Y, Lizee, G, Qin, H, Liu, S, Rabinovich, B, Kim, GJ, Wang, YH, Ye, Y, Sikora, AG, Overwijk, WW, Liu, YJ, Wang, G & Hwu, P 2008, 'Plasmacytoid dendritic cells induce NK cell-dependent, tumor antigen-specific T cell cross-priming and tumor regression in mice', *The Journal of clinical investigation*, vol. 118, no. 3, pp. 1165-1175.

Liu, C, Peng, W, Xu, C, Lou, Y, Zhang, M, Wargo, JA, Chen, JQ, Li, HS, Watowich, SS, Yang, Y, Frederick, DT, Cooper, ZA, Mbofung, RM, Whittington, M, Flaherty, KT, Woodman, SE, Davies, MA, Radvanyi, LG, Overwijk, WW, Lizée, G & Hwu, P 2013, 'BRAF Inhibition Increases Tumor Infiltration by T cells and Enhances the Antitumor Activity of Adoptive Immunotherapy in Mice', *Clinical Cancer Research*, vol. 19, no. 2, pp. 393-403.

Liu, J, Zhang, N, Li, Q, Zhang, W, Ke, F, Leng, Q, Wang, H, Chen, J & Wang, H 2011, 'Tumor-associated macrophages recruit CCR6+ regulatory T cells and promote the development of colorectal cancer via enhancing CCL20 production in mice', *PloS one*, vol. 6, no. 4, p. e19495.

Liu, Y, Masuda, E, Blank, MC, Kirou, KA, Gao, X, Park, MS & Pricop, L 2005, 'Cytokine-mediated regulation of activating and inhibitory Fc gamma receptors in human monocytes', *Journal of Leukocyte Biology*, vol. 77, no. 5, pp. 767-776.

Liu, YR, Sun, B, Zhao, XL, Gu, Q, Liu, ZY, Dong, XY, Che, N & Mo, J 2013, 'Basal caspase-3 activity promotes migration, invasion, and vasculogenic mimicry formation of melanoma cells', *Melanoma research*, vol. 23, no. 4, pp. 243-253.

Lominadze, D & McHedlishvili, G 1999, 'Red Blood Cell Behavior at Low Flow Rate in Microvessels', *Microvascular research*, vol. 58, no. 2, pp. 187-189.

Long, GV, Fung, C, Menzies, AM, Pupo, GM, Carlino, MS, Hyman, J, Shahheydari, H, Tembe, V, Thompson, JF & Saw, RP 2014, 'Increased MAPK reactivation in early resistance to dabrafenib/trametinib combination therapy of BRAF-mutant metastatic melanoma', *Nature communications*, vol. 5.

Long, GV, Atkinson, V, Cebon, JS, Jameson, MB, Fitzharris, BM, McNeil, CM, Hill, AG, Ribas, A, Atkins, MB, Thompson, JA, Hwu, W-J, Hodi, FS, Menzies, AM, Guminski, AD, Kefford, R, Shu, X, Ebbinghaus, S, Ibrahim, N & Carlino, MS 2016, 'Pembrolizumab (pembro) plus ipilimumab (ipi) for advanced melanoma: Results of the KEYNOTE-029 expansion cohort.', *Journal of Clinical Oncology*, vol. 34, no. suppl; abstr 9506.

Lun, AT, Chen, Y & Smyth, GK 2016, 'It's DE-licious: A Recipe for Differential Expression Analyses of RNA-seq Experiments Using Quasi-Likelihood Methods in edgeR', *Methods in Molecular Biology*, vol. 1418, pp. 391-416.

Maes, H, Van Eygen, S, Krysko, DV, Vandenabeele, P, Nys, K, Rillaerts, K & Garg, AD 2014, 'BNIP3 supports melanoma cell migration and vasculogenic mimicry by orchestrating the actin cytoskeleton', *Cell Death Dis*, vol. 5, p. e1127.

Mahoney, MG, Simpson, A, Aho, S, Uitto, J & Pulkkinen, L 2002, 'Interspecies conservation and differential expression of mouse desmoglein gene family', *Exp Dermatol*, vol. 11, no. 2, pp. 115-125.

Maniotis, AJ, Folberg, R, Hess, A, Seftor, EA, Gardner, LM, Pe'er, J, Trent, JM, Meltzer, PS & Hendrix, MJ 1999, 'Vascular channel formation by human melanoma cells in vivo and in vitro: vasculogenic mimicry', *Am J Pathol*, vol. 155, no. 3, pp. 739-752.

Martin, M 2011, 'Cutadapt removes adapter sequences from high-throughput sequencing reads', *EMBnet.journal*, vol. 17, no. 1, pp. 10-12.

Martinet, L, Garrido, I, Filleron, T, Le Guellec, S, Bellard, E, Fournie, J-J, Rochaix, P & Girard, J-P 2011, 'Human Solid Tumors Contain High Endothelial Venules: Association with T- and B-Lymphocyte Infiltration and Favorable Prognosis in Breast Cancer', *Cancer research*, vol. 71, no. 17, pp. 5678-5687.

Mattei, S, Colombo, MP, Melani, C, Silvani, A, Parmiani, G & Herlyn, M 1994, 'Expression of cytokine/growth factors and their receptors in human melanoma and melanocytes', *International Journal of Cancer*, vol. 56, no. 6, pp. 853-857.

McAllister, JC, Zhan, Q, Weishaupt, C, Hsu, MY & Murphy, GF 2010, 'The embryonic morphogen, Nodal, is associated with channel-like structures in human malignant melanoma xenografts', *J Cutan Pathol*, vol. 37 Suppl 1, pp. 19-25.

McComb, JG, Ranganathan, M, Liu, XH, Pilewski, JM, Ray, P, Watkins, SC, Choi, AMK & Lee, JS 2008, 'CX3CL1 Up-Regulation Is Associated with Recruitment of CX3CR1(+) Mononuclear Phagocytes and T Lymphocytes in the Lungs during Cigarette Smoke-Induced Emphysema', *Am J Pathol*, vol. 173, no. 4, pp. 949-961.

McDonald, DM, Munn, L & Jain, RK 2000, 'Vasculogenic Mimicry: How Convincing, How Novel, and How Significant?', *Am J Pathol*, vol. 156, no. 2, pp. 383-388.

McKay, K, Moore, PC, Smoller, BR & Hiatt, KM 2011, 'Association between natural killer cells and regression in melanocytic lesions', *Human pathology*, vol. 42, no. 12, pp. 1960-1964.

McLaughlin, F, Hayes, BP, Horgan, CM, Beesley, JE, Campbell, CJ & Randi, AM 1998, 'Tumor necrosis factor (TNF)-alpha and interleukin (IL)-1beta down-regulate intercellular adhesion molecule (ICAM)-2 expression on the endothelium', *Cell Adhes Commun*, vol. 6, no. 5, pp. 381-400.

McMahon, S, Charbonneau, M, Grandmont, S, Richard, DE & Dubois, CM 2006, 'Transforming Growth Factor β1 Induces Hypoxia-inducible Factor-1 Stabilization through Selective Inhibition of PHD2 Expression', *Journal of Biological Chemistry*, vol. 281, no. 34, pp. 24171-24181.

Mehnert, JM, McCarthy, MM, Jilaveanu, L, Flaherty, KT, Aziz, S, Camp, RL, Rimm, DL & Kluger, HM 2010, 'Quantitative expression of VEGF, VEGF-R1, VEGF-R2, and VEGF-R3 in melanoma tissue microarrays', *Human pathology*, vol. 41, no. 3, pp. 375-384.

Merighi, S, Benini, A, Mirandola, P, Gessi, S, Varani, K, Leung, E, Maclennan, S & Borea, PA 2006, 'Adenosine modulates vascular endothelial growth factor expression via hypoxia-inducible factor-1 in human glioblastoma cells', *Biochemical Pharmacology*, vol. 72, no. 1, pp. 19-31.

Middleton, J, Patterson, AM, Gardner, L, Schmutz, C & Ashton, BA 2002, 'Leukocyte extravasation: chemokine transport and presentation by the endothelium', *Blood*, vol. 100, no. 12, pp. 3853-3860.

Mikucki, M, Fisher, D, Matsuzaki, J, Skitzki, J, Gaulin, N, Muhitch, J, Ku, A, Frelinger, J, Odunsi, K & Gajewski, T 2015, 'Non-redundant requirement for CXCR3 signalling during tumoricidal T-cell trafficking across tumour vascular checkpoints', *Nature communications,* vol. 6.

Miracco, C, Mourmouras, V, Biagioli, M, Rubegni, P, Mannucci, S, Monciatti, I, Cosci, E, Tosi, P & Luzi, P 2007, 'Utility of tumour-infiltrating CD25+ FOXP3+ regulatory T cell evaluation in predicting local recurrence in vertical growth phase cutaneous melanoma', *Oncology reports,* vol. 18, no. 5, pp. 1115-1122.

Mishalian, I, Bayuh, R, Levy, L, Zolotarov, L, Michaeli, J & Fridlender, ZG 2013, 'Tumor-associated neutrophils (TAN) develop pro-tumorigenic properties during tumor progression', *Cancer Immunology, Immunotherapy,* vol. 62, no. 11, pp. 1745-1756.

Misra, RM, Bajaj, MS & Kale, VP 2012, 'Vasculogenic Mimicry of HT1080 Tumour Cells In Vivo: Critical Role of HIF-1α-Neuropilin-1 Axis', *PloS one,* vol. 7, no. 11, p. e50153.

Mizrahi, A, Crowley, JC, Shtoyerman, E & Katz, LC 2004, 'High-Resolution In Vivo Imaging of Hippocampal Dendrites and Spines', *The Journal of Neuroscience,* vol. 24, no. 13, pp. 3147-3151.

Molon, B, Ugel, S, Del Pozzo, F, Soldani, C, Zilio, S, Avella, D, De Palma, A, Mauri, P, Monegal, A & Rescigno, M 2011, 'Chemokine nitration prevents intratumoral infiltration of antigen-specific T cells', *Journal of Experimental Medicine,* vol. 208, no. 10, pp. 1949-1962.

Monastirli, A, Pasmatzi, E, Georgiou, S, Kapranos, N, Frangia, K, Braun, H, Ioannovich, J, Varakis, J & Tsambaos, D 2000, 'Lectin-binding pattern of primary malignant melanomas and melanocytic nevi', *J Cutan Pathol,* vol. 27, no. 3, pp. 103-107.

Montresor, A, Toffali, L, Constantin, G & Laudanna, C 2012, 'Chemokines and the Signaling Modules Regulating Integrin Affinity', *Front Immunol,* vol. 3, p. 127.

Mortier, A, Van Damme, J & Proost, P 2012, 'Overview of the mechanisms regulating chemokine activity and availability', *Immunology letters,* vol. 145, no. 1, pp. 2-9.

Motz, GT, Santoro, SP, Wang, LP, Garrabrant, T, Lastra, RR, Hagemann, IS, Lal, P, Feldman, MD, Benencia, F & Coukos, G 2014, 'Tumor endothelium FasL establishes a selective immune barrier promoting tolerance in tumors', *Nature medicine,* vol. 20, no. 6, pp. 607-615.

Mrowietz, U, Schwenk, U, Maune, S, Bartels, J, Kupper, M, Fichtner, I, Schroder, JM & Schadendorf, D 1999, 'The chemokine RANTES is secreted by human melanoma cells and is associated with enhanced tumour formation in nude mice', *British journal of cancer,* vol. 79, no. 7-8, pp. 1025-1031.

Murphy, EA, Majeti, BK, Barnes, LA, Makale, M, Weis, SM, Lutu-Fuga, K, Wrasidlo, W & Cheresh, DA 2008, 'Nanoparticle-mediated drug delivery to tumor vasculature suppresses metastasis', *Proceedings of the National Academy of Sciences,* vol. 105, no. 27, pp. 9343-9348.

Murphy, KM & Reiner, SL 2002, 'The lineage decisions of helper T cells', *Nature Reviews. Immunology,* vol. 2, no. 12, pp. 933-944.

Nakayama, T, Hieshima, K, Izawa, D, Tatsumi, Y, Kanamaru, A & Yoshie, O 2003, 'Cutting edge: profile of chemokine receptor expression on human plasma cells accounts for their efficient recruitment to target tissues', *Journal of Immunology,* vol. 170, no. 3, pp. 1136-1140.

Nandi, A, Estess, P & Siegelman, MH 2000, 'Hyaluronan Anchoring and Regulation on the Surface of Vascular Endothelial Cells Is Mediated through the Functionally Active Form of CD44', *Journal of Biological Chemistry,* vol. 275, no. 20, pp. 14939-14948.

Navarro, P, Ruco, L & Dejana, E 1998, 'Differential localization of VE- and N-cadherins in human endothelial cells: VE-cadherin competes with N-cadherin for junctional localization', *The Journal of Cell Biology,* vol. 140, no. 6, pp. 1475-1484.

Nazarian, R, Shi, H, Wang, Q, Kong, X, Koya, RC, Lee, H, Chen, Z, Lee, M-K, Attar, N & Sazegar, H 2010, 'Melanomas acquire resistance to B-RAF (V600E) inhibition by RTK or N-RAS upregulation', *Nature,* vol. 468, no. 7326, pp. 973-977.

Nesbit, M, Schaider, H, Miller, TH & Herlyn, M 2001, 'Low-level monocyte chemoattractant protein-1 stimulation of monocytes leads to tumor formation in nontumorigenic melanoma cells', *Journal of Immunology,* vol. 166, no. 11, pp. 6483-6490.

Nishikawa, H & Sakaguchi, S 2014, 'Regulatory T cells in cancer immunotherapy', *Current Opinion in Immunology,* vol. 27, pp. 1-7.

Nooijen, PT, Westphal, JR, Eggermont, AM, Schalkwijk, C, Max, R, de Waal, RM & Ruiter, DJ 1998, 'Endothelial P-selectin expression is reduced in advanced primary melanoma and melanoma metastasis', *Am J Pathol,* vol. 152, no. 3, pp. 679-682.

Noonan, FP, Zaidi, MR, Wolnicka-Glubisz, A, Anver, MR, Bahn, J, Wielgus, A, Cadet, J, Douki, T, Mouret, S, Tucker, MA, Popratiloff, A, Merlino, G & De Fabo, EC 2012, 'Melanoma induction by ultraviolet A but not ultraviolet B radiation requires melanin pigment', *Nature communications,* vol. 3, p. 884.

Obermajer, N, Muthuswamy, R, Odunsi, K, Edwards, RP & Kalinski, P 2011, 'PGE(2)-induced CXCL12 production and CXCR4 expression controls the accumulation of human MDSCs in ovarian cancer environment', *Cancer research,* vol. 71, no. 24, pp. 7463-7470.

Olbryt, M, Habryka, A, Student, S, Jarz?b, M, Tyszkiewicz, T & Lisowska, KM 2014, 'Global Gene Expression Profiling in Three Tumor Cell Lines Subjected to Experimental Cycling and Chronic Hypoxia', *PloS one,* vol. 9, no. 8, p. e105104.

Ostermann, G, Weber, KS, Zernecke, A, Schroder, A & Weber, C 2002, 'JAM-1 is a ligand of the beta(2) integrin LFA-1 involved in transendothelial migration of leukocytes', *Nature Immunology,* vol. 3.

Overmiller, AM, McGuinn, KP, Roberts, BJ, Cooper, F, Brennan-Crispi, DM, Deguchi, T, Peltonen, S, Wahl, JK, 3rd & Mahoney, MG 2016, 'c-Src/Cav1-dependent activation of the EGFR by Dsg2', *Oncotarget*, vol. 7, no. 25, pp. 37536-37555.

Ozaki, H, Ishii, K, Horiuchi, H, Arai, H, Kawamoto, T, Okawa, K, Iwamatsu, A & Kita, T 1999, 'Cutting edge: combined treatment of TNF-alpha and IFN-gamma causes redistribution of junctional adhesion molecule in human endothelial cells', *Journal of Immunology*, vol. 163, no. 2, pp. 553-557.

Paik, JH, Skoura, A, Chae, SS, Cowan, AE, Han, DK, Proia, RL & Hla, T 2004, 'Sphingosine 1-phosphate receptor regulation of N-cadherin mediates vascular stabilization', *Genes Dev*, vol. 18, no. 19, pp. 2392-2403.

Payne, AS & Cornelius, LA 2002, 'The role of chemokines in melanoma tumor growth and metastasis', *Journal of Investigative Dermatology*, vol. 118, no. 6, pp. 915-922.

Peitsch, WK, Doerflinger, Y, Fischer-Colbrie, R, Huck, V, Bauer, AT, Utikal, J, Goerdt, S & Schneider, SW 2014, 'Desmoglein 2 Depletion Leads to Increased Migration and Upregulation of the Chemoattractant Secretoneurin in Melanoma Cells', *PloS one*, vol. 9, no. 2, p. e89491.

Peng, W, Ye, Y, Rabinovich, BA, Liu, C, Lou, Y, Zhang, M, Whittington, M, Yang, Y, Overwijk, WW, Lizée, G & Hwu, P 2010, 'Transduction of Tumor-Specific T Cells with CXCR2 Chemokine Receptor Improves Migration to Tumor and Antitumor Immune Responses', *Clinical Cancer Research*, vol. 16, no. 22, pp. 5458-5468.

Petty, JM, Sueblinvong, V, Lenox, CC, Jones, CC, Cosgrove, GP, Cool, CD, Rai, PR, Brown, KK, Weiss, DJ, Poynter, ME & Suratt, BT 2007, 'Pulmonary Stromal-Derived Factor-1 Expression and Effect on Neutrophil Recruitment during Acute Lung Injury', *The Journal of Immunology*, vol. 178, no. 12, pp. 8148-8157.

Piali, L, Fichtel, A, Terpe, HJ, Imhof, BA & Gisler, RH 1995, 'Endothelial vascular cell adhesion molecule 1 expression is suppressed by melanoma and carcinoma', *The Journal of experimental medicine*, vol. 181, no. 2, pp. 811-816.

Piccard, H, Muschel, RJ & Opdenakker, G 2012, 'On the dual roles and polarized phenotypes of neutrophils in tumor development and progression', *Critical Reviews in Oncology/Hematology*, vol. 82, no. 3, pp. 296-309.

Pilichou, K, Nava, A, Basso, C, Beffagna, G, Bauce, B, Lorenzon, A, Frigo, G, Vettori, A, Valente, M, Towbin, J, Thiene, G, Danieli, GA & Rampazzo, A 2006, 'Mutations in Desmoglein-2 Gene Are Associated With Arrhythmogenic Right Ventricular Cardiomyopathy', *Circulation*, vol. 113, no. 9, pp. 1171-1179.

Piras, F, Colombari, R, Minerba, L, Murtas, D, Floris, C, Maxia, C, Corbu, A, Perra, MT & Sirigu, P 2005, 'The predictive value of CD8, CD4, CD68, and human leukocyte antigen-D-related cells in the prognosis of cutaneous malignant melanoma with vertical growth phase', *Cancer*, vol. 104, no. 6, pp. 1246-1254.

Pollock, PM, Harper, UL, Hansen, KS, Yudt, LM, Stark, M, Robbins, CM, Moses, TY, Hostetter, G, Wagner, U, Kakareka, J, Salem, G, Pohida, T, Heenan, P, Duray, P, Kallioniemi, O, Hayward, NK, Trent, JM & Meltzer, PS 2003, 'High frequency of BRAF mutations in nevi', *Nat Genet*, vol. 33, no. 1, pp. 19-20.

Ponce, ML 2009, 'Tube formation: an in vitro matrigel angiogenesis assay', *Methods in Molecular Biology*, vol. 467, pp. 183-188.

Postigo, AA, Marazuela, M, Sánchez-Madrid, F & de Landázuri, MO 1994, 'B lymphocyte binding to E- and P-selectins is mediated through the de novo expression of carbohydrates on in vitro and in vivo activated human B cells', *Journal of Clinical Investigation*, vol. 94, no. 4, pp. 1585-1596.

Poulikakos, PI, Persaud, Y, Janakiraman, M, Kong, X, Ng, C, Moriceau, G, Shi, H, Atefi, M, Titz, B, Gabay, MT, Salton, M, Dahlman, KB, Tadi, M, Wargo, JA, Flaherty, KT, Kelley, MC, Misteli, T, Chapman, PB, Sosman, JA, Graeber, TG, Ribas, A, Lo, RS, Rosen, N & Solit, DB 2011, 'RAF inhibitor resistance is mediated by dimerization of aberrantly spliced BRAF(V600E)', *Nature*, vol. 480, no. 7377, pp. 387-390.

Prasain, N & Stevens, T 2009, 'The actin cytoskeleton in endothelial cell phenotypes', *Microvascular research*, vol. 77, no. 1, pp. 53-63.

Pure, E & Cuff, CA 2001, 'A crucial role for CD44 in inflammation', *Trends Mol Med*, vol. 7, no. 5, pp. 213-221.

Racordon, D, Valdivia, A, Mingo, G, Erices, R, Aravena, R, Santoro, F, Bravo, ML, Ramirez, C, Gonzalez, P, Sandoval, A, González, A, Retamal, C, Kogan, MJ, Kato, S, Cuello, MA, Osorio, G, Nualart, F, Alvares, P, Gago-Arias, A, Fabri, D, Espinoza, I, Sanchez, B, Corvalán, AH, Pinto, MP & Owen, GI 2017, 'Structural and functional identification of vasculogenic mimicry in vitro', *Sci Rep*, vol. 7, no. 1, p. 6985.

Repo, H, Leirisalo, M & Kosunen, TU 1981, 'Neutrophil chemotaxis under agarose: a statistical analysis and comparison of the chemotactic response of cells from different donors', *Journal of Immunological Methods*, vol. 46, no. 2, pp. 227-242.

Richard, DE, Berra, E, Gothie, E, Roux, D & Pouyssegur, J 1999, 'p42/p44 mitogen-activated protein kinases phosphorylate hypoxia-inducible factor 1alpha (HIF-1alpha) and enhance the transcriptional activity of HIF-1', *The Journal of Biological Chemistry*, vol. 274, no. 46, pp. 32631-32637.

Rickelt, S, Franke, WW, Doerflinger, Y, Goerdt, S, Brandner, JM & Peitsch, WK 2008, 'Subtypes of melanocytes and melanoma cells distinguished by their intercellular contacts: heterotypic adherens junctions, adhesive associations, and dispersed desmoglein 2 glycoproteins', *Cell Tissue Res*, vol. 334, no. 3, pp. 401-422.

Robert, L, Tsoi, J, Wang, X, Emerson, R, Homet, B, Chodon, T, Mok, S, Huang, RR, Cochran, AJ, Comin-Anduix, B, Koya, RC, Graeber, TG, Robins, H & Ribas, A 2014, 'CTLA4 blockade broadens the peripheral T-cell receptor repertoire', *Clinical Cancer Research*, vol. 20, no. 9, pp. 2424-2432.

Robertson, RT, Levine, ST, Haynes, SM, Gutierrez, P, Baratta, JL, Tan, Z & Longmuir, KJ 2015, 'Use of labeled tomato lectin for imaging vasculature structures', *Histochem Cell Biol*, vol. 143, no. 2, pp. 225-234.

Robinson, LA, Nataraj, C, Thomas, DW, Cosby, JM, Griffiths, R, Bautch, VL, Patel, DD & Coffman, TM 2003, 'The chemokine CX 3 CL1 regulates NK cell activity in vivo', *Cellular immunology*, vol. 225, no. 2, pp. 122-130.

Robinson, MD, McCarthy, DJ & Smyth, GK 2010, 'edgeR: a Bioconductor package for differential expression analysis of digital gene expression data', *Bioinformatics*, vol. 26, no. 1, pp. 139-140.

Rofstad, EK & Halsør, EF 2000, 'Vascular Endothelial Growth Factor, Interleukin 8, Platelet-derived Endothelial Cell Growth Factor, and Basic Fibroblast Growth Factor Promote Angiogenesis and Metastasis in Human Melanoma Xenografts', *Cancer research*, vol. 60, no. 17, pp. 4932-4938.

Romani, N, Schuler, G & Fritsch, P 1983, 'Identical lectin binding patterns of human melanocytes and melanoma cells in vitro', *The Journal of Investigative Dermatology*, vol. 80, no. 4, pp. 272-277.

Romer, LH, McLean, NV, Yan, HC, Daise, M, Sun, J & DeLisser, HM 1995, 'IFN-gamma and TNF-alpha induce redistribution of PECAM-1 (CD31) on human endothelial cells', *Journal of Immunology*, vol. 154, no. 12, pp. 6582-6592.

Rosenberg, SA, Yang, JC, Sherry, RM, Kammula, US, Hughes, MS, Phan, GQ, Citrin, DE, Restifo, NP, Robbins, PF & Wunderlich, JR 2011, 'Durable complete responses in heavily pretreated patients with metastatic melanoma using T-cell transfer immunotherapy', *Clinical Cancer Research*, vol. 17, no. 13, pp. 4550-4557.

Rosenberg, SA & Restifo, NP 2015, 'Adoptive cell transfer as personalized immunotherapy for human cancer', *Science*, vol. 348, no. 6230, pp. 62-68.

Ruf, W, Seftor, EA, Petrovan, RJ, Weiss, RM, Gruman, LM, Margaryan, NV, Seftor, RE, Miyagi, Y & Hendrix, MJ 2003, 'Differential role of tissue factor pathway inhibitors 1 and 2 in melanoma vasculogenic mimicry', *Cancer research*, vol. 63, no. 17, pp. 5381-5389.

Ruhrberg, C, Gerhardt, H, Golding, M, Watson, R, Ioannidou, S, Fujisawa, H, Betsholtz, C & Shima, DT 2002, 'Spatially restricted patterning cues provided by heparin-binding VEGF-A control blood vessel branching morphogenesis', *Genes Dev*, vol. 16, no. 20, pp. 2684-2698.

Ryan, DH, Nuccie, BL, Abboud, CN & Winslow, JM 1991, 'Vascular cell adhesion molecule-1 and the integrin VLA-4 mediate adhesion of human B cell precursors to cultured bone marrow adherent cells', *Journal of Clinical Investigation*, vol. 88, no. 3, pp. 995-1004.

Sackstein, R, Schatton, T & Barthel, SR 2017, 'T-lymphocyte homing: an underappreciated yet critical hurdle for successful cancer immunotherapy', *Laboratory Investigation*, vol. 97, no. 6, pp. 669-697.

Salas, A, Shimaoka, M, Kogan, AN, Harwood, C, von Andrian, UH & Springer, TA 2004, 'Rolling adhesion through an extended conformation of integrin alphaLbeta2 and relation to alpha I and beta I-like domain interaction', *Immunity*, vol. 20, no. 4, pp. 393-406.

Schafer, S, Koch, PJ & Franke, WW 1994, 'Identification of the ubiquitous human desmoglein, Dsg2, and the expression catalogue of the desmoglein subfamily of desmosomal cadherins', *Experimental Cell Research*, vol. 211, no. 2, pp. 391-399.

Schaider, H, Oka, M, Bogenrieder, T, Nesbit, M, Satyamoorthy, K, Berking, C, Matsushima, K & Herlyn, M 2003, 'Differential response of primary and metastatic melanomas to neutrophils attracted by IL-8', *International Journal of Cancer*, vol. 103, no. 3, pp. 335-343.

Schenk, BI, Petersen, F, Flad, HD & Brandt, E 2002, 'Platelet-derived chemokines CXC chemokine ligand (CXCL)7, connective tissue-activating peptide III, and CXCL4 differentially affect and cross-regulate neutrophil adhesion and transendothelial migration', *Journal of Immunology*, vol. 169, no. 5, pp. 2602-2610.

Schilling, B, Sucker, A, Griewank, K, Zhao, F, Weide, B, Görgens, A, Giebel, B, Schadendorf, D & Paschen, A 2013, 'Vemurafenib reverses immunosuppression by myeloid derived suppressor cells', *International Journal of Cancer*, vol. 133, no. 7, pp. 1653-1663.

Schlecker, E, Stojanovic, A, Eisen, C, Quack, C, Falk, CS, Umansky, V & Cerwenka, A 2012, 'Tumor-infiltrating monocytic myeloid-derived suppressor cells mediate CCR5-dependent recruitment of regulatory T cells favoring tumor growth', *Journal of Immunology*, vol. 189, no. 12, pp. 5602-5611.

Schlegel, N, Meir, M, Heupel, WM, Holthofer, B, Leube, RE & Waschke, J 2010, 'Desmoglein 2-mediated adhesion is required for intestinal epithelial barrier integrity', *Am J Physiol Gastrointest Liver Physiol*, vol. 298, no. 5, pp. G774-783.

Schmitt, CJ, Franke, WW, Goerdt, S, Falkowska-Hansen, B, Rickelt, S & Peitsch, WK 2007, 'Homo- and heterotypic cell contacts in malignant melanoma cells and desmoglein 2 as a novel solitary surface glycoprotein', *The Journal of Investigative Dermatology*, vol. 127, no. 9, pp. 2191-2206.

Schnegg, CI, Yang, MH, Ghosh, SK & Hsu, M-Y 2015, 'Induction of vasculogenic mimicry overrides VEGF-A silencing and enriches stem-like cancer cells in melanoma', *Cancer research*, vol. 75, no. 8, pp. 1682-1690.

Seftor, RE, Seftor, EA, Koshikawa, N, Meltzer, PS, Gardner, LM, Bilban, M, Stetler-Stevenson, WG, Quaranta, V & Hendrix, MJ 2001, 'Cooperative interactions of laminin 5 gamma2 chain, matrix metalloproteinase-2, and membrane type-1-matrix/metalloproteinase are required for mimicry of embryonic vasculogenesis by aggressive melanoma', *Cancer research*, vol. 61, no. 17, pp. 6322-6327.

Semenza, GL 1998, 'Hypoxia-inducible factor 1 and the molecular physiology of oxygen homeostasis', *J Lab Clin Med*, vol. 131, no. 3, pp. 207-214.

Sheppard, KE, Cullinane, C, Martin, C, Kirby, L, Haynes, N, Waldeck, K, Young, R, VanArsdale, T & McArthur, G 2016, 'Abstract 2826: Sustained melanoma regression is achieved with continuous

palbociclib and PLX4720 treatment but not with intermittent or sequential dosing', *Cancer research*, vol. 76, no. 14 Supplement, pp. 2826-2826.

Shi, H, Moriceau, G, Kong, X, Lee, MK, Lee, H, Koya, RC, Ng, C, Chodon, T, Scolyer, RA, Dahlman, KB, Sosman, JA, Kefford, RF, Long, GV, Nelson, SF, Ribas, A & Lo, RS 2012, 'Melanoma whole-exome sequencing identifies (V600E)B-RAF amplification-mediated acquired B-RAF inhibitor resistance', *Nature communications*, vol. 3, p. 724.

Shi, H, Zhang, J, Han, X, Li, H, Xie, M, Sun, Y, Liu, W, Ba, X & Zeng, X 2017, 'Recruited monocytic myeloid-derived suppressor cells promote the arrest of tumor cells in the premetastatic niche through an IL-1beta-mediated increase in E-selectin expression', *International Journal of Cancer*, vol. 140, no. 6, pp. 1370-1383.

Sidibe, A, Ropraz, P, Jemelin, S, Emre, Y, Poittevin, M, Pocard, M, Bradfield, PF & Imhof, BA 2018, 'Angiogenic factor-driven inflammation promotes extravasation of human proangiogenic monocytes to tumours', *Nat Commun*, vol. 9, no. 1, p. 355.

Sinha, P, Clements, VK, Bunt, SK, Albelda, SM & Ostrand-Rosenberg, S 2007, 'Cross-talk between myeloid-derived suppressor cells and macrophages subverts tumor immunity toward a type 2 response', *The Journal of Immunology*, vol. 179, no. 2, pp. 977-983.

Sood, AK, Seftor, EA, Fletcher, MS, Gardner, LM, Heidger, PM, Buller, RE, Seftor, RE & Hendrix, MJ 2001, 'Molecular determinants of ovarian cancer plasticity', *Am J Pathol*, vol. 158, no. 4, pp. 1279-1288.

Stahl, JM, Sharma, A, Cheung, M, Zimmerman, M, Cheng, JQ, Bosenberg, MW, Kester, M, Sandirasegarane, L & Robertson, GP 2004, 'Deregulated Akt3 activity promotes development of malignant melanoma', *Cancer research*, vol. 64, no. 19, pp. 7002-7010.

Stark, M & Hayward, N 2007, 'Genome-Wide Loss of Heterozygosity and Copy Number Analysis in Melanoma Using High-Density Single-Nucleotide Polymorphism Arrays', *Cancer research*, vol. 67, no. 6, pp. 2632-2642.

Steffen, BJ, Breier, G, Butcher, EC, Schulz, M & Engelhardt, B 1996, 'ICAM-1, VCAM-1, and MAdCAM-1 are expressed on choroid plexus epithelium but not endothelium and mediate binding of lymphocytes in vitro', *Am J Pathol*, vol. 148, no. 6, pp. 1819-1838.

Steinberg, SM, Shabaneh, TB, Zhang, P, Martyanov, V, Li, Z, Malik, BT, Wood, TA, Boni, A, Molodtsov, A, Angeles, CV, Curiel, TJ, Whitfield, ML & Turk, MJ 2017, 'Myeloid Cells That Impair Immunotherapy Are Restored in Melanomas with Acquired Resistance to BRAF Inhibitors', *Cancer research*, vol. 77, no. 7, pp. 1599-1610.

Straetemans, T, Berrevoets, C, Coccoris, M, Treffers-Westerlaken, E, Wijers, R, Cole, DK, Dardalhon, V, Sewell, AK, Taylor, N, Verweij, J & Debets, R 2015, 'Recurrence of Melanoma Following T Cell Treatment: Continued Antigen Expression in a Tumor That Evades T Cell Recruitment', *Molecular Therapy*, vol. 23, no. 2, pp. 396-406.

Stylianopoulos, T & Jain, RK 2013, 'Combining two strategies to improve perfusion and drug delivery in solid tumors', *Proceedings of the National Academy of Sciences,* vol. 110, no. 46, pp. 18632-18637.

Sun, B, Zhang, D, Zhang, S, Zhang, W, Guo, H & Zhao, X 2007, 'Hypoxia influences vasculogenic mimicry channel formation and tumor invasion-related protein expression in melanoma', *Cancer letters,* vol. 249, no. 2, pp. 188-197.

Sun, WY, Pitson, SM & Bonder, CS 2010, 'Tumor Necrosis Factor-Induced Neutrophil Adhesion Occurs Via Sphingosine Kinase-1-Dependent Activation of Endothelial α(5)β(1) Integrin', *Am J Pathol,* vol. 177, no. 1, pp. 436-446.

Tan, LY, Mintoff, C, Johan, MZ, Ebert, BW, Fedele, C, Zhang, YF, Szeto, P, Sheppard, KE, McArthur, GA, Foster-Smith, E, Ruszkiewicz, A, Brown, MP, Bonder, CS, Shackleton, M & Ebert, LM 2016, 'Desmoglein 2 promotes vasculogenic mimicry in melanoma and is associated with poor clinical outcome', *Oncotarget,* vol. 7, no. 29, pp. 46492-46508.

Tan, LY, Martini, C, Fridlender, ZG, Bonder, CS, Brown, MP & Ebert, LM 2017, 'Control of immune cell entry through the tumour vasculature: a missing link in optimising melanoma immunotherapy?', *Clinical & Translational Immunology,* vol. 6, no. 3, p. e134.

Tanaka, K, Toiyama, Y, Okugawa, Y, Okigami, M, Inoue, Y, Uchida, K, Araki, T, Mohri, Y, Mizoguchi, A & Kusunoki, M 2014, 'In vivo optical imaging of cancer metastasis using multiphoton microscopy: a short review', *American Journal of Translational Research,* vol. 6, no. 3, pp. 179-187.

Tang, H, Wang, Y, Chlewicki, LK, Zhang, Y, Guo, J, Liang, W, Wang, J, Wang, X & Fu, Y-X 2016, 'Facilitating T Cell Infiltration in Tumor Microenvironment Overcomes Resistance to PD-L1 Blockade', *Cancer cell,* vol. 29, no. 3, pp. 285-296.

Tang, ML, Steeber, DA, Zhang, XQ & Tedder, TF 1998, 'Intrinsic differences in L-selectin expression levels affect T and B lymphocyte subset-specific recirculation pathways', *Journal of Immunology,* vol. 160, no. 10, pp. 5113-5121.

Tang, N, Wang, L, Esko, J, Giordano, FJ, Huang, Y, Gerber, HP, Ferrara, N & Johnson, RS 2004, 'Loss of HIF-1alpha in endothelial cells disrupts a hypoxia-driven VEGF autocrine loop necessary for tumorigenesis', *Cancer cell,* vol. 6, no. 5, pp. 485-495.

Taube, JM, Klein, A, Brahmer, JR, Xu, H, Pan, X, Kim, JH, Chen, L, Pardoll, DM, Topalian, SL & Anders, RA 2014, 'Association of PD-1, PD-1 ligands, and other features of the tumor immune microenvironment with response to anti-PD-1 therapy', *Clinical Cancer Research,* vol. 20, no. 19, pp. 5064-5074.

Tazzyman, S, Barry, ST, Ashton, S, Wood, P, Blakey, D, Lewis, CE & Murdoch, C 2011, 'Inhibition of neutrophil infiltration into A549 lung tumors in vitro and in vivo using a CXCR2-specific antagonist is associated with reduced tumor growth', *International Journal of Cancer,* vol. 129, no. 4, pp. 847-858.

Thorvaldsdottir, H, Robinson, JT & Mesirov, JP 2013, 'Integrative Genomics Viewer (IGV): high-performance genomics data visualization and exploration', *Brief Bioinform,* vol. 14, no. 2, pp. 178-192.

Tolcher, AW, Su, W-C, Lakhani, N, Gutheil, J, Melink, TJ, Chu, Y-W, Chen, Y-L & Chien, D-S 2017, 'Phase I dose escalation study of CVM-1118, a novel anti-vascular mimicry agent, in patients with advanced cancers', *Journal of Clinical Oncology,* vol. 35, no. 15_suppl, pp. 2580-2580.

Topalian, Suzanne L, Drake, Charles G & Pardoll, Drew M 2015, 'Immune Checkpoint Blockade: A Common Denominator Approach to Cancer Therapy', *Cancer cell,* vol. 27, no. 4, pp. 450-461.

Topczewska, JM, Postovit, LM, Margaryan, NV, Sam, A, Hess, AR, Wheaton, WW, Nickoloff, BJ, Topczewski, J & Hendrix, MJ 2006, 'Embryonic and tumorigenic pathways converge via Nodal signaling: role in melanoma aggressiveness', *Nature medicine,* vol. 12, no. 8, pp. 925-932.

Torisu, H, Ono, M, Kiryu, H, Furue, M, Ohmoto, Y, Nakayama, J, Nishioka, Y, Sone, S & Kuwano, M 2000, 'Macrophage infiltration correlates with tumor stage and angiogenesis in human malignant melanoma: Possible involvement of TNFα and IL-1α', *International Journal of Cancer,* vol. 85, no. 2, pp. 182-188.

Twyman-Saint Victor, C, Rech, AJ, Maity, A, Rengan, R, Pauken, KE, Stelekati, E, Benci, JL, Xu, B, Dada, H, Odorizzi, PM, Herati, RS, Mansfield, KD, Patsch, D, Amaravadi, RK, Schuchter, LM, Ishwaran, H, Mick, R, Pryma, DA, Xu, X, Feldman, MD, Gangadhar, TC, Hahn, SM, Wherry, EJ, Vonderheide, RH & Minn, AJ 2015, 'Radiation and dual checkpoint blockade activate non-redundant immune mechanisms in cancer', *Nature,* vol. 520, no. 7547, pp. 373-377.

Uotila, LM, Aatonen, M & Gahmberg, CG 2013, 'Integrin CD11c/CD18 alpha-chain phosphorylation is functionally important', *The Journal of Biological Chemistry,* vol. 288, no. 46, pp. 33494-33499.

Ustione, A & Piston, DW 2011, 'A simple introduction to multiphoton microscopy', *Journal of Microscopy,* vol. 243, no. 3, pp. 221-226.

Utoguchi, N, Mizuguchi, H, Saeki, K, Ikeda, K, Tsutsumi, Y, Nakagawa, S & Mayumi, T 1995, 'Tumor-conditioned medium increases macromolecular permeability of endothelial cell monolayer', *Cancer letters,* vol. 89, no. 1, pp. 7-14.

Van Belle, P, Rodeck, U, Nuamah, I, Halpern, AC & Elder, DE 1996, 'Melanoma-associated expression of transforming growth factor-beta isoforms', *Am J Pathol,* vol. 148, no. 6, p. 1887.

Van Coillie, E, Van Aelst, I, Wuyts, A, Vercauteren, R, Devos, R, De Wolf-Peeters, C, Van Damme, J & Opdenakker, G 2001, 'Tumor Angiogenesis Induced by Granulocyte Chemotactic Protein-2 as a Countercurrent Principle', *Am J Pathol,* vol. 159, no. 4, pp. 1405-1414.

van der Schaft, DW, Seftor, RE, Seftor, EA, Hess, AR, Gruman, LM, Kirschmann, DA, Yokoyama, Y, Griffioen, AW & Hendrix, MJ 2004, 'Effects of angiogenesis inhibitors on vascular network formation by human endothelial and melanoma cells', *Journal of the National Cancer Institute,* vol. 96, no. 19, pp. 1473-1477.

van Houdt, IS, Sluijter, BJ, Moesbergen, LM, Vos, WM, de Gruijl, TD, Molenkamp, BG, van den Eertwegh, AJ, Hooijberg, E, van Leeuwen, PA & Meijer, CJ 2008, 'Favorable outcome in clinically stage II melanoma patients is associated with the presence of activated tumor infiltrating T-lymphocytes and preserved MHC class I antigen expression', *International Journal of Cancer,* vol. 123, no. 3, pp. 609-615.

Varney, ML, Johansson, SL & Singh, RK 2005, 'Tumour-associated macrophage infiltration, neovascularization and aggressiveness in malignant melanoma: role of monocyte chemotactic protein-1 and vascular endothelial growth factor-A', *Melanoma research,* vol. 15, no. 5, pp. 417-425.

Varney, ML, Johansson, SL & Singh, RK 2006, 'Distinct Expression of CXCL8 and Its Receptors CXCR1 and CXCR2 and Their Association With Vessel Density and Aggressiveness in Malignant Melanoma', *American journal of clinical pathology,* vol. 125, no. 2, pp. 209-216.

Vartanian, A, Stepanova, E, Grigorieva, I, Solomko, E, Baryshnikov, A & Lichinitser, M 2011, 'VEGFR1 and PKCalpha signaling control melanoma vasculogenic mimicry in a VEGFR2 kinase-independent manner', *Melanoma research,* vol. 21, no. 2, pp. 91-98.

Vartanian, A, Gatsina, G, Grigorieva, I, Solomko, E, Dombrovsky, V, Baryshnikov, A & Stepanova, E 2013, 'The involvement of Notch signaling in melanoma vasculogenic mimicry', *Clin Exp Med,* vol. 13, no. 3, pp. 201-209.

Vergani, E, Di Guardo, L, Dugo, M, Rigoletto, S, Tragni, G, Ruggeri, R, Perrone, F, Tamborini, E, Gloghini, A, Arienti, F, Vergani, B, Deho, P, De Cecco, L, Vallacchi, V, Frati, P, Shahaj, E, Villa, A, Santinami, M, De Braud, F, Rivoltini, L & Rodolfo, M 2016, 'Overcoming melanoma resistance to vemurafenib by targeting CCL2-induced miR-34a, miR-100 and miR-125b', *Oncotarget,* vol. 7, no. 4, pp. 4428-4441.

Vestweber, D 2015, 'How leukocytes cross the vascular endothelium', *Nature Reviews Immunology,* vol. 15, no. 11, pp. 692-704.

Vianello, F, Papeta, N, Chen, T, Kraft, P, White, N, Hart, WK, Kircher, MF, Swart, E, Rhee, S, Palù, G, Irimia, D, Toner, M, Weissleder, R & Poznansky, MC 2006, 'Murine B16 Melanomas Expressing High Levels of the Chemokine Stromal-Derived Factor-1/CXCL12 Induce Tumor-Specific T Cell Chemorepulsion and Escape from Immune Control', *The Journal of Immunology,* vol. 176, no. 5, pp. 2902-2914.

Villanueva, J, Vultur, A, Lee, JT, Somasundaram, R, Fukunaga-Kalabis, M, Cipolla, AK, Wubbenhorst, B, Xu, X, Gimotty, PA, Kee, D, Santiago-Walker, AE, Letrero, R, D'Andrea, K, Pushparajan, A, Hayden, JE, Brown, KD, Laquerre, S, McArthur, GA, Sosman, JA, Nathanson, KL & Herlyn, M 2010, 'Acquired Resistance to BRAF Inhibitors Mediated by a RAF Kinase Switch in Melanoma Can Be Overcome by Cotargeting MEK and IGF-1R/PI3K', *Cancer cell,* vol. 18, no. 6, pp. 683-695.

Villarreal, G, Zhang, Y, Larman, HB, Gracia-Sancho, J, Koo, A & García-Cardeña, G 2010, 'Defining the Regulation of Klf4 Expression and Its Downstream Transcriptional Targets in Vascular Endothelial Cells', *Biochemical and biophysical research communications,* vol. 391, no. 1, pp. 984-989.

Vivier, E, Raulet, DH, Moretta, A, Caligiuri, MA, Zitvogel, L, Lanier, LL, Yokoyama, WM & Ugolini, S 2011, 'Innate or adaptive immunity? The example of natural killer cells', *Science*, vol. 331, no. 6013, pp. 44-49.

Vries, MHM, Wagenaar, A, Verbruggen, SEL, Molin, DGM & Post, MJ 2015, 'CXCL1 promotes arteriogenesis through enhanced monocyte recruitment into the peri-collateral space', *Angiogenesis*, vol. 18, no. 2, pp. 163-171.

Wagenblast, E, Soto, M, Gutierrez-Angel, S, Hartl, CA, Gable, AL, Maceli, AR, Erard, N, Williams, AM, Kim, SY, Dickopf, S, Harrell, JC, Smith, AD, Perou, CM, Wilkinson, JE, Hannon, GJ & Knott, SR 2015, 'A model of breast cancer heterogeneity reveals vascular mimicry as a driver of metastasis', *Nature*, vol. 520, no. 7547, pp. 358-362.

Walker, GJ, Flores, JF, Glendening, JM, Lin, A, Markl, ID & Fountain, JW 1998, 'Virtually 100% of melanoma cell lines harbor alterations at the DNA level within CDKN2A, CDKN2B, or one of their downstream targets', *Genes, Chromosomes and Cancer*, vol. 22, no. 2, pp. 157-163.

Wang, L, Fan, J, Thompson, LF, Zhang, Y, Shin, T, Curiel, TJ & Zhang, B 2011, 'CD73 has distinct roles in nonhematopoietic and hematopoietic cells to promote tumor growth in mice', *Journal of Clinical Investigation*, vol. 121, no. 6, pp. 2371-2382.

Wang, Y, Roche, O, Xu, C, Moriyama, EH, Heir, P, Chung, J, Roos, FC, Chen, Y, Finak, G, Milosevic, M, Wilson, BC, Teh, BT, Park, M, Irwin, MS & Ohh, M 2012, 'Hypoxia promotes ligand-independent EGF receptor signaling via hypoxia-inducible factor–mediated upregulation of caveolin-1', *Proceedings of the National Academy of Sciences of the United States of America*, vol. 109, no. 13, pp. 4892-4897.

Warso, MA, Maniotis, AJ, Chen, X, Majumdar, D, Patel, MK, Shilkaitis, A, Gupta, TKD & Folberg, R 2001, 'Prognostic significance of periodic acid-Schiff-positive patterns in primary cutaneous melanoma', *Clinical Cancer Research*, vol. 7, no. 3, pp. 473-477.

Weckbach, LT, Gola, A, Winkelmann, M, Jakob, SM, Groesser, L, Borgolte, J, Pogoda, F, Pick, R, Pruenster, M, Muller-Hocker, J, Deindl, E, Sperandio, M & Walzog, B 2014, 'The cytokine midkine supports neutrophil trafficking during acute inflammation by promoting adhesion via beta2 integrins (CD11/CD18)', *Blood*, vol. 123, no. 12, pp. 1887-1896.

Weidner , N, Semple , JP, Welch , WR & Folkman , J 1991, 'Tumor Angiogenesis and Metastasis — Correlation in Invasive Breast Carcinoma', *New England Journal of Medicine*, vol. 324, no. 1, pp. 1-8.

Weishaupt, C, Munoz, KN, Buzney, E, Kupper, TS & Fuhlbrigge, RC 2007, 'T-cell distribution and adhesion receptor expression in metastatic melanoma', *Clinical Cancer Research*, vol. 13, no. 9, pp. 2549-2556.

Wendel, M, Galani, IE, Suri-Payer, E & Cerwenka, A 2008, 'Natural Killer Cell Accumulation in Tumors Is Dependent on IFN-γ and CXCR3 Ligands', *Cancer research*, vol. 68, no. 20, pp. 8437-8445.

Wenger, RH, Kvietikova, I, Rolfs, A, Gassmann, M & Marti, HH 1997, 'Hypoxia-inducible factor-1 alpha is regulated at the post-mRNA level', *Kidney Int,* vol. 51, no. 2, pp. 560-563.

Wennerberg, E, Kremer, V, Childs, R & Lundqvist, A 2015, 'CXCL10-induced migration of adoptively transferred human natural killer cells toward solid tumors causes regression of tumor growth in vivo', *Cancer Immunology, Immunotherapy,* vol. 64, no. 2, pp. 225-235.

Wilmott, JS, Long, GV, Howle, JR, Haydu, LE, Sharma, RN, Thompson, JF, Kefford, RF, Hersey, P & Scolyer, RA 2012, 'Selective BRAF Inhibitors Induce Marked T-cell Infiltration into Human Metastatic Melanoma', *Clinical Cancer Research,* vol. 18, no. 5, pp. 1386-1394.

Winkler, F, Kozin, SV, Tong, RT, Chae, S-S, Booth, MF, Garkavtsev, I, Xu, L, Hicklin, DJ, Fukumura, D, di Tomaso, E, Munn, LL & Jain, RK 2004, 'Kinetics of vascular normalization by VEGFR2 blockade governs brain tumor response to radiation', *Cancer cell,* vol. 6, no. 6, pp. 553-563.

Wojciak-Stothard, B, Potempa, S, Eichholtz, T & Ridley, AJ 2001, '9Rgr; and Rac but not Cdc42 regulate endothelial cell permeability', *Journal of Cell Science,* vol. 114, no. 7, pp. 1343-1355.

Wu, X, Giobbie-Hurder, A, Liao, X, Lawrence, DP, McDermott, DF, Zhou, J, Rodig, SJ & Hodi, FS 2016, 'VEGF neutralization plus CTLA-4 blockade alters soluble and cellular factors associated with enhancing lymphocyte infiltration and humoral recognition in melanoma', *Cancer Immunology Research,* vol. 4, no. 10, pp. 856-868.

Wu, Y, Li, YY, Matsushima, K, Baba, T & Mukaida, N 2008, 'CCL3-CCR5 axis regulates intratumoral accumulation of leukocytes and fibroblasts and promotes angiogenesis in murine lung metastasis process', *Journal of Immunology,* vol. 181, no. 9, pp. 6384-6393.

Yakubenko, VP, Yadav, SP & Ugarova, TP 2006, 'Integrin αDβ2, an adhesion receptor up-regulated on macrophage foam cells, exhibits multiligand-binding properties', *Blood,* vol. 107, no. 4, pp. 1643-1650.

Yamada, M, Yanaba, K, Hasegawa, M, Matsushita, Y, Horikawa, M, Komura, K, Matsushita, T, Kawasuji, A, Fujita, T, Takehara, K, Steeber, DA, Tedder, TF & Sato, S 2006, 'Regulation of local and metastatic host-mediated anti-tumour mechanisms by L-selectin and intercellular adhesion molecule-1', *Clin Exp Immunol,* vol. 143, no. 2, pp. 216-227.

Yamaoka, T, Fujimoto, M, Ogawa, F, Yoshizaki, A, Bae, SJ, Muroi, E, Komura, K, Iwata, Y, Akiyama, Y, Yanaba, K, Shimizu, K & Sato, S 2011, 'The roles of P- and E-selectins and P-selectin glycoprotein ligand-1 in primary and metastatic mouse melanomas', *J Dermatol Sci,* vol. 64, no. 2, pp. 99-107.

Yan, M, Jene, N, Byrne, D, Millar, EKA, O'Toole, SA, McNeil, CM, Bates, GJ, Harris, AL, Banham, AH, Sutherland, RL & Fox, SB 2011, 'Recruitment of regulatory T cells is correlated with hypoxia-induced CXCR4 expression, and is associated with poor prognosis in basal-like breast cancers', *Breast Cancer Research,* vol. 13, no. 2, pp. R47-R47.

Yang, JP, Liao, YD, Mai, DM, Xie, P, Qiang, YY, Zheng, LS, Wang, MY, Mei, Y, Meng, DF, Xu, L, Cao, L, Yang, Q, Yang, XX, Wang, WB, Peng, LX, Huang, BJ & Qian, CN 2016, 'Tumor vasculogenic mimicry predicts poor prognosis in cancer patients: a meta-analysis', *Angiogenesis*, vol. 19, no. 2, pp. 191-200.

Yeo, L, Adlard, N, Biehl, M, Juarez, M, Smallie, T, Snow, M, Buckley, CD, Raza, K, Filer, A & Scheel-Toellner, D 2015, 'Expression of chemokines CXCL4 and CXCL7 by synovial macrophages defines an early stage of rheumatoid arthritis', *Annals of the Rheumatic Diseases*.

Yu, Q, Lou, XM & He, Y 2015, 'Preferential recruitment of Th17 cells to cervical cancer via CCR6-CCL20 pathway', *PloS one*, vol. 10, no. 3, p. e0120855.

Zheng, F, Jang, W-C, Fung, FKC, Lo, ACY & Wong, IYH 2016, 'Up-Regulation of ENO1 by HIF-1α in Retinal Pigment Epithelial Cells after Hypoxic Challenge Is Not Involved in the Regulation of VEGF Secretion', *PloS one*, vol. 11, no. 2, p. e0147961.

Zittermann, SI & Issekutz, AC 2006, 'Endothelial growth factors VEGF and bFGF differentially enhance monocyte and neutrophil recruitment to inflammation', *Journal of Leukocyte Biology*, vol. 80, no. 2, pp. 247-257.

Zuchtriegel, G, Uhl, B, Puhr-Westerheide, D, Pörnbacher, M, Lauber, K, Krombach, F & Reichel, CA 2016, 'Platelets Guide Leukocytes to Their Sites of Extravasation', *PLoS Biology*, vol. 14, no. 5, p. e1002459.